The synthesis and ring-opening polymerisation of novel cyclic esters from malic acid

by

Ryan Jonathon Pounder

A thesis submitted in partial fulfillment of the requirements for the degree of

Doctor of Philosophy in Chemistry

Department of Chemistry

University of Warwick

August 2010

Table of Contents

List of Figures

List of Schemes

List of Tables

Abbreviations

λ	Wavelength
δ	Chemical shift
β-PL	β-Propiolactone
δ-VL	δ-Valerolactone
ε-CL	ε-Caprolactone
AIBN	2,2-Azo-bis-isobutyronitrile
ATRP	Atom transfer radical polymerisation
BMD	3-(*S*)-[(Benzyloxycarbonyl)methyl]-1,4-dioxane-2,5-dione
CMC	Critical micelle concentration
COD	Cyclooctadiene
DBU	1,8-Diazabicyclo[5.4.0]undec-7-ene
DBN	1,5-Diazabicyclo[4.3.0]non-5-ene
DCC	Dicyclohexylcarbodiimide
DIAD	Diisopropylazodicarboxylate
DIEA	Diisopropylethylamine
DMAP	4-Dimethylaminopyridine
DLS	Dynamic light scattering
DP	Degree of polymerisation
DRI	Differential refractive index
DSC	Differential scanning calorimetry
DSDOP	2,2-Dibutyl-2-stanna-1,3-dioxepane
ESI MS	Electrospray ionisation mass spectrometry
GPC	Gel permeation chromatography
HMPA	Hexamethylphosphoramide
HPCE	High performance capillary electrophoresis
HEMA	2-Hydroxyethyl methacrylate
HMTETA	1,1,4,7,10,10-Hexamethyltriethylenetetraamine

LA	Lactide
LCST	Lower critical solution temperature
LDA	Lithium diisopropyl amide
M_n	Number-averaged molecular weight
M_w	Weight-averaged molecular weight
MA	Malic acid
MALDI-TOF MS	Matrix-assisted laser desorption and ionisation time-of-flight mass spectrometry
*m*CPBA	*meta*-Chloroperoxybenzoic acid
mDEG	10-Azido-2,5,8-trioxadecane
MLABz	Benzyl β-malolactone
MMA	Methyl methacrylate
MWCO	Molecular weight cut-off
NBS	*N*-Bromosuccinimide
NMO	*N*-Methylmorpholine-*N*-oxide
NMR	Nuclear magnetic resonance
OCA	*O*-Carboxyanhydride
*p*TsOH	*para*-Toluenesulfonic acid
PBMA	Poly(benzyl α-malate)
PBMD	Poly(glycolic acid-*co*-benzyl α-malate)
PCC	Pyridinium chlorochromate
PCL	Poly(ε-caprolactone)
PDC	Pyridinium dichromate
PDI	Polydispersity index
PEG	Poly(ethylene glycol)
PEO	Poly(ethylene oxide)
PGMA	Poly(glycolic acid-*co*-α-malic acid)
PLA	Poly(lactide)
PLLA	Poly(*L*-lactide)
PDLA	Poly(*D*-lactide)

PDLLA	Poly(*rac*-lactide)
PGA	Poly(glycolic acid)
PMA	Poly(malic acid)
PMDETA	*N*,*N*,*N*',*N*',*N*-Pentamethyldiethylenetriamine
PMMA	Poly(methyl methacrylate)
PNIPAM	Poly(*N*-isopropylacylamide)
PPL	Poly(β-propiolactone)
PVL	Poly(δ-valerolactone)
ROMP	Ring-opening metathesis polymerisation
ROP	Ring-opening polymerisation
T_g	Glass transition temperature
T_m	Melting transition temperature
TBD	1,5,7-Triazabicyclo[4.4.0]dec-5-ene
TEM	Transmission electron microscopy
TFA	Trifluoroacetic acid
TFAA	Trifluoroacetic anhydride
TGA	Thermogravimetric analysis
TMSEMA	Trimethylsilyloxyethyl methacrylate
TPP	Triphenylphosphine
UV	Ultra-violet

Acknowledgements

Firstly, I would like to thank my academic supervisor Dr Andrew Dove for his constant encouragement, enthusiasm and advice that he has given me throughout my studies over the past four years. I also thank the EPSRC for providing me with funding for this project.

I would also like to thank Matthew Stanford for being a great person to have worked alongside (if you ignore the mess) and for the great laughs and memories as part of Team Lilac. I would also like to acknowledge the rest of the Dove group for putting up with me over the last months of my studies when the stress took over a little.

I am grateful to Dr Helen Willcock from the “O’Reilly group” for all her help and guidance with the work in my final chapter. I would also like to acknowledge Dr Adam Clarke and Dr Ivan Prokes for all there advice and assistance with NMR measurements. A special thanks to Dr Lijang Song who helped me tirelessly with any mass spectrometry problems I encountered and provided some great data on my degradation studies.

Finally, I would like to thank my family and friends for always being there and for their constant support during my years of study. I am especially grateful to Katherine Burley; thank you for seeing me through the ups and downs, I couldn’t have done it without you. You have been amazing!

Declaration

Experimental work contained in this thesis is original research carried out by the author, unless otherwise stated, in the Department of Chemistry at the University of Warwick, between October 2006 and August 2010. No material contained herein has been submitted for any other degree, or at any other institution.

Results from other authors are referenced in the usual manner throughout the text.

_____ Date: _____

Ryan Jonathon Pounder

Abstract

The work in this thesis is directed towards the preparation of cyclic ester monomers using malic acid as a renewable resource. Their subsequent controlled ring-opening polymerisation (ROP) to yield functionalised poly(ester)s is studied and application in micellar self-assembly reported.

Chapter 1 reviews the many synthetic strategies that have been employed in the preparation of functional glycolides, lactides, ε-caprolactones, δ-valerolactones and β-propiolactones. Their subsequent polymerisation and applications are also discussed.

Chapter 2 describes the improved synthesis of 3-(*S*)-[(benzyloxycarbonyl)methyl]- and 3,6-(*S*)-[di(benzyloxycarbonyl)methyl]-1,4-dioxane-2,5-diones, BMD and malide respectively, from *L*-malic acid. Controlled organocatalytic ROP of BMD realised functional poly(glycolic acid-*co*-benzyl α-malate)s (PBMD) with the choice of initiator proving important in determining the resulting molecular weight. Successful hydrogenolysis of these poly(glycolic acid-*co*-benzyl α-malate)s yielded hydrophilic poly(glycolic acid-*co*-α-malic acid)s (PGMA) with subsequent degradation studies in H_2O observing complete degradation after six days.

In Chapter 3, the synthesis of 5-(*S*)- and 5-(*R*)-[(benzyloxycarbonyl)methyl]-1,3-dioxolane-2,4-dione (*L*-malOCA and *D*-malOCA respectively) from *L*- and *D*-malic acid respectively is reported. ROP of malOCA with a range of pyridine based catalysts enabled the synthesis of functional poly(benzyl α-malate)s (PBMA). Mechanistic studies revealed the formation of several side products that were eliminated *via* judicious choice of catalyst and column chromatography.

Subsequent hydrogenolysis realised hydrophilic poly(α-malic acid)s (PMA) with degradation studies in H_2O observing complete degradation after 10 days.

Chapter 4 reports the synthesis of novel amphiphilic PEO-*b*-PBMA block copolymers by the ROP of *L*-malOCA or *D*-malOCA from PEO macroinitiators with subsequent self-assembly realising polymeric micelles. Variation in both size dimensions and stability of the micelles through changes in both the hydrophobic and hydrophilic block lengths and their relative ratios was demonstrated. The self-assembly of an equimolar mixture of homochiral PEO-*b*-P(*L*-BMA) and PEO-*b*-P(*D*-BMA) resulted in the formation of stereocomplexed polymeric micelles.

Chapter 5 provides a summary of the findings in chapters 2 – 4 with chapter 6 providing the corresponding experimental data.

Chapter 1 - Synthesis and ring-opening polymerisation of functional cyclic esters.

1.1 Introduction

The ring-opening polymerisation (ROP) of lactones and lactides to produce aliphatic poly(ester)s provides versatile biocompatible and biodegradable polymers possessing good mechanical properties. These advantages have seen aliphatic poly(ester)s receive increasing attention over the last few years, driven by both their application in the biomedical field and as biodegradable substitutes for conventional commodity thermoplastics.[1-11] Among the family of biodegradable polymers, aliphatic poly(ester)s possess the leading position as a consequence of the ready metabolisation of the degradation products in most cases. Poly(ester)s can be prepared from a wide range of materials with judicious choice of monomer feedstock able to modulate the physio-chemical properties including glass transition temperatures, toughness, stiffness and degradability *etc*. Aliphatic poly(ester)s are prepared through one of two routes; the first is step-growth polycondensation of a hydroxy acid or between a diacid and a diol enabling access to a large range of monomer feedstocks (Scheme 1.1a). However, the molecular weights are generally limited and any minor deviations in the stoichiometry is detrimental to the chain length. Furthermore, long reaction times and high temperatures are often required resulting in unfavourable side reactions.[12] The second route for the synthesis of aliphatic poly(ester)s is *via* ring-opening polymerisation (ROP). By this methodology the preparation of high molecular weight aliphatic poly(ester)s is possible while maintaining high levels of control over their molecular characteristics under relatively mild conditions (Scheme 1.1b).

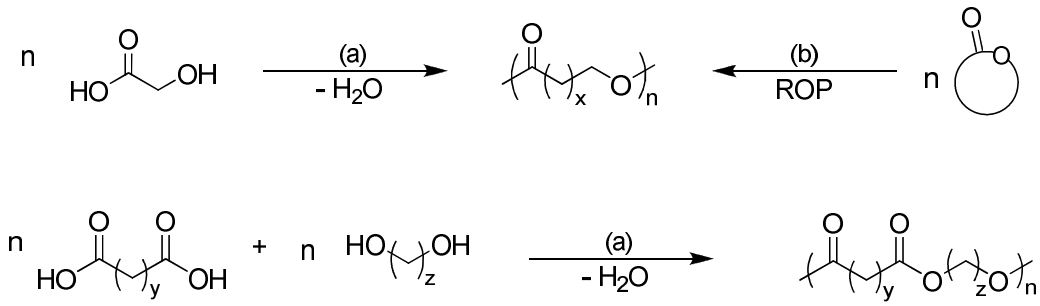

Scheme 1.1. Synthesis of poly(ester)s by (a) step-growth polycondensation or (b) ring-opening polymerisation.

A large amount of research has been directed towards the controlled ROP of commercially available renewable cyclic esters including glycolide, lactide, ε-caprolactone, δ-valerolactone and β-propiolactone to result in aliphatic poly(ester)s with highly controlled molecular parameters. A variety of catalytic systems have been investigated to more efficiently mediate the ROP process including the development of well-defined metal complexes, organic catalysts and the study of enzymatic catalysis and have resulted in high levels of control over polymer molecular weight, tacticity, polydispersity and end-group fidelity.[8,12-14] Additionally, work has been directed towards the formation of architecturally diverse poly(ester)s, including stars, brushes, cycles, cross-linked materials and hyper branched poly(ester)s, to improve mechanical properties, hydrophilicity and degradability profiles.[15-21] While the physical properties of these polymers can be further tailored *via* copolymerisation,[2,22-28] a major limitation towards application of these polymers in new arenas results from the lack of readily accessible side-chain functionality and thus also their hydrophobicity. The introduction of functional groups throughout the polymer chain using ROP methodology remains highly challenging but yields degradable polymers with tuneable properties including increased hydrophilicity, post-

polymerisation modification as well as further fine tuning of the physical properties.

1.2 Functional poly(ester)s from cyclic diesters

Poly(lactide) and its copolymers with glycolide or other cyclic esters are widely used in the medical field as sutures, oral implants, and microspheres for drug encapsulation and delivery.[1,4,8-10] Despite the widespread application of this family of polymers, their high crystallinity, brittleness, hydrophobicity and thermal instability present limitations of the materials. A more versatile alternative to copolymerisation is the synthesis and ROP of functional cyclic diesters (1,4-dioxane-2,5-diones). Two main strategies for the synthesis of functionalised cyclic diester monomers have been reported by *(i)* the self condensation of α-hydroxy acids catalysed by *p*-toluenesulfonic acid (*p*TsOH) or cracking of oligoesters by ZnO/$Sn(Oct)_2$ (Route 1, Scheme 1.2) or *(ii)* the step-by-step condensation of an α-hydroxy acid and an α-haloacyl halide with subsequent base-mediated cyclisation (Route 2, Scheme 1.2).

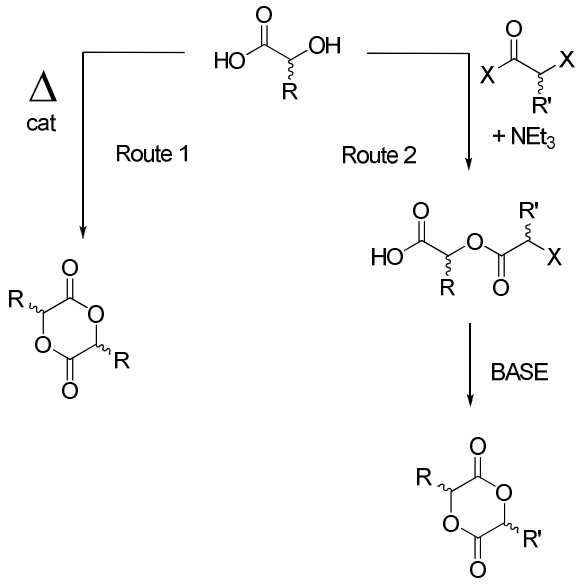

Scheme 1.2. General synthetic routes for the synthesis of cyclic diesters from α-hydroxy acids.

1.2.1 Alkyl- and aryl-functional glycolides

Using the methodologies previously described, an array of functional cyclic diesters have been synthesised including a variety of simple alkyl-functional 1,4-dioxane-2,5-diones. The variation of the poly(ester) side-chain alkyl substituent has resulted in the ability to significantly affect the physical properties of the polymers, especially the glass transition temperature (T_g). Baker *et al.* reported the synthesis of 3,6-diethyl- (**I**), 3,6-diisobutyl- (**II**) and 3,6-di-*n*-hexyl-1,4-dioxane-2,5-diones (**III**) (Figure 1.1) from their respective α-hydroxy acids by acid catalysed oligomerisation followed by cracking with ZnO at 180 °C. Bulk polymerisation of these monomers (statistical mixtures of *R,R*, *S,S* and *R,S*) was investigated at 130 °C using a range of different organometallic catalysts and resulted in the preparation of high molecular weight poly(ester)s. Under comparable conditions (bulk, 130 °C, [monomer]:[stannous(II) octanoate]:[ROH] 100:1:1) the rate of propagation for each monomer decreased with increasing

steric bulk of the side chains such that *L*-lactide (*L*-LA)>**I**>**III**>**II**. T_g values of the resulting poly(ester)s were reported to be 22, 12 and -37 °C for poly(**II**), poly(**I**) and poly(**III**) respectively, lower than that of isotactic poly(*L*-lactide) (PLLA) (55-60 °C).[29] A further study investigated the preparation of 3,6-dibenzyl-1,4-dioxan-2,5-dione, phenyllactide (**IV**) (Figure 1.1), through *p*TsOH catalysed dimerisation of *L*-phenyllactic acid. ROP of phenyllactide with stannous(II) octanoate ($Sn(Oct)_2$) in toluene resulted in amorphous poly(phenyllactide) with a T_g value of 50 °C. Subsequent hydrolytic degradation of the poly(ester) at 55 °C and pH 7.4 was shown to occur five times slower than poly(*rac*-LA) (PDLLA), attributed to the increased hydrophobicity of poly(phenyllactide) in comparison to PLA that resulted from the aromatic rings on the polymer side chain.[30]

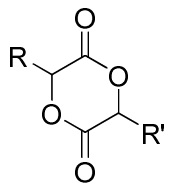

I: R = CH_2CH_3, R' = CH_2CH_3 (63%)
II: R = $CH_2CH(CH_3)_2$, R' = $CH_2CH(CH_3)_2$ (71%)
III: R = $(CH_2)_5CH_3$, R' = $(CH_2)_5CH_3$ (65%)
IV: R = $CH_2C_6H_5$, R' = $CH_2C_6H_5$(40-90%)
V: R = $CH(CH_3)_2$, R' = Me (35%)
VI: R = $(CH_2)_5CH_3$, R' = Me (45%)
VII: R = $CH_2C_6H_5$, R' = Me (35%)
VIII: R = $(CH_3)_2$, R' = Me (46%)
IX: R = $(CH_2)_3CH_3$, R' = Me (40%)
X: R = C_6H_5, R' = C_6H_5 (91%)
XI: R = C_6H_{11}, R' = C_6H_{11} (21-40%)
XII: R= C_6H_{11}, R' = Me (59%)
XIII: R = $CH(CH_3)_2$, R' = $CH(CH_3)_2$ (16%)

Figure 1.1. Synthesis of 3,6-difunctional glycolides (**I – XIII**); yields in parentheses.

The synthesis of a further range of alkyl-functionalised cyclic diesters including 3-methyl-6-isopropyl- (**V**), 3-methyl-6-*n*-hexyl- (**VI**), 3-benzyl-6-methyl- (**VII**), 3,6,6-trimethyl- (**VIII**) and 3-methyl-6-*n*-butyl-1,4-dioxane-2,5-diones (**IX**)

(Figure 1.1) have been reported through coupling of their respective α-hydroxy acids with 2-bromopropionyl bromide and cyclised with triethylamine (NEt_3). With the exception of 3,6,6-trimethyl-1,4-dioxane-2,5-dione, **VIII**, all the monomers were successfully polymerised with either $Sn(Oct)_2$, stannous(II) trifluoromethanesulfonate ($Sn(OTf)_2$) and/or dimethylaminopyridine (DMAP) with good control of molecular weight and PDI. DMAP proved a more efficient catalyst for greater sterically hindered monomers. This study also noted the decrease in T_g values of the poly(ester)s with increasing hydrophobic substituents such that with relatively short polymers (~ 4 000 $g.mol^{-1}$) T_g values were reduced from 41 to -17 to -47 °C for lactide, mono-hexyl and di-hexyl monomers respectively. [31] Poly(**VI**), (PmHLA), and poly(**III**), (PdiHLA), have been further studied as possible hydrophobic drug delivery systems. Hydrolytic degradation in a phosphate buffered solution at 37 °C and pH 7.4 of PmHLA with a T_g of ~ -15 °C was found to be slightly faster than an analogous PLA attributed to the flexible rubbery state of PmHLA at physiological temperature that favours degradation in comparison to the rigid and glassy PLA (T_g ~ 40 °C). In contrast, degradation studies at 60 °C, above the glass transition temperatures of both polymers, resulted in slower degradation for the sterically more hindered PmHLA compared to PLA. Release studies in phosphate buffered solution at 37 °C and pH 7.4 found the model drug tetracycline was released faster and in higher amounts in its active form from a PmHLA matrix than from a standard PLA matrix.[32] Amphiphilic copolymers of PmHLA/PdiHLA and PEO were also synthesised using a monomethylether poly(ethylene oxide) (PEO) (~ 2 000 $g.mol^{-1}$) as a macroinitiator resulting in block copolymers capable of self-assembly. The resulting micelles, with a PHLA core and PEO corona, displayed

decreased mean diameters with increased hydrophobicity. Incorporation of model hydrophobic drugs including Nile Red and Griseofulvin into the micelles was increased with increased concentration of hydrophobic *n*-hexyl groups in the core.[33]

In an attempt to realise a higher T_g poly(ester) the synthesis of mandelide (3,6-diphenyl-1,4-dioxan-2,5-dione, **X**) (Figure 1.1) by the dimerisation of *rac*-mandelic acid in the presence of acidic catalyst was investigated, yielding a statistical mixture of *LL*-, *DD*- and *meso*- diastereomers. Separation of the *rac*- and *meso*- isomers before polymerisation proved unnecessary as the benzylic methine proton readily racemised under the polymerisation conditions. Bulk polymerisation of mandelide with $Sn(Oct)_2$ at 160 °C resulted in amorphous polymers with molecular weights closely matching those predicted from the degree of polymerisation with PDIs < 3. The T_g of poly(mandelide) was reported to be 100 °C, comparable to that of poly(styrene), with poly(mandelide) also displaying other similar properties to poly(styrene) such as terminal viscosity and storage modulus. Despite its high T_g value and poly(styrene)-like properties, poly(mandelide) suffers from thermal and photochemical degradation attributed to the reactivity of the benzylic methine proton. Hydrolytic degradation of poly(mandelide) in phosphate buffered solution at 55 °C and pH 7.4 proceeded 100 times slower than an analogous PLA.[34] In an attempt to reduce the reactivity of the methine group in both the monomer and polymer while maintaining chain rigidity in the functional poly(ester), replacement of the aromatic ring with a cyclohexyl group was investigated. Synthesis of *rac*-, *meso*- and *R,R*-3,6-dicyclohexyl-1,4-dioxane-2,5-dione, **XI**, along with *rac*-3-cyclohexyl-6-methyl-1,4-dioxane-2,5-dione, **XII**, (Figure 1.1) was achieved from 2-cyclohexyl-2-

hydroxyacetic acid, prepared from the catalytic hydrogenation of mandelic acid using rhodium on alumina, by either dimersation in the presence of *p*TsOH or coupling with 2-bromopropionyl bromide and subsequent cyclisation with NEt_3. Solution polymerisation in ~0.2 M toluene at 90 °C and bulk polymerisation at 200 °C of **XI** using $Sn(Oct)_2$ resulted in poly(ester)s with T_g values comparable to poly(mandelide), whereas poly(**XII**) possessed a T_g value ~20 °C lower than poly(**XI**). Hydrolytic degradation studies on poly(**XI**) revealed no appreciable loss in polymer molecular weight after 100 days in pH 7.4 phosphate buffer at 55 °C. The effects of stereoregularity on the poly(ester) properties were investigated through comparison of the poly(**XI**)s prepared from *rac*, *meso*, and *R*,*R*-3,6-dicyclohexyl-1,4-dioxane-2,5-diones. Optically pure poly(*R*,*R*-dicyclohexylglycolide) had the highest T_g of 104 °C, whereas the *rac*- and *meso*-derivatives resulted in only slightly lower T_g values of 98 °C and 96 °C respectively being observed which implied that the stereosequence distribution is less important in determining the properties of poly(**XI**)s than observed in PLAs. In the same study the synthesis of *rac*-3,6-diisopropyl-1,4-dioxan-2,5-dione, **XIII**, (Figure 1.1) was realised through dimerisation of the respective α-hydroxy acid in the presence of *p*TsOH. ROP with $Sn(Oct)_2$ under analogous conditions to **XI** and **XII** yielded poly(**XIII**) with a significantly lower T_g value of 41 °C. Comparison of poly(**XI**), poly(**XII**), poly(**XIII**) and PLA revealed that the increase in T_g related to steric bulk and stereoregularity of the poly(ester) ([M]/[I] = 300) such that poly(*R*,*R*-**XI**) > poly(*meso*-**XI**) ~ poly(*rac*-**XI**) > poly(*rac*-**XII**) > PLA > poly(*rac*-**XIII**) (T_g = 104, 96, 98, 73, 55 and 41 °C respectively).[35]

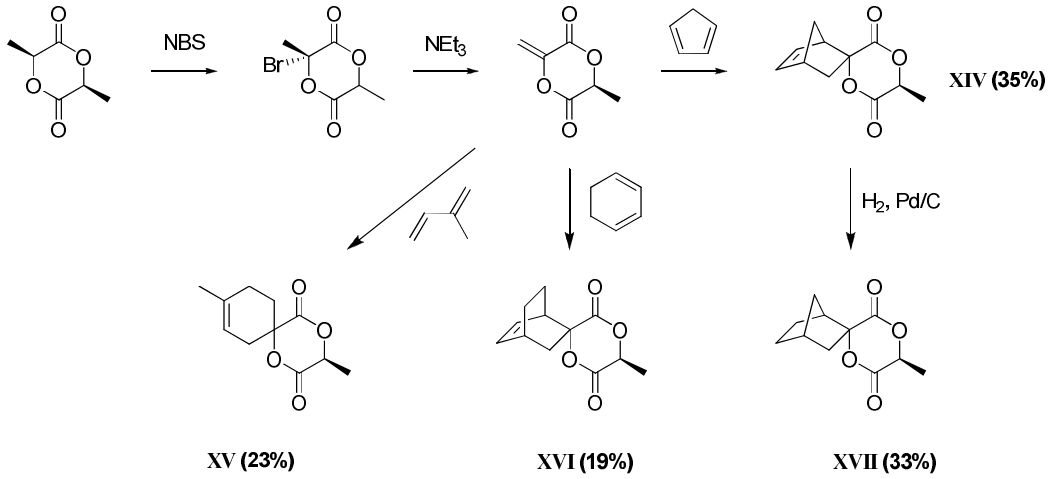

Scheme 1.3. Synthesis of (6*S*)-spiro[6-methyl-1,4-dioxane-2,5-dione-3,2'-bicyclo[2.2.1]hept[5]ene (**XIV**), (6*S*)-spiro[6-methyl-1,4-dioxane-2,5-dione-3,4'-(1-methyl)cyclohex-1-ene] (**XV**), (6*S*)-spiro[6-methyl-1,4-dioxane-2,5-dione-3,2'-bicyclo[2.2.2]oct[5]ene] (**XVI**), and (6*S*)-spiro[6-methyl-1,4-dioxane-2,5-dione-3,2'-bicyclo[2.2.1]hept[5]ane (**XVII**) (overall yields from *L*-LA in parentheses).

Recently Hillmyer *et al*. reported the synthesis of a bifunctional monomer, **XIV**, from *L*-lactide (Scheme 1.3) that is capable of both ROP and ring-opening metathesis polymerisation (ROMP). *L*-Lactide was first brominated with *N*-bromosuccinimide (NBS) followed by elimination of HBr with NEt_3 to result in (6*S*)-3-methylene-6-methyl-1,4-dioxane-2,5-dione. The captodative alkene was then used as a dienophile in a Diels-Alder reaction to construct a new tricyclic compound (spiro[6-methyl-1,4-dioxane-2,5-dione-3,2'-bicyclo[2.2.1]hept[5]ene], **XIV**). 1,5,7-triazabicyclo[4.4.0]dec-5-ene (TBD) was employed to catalyse the ROP of **XIV** with lower temperatures improving monomer conversion. This was consistent with the bulky nature of the norbornene side group limiting the exothermicity of the polymerisation reaction, such that at -20 °C, 94% conversion after 24 h was achieved whereby at room temperature conversion plateaued at 84% after an identical time. The resulting high molecular weight poly(ester) (M_n

= 30 100 g.mol^{-1}; PDI = 1.69) exhibited a T_g of 113 °C. The bifunctional nature of this monomer enabled the preparation of novel PLA composites with poly(1,5-cyclooctadiene) (poly(COD)) through both ROMP and ROP. Preparation of a statistical copolymer of **XIV** and COD (3:97) by ROMP followed by addition of this copolymer to a TBD catalysed ROP of *rac*-LA (COD/**XIV**:*rac*-LA = 20:80 by weight) resulted in a PLA-based material that displayed improved toughness over an equivalent blended PLA-poly(COD) material and the performance of PLA.[36] Further application of this chemistry involved the synthesis of **XV** and **XVI** that were prepared through the Diels-Alder reaction between the captodative alkene, (6*S*)-3-methylene-6-methyl-1,4-dioxane-2,5-dione, and isoprene or 1,3-cyclohexadiene respectively. In the same study **XIV** was successfully hydrogenated using H_2 and Pd/C yielding **XVII** (Scheme 1.3). ROP of **XV**, **XVI** and **XVII** with TBD resulted in homopolymers with T_g values of 77, 119 and 107 °C respectively, with 119 °C being the highest reported to date among all functional poly(lactide)s.[37]

1.2.2 Functional glycolides from amino acids

While substantial progress has been made in the synthesis and polymerisation of many alkyl functionalisation cyclic diesters, the hydrophobic nature of the resulting poly(ester)s limits their application. Further diversity, including the introduction of functional groups capable of increasing the hydrophilicity of the resultant polymer and enabling post-polymerisation reactions has provided further development of the library of functional cyclic diesters. As a consequence of the large range of terminal functional groups available, a common method to introduce such functional groups stems from the application of amino acid

starting materials (or their protected derivatives). An early example of this was the synthesis of 3-(*S*)-[(benzyloxycarbonyl)methyl]-1,4-dioxane-2,5-dione (BMD, **XVIII**) from *L*-aspartic acid (Figure 1.2). Initial protection of the β-carboxylic acid group of *L*-aspartic acid with benzyl alcohol followed by diazotisation with sodium nitrite ($NaNO_2$) afforded the α-hydroxy acid that after coupling with bromoacetyl bromide with NEt_3, was cyclised to BMD using sodium hydrogen carbonate ($NaHCO_3$). Polymerisations of BMD with $Sn(Oct)_2$ both in bulk at 160 °C and in toluene solution at 100 °C resulted in the isolation of polymers with M_n < 22 000 g.mol^{-1} that displayed broad polydispersities (PDI > 1.4) attributed to a reversible depolymerisation process.[38] Copolymerisation of BMD with *L*-LA (95, 91 and 86 mol% *L*-LA) in bulk at 160 °C yielded copolymers with a T_g of ~ 20 °C with higher compositions of BMD resulting in decreasing melting temperatures (T_m).

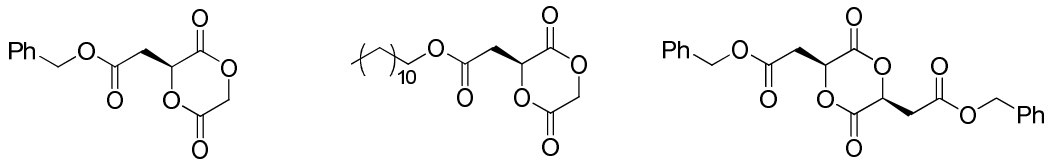

XVIII **XIX** **XX**

Figure 1.2. 3-(*S*)-[(benzyloxycarbonyl)methyl]-1,4-dioxane-2,5-dione (BMD, **XVIII**), 3-(*S*)-[(dodecyloxycarbonyl)methyl]-1,4-dioxane-2,5-dione (DMD, **XIX**) and 3,6-(*S*)-[di(benzyloxycarbonyl)methyl]-1,4-dioxane-2,5-dione (malide, **XX**).

Deprotection *via* catalytic hydrogenolysis of the benzyl groups using both PtO_2 and Pd/C catalysts was successful without any scission of the polymer chain as evidenced by gel permeation chromatography (GPC) analysis. Although the deprotected poly(ester)s did not display any change in T_g values they did show an

enhanced *in vitro* hydrolysis rate compared to PLA both as bulk materials and within PEO-*b*-poly(DLLA-*co*-BMD) nanoparticles.[39-40] Films of deprotected random copolymers of BMD and analogously synthesised 3-(*S*)-[(dodecyloxycarbonyl)methyl]-1,4-dioxane-2,5-dione (DMD, **XIX**) (5 and 10 mol%) (Figure 1.2) with *L*-LA (poly(BMD-*co*-LLA) and poly(DMD-*co*-LLA)) enabled the attachment of cell-binding Arg-Gly-Asp tripeptide (RGD) *via* a dicyclohexylcarbodiimide (DCC) coupling reaction. These RGD-immobilised copolymers exhibited improved cell attachment with an increasing amount of immobilised RGD achieved from increasing the α-malate unit content in the copolymer.[41] Amphiphilic block copolymers of PEO, *L*-LA and a small incorporation of BMD (3 – 9 wt%) were prepared using monomethylether poly(ethylene oxide) (M_n = 5 350 g.mol^{-1}) as a macroinitiator for the statistical bulk copolymerisation of *L*-LA and BMD with $Sn(Oct)_2$ at 160 °C. Deprotection of the BMD units *via* hydrogenolysis in the resulting block copolymer with subsequent self-assembly resulted in nanoparticles with diameters ranging from 30 – 40 nm suitable as an injectable drug carrier. The drug loading capacity of these micelles was studied using papaverine (PAP) introduced in excess during the self-assembly process. PAP incorporation was dramatically increased with increasing carboxylic acid group contents in the block copolymer attributed to increased hydrogen bonding between the carboxylic acid groups and PAP. Hydrolytic degradation of these micelles in pH 7.4 phosphate buffer at 37 °C was three times faster than the respective unfunctionalised particles and was complete within two days.[40]

The difunctional derivative of BMD, 3,6-(*S*)-[di(benzyloxycarbonyl)methyl]-1,4-dioxane-2,5-dione (malide, **XX**), was reported at a similar time (Figure 1.2).[42]

Malide was prepared from the dimerisation of benzyl α-(*L*)-malate, from both *L*-malic acid and *L*-aspartic acid, in the presence of a ZnO catalyst. Polymerisation of malide in bulk at temperatures ranging from 100 to 220 °C with different organotin catalysts proved challenging with only low molecular weight poly(ester)s (M_n < 4 000 g.mol^{-1}) being obtained, attributed to the steric hindrance present from the bulky pendant groups.[42]

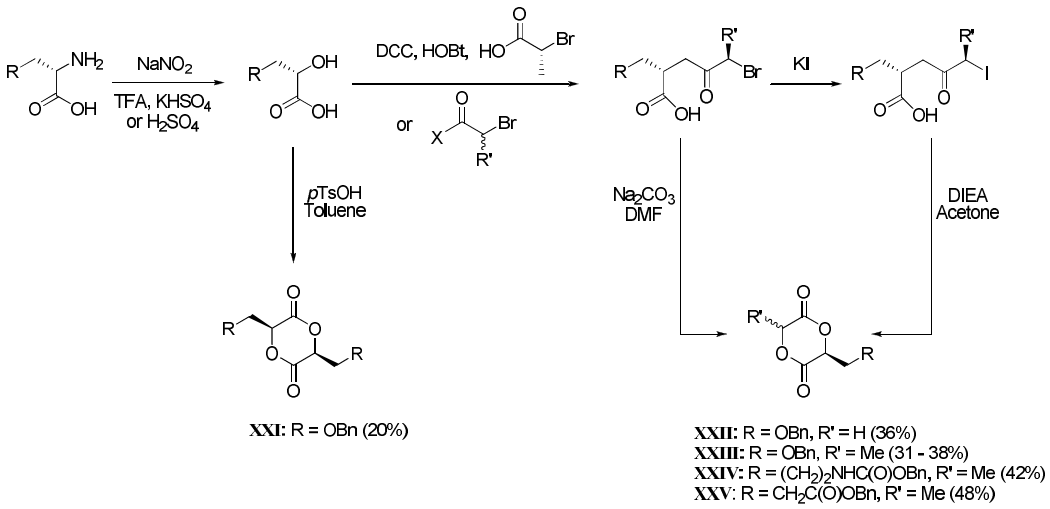

Scheme 1.4. Synthesis of cyclic diester monomers (**XXI** – **XXV**) from amino acids (overall yields from the amino acids in parentheses).

Benzyl protected *L*-serine, *L*-lysine and *L*-glutamic acid have also been applied in the synthesis of functional poly(ester)s *via* ROP. Following diazotisation to the respective α-hydroxy acids, a range of monomers have been synthesised including cyclic dimers (**XXI**) with *p*TsOH and those derived from one functional α-hydroxy acid with either lactic or glycolic acid units from coupling with an α-acyl halide and subsequent cyclisation with either *N*,*N*-diisopropylethylamine (DIEA) or Na_2CO_3 (**XXII** – **XXV**) (Scheme 1.4). High molecular weight polymers were realised *via* the bulk copolymerisation of **XXI** -

XXV with *rac*-LA by $Sn(Oct)_2$ at 140 °C. The copolymers showed T_g values significantly lower than PLA (5 to 27 °C). Subsequent deprotection of the copolymers through either hydrogenation with H_2 and $Pd(OH)_2$ for the *L*-serine and *L*-glutamic acid polymers or *via* HBr(33%)/AcOH for the *L*-lysine polymers to reveal alcohol, carboxylic acid or amine functionality respectively was achieved without poly(ester) degradation.[43] Möller *et al.* recently reported the use of **XXV** (mBzCLA), **III** and **IV** in the preparation of a range of novel degradable nanoparticles. These polymeric micelles consisted of hydrophilic coronas of either PEO or PmCLA with the latter resulting from the deprotection of poly(**XXV**) and hydrophobic cores of either PLA, poly(**III**) or poly(**IV**) all possessing average hydrodynamic diameters below 100 nm and low CMC values between 5×10^{-3} and 100×10^{-3} $g.L^{-1}$.[44]

Hennink *et al.* also reported an additional route into both (*S*)-3-(benzyloxymethyl)-1,4-dioxane-2,5-dione (**XXII**) and (*S*)-6-methyl-3-(benzyloxymethyl)-1,4-dioxane-2,5-dione (**XXIII**). Initial coupling of *O*-benzyl-*L*-serine with either benzyl (*S*)-lactate or benzyl glycolate with subsequent orthogonal deprotection steps and cyclisation with cyanuric chloride yielded **XXII** and **XXIII** while maintaining the chirality of the original hydroxyl acid; this synthesis was also successfully applied to the synthesis of *L*-LA and glycolide (Scheme 1.5).[45]

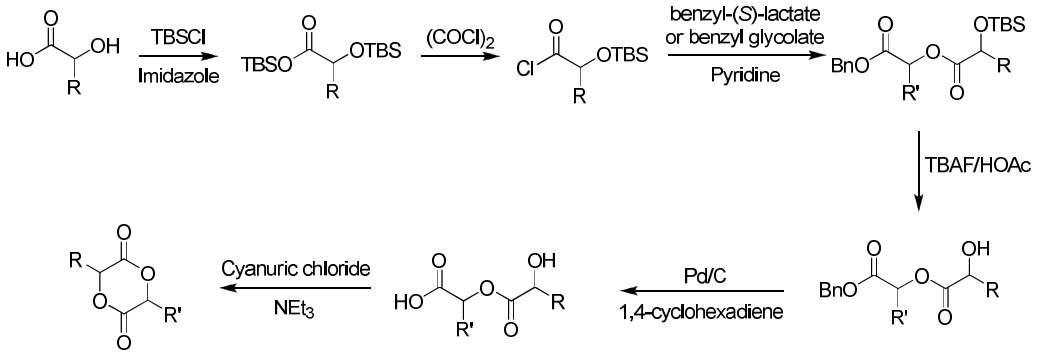

XXII: R = OBn; R' = H (4%)
XXIII: R = OBn; R' = Me (14%)

Scheme 1.5. Synthesis of cyclic diester monomers **XXII** and **XXIII** *via* an alternative method from *O*-benzyl-*L*-serine (overall yields from *O*-benzyl-*L*-serine in parentheses).

Several studies have focused on the *L*-serine-based cyclic diesters, **XXI**, **XXII** and **XXIII** (Scheme 1.4). Homo- and copolymerisations of **XXII** and **XXIII** have been attempted with a range of catalysts including $Sn(Oct)_2$ in bulk at 110 °C and 130 °C and an ethylzinc phenolate ((2-((dimethylamino) methyl)-4,6-dimethylphenoxy)(ethyl)zinc)) in solution at 35 °C. ROP mediated with $Sn(Oct)_2$ led to relatively low molecular weight poly(ester)s, whereas ROP with the ethylzinc phenolate catalyst realised high molecular weight poly(ester)s (M_n = 38 000 g.mol^{-1}; PDI = 1.7) with T_g values ranging from 15 to 30 °C depending on molecular weight. Both random and block copolymers involving **XXII** and **XXIII** were prepared with *L*-LA (25, 50 and 75 mol%) resulting in a decrease in T_g value with increasing *L*-serine monomer incorporation. Bulk copolymerisation of **XXI** with *L*-LA (95 mol%) using $Sn(Oct)_2$ at 140 °C realised poly(ester)s with molecular weights up to 7.7 x 10^4 g.mol^{-1} with a T_g of 56 °C.[46] Deprotection of homo- and copolymers containing **XXI** and **XXII** *via* hydrogenation using H_2 over either Pd/C (10%) or $Pd(OH)_2$ gave the hydroxyl functionalised poly(ester)s with no significant change in T_g and in the absence of any chain scission.[47] The

deprotected poly(**XXII**) was semicrystalline with a T_g of -4 °C and a T_m of 135 °C while the deprotected poly(**XXIII**) was amorphous with a T_g of 30 °C.[46] Hydrolytic degradations of the deprotected poly(**XXIII**) homo- and copolymers were further studied in pH 7.4 phosphate buffer at 37 °C. The deprotected poly(**XXIII**-*co*-LLA) showed both a decrease in T_g and degradation times with increasing *L*-serine monomer content as a result of the increased hydrophilicity of the poly(ester). Complete degradation of poly(**XXIII**) was observed after 1 day with degradation rates decreasing with increasing *L*-LA content to 25, 50 and 75 mol% resulting in complete degradation requiring ~ 1 week, ~ 1 month and ~ 2 months respectively.[46] Modification of a deprotected poly(**XXI**-*co*-LLA) (5 mol% incorporation) has been achieved with succinic anhydride realising pendant carboxylic acid groups observing a small increase in T_g to 61 °C from 57 °C observed with the deprotected poly(**XXI**-*co*-LLA). Attachment of an amine-substituted biotin derivative and a RGD-containing peptide (GGRGDSPGGK) conjugated to a fluorescein derivative (FITC) *via* a dicyclohexylcarbodiimide (DCC) coupling led to poly(ester) films with increased epithelial cell adhesion performance compared to their respective unfunctionalised copolymer films.[47]

Random copolymers (50:50) of **XXII** and ε-caprolactone (εCL), chosen for its slow degradation rate, low T_g and crystallinity, were also prepared with $Sn(Oct)_2$ at 110 °C, 130 °C and 150 °C resulting in amorphous copolymers with T_g values of -16, -29 and -28 °C respectively. Deprotection of the copolymers resulted in a subtle increase in the T_g values to -10, -22 and -19 °C respectively. In an attempt to prepare more crystalline materials, a triblock copolymer was prepared by initiation of **XXII** from a telechelic poly(ε-caprolactone) (PCL) macroinitiator with varying poly(**XXII**) and PCL lengths. The protected triblock copolymers

were amorphous with T_g values ranging from -44 to -10 °C, however, upon deprotection the triblock copolymers showed phase separation and were semicrystalline with the PCL segments crystallising with T_m values ranging from 39 to 46 °C.[48] Such melting temperatures just above body temperature enabled their investigation as materials for stable scaffolds in tissue engineering. The wettability of these poly(ester)s was shown to be tunable through percentage composition of **XXII** in the copolymer with increasing content resulting in an increase in hydrophilicity. The increased hydrophilicity resulted in an improved adherence of human mesenchymal stem cells (hMSCs) onto the polymeric surface with survival of the cells along with the ability to differentiate toward osteogenic lineage on the poly(**XXII**-*b*-εCL) surfaces.[49]

1.2.3 Miscellaneous functional glycolides

Amino acids provide simple and versatile starting materials for the synthesis of functionalised cyclic diesters. However, a more attractive route is the application of inexpensive and readily available starting materials capable of introducing the same versatility as amino acids.

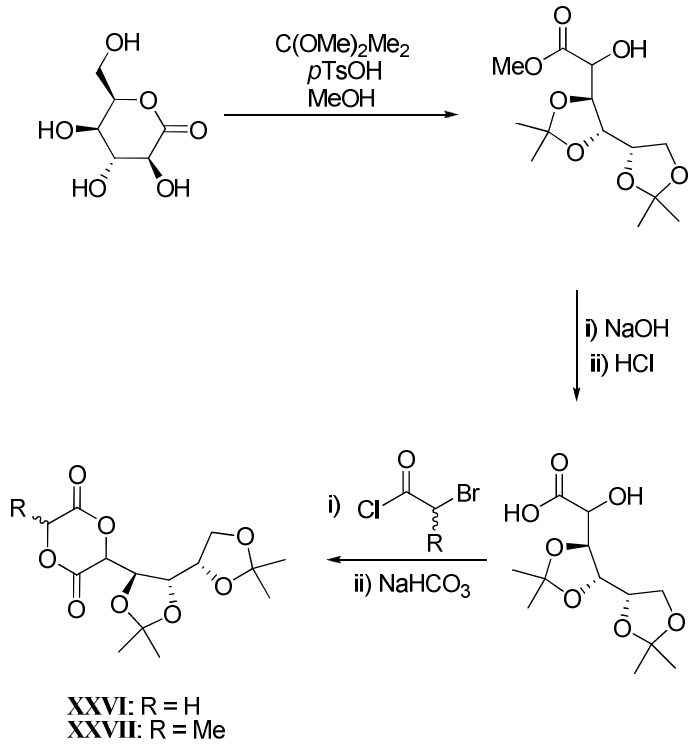

Scheme 1.6. Synthesis of 3-(1,2:3,4-tetraoxobutyl-di-*O*-isopropylidene)-(DIPAGYL, **XXVI**) and 3-methyl-6-(1,2:3,4-tetraoxobutyl-di-*O*-isopropylidene)-1,4-dioxane-2,5-diones (DIPALYL, **XXVII**) from δ-gluconolactone.

δ-Gluconolactone, a naturally occurring lactone derived from glucose, has been applied in the synthesis of 3-(1,2:3,4-tetraoxobutyl-di-*O*-isopropylidene)-(DIPAGYL, **XXVI**) and 3-methyl-6-(1,2:3,4-tetraoxobutyl-di-*O*-isopropylidene)-1,4-dioxane-2,5-diones (DIPALYL, **XXVII**). The synthesis of the monomers was achieved by the initial ring-opening and protection of δ-gluconolactone with dimethoxypropane/methanol to yield an isopropylidene-protected gluconic acid methyl ester. Hydrolysis of the methyl ester with sodium hydroxide resulted in 3,4:5,6-di-*O*-isopropylidenegluconic acid, that after coupling to either bromoacetyl chloride or 2-bromopropanoyl chloride was cyclised with $NaHCO_3$ resulting in DIPAGYL and DIPALYL respectively (Scheme 1.6). Bulk homopolymerisation of DIPAGYL with $Sn(Oct)_2$ at 120 °C resulted in high

molecular weight (M_w = *ca.* 20 000 g.mol^{-1}) poly(DIPAGYL) as a brittle amorphous poly(ester) with a T_g ~ 95 °C. Homopolymerisation of DIPALYL, however, only resulted in oligomers with M_n ~ 2 000 g.mol^{-1}.[50] Deprotection of the isopropylidene groups to reveal hydroxyl groups initially proved difficult with iodine in methanol or acetic acid cleaving only *ca.* 60% of the protecting groups acid,[50] refluxing acetic acid/acetone (50:50) was able to increase this deprotection to 90%, however, only oligomers were isolated.[51] Bulk copolymerisation of DIPAGYL with *rac*-LA (70 mol% of *rac*-LA) resulted in an amorphous copolymer with a T_g of 73 °C while incorporation of DIPALYL (17 mol%) yielded a copolymer with a T_g of 58 °C.[52] Further investigation into poly(DIPAGYL-*co*-LLA)s, with *L*-LA incorporation ranging from 30 to 98 mol%, led to observed T_g values increasing with increasing DIPAGYL content ranging from 61 to 77 °C, with copolymers containing less than 90% *L*-LA being amorphous.[51] Deprotection of poly(DIPAGYL-*co*-LLA) required treatment with trifluoroacetic acid (TFA) to realise copolymers with various degrees of hydroxylation. The resulting T_g values of the polymers increased from 74 to 93 °C with rising number of pendant hydroxyl groups. Deprotection was complete at the 5/6 position, whereas only partial deprotection occurred at the 3/4 position along with partial degradation of the aliphatic poly(ester).[51] Further modification of the poly(ester) backbone was demonstrated with coupling of napthoyl chloride to the exposed hydroxyl group at the 6-position on a deprotected poly(DIPAGYL-*co*-DLLA) with confirmation by GPC showing the binding of the fluorescent label.[53]

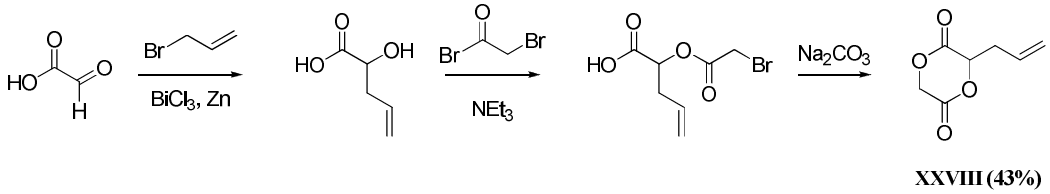

Scheme 1.7. Synthesis of 3-allyl-1,4-dioxane-2,5-dione (**XXVIII**) from glyoxylic acid (overall yield from glycoxylic acid in parentheses).

The synthesis of an allyl functionalised aliphatic poly(ester) has been realised from the synthesis and ROP of 3-allyl-1,4-dioxane-2,5-dione (allylglycolide, **XXVIII**). A simple synthetic procedure from glyoxylic acid monohydrate involving a Barbier-type addition of allyl bromide gave allylglycolic acid, that was then coupled to bromoacetyl bromide in the presence of NEt_3 and subsequently cyclised with Na_2CO_3 (Scheme 1.7). Bulk homo- and copolymerisation of allylglycolide with *L*-LA (25, 50 and 75%) by $Sn(Oct)_2$ at 110 °C resulted in amorphous poly(ester)s with T_g values of 14 °C for poly(allylglycolide) and ranging from 19 to 42 °C for poly(allylglycolide-*co*-LLA) with increasing *L*-LA content. Modification of the allyl groups was investigated by oxidation with *m*-chloroperoxybenzoic acid (*m*CPBA) to reveal synthetically versatile epoxide groups; these amorphous polymers displayed T_g values higher than the parent allyl polymers.[54]

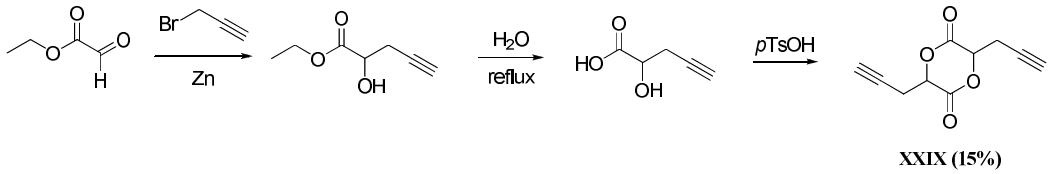

Scheme 1.8. Synthesis of 3,6-di-2-propynyl-1,4-dioxane-2,5-dione (**XXIX**) from ethyl glyoxylate (overall yield from ethyl glyoxylate in parentheses).

In a comparable synthetic procedure, 3,6-di-2-propynyl-1,4-dioxane-2,5-dione (dipropargyl glycolide, **XXIX**) has been synthesised from ethyl glyoxylate. Coupling of propargyl bromide *via* a Reformatsky-type reaction with subsequent hydrolysis provided the propargylglycolic acid that was cyclised with *p*TsOH in refluxing toluene (Scheme 1.8). Bulk homo- and copolymerisations with *rac*-LA were successfully performed with $Sn(Oct)_2$ at 130 °C realising poly(ester)s with varying degree of pendant alkyne functionality. These pendant groups enabled the quantitative attachment of both a poly(ethylene oxide)-550 monomethylether azide (PEO-550 azide) and 1-azidodecane *via* Cu(I)-catalysed Huisgen 1,3-dipolar cycloaddition click reactions ($CuSO_4$/sodium ascorbate) yielding water soluble poly(ester)s without any polymer degradation. Furthermore, grafting mixtures of 10-azido-2,5,8-trioxadecane (mDEG) and 1-azidodecane provided water-soluble polymers that demonstrated lower critical solution temperature (LCST) behavior. Simple and precise adjustment of the cloud point temperature between 25 to 65 °C was possible through variation of the mole fraction of mDEG and 1-azidodecane.[55]

An additional route into water-soluble thermoresponsive PEO-grafted poly(ester)s was realised through the synthesis and ROP of cyclic diesters with pendant oligo(ethylene oxide) chains alleviating the requirement for post-polymerisation functionalisation. This approach involved the coupling of short chain monomethyl ether PEOs (1-4 ethylene oxide repeat units) with 1,6-dibromohexane generating a hexyl bromide capped PEO. Reaction of this with magnesium yielded the respective Grignard reagent that was then reacted with diethyl glycolate that after subsequent catalytic hydrogenation and hydrolysis with H_2, Pt/C and KOH respectively yielded the corresponding α-hydroxyacid

that was then cyclised using *p*TsOH to give diPEO functionalised cyclic diesters with varying pendant oligo(ethylene oxide) chain lengths, **XXX** (Scheme 1.9).[56]

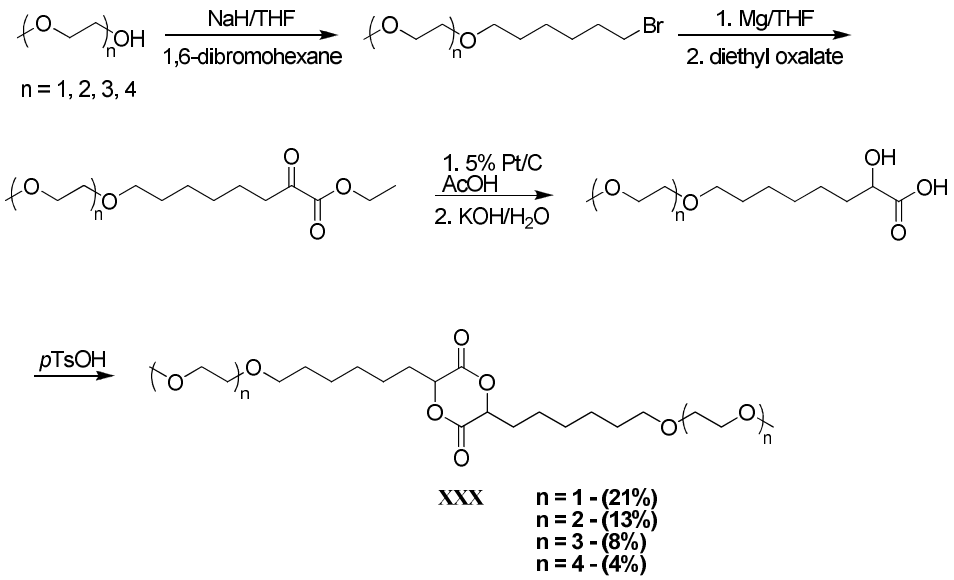

Scheme 1.9. Synthesis of diPEO functionalised cyclic diesters (**XXX**) from short chain monomethylether PEOs (1-4 ethylene oxide repeat units) (overall yield from short chain monomethylether PEOs in parentheses).

Bulk homopolymerisation of **XXX** with $Sn(Oct)_2$ at 130 °C yielded PEO grafted poly(ester)s observing T_g values ~ -25 °C. The grafted polymers with longer monomethylether PEO pendant chains (3 and 4 ethylene oxide repeat units) were water-soluble and exhibited LCSTs with cloud points at ~ 19 and 39 °C respectively.[56]

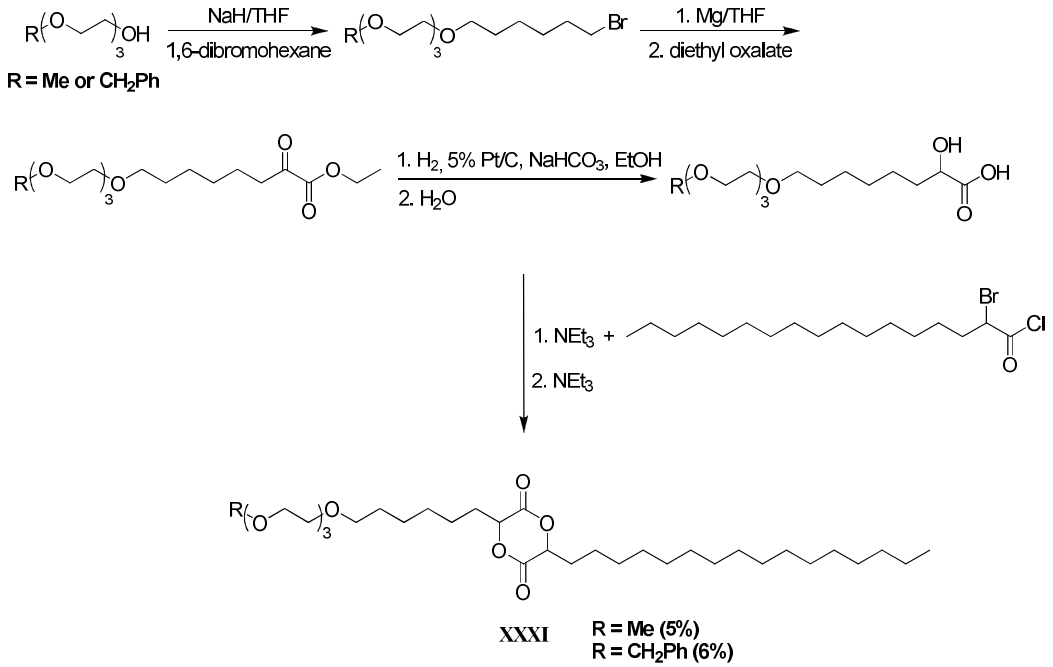

Scheme 1.10. Synthesis of PEO functionalised cyclic diesters (**XXXI**) from either a short chain monomethylether or monobenzylether PEO (3 ethylene oxide repeat units) (overall yield from the short chain monomethylether or monobenzylether PEOs in parentheses).

In a similar synthetic procedure, two cyclic diesters possessing either a monomethylether or monobenzylether triethylene glycol chain and one long alkyl chain have been synthesised. The short PEGs were functionalised with an α-hydroxy acid end group as before with 1,6-dibromohexane. Subsequent coupling to 2-bromooctadecanoyl chloride, synthesised from steric acid, in the presence of NEt_3 followed by cyclisation with the same base resulted in the two novel PEO functionalised cyclic diesters, **XXXI** (Scheme 1.10). Bulk homopolymerisations of **XXXI** with $Sn(Oct)_2$ at 130 °C resulted in amphiphilic polymers with T_m values ~ 17 °C, attributed to side chain crystallisation of the alkyl chains, and T_g values ~ -60 °C, assigned to the PEO side chains rather than the poly(ester) backbone. Deprotection of the monobenzylether PEO end group, *via* catalytic hydrogenation with Pd/C, successfully revealed pendant hydroxyl groups without

any chain scission. Polymeric micelles prepared using **XXXI** with the monomethylether PEO end group were capable of encapsulating azobenzene observing an average hydrodynamic diameter of 60 nm determined from dynamic light scattering along with UV-vis characterisation confirming incorporation of the hydrophobic dye.[57]

1.3 Functional poly(ester)s from O-carboxyanhydride monomers.

Recent work by Bourissou, Martin-Vaca and coworkers has demonstrated that synthesis and ROP of *O*-carboxyanhydrides (OCAs) provides facile access to functional poly(ester) derivatives with structures analogous to those realised through the ROP of cyclic diesters.[58-59] ROP of OCAs mediated by 4-dimethylaminopyridine (DMAP) is entropically driven by loss of CO_2 rather than enthalpically driven through release of ring strain and hence the thermodynamic effects of ring-substitution are lessened. *L*-gluOCA (**XXXII**) was derived from commercially available *O*-benzyl-*L*-glutamic acid. Initial diazotisation to afford the respective α-hydroxy acid, followed by conversion to the dicyclohexylamine salt and subsequent cyclisation with diphosgene in the presence of polystyrene-supported diisopropylethylamine (PS-DIEA) yielded *L*-gluOCA (Scheme 1.11). Homopolymerisation of *L*-gluOCA was achieved with DMAP at 25 °C in dichloromethane within 5 min for a targeted [M]/[I] of 50 while maintaining excellent control over the polymerisation (M_n = 6 300 g.mol^{-1}, PDI = 1.18). Subsequent acetylation of the hydroxyl-end group with acetic anhydride enabled the successful hydrogenolysis with Pd/C of the pendant benzyl groups in the absence of any chain scission of the poly(ester). Block and statistical copolymerisations with *L*-lacOCA, an OCA derived from *L*-lithium lactate *via* a

similar procedure, were also successful.[58] ROP of both *L*-lacOCA and *L*-gluOCA with DMAP at a targeted [M]/[I] of 20 realised full monomer conversion in 5 min while under analogous conditions the ROP of *L*-lactide ([M]/[I] = 10) required 4 days to achieve 93% monomer conversion. Interestingly, *L*-gluOCA proved slightly more reactive than *L*-lacOCA which was a marked contrast to the pronounced deactivation induced by the introduction of pendant functional groups to 1,4-dioxane-2,5-diones.

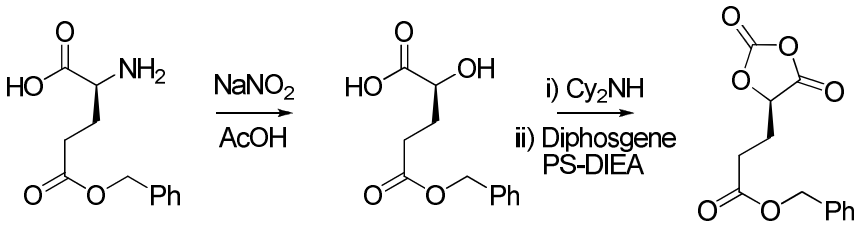

Scheme 1.11. Synthesis of *L*-gluOCA (**XXXII**) from *O*-benzyl-*L*-glutamic acid. (overall yield from *L*-glutamic acid in parentheses).

1.4 Functional poly(ester)s from ε-caprolactone

A large amount of research has also been undertaken in the preparation and ROP of functional ε-caprolactones (εCL). Poly(ε-caprolactone) (PCL) displays attractive characteristics including biocompatibility, biodegradability and miscibility with a wide range of polymers, however extending its possible applications again requires changes to the hydrophilicity and control over biodegradation rate and mechanical properties of the materials. Synthesis of PCLs with pendant functionality enabling drug attachment, tuning of biodegradation rate and improved biocompatibility is most commonly achieved through the ROP of a functional εCL. In turn, these monomers are most

commonly accessed by the ring-expansion *via* a Bayer-Villiger oxidation with *meta*-chloroperoxybenzoic acid (*m*CPBA) of the corresponding cyclohexanone (Scheme 1.12).

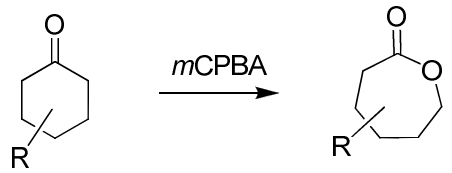

Scheme 1.12. General procedure for the preparation of functional εCL from functional cyclohexanones by ring-expansion *via* a Bayer-Villiger oxidation with *m*CPBA.

1.4.1 εCLs from cyclohexane-1,4-diol and related compounds

An early application of this procedure was in the preparation of 4-(*tert*-butyldimethylsilyloxy)-εCL (SCL, **XXXIII**) from cyclohexane-1,4-diol. Oxidation of one of the alcohol groups to 4-hydroxycyclohexanone with Jones reagent followed by protection of the remaining hydroxyl group with *tert*-butyldimethylsilyl chloride in the presence of imidazole afforded the respective functionalised cyclohexanone. Ring-expansion *via* oxidation with *m*CPBA realised the respective functionalised εCL, SCL (Scheme 1.13). Protection of the hydroxyl group was vital as the functional monomer was shown to rearrange to the more stable five-membered lactone, 3-(2-hydroxyethyl)-γ-butyrolactone. Bulk copolymerisation of SCL with εCL, δ-valerolactone (δVL) and varying proportions of cross-linking agent 2,2-bis(ε-caprolacton-4-yl)propane (BCP) at 140 °C with $Sn(Oct)_2$ resulted in a series of elastomers with varying crosslink density. Deprotection of the *tert*-butyldimethylsilyl group to reveal pendant hydroxyl groups was not successful without inducing polymer degradation.[60]

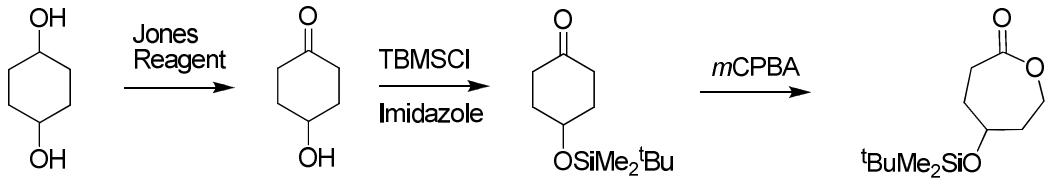

XXXIII (35%)

Scheme 1.13. Synthesis of 4-(*tert*-butyldimethylsilyloxy)-εCl (SCL, **XXXIII**) from cyclohexane-1,4-diol (overall yield from cyclohexane-1,4-diol in parentheses).

The synthesis of 1,4,8-trioxaspiro[4.9]-9-undecanone (TOSUO, **XXXIV**), achieved in a single step from commercially available 1,4-cyclohexanedione monoethylene acetal through treatment with *m*CPBA, was also investigated as a route to hydroxyl functionalised poly(ester)s (Scheme 1.14). Homo- and copolymerisations of TOSUO with εCL were undertaken with aluminium tris(isopropxide) ($Al(O^iPr)_3$) at 25 °C in toluene. Subsequent deprotection of the pendant acetal groups in poly(TOSUO) to hydroxyl groups was successful through treatment with triphenylcarbenium tetrafluoroborate and subsequently sodium borohydride ($NaBH_4$) with no observed chain scission evidenced *via* GPC.[61] Poly(TOSUO) was further used as a macroinitiator for the ROP of εCL and *visa versa* using identical conditions as before in the formation of block copolymers. The T_g values of poly(TOSUO) increase from -35 °C to -14 °C with increase in molecular weight as do T_m values, increasing from 49 to 60 °C. A subtle increase in both T_g and T_m values was observed upon conversion of the acetal groups on a poly(TOSUO-*b*-εCL) to ketone groups and further still upon ketone conversion to hydroxyl groups *via* conditions previously described.[62]

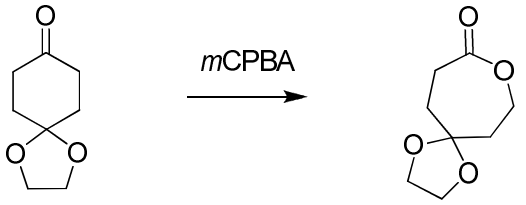

XXXIV (73%)

Scheme 1.14. Synthesis of 1,4,8-trioxaspiro[4.9]-9-undecanone (TOSUO, **XXXIV**) from 1,4-cyclohexanedione monoethylene acetal (overall yield from 1,4-cyclohexanedione monoethylene acetal in parentheses).

Further investigation of poly(γ-ketone-5-εCL) (polyKCL), prepared from the deacetalisation of poly(TOSUO) as described before, observed a dramatic increase in both T_g and T_m to 41 and >140 °C respectively. This substantial improvement in thermal properties of the polymer, particularly in T_m, overcomes the limitation commonly placed on PCL (T_m ~ 59 °C) applications.[63] An additional route into poly(KCL) is through the synthesis and ROP of 2-oxepane-1,5-dione (ODP, **XXXV**) with $Sn(Oct)_2$ in toluene at 90 °C. ODP was synthesised from the ring-expansion of commercially available 1,4-cyclohexanedione, providing a direct route into the formation of poly(ODP), analogous to poly(KCL), without requiring any post-polymerisation modifications (Scheme 1.15).[64] Investigation into aminoxy/ketone reactions for the preparation of intramolecular crosslinking of poly(ODP-*co*-εCL) prepared using $Al(O^iPr)_3$ at 25 °C was investigated by Wooley and van Horne.[65-67] In early attempts, reductive amination of a poly(ODP-*co*-εCL) with primary diamines to afford covalently cross-linked poly(ester) materials was unsuccessful due to side reactions that resulted in chain scission and rearrangement products through intramolecular lactamisation.[67] The application of 1,6-bis(aminooxy)hexane afforded an improved methodology for these transformations such that cross-

linking of poly(ODP-*co*-εCL) catalysed with *p*TsOH was successful resulting in an insoluble cross-linked PCL gel observing melting temperatures lower than their polymer precursors.[66] Applying these conditions, a mixture of *O*-dodecylhydroxylamine, *O*-benzylhydroxylamine and dansyl hydrazine, a sulfonylhydrazine-terminated fluorophore have been grafted to poly(ODP-*co*-εCL) *via* both sequential and single-step processes without degradation of the polymer backbone. Dansyl hydrazine resulted in considerable deviations in the product composition relative to the feed stoichiometries resulting from the reduced nucleophilicity along with the differences in relative stabilities of the sulfonyl hydrazone and ketoxime ether linkages under the acidic conditions. Application of a single-step, one-pot strategy for this grafting was also successful with varying mixtures of the three compounds leading to the simple preparation of multifunctional poly(ester)s.[65]

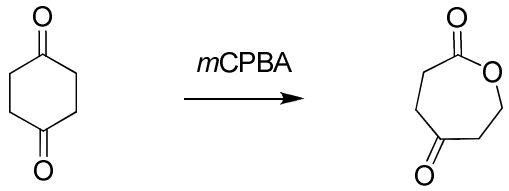

XXXV (45%)

Scheme 1.15. Synthesis of 2-oxepane-1,5-dione (ODP, **XXXV**) from 1,4-cyclohexanedione (overall yield from 1,4-cyclohexanedione in parentheses).

Terpolymerisation of εCL, TOSUO and γ-(triethylsilyloxy)-εCL (TeSCL) (90:5:5) with $Al(O^iPr)_3$ at 25 °C yielded terpolymers with two types of protected hydroxyl groups enabling sequential deprotection. TeSCL synthesised in an analogous manner to SCL (**XXXIII**) (Scheme 1.13), with chlorotriethylsilane

rather than *tert*-butyldimethylsilyl, was selectively deprotected using trifluoroacetic acid (TFA) without polymer degradation leaving hydroxyl groups available for grafting of εCL using $AlEt_3$ at 25 °C. Deprotection of the acetal groups of TOSUO was again achieved using triphenylcarbenium tetrafluoroborate with subsequent treatment with $NaBH_4$ exposing hydroxyl groups applied in a second grafting using *rac*-LA under identical conditions used for the ROP of εCL.[68] In addition to the synthesis of SCL, cyclohexane-1,4-diol has been extensively applied in the preparation of functional εCLs including ACL (**XXXVI**), γ-benzyl-εCL (**XL**), γ-(2,2-bis(phenyldioxymethyl)propionate)-εCL (**XLI**) and γ-(2-bromo-2-methylpropionyl)-εCL (**XLIV**).

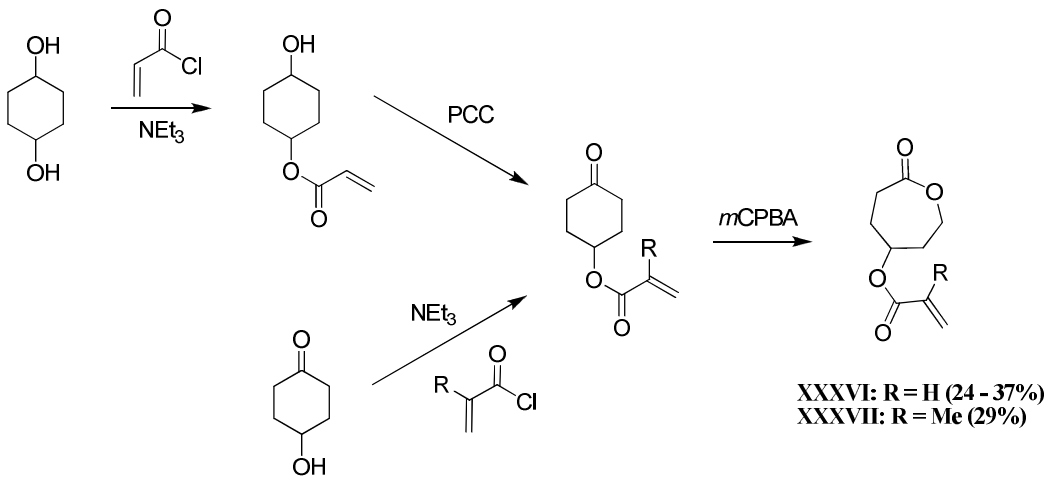

Scheme 1.16. Synthesis of both 4-(acryloyloxy)-εCL (ACL, **XXXVI**) and γ-methacryloyloxy-εCL (MCL, **XXXVII**) from cyclohexane-1,4-diol and 4-hydroxycyclohexanone (overall yields from cyclohexane-1,4-diol and 4-hydroxycyclohexanone in parentheses).

4-(Acryloyloxy)-εCL (ACL, **XXXVI**), a difunctional monomer capable of being selectively polymerised *via* two different living/controlled methods was prepared by coupling of cyclohexane-1,4-diol with acryloyl chloride, subsequent oxidation of the remaining hydroxyl group with pyridinium chlorochromate (PCC) and

ring-expansion with *m*CPBA (Scheme 1.16).[69] ACL has also been prepared *via* a similar procedure directly from 4-hydroxycyclohexanone, avoiding the need for the oxidation of the hydroxyl group (Scheme 1.16).[70] Homopolymerisation of ACL was achieved through both atom transfer radical polymerisation (ATRP) using $NiBr_2(PPh)_3$ at 90 °C and ROP with $Al(O^iPr)_3$ in toluene at 25 °C realising amorphous polymers with T_g values of 95 and -60 °C respectively. Bulk copolymerisation with εCL or *L*-LA by $Sn(Oct)_2$ at 110 °C proceeded with no crosslinking of the pendant acrylate groups despite the high polymerisation temperatures.[69] Poly(ACL-*co*-εCL) prepared using $Al(O^iPr)_3$ in toluene at 25 °C was transformed into unimolecular particles in ultradilute conditions by self-crosslinking using the radical initiator 2,2-azo-bis-isobutyronitrile (AIBN) at 65 °C. The nanoparticles showed an increase in T_g from -62 °C in the copolymer to -45 °C.[71] Poly(ester)s containing ACL have also been applied in cathodic electrografting processes providing a substitute for traditional low molecular weight acrylates with the advantage of chemisorbing chains with predetermined characteristics.[72]

A similar functional monomer, γ-methacryloyloxy-εCL (MCL, **XXXVII**), has been synthesised using methacryloyl chloride in place of acroyl chloride in analogous fashion to ACL (Scheme 1.16). Copolymerisation of MCL with εCL at 25 °C by $Al(O^iPr)_3$ in toluene resulted in poly(ester)s films capable of photo-crosslinking *via* irradiation with UV light (λ = 366 nm) providing a range of novel resins with a variety of structures.[70] The pendant acrylate functionalities in poly(ACL-*co*-εCL) has enabled the Michael-type addition of mercaptoacetic acid and an oligomeric thiol, α-methoxy-ω-mercapto-poly(ethylene oxide) (PEO-SH), in the presence of pyridine. No polymer degradation was observed during the

grafting thus yielding amphiphilic copolymers with steric effects determining the grafting yield.[73] A further approach to realise amphiphilic copoly(ester)s was realised by the incorporation of PEO chains onto a polymerisable monomer alleviating the necessity for post-polymerisation modification. Two macromonomers have been prepared using 1,4-dioxaspiro[4.5]decan-8-ol, in turn prepared from the reduction of 1,4-dioxaspiro[4.5]decan-8-one with lithium aluminium hydride ($LiAlH_4$), as an initiator for the polymerisation of ethylene oxide (10 or 20 repeat units) with potassium alkoxide. The PEO ω-end group was methyl capped with methyl iodide followed by removal of the acetal protecting group using 0.1 M HCl with subsequent oxidation using *m*CPBA to realise two PEO functionalised εCL macromonomers (n = 10 and 20 ethylene oxide repeat units) (**XXXVIII**) (Scheme 1.17). Copolymerisation of **XXXVIII** with εCL was performed with $AlEt_3$ in toluene at 25 °C, realising amphiphilic graft copolymers of M_n ~ 35 000 g.mol^{-1}.[74]

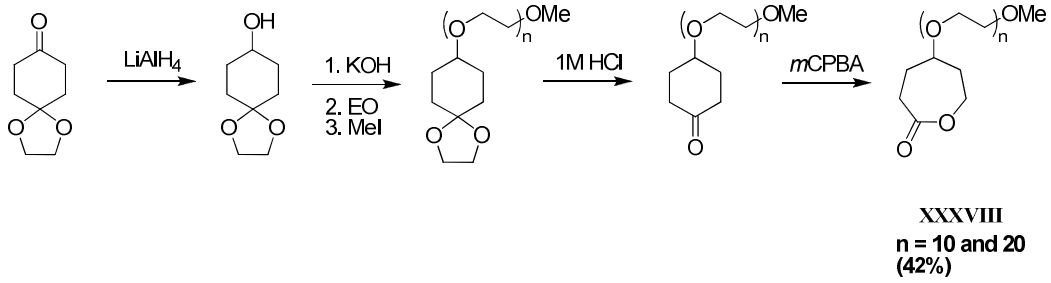

Scheme 1.17. Synthesis of PEO functionalised εCL macromonomers (**XXXVIII**) from 1,4-cyclohexanedione monoethylene acetal (overall yield from 1,4-cyclohexanedione monoethylene acetal in parentheses).

Preparation of hyperbranched poly(ester)s have been realised using 4-(2-hydroxyethyl)-εCL (**XXXIX**), possessing both a polymerisable εCL ring and a initiating primary alcohol. 1,4-dioxaspiro[4.5]decan-8-one was initially reacted

with dimethyl carbethoxymethylphosphonate and subsequently hydrogenated with H_2 and Pd/C to yield 8-(carbethoxymethyl)-1,4-dioxaspiro[4.5]decan-8-one. Reduction of the remaining ethyl ester with $LiAlH_4$ followed by treatment with benzyl bromide and deprotection of the acetyl group with *p*TsOH resulted in 4-(2-(benzyloxy)ethyl)cyclohexanone. Subsequent oxidation with *m*CPBA and hydrogenolysis of the benzyl group with H_2 and Pd/C realised using 4-(2-hydroxyethyl)-εCL (Scheme 1.18). Bulk polymerisation of **XXXIX** carried out with $Sn(Oct)_2$ at 110 °C realised hyperbranched polymers with number-averaged molecular weights between 65 000 and 85 000 $g.mol^{-1}$ and polydispersities of ~3.2. Surface modification of the hydroxyl chain ends was demonstrated with simple quantitative end capping by acetyl chloride affording hyperbranched poly(ester)s with dramatically different solubilities.[75]

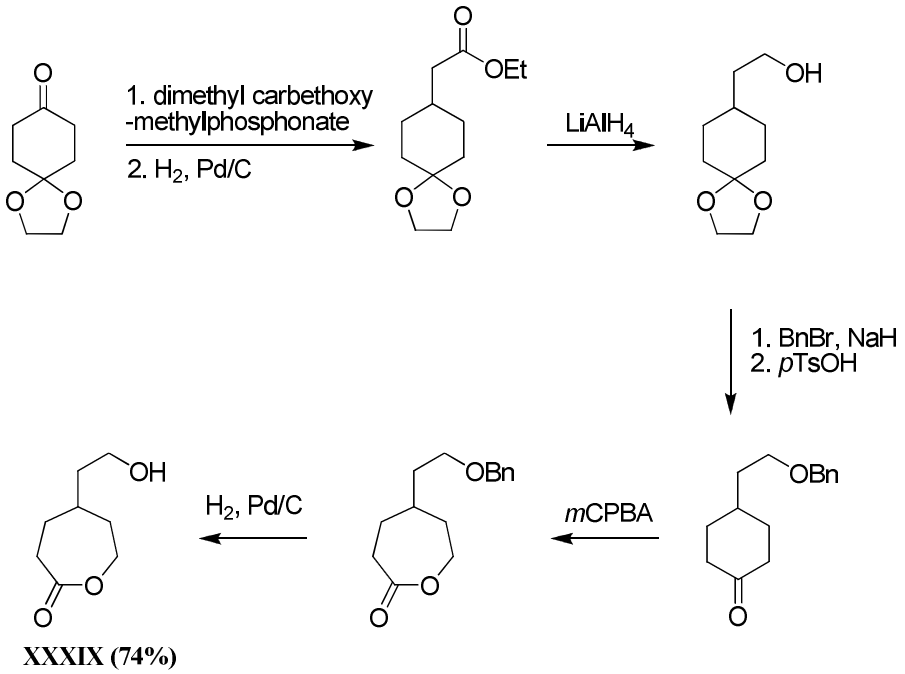

Scheme 1.18. Synthesis of 4-(2-hydroxyethyl)-εCL (**XXXIX**) from 1,4-cyclohexanedione monoethylene acetal (overall yield from 1,4-cyclohexanedione monoethylene acetal in parentheses).

Hedrick *et al.* reported the further use of cyclohexane-1,4-diol in the synthesis of γ-benzyloxy-εCL, **XL**, and γ-(2,2-bis(phenyldioxymethyl)propionate)-εCL, **XLI**, through initial monoprotection of the hydroxyl group with either benzyl bromide and 2,2'-bis(phenyldioxymethyl)propionyl chloride respectively. Oxidation with PCC of the remaining hydroxyl groups followed by ring-expansion yielded the desired functionalised εCLs (Scheme 1.19).[76]

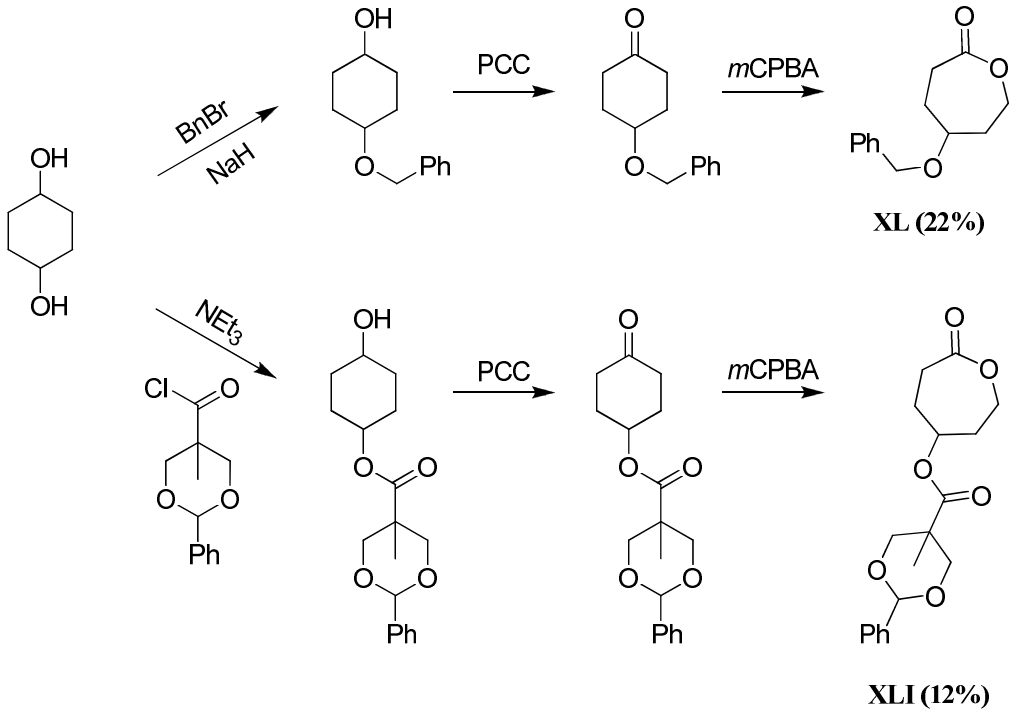

Scheme 1.19. Synthesis of γ-benzyloxy-εCL (**XL**) and γ-(2,2-bis(phenyldioxymethyl)propionate)-εCL (**XLI**) from cyclohexane-1,4-diol (overall yield from cyclohexane-1,4-diol in parentheses).

Hedrick *et al.* also reported a similar oxidation of commercially available ethyl-4-hydroxycyclohexyl carboxylate followed by hydrolysis of the ethyl ester with dilute sulfuric acid yielding 4-ketocyclohexanecarboxylic acid that was coupled to both benzyl bromide and *tert*-butyl alcohol with subsequent ring-expansion

through treatment with *m*CPBA yielding benzyl γ-(εCL)carboxylate and *tert*-butyl-γ-(εCL)carboxylate respectively, **XLII** (Scheme 1.20).[76]

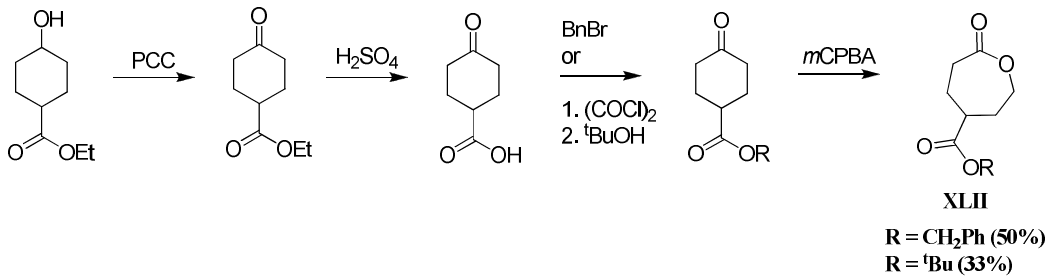

Scheme 1.20. Synthesis of benzyl γ-(εCL)carboxylate and *tert*-butyl-γ-(εCL)carboxylate (**XLII**) from ethyl-4-hydroxycyclohexyl carboxylate (overall yields from ethyl-4-hydroxycyclohexyl carboxylate in parentheses).

4-Trifluoroacetyl-7-oxo-1,4-oxazaperhydropine, **XLIII**, prepared from 1,4-dioxa-7-azaspiro[4, 5]decane was also reported in this study through attachment of a trifluoroacetyl group with trifluoroacetic anhydride (TFAA) with subsequent conversion of the acetal group to a ketone with *p*TsOH, followed by ring-expansion to **XLIII** with *m*CPBA (Scheme 1.21).[76]

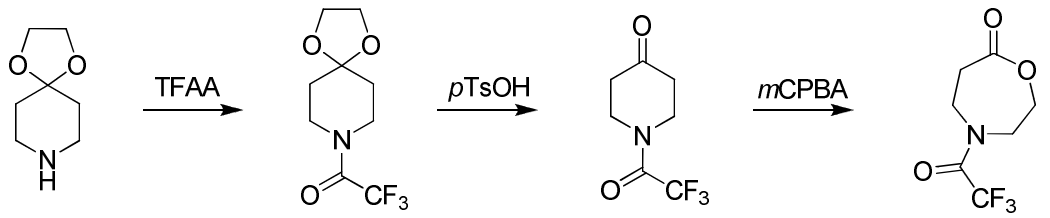

Scheme 1.21. Synthesis of 4-trifluoroacetyl-7-oxo-1,4-oxazaperhydropine (**XLIII**) from 1,4-dioxa-7-azaspiro[4, 5]decane (overall yield from 1,4-dioxa-7-azaspiro[4, 5]decane in parentheses).

Bulk polymerisation of these monomers was accomplished with $Sn(Oct)_2$ at 110 °C in toluene and $Al(O^iPr)_3$ at 25 °C in THF. Deprotection of the benzyl protecting groups in poly(**XL**), poly(**XLI**) and poly(**XLII**) was achieved *via* catalytic hydrogenation with Pd/C resulting in poly(ester)s with low T_g values. The *tert*-butyl groups of poly(**XLII**) (R = ^{t}Bu) were also successfully removed using trifluoromethanesulfonic acid without degradation of the polymer. Deprotection of poly(**XLIII**) to yield amino functionalised poly(ester)s was complicated due to the sensitivity of the polymer backbone under the deprotection conditions; $NaBH_4$ proved to be the most effective reagent for this transformation.[76] Bulk homo- and copolymerisation of the deprotected analogue of (**XLI**) with εCL at 110 °C with $Sn(Oct)_2$ resulted in hyperbranched aliphatic poly(ester)s.[77]

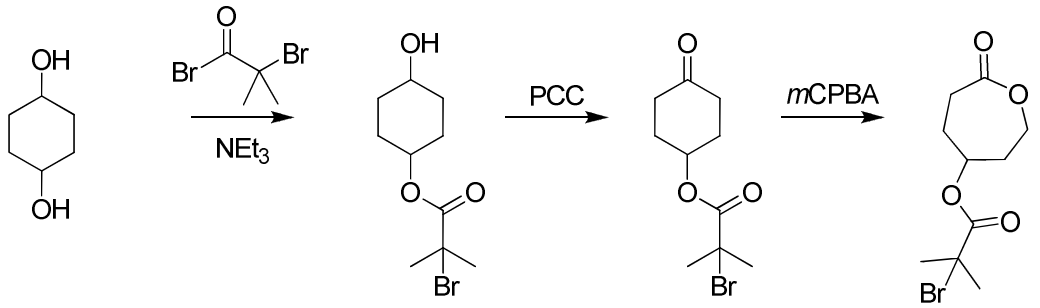

XLIV (17%)

Scheme 1.22. Synthesis of γ-(2-bromo-2-methylpropionyl)-εCL (**XLIV**) from cyclohexane-1,4-diol (overall yield from cyclohexane-1,4-diol in parentheses).

The synthesis and ROP of a functional εCL possessing a pendant atom transfer radical polymerisation (ATRP) initiator has been reported from cyclohexane-1,4-diol. γ-(2-Bromo-2-methylpropionyl)-εCL, **XLIV**, was synthesised *via* an identical procedure to the synthesis of **XLI** using 2-bromoisobutyryl bromide

rather than 2,2'-bis(phenyldioxymethyl)propionyl chloride (Scheme 1.22). Preparation of poly(εCL-*g*-poly(methyl methacrylate)) (poly(εCL-*g*-MMA)) was achieved through combination of ATRP with $NiBr_2(PPh_3)_2$ and ROP with $Al(O^iPr)_3$ of **XLIV**, methyl methacrylate and εCL either sequentially or in one pot. Incorporation of trimethylsilyloxyethyl methacrylate (TMSEMA) with subsequent deprotection leads to an amphiphilic copolymers that were further successfully used as macroinitiators realising amphiphilic graft copolymers.[78] Sequential and concurrent polymerisation of **XLIV** with 2-hydroxyethyl methacrylate (HEMA) has resulted in the isolation of branched copolymers. Both monomers possess initiating centers that are required for polymerisation of the opposite monomer (*via* ROP and ATRP) ensuring copolymerisation and branching. Concurrent bulk polymerisations carried out with $Sn(Oct)_2$ and $NiBr_2(PPh_3)_2$ at 85 – 100 °C resulted in branched copolymers with M_n of 5 000 $g.mol^{-1}$ and PDI of 2.2. Versatility of the macromolecular architecture was realised through introduction of both εCL and MMA in the polymerisation capable of altering the grafting density within the branched copolymer observing a M_n of 15 000 $g.mol^{-1}$ and a broad multimodal molecular weight distribution (PDI = 2.30).[79] Chemical modification of poly(**XLIV**-*co*-εCL), prepared using $Al(O^iPr)_3$ in toluene at 25 °C, was demonstrated through dehydrohalogenation of the tertiary alkyl bromide with 1,5-diazabicyclo[4.3.0]non-5-ene (DBN) resulting in the formation of a methacrylic double bond. Nucleophilic substitution of the bromine atom with pyridine was also successful, yielding the pyridinium salt, however some side reactions were observed limiting the reaction yield. Despite this, quaternisation of the bromide groups along the poly(**XLIV**-*co*-εCL) chain proved quantitative without degradation of the poly(ester) chains.[80]

1.4.2 Halogen-functional εCLs

Halogenated monomers are a useful addition to the family of functional εCLs. γ-Bromo-εCL, **XLV**, has been synthesised from 7-oxabicyclo[2.2.1]heptane. Conversion of 7-oxabicyclo[2.2.1]heptane to *trans*-4-bromocyclohexanol was achieved using aqueous hydrobromic acid with subsequent PCC oxidation of the hydroxyl group and final ring-expansion with *m*CPBA (Scheme 1.23).[81] The synthesis of an analogous monomer with the bromine functionality at the α position of εCL has also been reported *via* two methods, **XLVI**. The first method required the conversion of cyclohexene to 2-bromo-cyclohexanol through treatment with *N*-bromosuccinimide (NBS) followed by oxidation and ring-expansion with PCC and *m*CPBA respectively yielding **XLVI** (Scheme 1.24).[82] The second involved the treatment of cyclohexanone with bromine followed by ring-expansion (Scheme 1.25).[83]

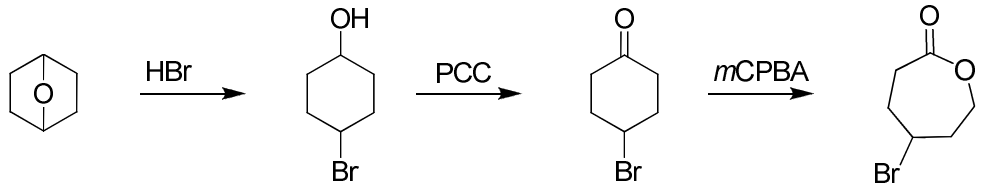

XLV (50%)

Scheme 1.23. Synthesis of γ-bromo-εCL (**XLV**) from 7-oxabicyclo[2.2.1]heptane (overall yield from 7-oxabicyclo[2.2.1]heptane in parentheses).

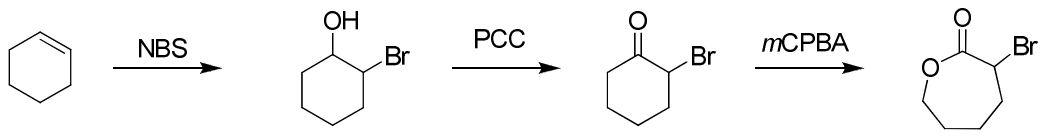

XLVI (28%)

Scheme 1.24. Synthesis of α-bromo-εCL (**XLVI**) from cyclohexene (overall yield from cyclohexene in parentheses).

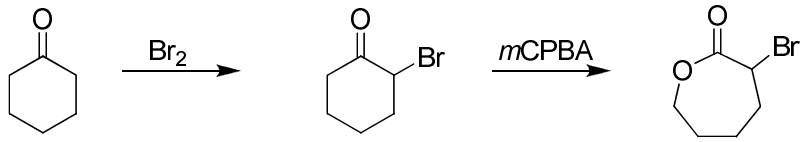

XLVI (37%)

Scheme 1.25. Synthesis of α-bromo-εCL (**XLVI**) from cyclohexanone (overall yield from cyclohexanone in parentheses).

Homo- and copolymerisation of γ-bromo-εCL with εCL by $Al(O^iPr)_3$ at 0 °C in toluene yielded amorphous bromine functionalised poly(ester)s with a T_g value of -17 °C. Increased γ-bromo-εCL content in the random copolymers resulted in an increase in T_g and a corresponding decrease in T_m compared to PCL.[81] The bromine groups of a poly(γ-bromo-εCL-*co*-εCL) were successfully quaternised with pyridine at 50 °C without elimination or degradation of the poly(ester). Quaternised poly(γ-bromo-εCL-*b*-εCL) and poly(γ-bromo-εCL-*co*-εCL) were further investigated as possible non-viral gene delivery systems. Poly(γ-bromo-εCL-*co*-εCL) consisting of γ-bromo-εCL (50 and 80 mol%) were formulated with encapsulation of DNA into nanoparticle systems with sizes between 150 and 400 nm depending on the composition of the polymer. Cytotoxicity and transfection efficiency of these nanoparticles was found to be comparable to polyethylenamine 50 kDa, a polycation commonly used for gene delivery applications.[84] Post-polymerisation modification of structurally analogous poly(α-bromo-εCL-*b*-εCL) prepared with $Sn(OTf)_2$ in toluene at 30 °C with sodium azide (NaN_3) enabled the coupling of alkynyl saccharides resulting in the formation of amphiphilic block glycopolymers. Self-assembly of these diblock glycopolymers resulted in spherical aggregates with average hydrodynamic diameters of 40 – 120 nm capable of binding reversibly with Concanavalin A.[82]

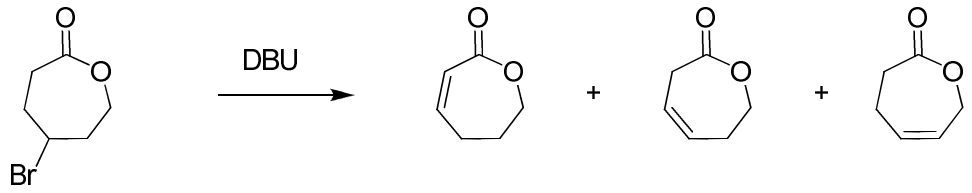

Scheme 1.26. Synthesis of 6,7-dihydro-(5H)-2-oxepinone (DHO, **XLVII**), 6,7-dihydro-(3H)-2-oxepinone (DHO2, **XLVIII**) and 4,7-dihydro-(3H)-2-oxepinone (DHO3, **XLIX**) from **XLV**.

Dehydrohalogenation of γ-bromo-εCL with 1,8-diazabicyclo[5.4.0]undec-7-ene (DBU) resulted in a mixture of three unsaturated εCLs (6,7-dihydro-(5H)-2-oxepinone (DHO, **XLVII**), 6,7-dihydro-(3H)-2-oxepinone (DHO2, **XLVIII**) and 4,7-dihydro-(3H)-2-oxepinone (DHO3, **XLIX**) (Scheme 1.26). Separation of DHO from DHO2 and DHO3 was possible through column chromatography while further separation of DHO2 and DHO3 was not successful. Polymerisations were carried out with $Al(O^iPr)_3$ at 25 °C in toluene on both the mixture of DHO2 and DHO3 mixture and the homopolymerisation of DHO with poly(DHO) realising a semicrystalline unsaturated aliphatic poly(ester) with a T_g of -50 °C and a T_m of 35 °C. Block and random copolymers were also prepared with εCL with increasing DHO content resulting in a decrease in T_m and increase in T_g compared to PCL.[80,85]

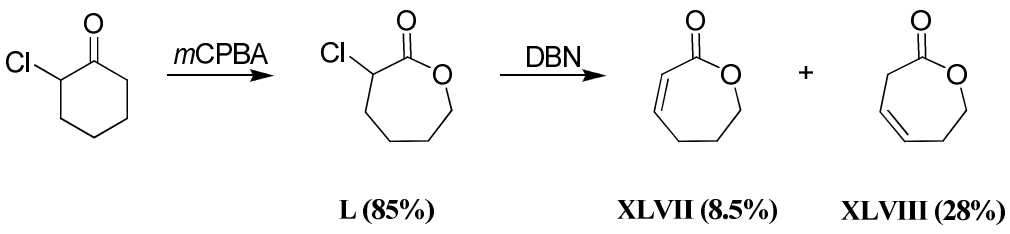

Scheme 1.27. Synthesis of α-chloro-εCL, **L**, 6,7-dihydro-(5H)-2-oxepinone (DHO, **XLVII**) and 6,7-dihydro-(3H)-2-oxepinone (DHO2, **XLVIII**) from 2-chlorocyclohexane (overall yields from 2-chlorocyclohexane in parentheses).

A synthetic route to pure DHO2 was achieved using α-chloro-εCL, **L**, synthesised from the oxidation of commercially available 2-chlorocyclohexanone.[86] Dehydrohalogenation of α-chloro-εCL with 1,5-diazabicyclo[4.3.0]non-5-ene (DBN) resulted in a mixture of DHO and DHO2 that as previously outlined, are easily separated *via* column chromatography. Homopolymerisation of DHO2 and its copolymerisation with εCL were performed with $Al(O^iPr)_3$ either at 0 °C or 25 °C in toluene, with the T_g values of poly(DHO2-*co*-εCL) showing a slight dependence on the composition. Poly(DHO2-*co*-εCL) was successfully epoxidised leading to a more rigid polymer as observed by an increase in T_g. Complete amination of the resulting epoxide functionalised copolymer with *N*,*N*-diethylminoethanethiol with subsequent quaternisation of the free amine groups with benzyl bromide yielded hydrophilic copolymers without any competing side reactions or polymer degradation.[86] DHO2 has also been applied to ring-opening metathesis polymerisation (ROMP). Bulk polymerisation of DHO2 at 60 °C with molybdenum-based Schrock catalyst enabled the preparation of high molecular weight unsaturated poly(ester)s, however, intramolecular side reactions also occurred. Bulk copolymerisation with norbornene, *cis*-cyclooctene, and 1,5-cyclooctadiene resulted in copolymers with tapered diblock structures.[87]

The previously described halogen-functionalised εCL α-chloro-εCL, **L**, has been investigated in the preparation of functional poly(ester)s (Scheme 1.27). Copolymers of α-chloro-εCL and εCL have been prepared using 2,2-dibutyl-2-stanna-1,3-dioxepane (DSDOP) at 20 °C in toluene with decrease in T_m upon increasing α-chloro-εCL content with the poly(ester)s being observed. The polymer became completely amorphous at >50% incorporation with a T_g value of

-56 °C. Triblock polymer formation using poly(α-chloro-εCL-*co*-εCL) as a macroinitiator for the ATRP of MMA initiated from the pendant chlorine groups with CuCl/1,1,4,7,10,10-hexamethyltriethylenetetraamine (HMTETA) resulted in poly((α-chloro-εCL-*co*-εCL)-*g*-MMA) possessing a T_g value of 105 °C and T_m value of 50 °C. 3-butenyl benzoate was also successfully reacted with poly(α-chloro-εCL-*co*-εCL) in DMF at 60 °C with the resulting copolymer exhibiting a T_g value of -50 °C with no degradation of the polymer observed.[88] 3-Buten-1-ol, vinylacetic acid and 2-epoxyhex-5-ene have also been successfully grafted to poly(α-chloro-εCL-*co*-εCL) under these conditions without degradation yielding poly(ester)s with T_g values of -54, -48 and -42 °C respectively.[89] Heterografted copolymers were further realised from poly(α-chloro-εCL-*co*-εCL) synthesised as described above. Two α-MeO-ω-(CO_2-CH_2-CH=CH_2) functionalised PEOs (M_w = 750 and 350 g.mol^{-1}) prepared from reaction of the respective PEO and vinylacetic acid were grafted to poly(α-chloro-εCL-*co*-εCL) at a ~20% efficiency using CuBr/Me_6-Tren in DMF at 60 °C. The residual chlorinated units were advantageously used to initiate the ATRP of styrene using CuBr/Me_6-Tren in DMF at 110 °C realising heterografted PCL without polymer degradation.[90]

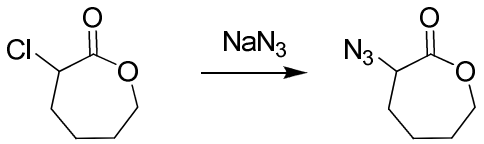

L **LI (85%)**

Scheme 1.28. Synthesis of α-azide-εCL (**LI**) from **L** prepared from 2-chlorocyclohexane (overall yield from 2-chlorocyclohexane in parentheses).

Azide functional copoly(ester)s have also been prepared by both the direct polymerisation of an azide containing monomer (α-azido-εCL, **LI**) and by post-polymerisation modification of both chloro- and bromo-containing PCLs. The synthesis of α-azido-εCL was realised from reaction of NaN_3 with α-chloro-εCL that was also successful in conversion of chloro- and bromo-containing PCLs to azide groups (Scheme 1.28). The T_g values of the poly(α-azido-εCL-*co*-εCL) were dependant on the α-azido-εCL content with values between -60 °C for PCL and -43 °C for poly(α-azido-εCL). Application of Cu(I)-catalysed Huisgen 1,3-dipolar cycloaddition click reactions resulted in the successful grafting of propargyl benzoate, 3-amino-dimethyl-1-propyne and *N*,*N*,*N*-triethylpropargyl ammonium bromide catalysed with DBU and CuI at 35 °C without any polymer degradation. A range of other alkynes have been attached to poly(α-azido-εCL-*co*-εCL) under similar conditions including but-3-yn-1-ol yielding pendant hydroxyl groups with a T_g of -50 °C and propargyl acrylate capable of UV cross-linking with a T_g of -40 °C. Attachment of propargyl bromoisobutyrate yielded a polymer with a T_g of -43 °C enabling the formation of graft copolymers through initiation of the ATRP of styrene with $CuCl/CuCl_2$-HMTETA at 110 °C. Amphiphilic graft copolymers were realised through the grafting of *N*,*N*,*N*-triethylpropargyl ammonium bromide end grouped PEO and an α-methoxy-ω-alkyne-PEO. The one-pot synthesis of functional PCLs was also demonstrated through reaction of poly(α-chloro-εCL-*co*-εCL) and NaN_3 with subsequent addition of 3-(dimethylamino)-1-propyne in the presence of CuI in THF at 35 °C.[91-92]

Direct functionalisation of εCL has also been successful through iodination of the α-position through anionic activation using lithium diisopropyl amide (LDA) at

-78 °C with subsequent quenching of the lithium carbanion with iodine monochloride yielding α-iodo-εCL, **LII** (Scheme 1.29). Homo- and copolymerisations of α-iodo-εCL with εCL were carried out by $Sn(Oct)_2$ at 100 °C in toluene yielding iodine-functionalised PCLs with predictable molecular weights and low polydispersities.[93] Post-polymerisation modification of poly(α-iodo-εCL-*co*-εCL) with NaN_3 followed by hydrogenolysis of the new azide groups using H_2 and Pd/C yielded pendant primary amines along the poly(ester) backbone, however, partial polymer degradation was also observed.[94]

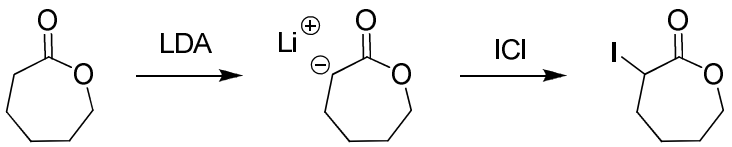

LII (29%)

Scheme 1.29. Synthesis of α-iodo-εCL (**LII**) prepared from εCL (overall yield from εCL in parentheses).

1.4.3 Miscellaneous functional εCLs

Other functional εCLs that have been prepared include 7-allyl-1-oxa-cycloheptan-2-one, **LIII**, from the ring expansion of commercially available 2-allyl cyclohexanone with *m*CPBA. Column chromatography was required to separate **LIII** from its respective epoxide functional monomer, **LIV** (Scheme 1.30).

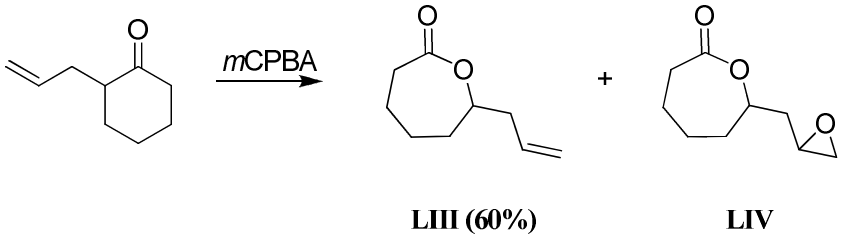

LIII (60%) **LIV**

Scheme 1.30. Synthesis of 7-allyl-1-oxa-cycloheptan-2-one (**LIII**) prepared from 2-allyl cyclohexanone (overall yield from 2-allyl cyclohexanone in parentheses).

Bulk homo- and copolymerisations of **LIII** with εCL were successful with $Sn(Oct)_2$ at 110 °C with the homopolymer being an amorphous poly(ester) with a T_g of -62 °C. The poly(ester) pendant allyl groups were chemical modified *via* epoxidation with *m*CPBA, bromination with bromine and hydrosilylation with phenyl dimethyl silane without any polymer degradation.[95]

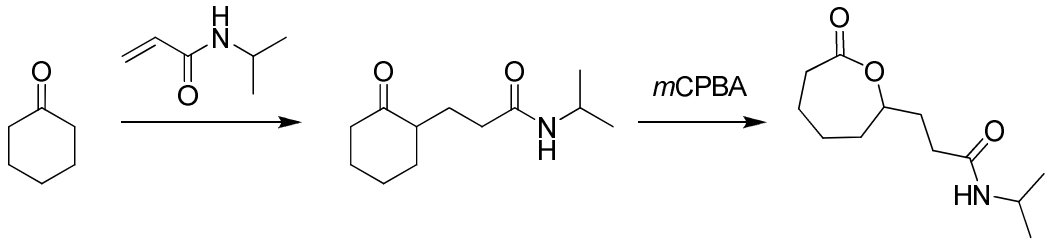

LV (70%)

Scheme 1.31. Synthesis of *N*-isopropyl-2-carbamoylethyl-εCL (**LV**) prepared from cyclohexanone (overall yield from cyclohexanone in parentheses).

Further direct functionalisation at the 6 position of εCL includes the synthesis of *N*-isopropyl-2-carbamoylethyl-εCL (CCL, **LV**) *via* a Michael-type reaction of cyclohexanone and *N*-isopropylacrylamide resulting in the cyclohexanone α-alkylation derivative that was subsequently oxidised to CCL through treatment with *m*CPBA (Scheme 1.31). Bulk copolymerisation of CCL with εCL using $Sn(Oct)_2$ at 130 °C indicated that the CCL content in poly(CCL-*co*-εCL) had a

strong effect on its T_m value increasing from 42 to 53 °C with decreasing CCL content. Increasing the CCL content resulted in an increase in the hydrophilicity of the copolymer leading to a more rapid degradation than observed for PCL in a phosphate buffered solution at pH 7.4 at 37 °C such that after 70 days the weight of poly(CCL-*co*-εCL) had decreased by 25 wt.% while PCL showed no significant change.[96]

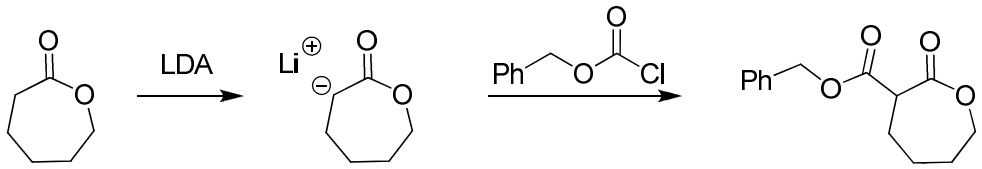

LVI (54%)

Scheme 1.32. Synthesis of α-benzyl carboxylate εCL (**LVI**) prepared from εCL (overall yield from εCL in parentheses).

PCL functionalised with a pendant carboxylic acid group has been realised through the synthesis and ROP of a monomer possessing a benzyl protected carboxylic acid in the α-position of εCL (α-benzyl carboxylate-εCL, **LVI**). α-Benzyl carboxylate-εCL was synthesised *via* a similar method to α-iodo-εCL through electrophilic substitution of the lithium carbanion εCL with benzyl chloroformate (Scheme 1.32). Bulk homo- and copolymerisation of α-benzyl carboxylate εCL and εCL was initiated from a monomethylether PEO (M_n ~ 5 000 g.mol^{-1}) with $Sn(Oct)_2$ at 140 °C resulting in the formation of block copolymers, poly(α-benzyl carboxylate εCL-*b*-PEO) and poly(α-benzyl carboxylate εCL-*co*-εCL-*b*-PEO). Deprotection of the benzyl carboxylate groups through hydrogenolysis with H_2 and Pd/C provided carboxylic acid functionalised block copolymers without any polymer degradation. The

amphiphilic poly(α-benzyl carboxylate εCL-*b*-PEO) self-assembled into polymeric micelles with an average diameter of 62 nm while the self-assembled deprotected poly(α-benzyl carboxylate εCL-*b*-PEO) showed a significantly smaller average diameter of 20 nm.[97]

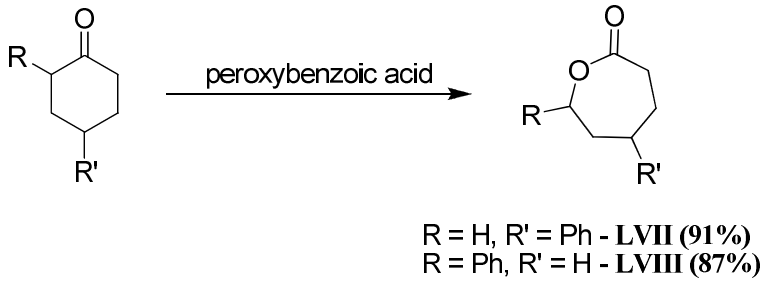

R = H, R' = Ph - **LVII (91%)**
R = Ph, R' = H - **LVIII (87%)**

Scheme 1.33. Synthesis of 3-phenyl-εCL (**LVII**) and 5-phenyl-εCL (**LVIII**) prepared from 2- and 4-phenylcyclohexanone respectively (overall yields from 2- and 4-phenylcyclohexanone in parentheses).

The effect of the substitution position of functionality on the εCL ring on the resulting poly(ester)s physical properties was demonstrated *via* synthesis of two phenyl substituted εCLs from the oxidation of 2-phenylcyclohexanone and 4-phenylcyclohexanone with peroxybenzoic acid yielding 3-phenyl- (**LVII**) and 5-phenyl-εCLs (**LVIII**) respectively (Scheme 1.33). Polymerisations of these monomers with $SnCl_2$ or $Sn(Oct)_2$ in the melt at 150 °C and $Al(O^iPr)_3$ or cyclopentadienyl sodium (CpNa) from 0 to 70 °C in toluene yielded poly(5-phenyl-εCLs) as an amorphous material with a T_g of 18 °C and poly(3-phenyl-εCLs) with significantly different physical properties, notably a T_g of -47 °C and a T_m of 30 °C.[98]

A method of improving the physical properties of both homo- and copolymers is through crosslinking, often achieved as a post-polymerisation modification. 2,2-bis(ε-caprolactone-4-yl)propane (BCP, **LIX**) and bis(ε-caprolactone-4-yl) (BCY,

LX) possess two ajoining εCL cyclic esters that enable crosslinking to occur throughout the polymerisation process. Synthesis of BCP and BCY initially involved the oxidation of 2,2-bis(4-hydroxycyclohexyl)propane with CrO_3 and dicyclohexyl-4,4'-diol with Jones reagent respectively. Ring-expansion of the resulting diketones with *m*CPBA yielded the tetrafunctional BCP and BCY monomers (Schemes 1.34 and 1.35).[99] Bulk copolymerisation of BCP and BCY with 1,5-dioxepan-2-one (DXO, **LXI**) by $Sn(Oct)_2$ at a range of temperatures prepared perfectly random crosslinked elastic films with T_g values increasing from -39 °C for pure poly(DXO) to -35 °C for BCP crosslinked films and -21 °C for BCY crosslinked films. DXO was prepared from oxidation of tetrahydro-4H-pyran-4-one that was synthesised *via* the Friedel-Craft acylation of ethylene with chloroproponylchloride followed by ring closure with H_3PO_4 and NaH_2PO_4 (Scheme 1.36).[99]

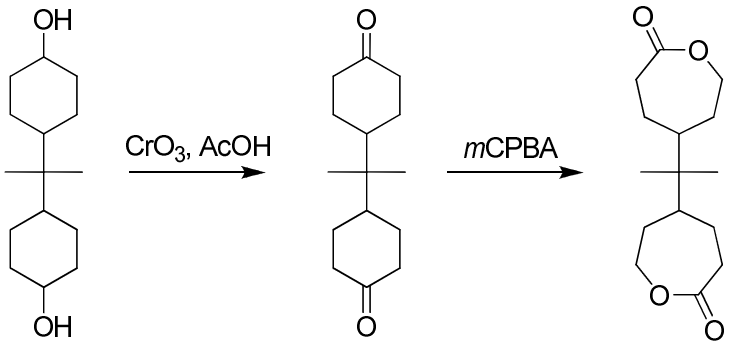

LIX (57%)

Scheme 1.34. Synthesis of 2,2-bis(ε-caprolactone-4-yl)propane (**LIX**) prepared from 2,2-bis(4-hydroxycyclohexyl)propane (overall yield from 2,2-bis(4-hydroxycyclohexyl)propane in parentheses).

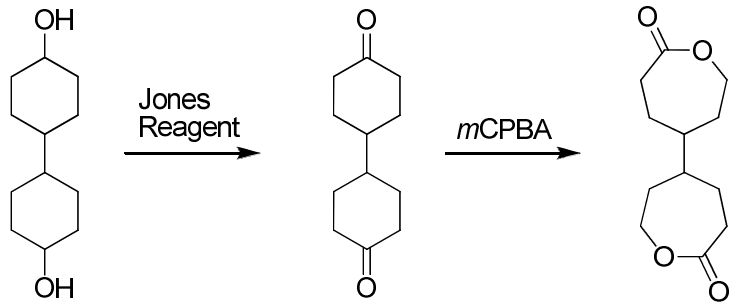

LX (79%)

Scheme 1.35. Synthesis of bis(ε-caprolactone-4-yl) (**LX**) prepared from dicyclohexyl-4,4'-diol (overall yield from dicyclohexyl-4,4'-diol in parentheses).

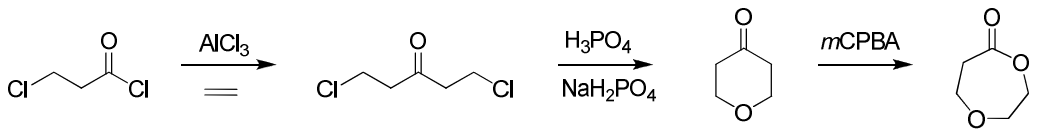

LXI (48%)

Scheme 1.36. Synthesis of 1,5-dioxepan-2-one (DXO, **LXI**) prepared from chloropropionylchloride (overall yield from chloropropionylchloride in parentheses).

(-)-Menthide, **LXII**, prepared from the simple *m*CPBA oxidation of the natural product (-)-menthone is one of the few examples of functional εCLs derived from renewable resources (Scheme 1.37).[100] Homopolymerisation of (-)-menthide was carried out with a discrete zinc alkoxide catalyst at 25 °C in toluene under an inert atmosphere yielding an amorphous high molecular weight polymer with a T_g of -25 °C. Further work has focused on the synthesis of telechelic ABA triblock copolymers with *rac*-LA to alter the mechanical properties of PLA resulting in a T_g value of -22 °C corresponding to the poly((-)-menthide) block and T_g values for the PLA block varying from 20 to 51 °C depending on the PLA molecular weight.[100-102] Hydrolytic degradation of poly((-)-menthide) in a phosphate

buffered solution at pH 7.4 at 37 °C revealed a slower degradation than PLA with little mass loss even after 48 weeks.[103]

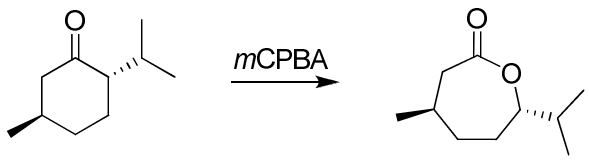

LXII (70%)

Scheme 1.37. Synthesis of (-)-menthide (**LXII**) prepared from (-)-menthone. (overall yield from (-)-menthone in parentheses).

(+)-Dihydrocarvone has also been applied in the synthesis of 7-methyl-4-(2-methyloxiran-2-yl)oxepan-2-one, **LXIII** (Scheme 1.38).[104] Oxidation of the natural product with *m*CPBA resulted in both ring-expansion of the 6-membered ring and epoxidation of the pendant propenyl group resulting in an epoxide-functional εCL, **LXIII**. Homopolymerisation of **LXIII** was carried out with $ZnEt_2$ and $Sn(Oct)_2$ at temperatures ranging from 20 to 120 °C resulting in both lactone and epoxide ring-opening to yield low molecular weight branched oligomers. Copolymerisation with εCL and δ-valerolactone (δVL) catalysed by $ZnEt_2$ or $Sn(Oct)_2$ at 60 and 120 °C also resulted in branched polymers with increasing T_g and decreasing T_m with increasing **LXIII** content. Copolymers containing less than 10% incorporation of **LXIII** exhibited excellent shape memory behavior even after repeated bending.[104]

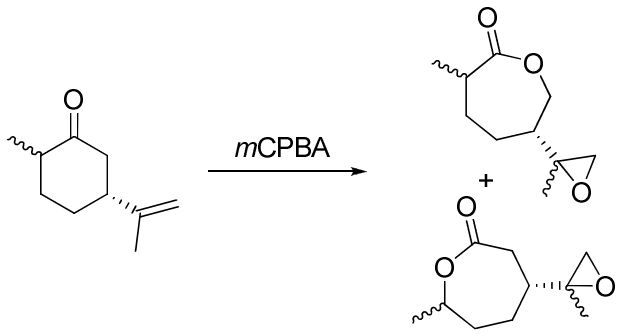

LXIII (25%)

Scheme 1.38. Synthesis of 7-methyl-4-(2-methyloxiran-2-yl)oxepan-2-one (**LXIII**) prepared from (+)-dihydrocarvone (overall yield from (+)-dihydrocarvone in parentheses).

The ε-lactone, 2,3,4,5-tetra-*O*-methyl-*D*-glucono-1,6-lactone, **LXIV**, has also been synthesised and studied as a monomer in ROP. Synthesis of **LXIV** has been reported by three routes. In the first reported synthesis, protection of the primary alcohol group of methyl α-*D*-glucopyranoside with trityl chloride was followed by the subsequent protection of the secondary alcohol groups with methyl iodide. Removal of the 6-*O*-triphenylmethyl group by acidic hydrolysis was then followed by protection with benzyl bromide. Further acid hydrolysis with acetic anhydride and subsequent oxidation with acetic anhydride/dimethyl sulfoxide gave 6-*O*-benzyl-2,3,4-tri-*O*-methyl-*D*-glucono-1,5-lactone. Ring-opening of this δ-lactone with methyl iodide and potassium hydroxide, removal of the benzyl group and lactonisation with dicyclohexylcarbodiimide (DCC) and dimethylaminopyridine (DMAP) yielded **LXIV** (Scheme 1.39).[105]

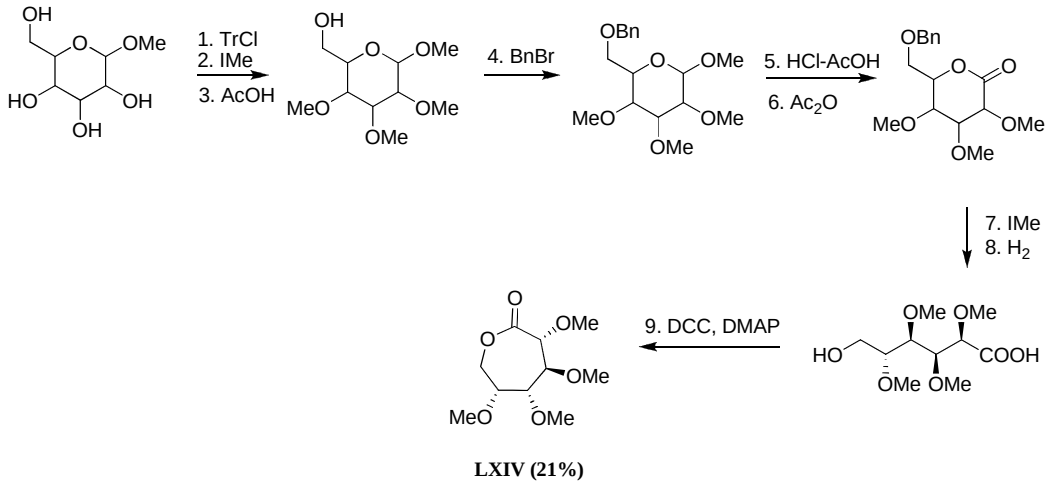

Scheme 1.39. Synthesis of 2,3,4,5-tetra-*O*-methyl-*D*-glucono-1,6-lactone (**LXIV**) prepared from methyl α-*D*-glucopyranoside (overall yield from methyl α-*D*-glucopyranoside in parentheses).

Alternatively this monomer has been prepared from *D*-glucose diethylmercaptal by first protecting the primary and secondary alcohols with trityl chloride and methyl iodide respectively before removal of the diethylmercaptal protecting group and oxidation of the resulting aldehyde with $Hg(ClO_4)_2$ and pyridinium dichromate (PDC) respectively. The triphenylmethyl protected alcohols of the resultant 6-*O*-triphenylmethyl-2,3,4,5-tetra-*O*-methyl-*D*-gluconic acid were liberated in acidic conditions before lactonisation with DCC and DMAP yielded **LXIV** (Scheme 1.40).[105]

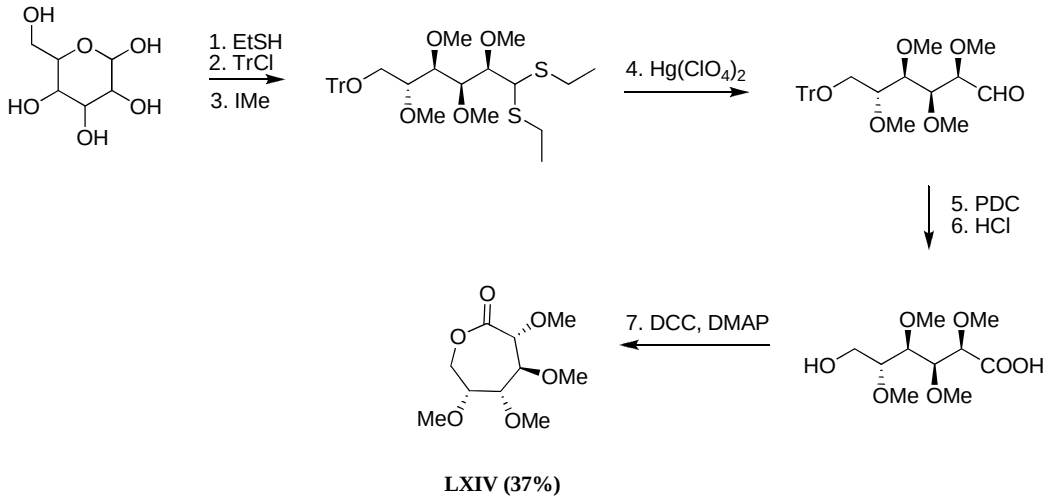

Scheme 1.40. Synthesis of 2,3,4,5-tetra-*O*-methyl-*D*-glucono-1,6-lactone (**LXIV**) prepared from *D*-glucose (overall yield from methyl *D*-glucose in parentheses).

The final reported synthetic route for this monomer applies the commercially available reduced sugar *D*-dulcitol as its starting material. Initial protection of the primary and secondary alcohols with trityl chloride and methyl iodide respectively is followed by removal of the trityl groups under acidic conditions with subsequent cyclisation by oxidation using Shvo's catalyst (Scheme 1.41).[106]

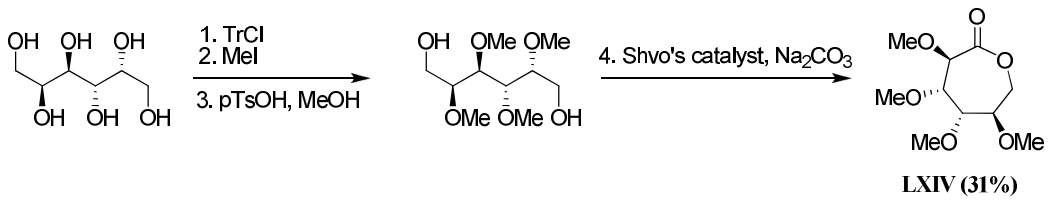

Scheme 1.41. Synthesis of 2,3,4,5-tetra-*O*-methyl-*D*-glucono-1,6-lactone (**LXIV**) prepared from *D*-dulcitol (overall yield from *D*-dulcitol in parentheses).

LXIV was initially copolymerised with *L*-LA (~ 16 mol%) in bulk using $Sn(Oct)_2$ at 110 °C. The resultant poly(**LXIV**-*co*-LLA) contained differing amounts of carbohydrate monomer with the highest incorporation being 2.2% of **LXIV** (M_n

= 14 900 g.mol^{-1} and PDI = 1.2).[107] Further screening of catalysts for the ROP of **LXIV** resulted in the discovery that Y(O^{i}Pr)$_3$ was able to efficiently catalyse the ROP at 25 °C in toluene in a living manner to obtain amorphous poly(**LXIV**) displaying a T_g of 52 °C. Block copolymerisations with εCL were also successful. Surface plasmon resonance (SPR) sensograms demonstrated that both the homo- and block copolymers exhibit excellent resistance to fibrinogen and lysozyme and therefore could be extended to use in biomaterials applications.[106]

1.5 Functional poly(ester)s from δ-valerolactones

Unlike cyclic diesters and εCLs, there has been relatively little research into the synthesis and ROP of functional δ-valerolactones (δVL). This is largely a consequence of both the significantly less versatile syntheses and the lowered reactivity towards ROP of this family of monomers with several commonly applied catalysts. As with the other aliphatic poly(ester)s, polymers prepared from δVL have attractive physical properties, however, in common with other poly(ester)s their applications are restricted due to hydrophobicity, lack of tailorability of degradation times and mechanical properties.

A general synthetic method for the functionalisation of δVLs relies on the increased acidity of the α-methylene group on δVL such that lithiation with LDA and subsequent quenching with an alkyl halide in hexamethylphosphoramide (HMPA) yields the desired functional δVL with general structure shown in Scheme 1.42.

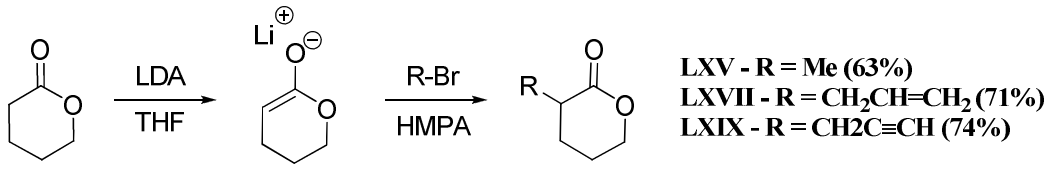

Scheme 1.42. General synthetic procedure for the preparation of functional δVL monomers **LXV, LXVII** and **LXIX** from δVL (overall yields from δVL in parentheses).

An early example of this functionalisation methodology was the synthesis of α-methyl-δVL, **LXV**, in which the excipient enolate was quenched with methyl iodide at -40 °C (Scheme 1.42). Homopolymerisation of this monomer has only been achieved in the bulk under argon with a lipase catalyst derived from *Candida antarctica* (lipase CA) at 35 °C obtaining poly(α-methyl-δVL) exhibiting a M_n of 8 500 g.mol^{-1} and PDI of 2.1.[108]

A similar monomer has been synthesised *via* an alternative procedure between acrolein with isobutyraldehyde in the presence of sodium hydroxide that after subsequent acidification yields γ,γ-dimethyl-δVL (DMVL, **LXVI**) (Scheme 1.43). Homopolymerisation of DMVL was carried out with *n*-butyllithium and range of other catalysts resulting in poly(DMVL) as a crystalline polymer with a T_m of 110 – 120 °C, approximately 70 °C higher than that of poly(δVL) (PVL) (55 – 65 °C).[109]

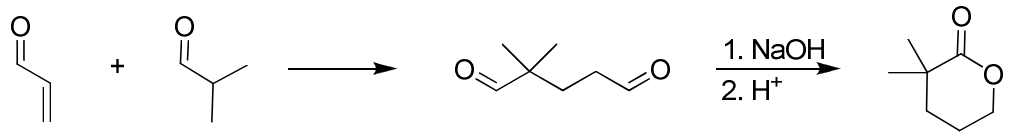

LXVI (63%)

Scheme 1.43. Synthesis of γ,γ-dimethyl-δVL (DMVL, **LXVI**) prepared from acrolein (overall yield from acrolein in parentheses).

Although alkyl functional δVLs provide a variation in physical properties to PVL, they are not able to introduce hydrophilicity and/or participate in post-polymerisation reactions. In an attempt to introduce these desired properties α-allyl-δVL, **LXVII**, was synthesised *via* the general method described above using allyl bromide (Scheme 1.42). Polymerisations performed with $Sn(OTf)_2$ at 25 °C in THF yielded amorphous poly(allyl-δVL) whereas the respective poly(allyl-δVL-*co*-εCL) and poly(allyl-δVL-*co*-δVL) copolymers showed decreasing T_m values correlating with increased allyl-δVL incorporation with no melting transitions being observed at >25% and >15% for poly(allyl-δVL-*co*-εCL) and poly(allyl-δVL-*co*-δVL) respectively. Post-polymerisation modification of poly(allyl-δVL-*co*-εCL) through dihydroxylation with osmium tetraoxide (OsO_4) resulted in complete conversion of the pendant allyl groups to hydroxyalkyl groups without polymer degradation.[110]

Applying allyl-δVL as a starting material, the synthesis of α-cyclopentene-δVL, **LXVIII**, was achieved through allylation with allyl bromide and LDA as before yielding α,α-diallyl-δVL with subsequent ring-closing metathesis catalysed by a ruthenium benzylidene complex (Scheme 1.44).[111] Copolymerisations of α-cyclopentene-δVL and εCL were successful with $Sn(OTf)_2$ at 25 °C in THF while the homopolymerisation of α-cyclopentene-δVL proved ineffective. The pendant olefins of poly(α-cyclopentene-δVL-*co*-εCL) were completely dihydroxylated with OsO_4 yielding hydroxyl functionalised copolymers without poly(ester) degradation. DCC coupling of succinic acid ester derivatives of various monomethylether PEOs to the pendant hydroxyl groups realised amphiphilic PEO-grafted aliphatic poly(ester)s.[111]

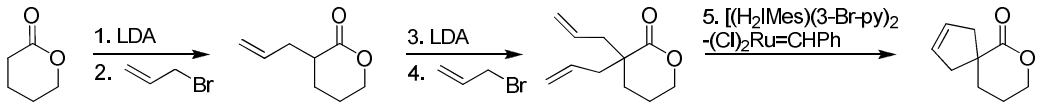

LXVIII (57%)

Scheme 1.44. Synthesis of α-cyclopentene-δVL (**LXVIII**) prepared from δVL (overall yield from δVL in parentheses).

An alkyne derivative of α-allyl-δVL has also been synthesised in analogous fashion using propargyl bromide to yield α-propargyl-δVL, **LXIX** (Scheme 1.42). Bulk homopolymerisation of α-propargyl-δVL was successfully catalysed with $Sn(OTf)_2$ at 25 °C while control over pendant alkyne density was achieved *via* copolymerisation with εCL. Alkyne groups along the poly(ester) backbone enabled grafting of different functional azides *via* Cu(I)-catalysed Huisgen 1,3-dipolar cycloaddition click reactions. An α,ω-PEO-1100-monomethylether azide, prepared from the mesylation of PEO-1100 monomethyl ether followed by nucleophilic substitution with NaN_3, was grafted to the alkyne functionalised poly(ester)s with copper(II) sulphate and sodium ascorbate at 80 °C in water without degradation of the poly(ester). The resulting grafted amphiphilic copolymers were crystalline with a T_m of 32 °C and were further shown to be biocompatible. Along with a PEO chain, an azide-terminated oligopeptide was also grafted onto the alkyne functional copolymers under similar conditions with slightly elevated temperatures (100 °C) without polymer degradation enabling "biotailoring" of aliphatic poly(ester)s.[112] Further work on poly(α-propargyl-δVL-*co*-εCL) involved grafting an azide-functionalised camptothecin using bromotris(triphenylphosphine)copper(I) *N*,*N*-diisopropylethylamine in dichloromethane (resulting from the poor aqueous solubility of the functionalised camptothecin). Although hydrophobic polymer-drug conjugates can be used to

prepare microparticles, further grafting of α,ω-PEO-1100-monomethylether azide resulted in a highly water soluble poly(ester)-camptothecin conjugate.[113] Poly(α-propargyl-δVL) and terpolymers with ε-CL and *L*-LA have been subjected to further "click" reactions with the grafting of phosphorylcholine (PC) moieties that possess excellent biocompatibilities. An azide functionalised PC (PC-azide) was successfully grafted onto poly(α-propargyl-δVL) with copper(I) sulphate and sodium ascorbate under constant microwave radiation. Reaction of PC azide with the terpolymers required CuBr-*N*,*N*,*N*',*N*',*N*-Pentamethyldiethylenetriamine (PMDETA) to achieve complete grafting of the PC-azide. The resulting poly(ester)s demonstrated good cell viability suggesting their usefulness for integration into medical devices, biomaterials, and drug delivery vehicles.[114]

Copolymerisation of δVL, α-allyl-δVL, α-propargyl-δVL and ODP using $Sn(Oct)_2$ at 105 °C in THF realised multifunctional poly(ester) particles that were subjected to a variety of chemical transformations as result of the diverse range of pendant functionalities. The pendant allyl groups were converted to epoxides with *m*CPBA and subsequently added dropwise to a refluxing solution of 2,2'-(ethylenedioxy)bis(ethylamine) resulting in crosslinked amorphous nanoparticles. The nanoscopic size dimensions of the poly(ester) nanoparticles were dependant on the amount of diamine crosslinker present during the crosslinking process and could be further tailored *via* changing the epoxide density in the nanoparticle. Utilisation of the intergrated functionalities in the nanoparticle was demonstrated through reductive amination reaction of the keto groups introduced from ODP with *N*-boc-ethylenediamine.[115] Conjugation of dye-labelled NHS ester Alexa Fluor® 594 to the resulting free amine groups enabled the monitoring of uptake and transport of these nanoparticles. Partial oxidation of the allyl groups before

nanoparticle formation enabled preparation of allyl functionalised poly(ester) nanoparticles *via* a novel one-pot reaction with no significant change in dimensions. Applying 'thiol-ene' chemistry, a thiol functionalised dendritic molecular transporter and targeting peptides for radiated and non-radiated tumor vasculature, HVGGSSV and a novel CRGD, with incorporated cysteine residues were successfully attached to the allyl functionalised nanoparticles. Combination of this with reductive amination of the keto functionality enabled the preparation of conjugate materials including nanoparticle-peptide-dye (NP-P-dye/NP-P), nanoparticle-dendritic-molecular transporter-dye (NP-MT-dye) and nanoparticle-peptide-molecular transporter-dye (NP-P-MT-dye).[116]

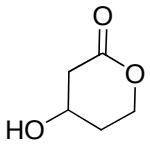

LXX

Figure 1.3. Structure of commercially available mevalonolactone (**LXX**).

Mevalonolactone (ML, **LXX**) is a commercially available functional derivative of δVL possessing a pendant hydroxyl group (Figure 1.3). ML has been used as a bifunctional comonomer in the bulk copolymerisation with *L*-LA (90 mol%) with $Sn(Oct)_2$ at 130 °C and tin distannoxane at 110 °C resulting in branched PLAs with T_g and T_m values lower than those of linear PLA.[117]

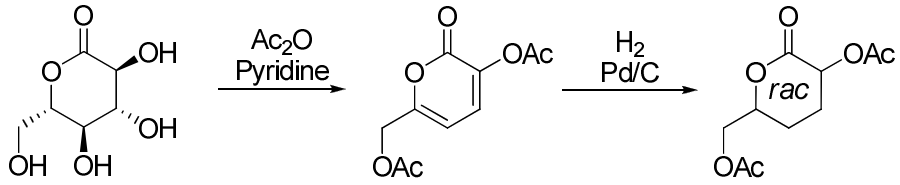

Scheme 1.45. Synthesis of (5-acetoxy-6-oxotetrahydro-2H-pyran-2-yl)methyl acetate (**LXXI**) prepared from *D*-gluconolactone (overall yield from *D*-gluconolactone in parentheses).

Synthesis of (5-acetoxy-6-oxotetrahydro-2H-pyran-2-yl)methyl acetate, **LXXI** with acetyl protected hydroxyl groups has been prepared from *D*-gluconolactone. *D*-Gluconolactone was first converted to 3-acetoxy-6-acetoxymethyl-pyran-2-one with acetic anhydride and pyridine followed by hydrogenolysis with H_2 and Pd/C yielding the carbohydrate lactone as a racemic mixture (Scheme 1.45). ROP was achieved with $Sn(OBu)_2$ at 80 °C in toluene realising amorphous poly(**LXXI**)s with no T_m and a T_g value of 18 °C with modest molecular weights (M_n ranging from 1 800 – 7 300 $g.mol^{-1}$). The absence of any end-group resonances in ^1H NMR spectra and MALDI-TOF MS analysis determined the major product as cyclic polymers resulting from a similar rate of propagation to transesterification due to the low ring strain of the monomer.[118]

1.6 Functional poly(ester)s from β-propiolactone

As noted with δVL derivatives, there has been significantly less attention toward the synthesis and controlled ROP of functional β-propiolactones (β-PL) in comparison to cyclic diesters and εCLs in part a reflection of challenges in achieving a controlled ROP.[119] Nonetheless, functional β-PLs do provide another useful route into functional poly(ester)s. Functional β-PLs are commonly

synthesised from either aspartic acid or malic acid. Monomers synthesised from *L*-aspartic acid are generally realised by diazotisation of the amino acid with NaBr and sodium nitrite to yield *L*-(-)-bromosuccinic acid that when subsequently treated with trifluoroacetic anhydride (TFAA) result in *L*-(+)-bromosuccinic anhydride. Ring-opening with an alcohol yields an optically active mixture of bromosuccinic acid mono alcohol protected benzyl ester isomers that are subsequently cyclised with sodium hydroxide realising functional β-PLs (Scheme 1.46). Two routes from *L*-malic acid have also been reported with the first involving the protection of both carboxylic acid groups with benzyl alcohol followed by mesylation of the free hydroxyl group with mesyl chloride. Subsequent removal of the benzyl groups, cyclisation with TFAA and reaction with an alcohol affords the desired product. An improvement on this route involves the ring-closure of *L*-malic acid with TFAA and subsequent ring-opening with an alcohol resulting in the respective β-hydroxy acid that is cyclised with diisopropylazodicarboxylate (DIAD) and triphenylphosphine (TPP) yielding the functional β-PLs (Scheme 1.46).

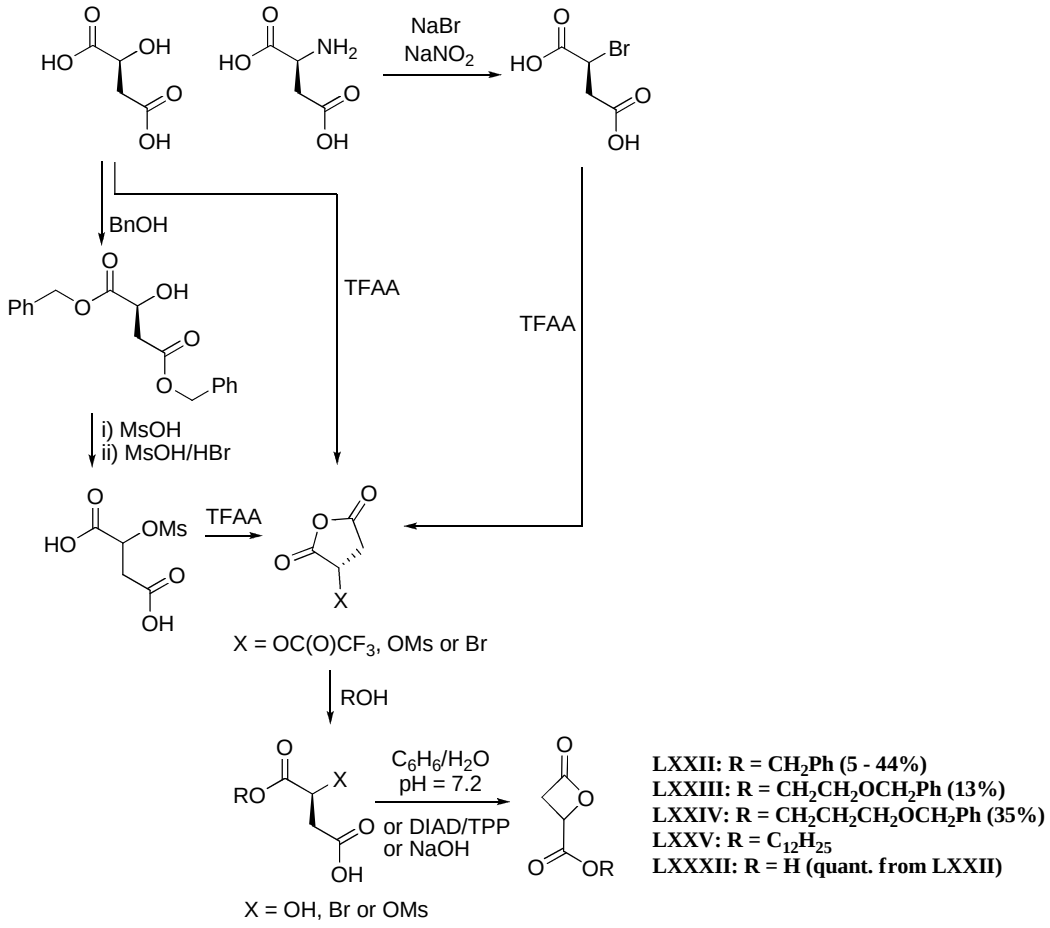

Scheme 1.46. General synthetic procedures for the preparation of functional β-PL monomers **LXXII**, **LXXIII**, **LXXIV**, **LXXV** and **LXXXII** from *L*-aspartic acid or *L*-malic acid (overall yields from *L*-aspartic acid or *L*-malic acid in parentheses if available).

Benzyl β-malolactone (MLABz, **LXXII**) has received much attention providing a controlled route into highly desirable poly(β-malic acid) (PMA) (Scheme 1.46). Early work in which the ROP of MLABz was performed with NEt_3 at 70 °C yielded only low molecular weight poly(MLABz) with M_n ~ 6 000 g.mol^{-1} with no correlation between molecular weight and monomer to initiator ratio. Preparation of high molecular weight poly(MLABz) with reproducible results was achieved by extensive purification of the monomer before polymerisation

with tetraethylammonium benzoate at 37 °C realising poly(MLABz) close to theoretical molecular weights (M_n > 170 000 g.mol^{-1}). Conversion of poly(MLABz) to PMA was realised through catalytic hydrogenolysis with H_2 and Pd/C at 25 °C yielding water soluble poly(ester)s without polymer degradation.[120-121] Additionally, partial and complete deprotection of poly(MLABz) was achieved with Pd/C catalysed hydrogenolysis by controlling the reaction time and conditions to yield copolymers of MLABz and malic acid (MA) with non-random distribution throughout the polymer forming "blocky" copolymers.[122] Oligomer formation during the degradation of PMA was monitored and quantified by aqueous GPC and high performance capillary electrophoresis (HPCE). The degradation rate was found to increase with increasing pendant acid group content in the poly(ester).[123] More recently, MLABz has been copolymerised with *L*-LA by $Sn(Oct)_2$ in the melt at 110 °C with simple removal of the benzyl ester from the resulting poly(MLABz-*co*-LLA) through hydrogenolysis obtaining pendant carboxylic acid groups with composition simply controlled through adjustment of the MLABz:*L*-LA ratio. The morphology of poly(MLABz-*co*-LLA) changed from crystalline to amorphous with increasing MLABz content (8 to 41 mol%) with decreases in T_g values from 59 to 45 °C. T_g values of the resulting deprotected poly(MA-*co*-LLA) were higher than that of the parent poly(MLABz-*co*-LLA)s.[124] Similar observations were reported for the correlation between MLABz/MA content and T_g values of analogously prepared poly(MLABz-*co*-DLLA) and poly(MLA-*co*-DLLA) using *rac*-LA. [125]

A telechelic ABA triblock, poly(εCL-*co*-MLA-*co*-εCL), was prepared by initial homopolymerisation of MLABz with potassium 11-hydroxydodecanoate in THF

at 0 °C with initiation from 18-crown-6 ether (HDD) affording poly(MLABz) with an α-hydroxyl and ω-carboxylic acid end group. Reduction of the carboxylic acid end group with a borane-tetrahydrofuran complex (BH_3:THF) at 0 °C resulted in poly(MLABz) with two hydroxyl end groups that was applied as a telechelic macroinitiator in the telechelic ROP of εCL with $AlEt_3$ in toluene at 25 °C to realise the telechelic ABA triblock poly(εCL-*co*-**LXXII**-*co*-εCL). Hydrogenolysis of the MLABz realised the amphiphilic triblock poly(εCL-*co*-MLA-*co*-εCL) without poly(ester) degradation. Ultra-violet (UV) spectroscopy with pyrene demonstrated that poly(εCL-*co*-MLA-*co*-εCL) formed flower-type micelles in pure water.[126] Further work involved using lactic acid as an initiator for the homopolymerisation of MLABz catalysed by TFA at 80 °C with subsequent conversion of the α-carboxylic acid end group to an acid chloride with oxalyl chloride. Linoleic chloride, synthesised from linoleic acid, and the poly(MLABz) acid chloride were grafted to chitosan with subsequent removal of the benzyl groups with methanesulfonic acid realising amphiphilic chitosan derivatives (LMCs). LMC self-assembly in water resulted in nanoparticles with average diameters of 190 – 350 nm. Paclitaxel (PTX) was incorporated into the LMC nanoparticles with high loading efficiency with the release rate controlled by the linoleic acid content and PMA chain length.[127]

(*R,S*)-benzyloxyethyl-β-malolactonate (MABE, **LXXIII**) similar to MLABz possessing a benzyl protected alcohol rather than carboxylic acid was synthesised in analogous fashion using benzyloxyethanol prepared from ethane-1,2-diol and benzoyl chloride (Scheme 1.46). Bulk copolymerisation of MABE with *rac*-LA by $Sn(Oct)_2$ at 130 °C followed by deprotection through hydrogenolysis catalysed by Pd/C resulted in amorphous poly(MABE-*co*-DLLA) with relatively long

pendant hydroxyl arms increasing the hydrophilicity while maintaining relatively long-term degradation stability compared to carboxylic acid functionalised poly(ester)s.[128] 3-Benzyloxypropylmalolactonate, **LXXIV**, providing a structurally comparable monomer to MABE, was synthesised and homopolymerised *via* the similar methods yielding poly(**LXXIV**) displaying a T_g value of -21 °C. Subsequent deprotection resulted in a hydrophilic poly(ester) while observing no change in T_g from the parent protected poly(**LXXIV**). Bulk copolymerisation of **LXXIV** with both ethyladamantylmalolactonate and butyl malolactonate, prepared by comparable syntheses to MABE, resulted in copolymers with T_g values from -15 and -19 °C respectively changing to -27 and 25 °C upon deprotection.[129]

Preparation of (*R*,*S*)-β-dodecyl malolactonate (**LXXV**), a hydrophobic functional β-PL, from 1-dodecanol *via* the general strategy (Scheme 1.46) has been used in nanoparticle formation for the encapsulation of small double-stranded RNA molecules (siRNA) used to abolish the production of a given protein. Bulk copolymerisation of **LXXV** and εCL from a PEO (M_w ~ 2 000 g.mol^{-1}) macroinitiator with $Sn(Oct)_2$ at 115 °C resulted in amphiphilic PEO-*b*-poly(εCL-*co*-**LXXV**) with the ability to self-assemble into nanoparticles in water. The presence of **LXXV** in the nanoparticles resulted in an increase of siRNA incorporation due to its long hydrophobic tail increasing the hydrophobic interactions.[130]

Butyl malolactonate (**LXXVI**) and butyl 3-methylmalolactonate (**LXXVII**) have also been prepared *via* the general procedure with 1-butanol using 3-methylaspartic acid and *L*-aspartic acid as starting materials respectively (Scheme 1.46 and Figure 1.4). A poly(MLABz) prepared using a potassium pentenoate/6-

crown-18 ether complex was used as a macroinitiator for the homopolymerisations of both **LXXVI** or **LXXVII** to yield block copolymers. Catalytic hydrogenolysis with H_2 and Pd/C of the benzyl ester groups afforded amphiphilic block copolymers capable of forming macromolecular micelles with characteristics dependant on block chain length and chemical structure of the hydrophobic block demonstrating average hydrodynamic diameters between 35 to 90 nm for poly(MLA-*b*-**LXXVII**) and poly(MLA-*b*-**LXXVI**).[131]

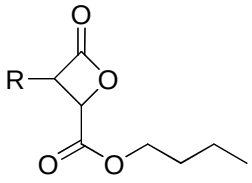

LXXVI: R = H
LXXVII: R = Me

Figure 1.4. Structures of butyl malolactonate (**LXXVI**) and butyl 3-methylmalolactonate (**LXXVII**) prepared from 3-methylaspartic acid and *L*-aspartic acid respectively.

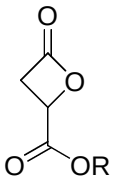

LXXVIII: R = $(CH_2)_5CH_3$
LXXIX: R = $CH_2CH_2C(CH_3)_3$
LXXX: R = $CH_2CH{=}CH_2$

Figure 1.5. Structures of hexyl malolactonate (**LXXVIII**), neohexyl malolactonate (**LXXIX**) and allyl malolactonate (**LXXX**) prepared from aspartic acid using hexanol, neohexanol and allyl alcohol respectively.

Other functional β-PLs synthesised include hexyl malolactonate (**LXXVIII**) and neohexyl malolactonate (**LXXIX**) from aspartic acid using hexanol and 3,3-

dimethyl-1-butanol (neohexanol) respectively (Figure 1.5). Poly(**LXXVIII**) and poly(**LXXIX**) prepared from anionic ROP observed T_g values of -10 and 22 °C respectively while copolymerisation with MLABz (10 mol%) and subsequent deprotection resulted in amphiphilic poly(MLA-*co*-**LXXVIII**) and poly(MLA-*co*-**LXXIX**) with similar T_g values. Self-assembly of these amphiphilic block copolymers yielded degradable nanoparticles displaying average hydrodynamic diameters varying from 90 to 171 nm depending on the poly(ester) composition. Allyl malolactonate (**LXXX**) (Figure 1.5) also prepared *via* the general procedure using allyl alcohol was subjected to terpolymerisation with MLABz and **LXXVI** resulting in a poly(ester) with a T_g value of 17 °C. Chemical modification of the pendant allyl chains with *m*CPBA, hydrogenation with H_2 catalysed with Pd/C and $Na_2S_2O_5$ afforded a terpolymer demonstrated effectiveness in bone defect treatment with a wound healing capacity close to that of carboxymethyl benzylamine sulfonate dextrans (CMDBS).[132]

Another synthetic route to access allyl-functional β-PLs is the synthesis of *rac*-allyl-β-BL, **LXXXI**, by the carbonylation of 1,2-epoxy-5-hexene catalysed by $[(C_6H_5)_3P=]_2NCo(CO)_4$ and $BF_3{\bullet}Et_2O$ (Scheme 1.47).[133] Homo- and copolymerisation of *rac*-allyl-β-PL with β-BL by a discrete amino-alkoxybis(phenolate)yttrium amido complex at 20 °C in toluene yielded highly syndiotactic polymers. Poly(*rac*-allyl-β-PL) is an amorphous polyester with a T_g of -44 °C while increasing the content of *rac*-allyl-β-PL in the copolymer resulted in an decrease in both the T_m and T_g. Quantitative hydroxylation, dihydroxylation and epoxidation of the pendant allyl groups was performed with either pinacolborane in the presence of Wilkinson's catalyst ($RhCl(PPh_3)_3$), OsO_4 and

N-methylmorpholine-*N*-oxide (NMO) or *m*CPBA respectively without any poly(ester) degradation.[134]

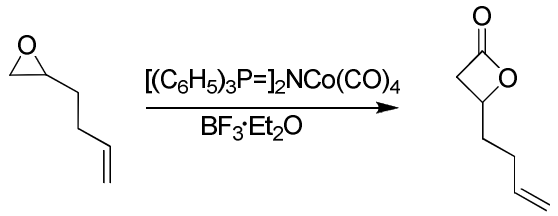

LXXXI (63%)

Scheme 1.47. Structures of *rac*-allyl-β-PL (**LXXXI**) prepared from 1,2-epoxy-5-hexene (overall yield from 1,2-epoxy-5-hexene in parentheses).

The preparation of malolactonic acid, **LXXXIII**, from the hydrogenolysis of MLABz provides a versatile compound possessing a pendant carboxylic acid group that can be reacted further yielding a range of possible functional β-PLs (Scheme 1.46). A poly(DLLA) was successfully coupled to malolactonic acid through DCC coupling yielding a bulky macromonomer, **LXXXIII**, (Scheme 1.48) that was polymerised using tetraethylammonium benzoate realising a simple route into PLA grafted PMA with a T_g of -17 °C and a T_m of 37 °C. In targeting artificial membranes, synthesis of a cholesterol functionalised β-PL, **LXXXIV**, was prepared *via* an analogous route (Scheme 1.48) with subsequent polymerisation yielding a cholesterol grafted PMA with a T_g of -8 °C and a T_m of 290 °C.[132]

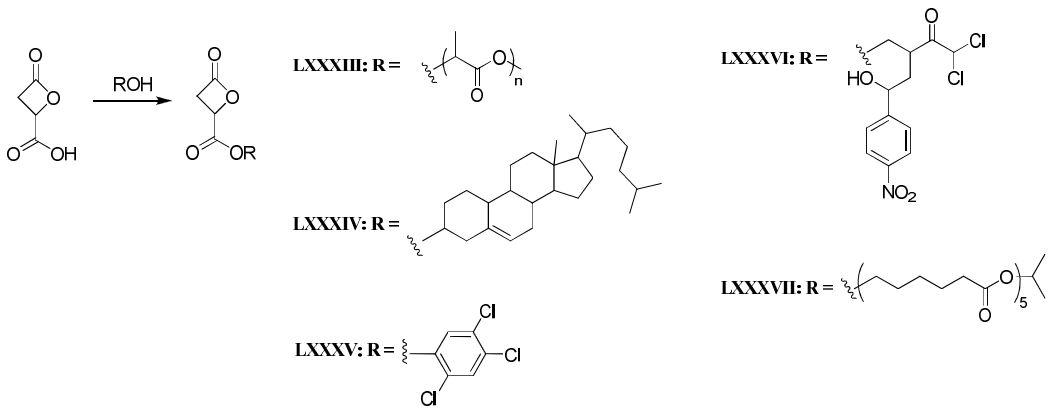

Scheme 1.48. Structures of poly(DLLA) malolactonate (**LXXXIII**), cholesterol malolactonate (**LXXXIV**), 2,4,5-trichlorophenylmalolactonate (**LXXXV**), (4 *RS*)-4-(chloramphenicol)oxycarbonyl-2-oxetanone (**LXXXVI**) and poly(εCL)$_5$ malolactonate (**LXXXVII**) prepared from aspartic acid and their respective alcohols.

Other monomers prepared using malolactonic acid include 2,4,5-trichlorophenylmalolactonate, **LXXXV**, and (4 *RS*)-4-(chloramphenicol)oxycarbonyl-2-oxetanone, **LXXXVI**, from their respective alcohols (Scheme 1.48). Bulk copolymerisation of **LXXXV** and **LXXXVI** with **LXXXII** (70 mol%) by tetramethylammonium benzoate at 70 °C realised copolymers with molecular weights between 3 000 and 4 000 g.mol^{-1}.[135] A well-defined low molecular weight PCL-OH chain (5 repeat units) has been coupled to malolactonic acid using DCC in the preparation of a macromonomer (**LXXXVII**) with homo- and copolymerisations carried out with potassium 11-hydroxydodecanoate at 0 °C in THF. Copolymerisations of **LXXXVII** and MLABz realised poly(ester)s with pendant poly(εCL)$_5$ chains with various compositions. Quantitative hydrogenolysis of the MLABz groups yielded the respective amphiphilic poly(MA-*co*-**LXXXVII**). Amphiphilic poly(MA-*co*-**LXXXVII**) was also prepared *via* a grafting from approach using poly(**LXXX**-*co*-MLABz). Conversion of the pendant allyl groups from **LXXX** to hydroxyl

groups by reaction with mercaptoethanol in the presence of AIBN at 70 °C enabled the introduction of pendant hydroxyl groups that were used to polymerise εCL using $AlEt_3$ with subsequent hydrogenolysis of the MLABz components realising an analogous amphiphilic poly(MA-*co*-**LXXXVII**).[136]

Bizzarri *et al.* has reported the synthesis and polymerisation of a wide range of monomers, **LXXXVIII – XCV**, applying both commonly used synthetic procedures (Scheme 1.49). Homo- and copolymerisations of all these functional β-PL monomers with tetraethylammonium benzoate at ~ 40 °C in THF yielded amorphous poly(ester)s with T_g values ranging from -34 to 42°C, depending on length and nature of the side groups.[137]

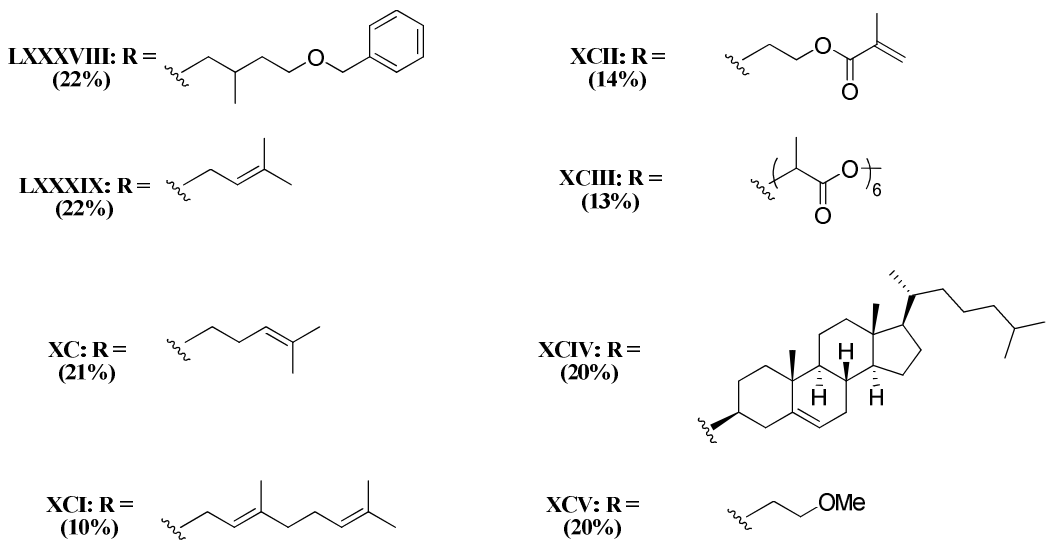

Scheme 1.49. Structures of a range of functional β-PL monomers synthesised by Bizzarri *et al.* by either procedure applied in Scheme 1.46 (**LXXXVIII – XCII**) or procedure applied in Scheme 1.48 (**XCIII – XCV**) from *rac*-aspartic acid (overall yields from *rac*-aspartic acid in parentheses).

Through a different synthesis (*R*,*S*)-4-alkyloxycarbonyl-3,3-dimethyl-2-oxetanones, **XCVI – XCIX**, were realised from commercially available diethyl

oxalpropionate through initial alkylation with potassium *t*-butoxide and methyl iodide. Reduction of the carbonyl with $NaBH_4$ and hydrolysis of the ester groups afforded 3,3-dimethylmalic acid. TFAA was used to prepare the cyclic anhydride intermediate with ring-opening *via* the desired alcohol with final cyclisation with DIAD and TPP yields the (*R*, *S*)-4-alkyloxycarbonyl-3,3-dimethyl-2-oxetanones. Several functional derivatives have been synthesised *via* this procedure possessing pendant functionality including benzyl (**XCVI**), allyl (**XCVII**), 1-methylpropyl (**XCVIII**) and hexyl (**XCIX**) (Scheme 1.50).[138]

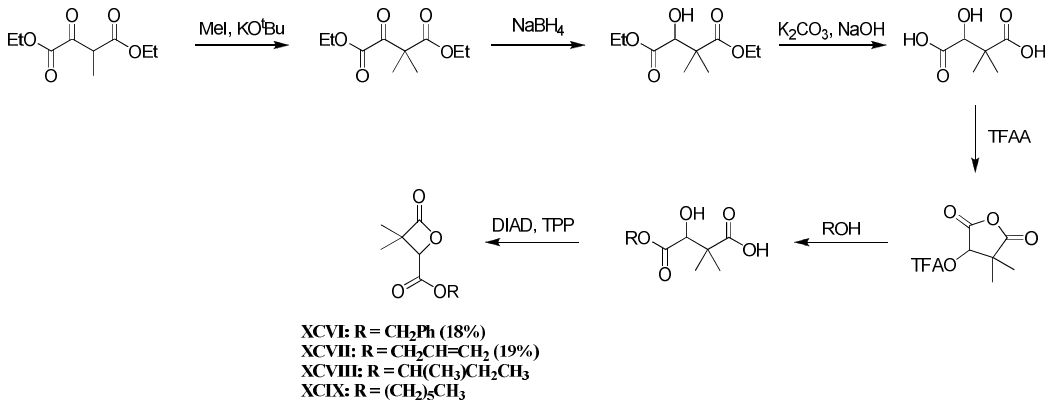

Scheme 1.50. Synthesis of (*R*, *S*)-4-alkyloxycarbonyl-3,3-dimethyl-2-oxetanones (**XCVI** – **XCIX**) prepared from diethyl oxalpropionate (overall yields from diethyl oxalpropionate in parentheses if available).

Bulk homopolymerisation of 4-benzyloxycarbonyl-3,3-dimethyl-2-oxetanone (**XCVI**) with tetraethylammonium benzoate at 37 °C found that the two methyl groups adjacent to the carbonyl had a large effect on both the polymerisation mechanism and physical properties with a T_g of 54 °C, 22 °C higher than structurally similar poly(MLABz). Deprotection of poly(**XCVI**) through catalytic hydrogenation catalysed with palladium was successful without polymer degradation. Hydrolytic degradation of the resulting poly(ester) was conducted in

a sodium phosphate buffer at pH 7 at both 37 and 50 °C. At 50 °C degradation to mainly oligomers was observed *via* GPC analysis after two months**.** A terpolymer of **XCVI**, **XCVII** and **XCVIII** was prepared by simultaneous bulk copolymerisation at 37 °C with tetraethylammonium benzoate yielding an amorphous poly(ester) with a T_g value of 44 °C.[138] Further work with **XCVI** involved its copolymerisation with β-butyrolactone (β-BL) *via* metal-free catalysis with 1,3,4-triphenyl-4,5-dihydro-*1H*-1,2,4-triazol-5-ylidene (triazole carbene) at 50 °C in toluene in the presence of *t*-BuOH achieving poly(**XCVI**-*co*-β-BL) with low polydispersities between 1.09 and 1.27. The resulting α,ω-dihydroxy poly(**XCVI**-*co*-β-BL) was further used as a macroinitiator for the telechelic polymerisation of *L*-LA at 90 °C in toluene catalysed with the triazole carbene yielding α,ω-dihydroxy PLLA-*b*-poly(**XCVI**-*co*-β-BL)-*b*-PLLA that was subsequently subjected to catalytic hydrogenolysis with H_2 and a Pd/C catalyst resulting in the respective amphiphilic triblock poly(ester). Self-assembly of the amphiphilic triblock poly(ester) at low temperatures (4 °C) resulted in flower-type micelles with microgelation occurring at 25 °C and dissolution of the microgel at 40 °C.[139]

L-Serine has been applied to the synthesis of functional β-PLs. A first example involved tritylation of the amine with triphenylchloromethane followed by cyclisation with DCC and DMAP resulting in the *N*-tritylated *L*-serine β-PL, **C** (Scheme 1.51). Homopolymerisations with tetrabutylammonium acetate at 80 °C in THF obtained poly(**C**) with low polydispersities between 1.2 – 1.3 with deprotection of the trityl group with TFA resulting in some degradation of the polymer backbone.[140] Another functional β-PL derived from *L*-serine involved the cyclisation of the commercially available *N*-(benzyloxycarbonyl)-*L*-serine

(**CI**) with *N*-phosphonium adduct of Ph_3P and dimethyl azodicarboxylate (DMAD) yielding *N*-(benzyloxycarbonyl)-*L*-serine β-PL (**CI**) (Scheme 1.51). Primarily, thermally-initiated melt polymerisation of **CI** carried out at 135 °C resulted in the formation of low molecular weight oligomers along with thermal degradation of the monomer. Therefore solution polymerisation in THF was attempted with a range of catalysts at 35 °C with only tetraethylammonium benzoate and potassium acetate/dicyclohexyl-18-crown ether-6 producing reproducible high molecular weight poly(**CI**)s. Deprotection of poly(**CI**) *via* catalytic hydrogenolysis with formic acid yielded the respective poly(*L*-serine ester). Copolymerisation of **CI** with *N*-(*tert*-butyloxycarbonyl)-*L*-serine β-BL (**CII**) at 20 °C prepared and polymerised using procedures developed for **CI** realised copolymers with molecular weights of 40 000 $g.mol^{-1}$.[141] Homopolymerisation of **CI** has also been achieved with mesyl chloride and Na_2CO_3 at 20 °C in acetone, however, no relationship between experimental conditions and molecular weight resulted with M_n constantly around 20 000 $g.mol^{-1}$. Improved deprotection of poly(**CI**) was achieved with HBr/acetic acid mixtures resulting in the bromide salt of the deprotected poly(**CI**) that combined with poly(β-malic acid) and/or its respective sodium salt formed polyelectrolyte complexes.[142]

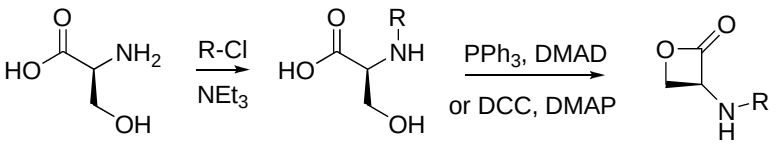

C: R = C(Ph)$_3$ (8%)
CI: R = C(O)OCH$_2$Ph (81%)
CII: R = C(O)OC(CH$_3$)$_3$

Scheme 1.51. Synthesis of *N*-tritylated *L*-serine β-PL (**C**), *N*-(benzyloxycarbonyl)-*L*-serine β-PL (**CI**) and *N*-(*tert*-butyloxycarbonyl)-*L*-serine β-BL (**CII**) from *L*-serine (overall yields from *L*-serine in parentheses if available).

Synthesis and ROP of α-chloromethyl-α-methyl-β-propiolactone (**CIII**), a halogenated functional β-PL, provided a useful reactive functional group requiring no protective group chemistry unlike hydroxyl and amine groups *etc*. Bis(2,2'-hydroxymethyl)propionic acid was used as the starting material with initial conversion of the hydroxyl and carboxylic acid groups into chlorine and acid chlorides respectively with thionyl chloride. Subsequent hydrolysis followed by lactonisation with KOH realised **CIII** (Scheme 1.52) that was successfully homopolymerised with a range of catalysts at different temperatures resulting in poly(**CIII**) with T_m values > 214 °C, depending on choice of catalyst. Polymers synthesised with $Sn(Oct)_2$ as the catalyst achieved the highest crystallinity with a T_m value of 250 °C as determined by differential scanning calorimetry (DSC) analysis. Solution polymerisations were also successful with $Sn(Oct)_2$ at 90 °C requiring chlorobenzene as the solvent to overcome solubility issues of the resulting poly(**CIII**).[143] Bulk copolymerisation of **CIII** and εCL with $Al(O^iPr)_3$ at 160 °C observed T_m values decreasing with increasing εCL content obtaining amorphous copolymers at >50% εCL content. Subsequent reaction of the pendant chloromethyl groups with pyridine formed the quaternary pyridinium salt with almost complete conversion resulting in increasing the hydrophilicity of the poly(ester)s.[144]

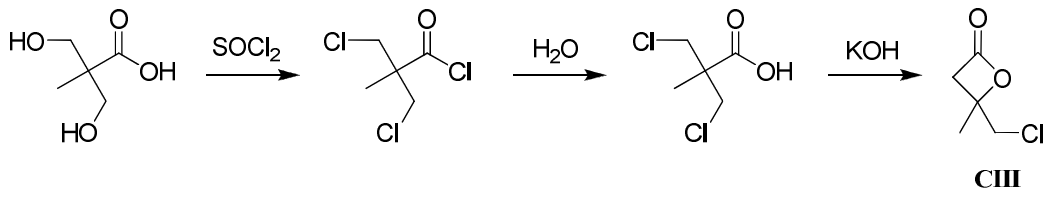

CIII

Scheme 1.52. Synthesis of α-chloromethyl-α-methyl-β-propiolactone (**CIII**) from bis(2,2'-hydroxymethyl)propionic acid.

1.7 Conclusions

There are many examples reported in the scientific literature of functional cyclic esters capable of ROP resulting in a wide variety of aliphatic poly(ester)s. A whole range of functionality has been incorporated into cyclic esters including hydrophilic, halogenated and unsaturated groups. Homo- and copolymerisation of these monomers can realise poly(ester)s with greatly varying physical properties with many of these functional poly(ester)s showing possible applications in a wide variety of fields due to their highly attractive properties including biodegradability and biocompatibility.

1.8 References

(1) Albertsson, A. C.; Varma, I. K. *Biomacromolecules* **2003**, *4*, 1466.

(2) Daniels, A. U.; Chang, M. K. O.; Andriano, K. P.; Heller, J. *J. Appl. Biomater.* **1990**, *1*, 57.

(3) Middleton, J. C.; Tipton, A. J. *Biomaterials* **2000**, *21*, 2335.

(4) Uhrich, K. E.; Cannizzaro, S. M.; Langer, R. S.; Shakesheff, K. M. *Chem. Rev.* **1999**, *99*, 3181.

(5) Place, E. S.; George, J. H.; Williams, C. K.; Stevens, M. M. *Chem. Soc. Rev.* **2009**, *38*, 1139.

(6) Sabir, M. I.; Xu, X. X.; Li, L. *Mater. Sci.* **2009**, *44*, 5713.

(7) Auras, R.; Harte, B.; Selke, S. *Macromol. Biosci.* **2004**, *4*, 835.

(8) Dechy-Cabaret, O.; Martin-Vaca, B.; Bourissou, D. *Chem. Rev.* **2004**, *104*, 6147.

(9) Drumright, R. E.; Gruber, P. R.; Henton, D. E. *Adv. Mater.* **2000**, *12*, 1841.

(10) Tsuji, H. *Macromol. Biosci.* **2005**, *5*, 569.

(11) Bendix, D. *Polym. Degrad. Stab.* **1998**, *59*, 129.

(12) Albertsson, A. C.; Varma, I. K. *Adv. Polym. Sci.* **2002**, *157*, 1.

(13) Jerome, C.; Lecomte, P. *Adv. Drug. Del. Rev.* **2008**, *60*, 1056.

(14) Dove, A. P. *Chem. Commun.* **2008**, 6446.

(15) Choi, Y. R.; Bae, Y. H.; Kim, S. W. *Macromolecules* **1998**, *31*, 8766.

(16) Kricheldorf, H. R.; Eggerstedt, S. *Macromol. Chem. Phys.* **1999**, *200*, 587.

(17) Kricheldorf, H. R.; Fechner, B. *Macromolecules* **2001**, *34*, 3517.

(18) Kricheldorf, H. R.; Fechner, B. *Biomacromolecules* **2002**, *3*, 691.

(19) Kricheldorf, H. R.; Langanke, D. *Macromol. Chem. Phys.* **1999**, *200*, 1174.

(20) Ryner, M.; Finne, A.; Albertsson, A. C.; Kricheldorf, H. R. *Macromolecules* **2001**, *34*, 7281.

(21) Ryner, M.; Valdre, A.; Albertsson, A. C. *J. Polym. Sci., Part A: Polym. Chem.* **2002**, *40*, 2049.

(22) Chen, C. C.; Chueh, J. Y.; Tseng, H.; Huang, H. M.; Lee, S. Y. *Biomaterials* **2003**, *24*, 1167.

(23) Gilding, D. K.; Reed, A. M. *Polymer* **1979**, *20*, 1459.

(24) Jain, R. A. *Biomaterials* **2000**, *21*, 2475.

(25) Malin, M.; Hiljanen-Vainio, M.; Karjalainen, T.; Seppälä, J. *J. Appl. Polym. Sci.* **1996**, *59*, 1289.

(26) Miller, R. A.; Brady, J. M.; Cutright, D. E. *J. Biomed. Mater. Res.* **1977**, *11*, 711.

(27) Shen, Y. Q.; Sun, W. L.; Zhu, K. J.; Shen, Z. Q. *J. Biomed. Mater. Res.* **2000**, *50*, 528.

(28) Vion, J. M.; Jerome, R.; Teyssie, P.; Aubin, M.; Prudhomme, R. E. *Macromolecules* **1986**, *19*, 1828.

(29) Yin, M.; Baker, G. L. *Macromolecules* **1999**, *32*, 7711.

(30) Simmons, T. L.; Baker, G. L. *Biomacromolecules* **2001**, *2*, 658.

(31) Trimaille, T.; Moller, M.; Gurny, R. *J. Polym. Sci., Part A: Polym. Chem.* **2004**, *42*, 4379.

(32) Trimaille, T.; Gurny, R.; Moller, M. *J. Biomed. Mater. Res. Part A* **2007**, *80A*, 55.

(33) Trimaille, T.; Mondon, K.; Gurny, R.; Moller, M. *Int. J. Pharm.* **2006**, *319*, 147.

(34) Liu, T. Q.; Simmons, T. L.; Bohnsack, D. A.; Mackay, M. E.; Smith, M. R.; Baker, G. L. *Macromolecules* **2007**, *40*, 6040.

(35) Jing, F.; Smith, M. R.; Baker, G. L. *Macromolecules* **2007**, *40*, 9304.

(36) Jing, F.; Hillmyer, M. A. *J. Am. Chem. Soc.* **2008**, *130*, 13826.

(37) Fiore, G. L.; Jing, F.; Young, V. G.; Jr.; Cramer, C. J.; Hillmyer, M. A. *Polym. Chem.* **2010**, *1*, 870.

(38) Kimura, Y.; Shirotani, K.; Yamane, H.; Kitao, T. *Macromolecules* **1988**, *21*, 3338.

(39) Kimura, Y.; Shirotani, K.; Yamane, H.; Kitao, T. *Polymer* **1993**, *34*, 1741.

(40) Lee, J. Y.; Cho, E. C.; Cho, K. *J. Controlled Release* **2004**, *94*, 323.

(41) Yamaoka, T.; Hotta, Y.; Kobayashi, K.; Kimura, Y. *Int. J. Biol. Macromol.* **1999**, *25*, 265.

(42) Ouchi, T.; Fujino, A. *Makromol. Chem.* **1989**, *190*, 1523.

(43) Gerhardt, W. W.; Noga, D. E.; Hardcastle, K. I.; Garcia, A. J.; Collard, D. M.; Weck, M. *Biomacromolecules* **2006**, *7*, 1735.

(44) Nottelet, B.; Tommaso, C. D.; Mondon, K.; Gurny, R.; Möller, M. *J. Polym. Sci., Part A: Polym. Chem.* **2010**, *48*, 3244.

(45) Leemhuis, M.; van Steenis, J. H.; van Uxem, M. J.; van Nostrum, C. F.; Hennink, W. E. *Eur. J. Org. Chem.* **2003**, 3344.

(46) Leemhuis, M.; van Nostrum, C. F.; Kruijtzer, J. A. W.; Zhong, Z. Y.; ten Breteler, M. R.; Dijkstra, P. J.; Feijen, J.; Hennink, W. E. *Macromolecules* **2006**, *39*, 3500.

(47) Noga, D. E.; Petrie, T. A.; Kumar, A.; Weck, M.; Garcia, A. J.; Collard, D. M. *Biomacromolecules* **2008**, *9*, 2056.

(48) Loontjens, C. A. M.; Vermonden, T.; Leemhuis, M.; van Steenbergen, M. J.; van Nostrum, C. F.; Hennink, W. E. *Macromolecules* **2007**, *40*, 7208.

(49) Seyednejad, H.; Vermonden, T.; Fedorovich, N. E.; van Eijk, R.; van Steenbergen, M. J.; Dhert, W. J. A.; van Nostrum, C. F.; Hennink, W. E. *Biomacromolecules* **2009**, *10*, 3048.

(50) Benabdillah, K. M.; Coudane, J.; Boustta, M.; Engel, R.; Vert, M. *Macromolecules* **1999**, *32*, 8774.

(51) Saulnier, B.; Coudane, J.; Garreau, H.; Vert, M. *Polymer* **2006**, *47*, 1921.

(52) Marcincinova-Benabdillah, K.; Boustta, M.; Coudane, J.; Vert, M. *Biomacromolecules* **2001**, *2*, 1279.

(53) Saulnier, B.; Ponsart, S.; Coudane, J.; Garreau, H.; Vert, M. *Macromol. Biosci.* **2004**, *4*, 232.

(54) Leemhuis, M.; Akeroyd, N.; Kruijtzer, J. A. W.; van Nostrum, C. F.; Hennink, W. E. *Eur. Polym. J.* **2008**, *44*, 308.

(55) Jiang, X.; Vogel, E. B.; Smith, M. R.; Baker, G. L. *Macromolecules* **2008**, *41*, 1937.

(56) Jiang, X. W.; Smith, M. R.; Baker, G. L. *Macromolecules* **2008**, *41*, 318.

(57) Jiang, X. W.; Vogel, E. B.; Smith, M. R.; Baker, G. L. *J. Polym. Sci., Part A: Polym. Chem.* **2007**, *45*, 5227.

(58) du Boullay, O. T.; Bonduelle, C.; Martin-Vaca, B.; Bourissou, D. *Chem. Commun.* **2008**, 1786.

(59) du Boullay, O. T.; Marchal, E.; Martin-Vaca, B.; Cossio, F. P.; Bourissou, D. *J. Am. Chem. Soc.* **2006**, *128*, 16442.

(60) Pitt, C. G.; Gu, Z. W.; Ingram, P.; Hendren, R. W. *J. Polym. Sci., Part A: Polym. Chem.* **1987**, *25*, 955.

(61) Tian, D.; Dubois, P.; Grandfils, C.; Jerome, R. *Macromolecules* **1997**, *30*, 406.

(62) Tian, D.; Dubois, P.; Jerome, R. *Macromolecules* **1997**, *30*, 1947.

(63) Tian, D.; Halleux, O.; Dubois, P.; Jerome, R.; Sobry, R.; Van den Bossche, G. *Macromolecules* **1998**, *31*, 924.

(64) Latere, J. P.; Lecomte, P.; Dubois, P.; Jerome, R. *Macromolecules* **2002**, *35*, 7857.

(65) Van Horn, B. A.; Iha, R. K.; Wooley, K. L. *Macromolecules* **2008**, *41*, 1618.

(66) Van Horn, B. A.; Wooley, K. L. *Soft Mater.* **2007**, *3*, 1032.

(67) Van Horn, B. A.; Wooley, K. L. *Macromolecules* **2007**, *40*, 1480.

(68) Stassin, F.; Halleux, O.; Dubois, P.; Detrembleur, C.; Lecomte, P.; Jerome, R. *Macromol. Symp.* **2000**, *153*, 27.

(69) Mecerreyes, D.; Humes, J.; Miller, R. D.; Hedrick, J. L.; Detrembleur, C.; Lecomte, P.; Jerome, R.; San Roman, J. *Macromol. Rapid Commun.* **2000**, *21*, 779.

(70) Vaida, C.; Mela, P.; Keul, H.; Moller, M. *J. Polym. Sci., Part A: Polym. Chem.* **2008**, *46*, 6789.

(71) Mecerreyes, D.; Lee, V.; Hawker, C. J.; Hedrick, J. L.; Wursch, A.; Volksen, W.; Magbitang, T.; Huang, E.; Miller, R. D. *Adv. Mater.* **2001**, *13*, 204.

(72) Lou, X. D.; Jerome, C.; Detrembleur, C.; Jerome, R. *Langmuir* **2002**, *18*, 2785.

(73) Rieger, J.; Van Butsele, K.; Lecomte, P.; Detrembleur, C.; Jerome, R.; Jerome, C. *Chem. Commun.* **2005**, 274.

(74) Rieger, J.; Bernaerts, K. V.; Du Prez, F. E.; Jerome, R.; Jerome, C. *Macromolecules* **2004**, *37*, 9738.

(75) Liu, M. J.; Vladimirov, N.; Frechet, J. M. J. *Macromolecules* **1999**, *32*, 6881.

(76) Trollsas, M.; Lee, V. Y.; Mecerreyes, D.; Lowenhielm, P.; Moller, M.; Miller, R. D.; Hedrick, J. L. *Macromolecules* **2000**, *33*, 4619.

(77) Trollsas, M.; Lowenhielm, P.; Lee, V. Y.; Moller, M.; Miller, R. D.; Hedrick, J. L. *Macromolecules* **1999**, *32*, 9062.

(78) Mecerreyes, D.; Atthoff, B.; Boduch, K. A.; Trollsas, M.; Hedrick, J. L. *Macromolecules* **1999**, *32*, 5175.

(79) Mecerreyes, D.; Trollsas, M.; Hedrick, J. L. *Macromolecules* **1999**, *32*, 8753.

(80) Detrembleur, C.; Mazza, M.; Lou, X.; Halleux, O.; Lecomte, P.; Mecerreyes, D.; Hedrick, J. L.; Jerome, R. *Macromolecules* **2000**, *33*, 7751.

(81) Detrembleur, C.; Mazza, M.; Halleux, O.; Lecomte, P.; Mecerreyes, D.; Hedrick, J. L.; Jerome, R. *Macromolecules* **2000**, *33*, 14.

(82) Xu, N.; Wang, R.; Du, F. S.; Li, Z. C. *J. Polym. Sci., Part A: Polym. Chem.* **2009**, *47*, 3583.

(83) Wang, G.; Shi, Y.; Fu, Z.; Yang, W.; Huang, Q.; Zhang, Y. *Polymer* **2005**, *46*, 10601.

(84) Vroman, B.; Mazza, M.; Fernandez, M. R.; Jerome, R.; Preat, V. *J. Controlled Release* **2007**, *118*, 136.

(85) Lou, X.; Detrembleur, C.; Lecomte, P.; Jerome, R. *Macromolecules* **2001**, *34*, 5806.

(86) Lou, X. D.; Detrembleur, C.; Lecomte, P.; Jerome, R. *J. Polym. Sci., Part A: Polym. Chem.* **2002**, *40*, 2286.

(87) Lou, X. D.; Detrembleur, C.; Lecomte, P.; Jerome, R. *e-Polymers* **2002**.

(88) Lenoir, S.; Riva, R.; Lou, X.; Detrembleur, C.; Jerome, R.; Lecomte, P. *Macromolecules* **2004**, *37*, 4055.

(89) Riva, R.; Lenoir, S.; Jerome, R.; Lecomte, P. *Polymer* **2005**, *46*, 8511.

(90) Riva, R.; Rieger, J.; Jerome, R.; Lecomte, P. *J. Polym. Sci., Part A: Polym. Chem.* **2006**, *44*, 6015.

(91) Riva, R.; Schmeits, P.; Stoffelbach, F.; Jerome, C.; Jerome, R.; Lecomte, P. *Chem. Commun.* **2005**, 5334.

(92) Riva, R.; Schmeits, S.; Jerome, C.; Jerome, R.; Lecomte, P. *Macromolecules* **2007**, *40*, 796.

(93) El Habnouni, S.; Darcos, V.; Coudane, J. *Macromol. Rapid Commun.* **2009**, *30*, 165.

(94) Habnouni, S. E.; Blanquer, S.; Darcos, V.; Coudane, J. *J. Polym. Sci., Part A: Polym. Chem.* **2009**, *47*, 6104.

(95) Mecerreyes, D.; Miller, R. D.; Hedrick, J. L.; Detrembleur, C.; Jerome, R. *J. Polym. Sci., Part A: Polym. Chem.* **2000**, *38*, 870.

(96) Dai, W. F.; Huang, H.; Du, Z. Z.; Lang, M. D. *Polym. Degrad. Stab.* **2008**, *93*, 2089.

(97) Mahmud, A.; Xiong, X. B.; Lavasanifar, A. *Macromolecules* **2006**, *39*, 9419.

(98) Deng, X. M.; Yuan, M. L.; Cao, X. J.; Li, X. H. *Macromol. Chem. Phys.* **2001**, *202*, 2417.

(99) Palmgren, R.; Karlsson, S.; Albertsson, A.-C. *J. Polym. Sci., Part A: Polym. Chem.* **1997**, *35*, 1635.

(100) Zhang, D. H.; Hillmyer, M. A.; Tolman, W. B. *Biomacromolecules* **2005**, *6*, 2091.

(101) Wanamaker, C. L.; Bluemle, M. J.; Pitet, L. M.; O'Leary, L. E.; Tolman, W. B.; Hillmyer, M. A. *Biomacromolecules* **2009**, *10*, 2904.

(102) Wanamaker, C. L.; O'Leary, L. E.; Lynd, N. A.; Hillmyer, M. A.; Tolman, W. B. *Biomacromolecules* **2007**, *8*, 3634.

(103) Wanamaker, C. L.; Tolman, W. B.; Hillmyer, M. A. *Biomacromolecules* **2009**, *10*, 443.

(104) Lowe, J. R.; Tolman, W. B.; Hillmyer, M. A. *Biomacromolecules* **2009**, *10*, 2003.

(105) Pinilla, I. M.; Martínez, M. B.; Galbis, J. A. *Carbohydr. Res.* **2003**, *338*, 549.

(106) Urakami, H.; Guan, Z. *Biomacromolecules* **2008**, *9*, 592.

(107) Pinilla, I. M.; Martinez, M. B.; Galbis, J. A. *Carbohydr. Res.* **2003**, *338*, 549.

(108) Kullmer, K.; Kikuchi, H.; Uyama, H.; Kobayashi, S. *Macromol. Rapid Commun.* **1998**, *19*, 127.

(109) Hayashi, K. *Ind. Eng. Chem. Prod. Res. Dev.* **1974**, *13*, 193.

(110) Parrish, B.; Quansah, J. K.; Emrick, T. *J. Polym. Sci., Part A: Polym. Chem.* **2002**, *40*, 1983.

(111) Parrish, B.; Emrick, T. *Macromolecules* **2004**, *37*, 5863.

(112) Parrish, B.; Breitenkamp, R. B.; Emrick, T. *J. Am. Chem. Soc.* **2005**, *127*, 7404.

(113) Parrish, B.; Emrick, T. *Bioconjugate Chem.* **2007**, *18*, 263.

(114) Cooper, B. M.; Chan-Seng, D.; Samanta, D.; Zhang, X. F.; Parelkar, S.; Emrick, T. *Chem. Commun.* **2009**, 815.

(115) van der Ende, A. E.; Kravitz, E. J.; Harth, E. *J. Am. Chem. Soc.* **2008**, *130*, 8706.

(116) van der Ende, A.; Croce, T.; Hamilton, S.; Sathiyakumar, V.; Harth, E. *Soft Mater.* **2009**, *5*, 1417.

(117) Tasaka, F.; Ohya, Y.; Ouchi, T. *Macromol. Rapid Commun.* **2001**, *22*, 820.

(118) Tang, M.; White, A. J. P.; Stevens, M. M.; Williams, C. K. *Chem. Commun.* **2009**, 941.

(119) Coulembier, O.; Degée, P.; Hedrick, J. L.; Dubois, P. *Prog. Polym. Sci.* **2006**, *31*, 723.

(120) Cammas, S.; Renard, I.; Langlois, V.; Guerin, P. *Polymer* **1996**, *37*, 4215.

(121) Guerin, P.; Vert, M.; Braud, C.; Lenz, R. W. *Polym. Bull.* **1985**, *14*, 187.

(122) Caron, A.; Braud, C.; Bunel, C.; Vert, M. *Polymer* **1990**, *31*, 1797.

(123) Braud, C.; Vert, M. *Polym. Bull.* **1992**, *29*, 177.

(124) He, B.; Bei, J. Z.; Wang, S. G. *Polymer* **2003**, *44*, 989.

(125) He, B.; Poon, Y. F.; Feng, J.; Chan-Park, M. B. *J. Biomed. Mater. Res. Part A* **2008**, *87A*, 254.

(126) Coulembier, O.; Degee, P.; Dubois, P. *Macromol. Chem. Phys.* **2006**, *207*, 484.

(127) Zhao, Z. M.; He, M.; Yin, L. C.; Bao, J. M.; Shi, L. L.; Wang, B. Q.; Tang, C.; Yin, C. H. *Biomacromolecules* **2009**, *10*, 565.

(128) Wang, L.; Jia, X. H.; Chen, Y. S.; Che, Y. Z.; Yuan, Z. *J. Biomed. Mater. Res. Part A* **2008**, *87A*, 459.

(129) Barbaud, C.; Cammas-Marion, S.; Guerin, P. *Polym. Bull.* **1999**, *43*, 297.

(130) Bouclier, C.; Moine, L.; Hillaireau, H.; Marsaud, V.; Connault, E.; Opolon, P.; Couvreur, P.; Fattal, E.; Renoir, J. M. *Biomacromolecules* **2008**, *9*, 2881.

(131) Cammas-Marion, S.; Bear, M. M.; Harada, A.; Guerin, P.; Kataoka, K. *Macromol. Chem. Phys.* **2000**, *201*, 355.

(132) Cammas-Marion, S.; Guerin, P. *Macromol. Symp.* **2000**, *153*, 167.

(133) Lee, J. T.; Thomas, P. J.; Alper, H. *J. Org. Chem.* **2001**, *66*, 5424.

(134) Ajellal, N.; Thomas, C. M.; Carpentier, J. F. *J. Polym. Sci., Part A: Polym. Chem.* **2009**, *47*, 3177.

(135) LeboucherDurand, M. A.; Langlois, V.; Guerin, P. *Polym. Bull.* **1996**, *36*, 35.

(136) Coulembier, O.; Degee, P.; Gerbaux, P.; Wantier, P.; Barbaud, C.; Flammang, R.; Guerin, P.; Dubois, P. *Macromolecules* **2005**, *38*, 3141.

(137) Bizzarri, R.; Chiellini, F.; Solaro, R.; Chiellini, E.; Cammas-Marion, S.; Guerin, P. *Macromolecules* **2002**, *35*, 1215.

(138) Barbaud, C.; Fay, F.; Abdillah, F.; Randriamahefa, S.; Guerin, P. *Macromol. Chem. Phys.* **2004**, *205*, 199.

(139) Coulembier, O.; Mespouille, L.; Hedrick, J. L.; Waymouth, R. M.; Dubois, P. *Macromolecules* **2006**, *39*, 4001.

(140) Fietier, I.; Leborgne, A.; Spassky, N. *Polym. Bull.* **1990**, *24*, 349.

(141) Zhou, Q. X.; Kohn, J. *Macromolecules* **1990**, *23*, 3399.

(142) Rossignol, H.; Boustta, M.; Vert, M. *Int. J. Biol. Macromol.* **1999**, *25*, 255.

(143) Liu, X. Q.; Wang, M. X.; Li, Z. C.; Li, F. M. *Macromol. Chem. Phys.* **1999**, *200*, 468.

(144) Liu, X. Q.; Li, Z. C.; Du, F. S.; Li, F. M. *Macromol. Rapid Commun.* **1999**, *20*, 470.

Chapter 2 - Synthesis and organocatalytic ring-opening polymerisation of cyclic esters derived from *L*-malic acid.

2.1 Introduction

In order to investigate the potential for the synthesis of a versatile poly(ester) by ROP, malic acid (MA, **1**) was chosen as the feedstock. MA is a relatively inexpensive, commercially available α-hydroxy acid equivalent to aspartic acid, thus possessing a pendant carboxylic acid moiety that would potentially support a range of functional groups providing a high level of control over degradation times and physical properties of the resultant polymers. Previous studies to utilise MA in ROP include the synthesis of a range of β-lactones from ring closure between the hydroxyl group and β-carboxylic acid. These studies have resulted in a range of functional β-malolactones that through ROP result in a range of functional poly(hydroxyalkanoate)s including the highly desirable poly(β-malic acid) (PMA).[1-2] ROP of 6-membered rings derived from MA have received relatively little attention despite being previously reported. Kimura *et al*. reported the synthesis and ROP of 3-(*S*)-[(benzyloxycarbonyl)methyl]-1,4-dioxane-2,5-dione (BMD, **6**) (Figure 2.1). ROP of BMD mediated by stannous(II) octanoate ($Sn(Oct)_2$) resulted in relatively poorly defined poly(ester)s (*e.g*. [M]/[I] = 100; M_n = 10 500 g.mol^{-1}; PDI = 2.0). Despite this poor control, BMD and its statistical copolymers with lactide (LA) have received some study including micelle formation through self-assembly of an amphiphilic block copolymer with poly(ethylene oxide) (PEO).[3-6] Ouchi and coworkers also reported the synthesis of the cyclic diester of MA, 3,6-(*S*)-[di(benzyloxycarbonyl)methyl]-1,4-dioxane-2,5-dione (malide, **7**) (Figure 2.1). ROP of malide with different organotin catalysts between 130 and 220 °C led to polymers with low reactivities for ROP and unpredictable molecular parameters.[7] In both cases the relatively poor control compared to that of less hindered cyclic esters is thought to be a result of

transesterification reactions. In all cases reported to date, ROP has been catalysed by $Sn(Oct)_2$, that while being extensively applied in ROP, is known to readily mediate transesterification reactions that may therefore limit control over the polymerisation.

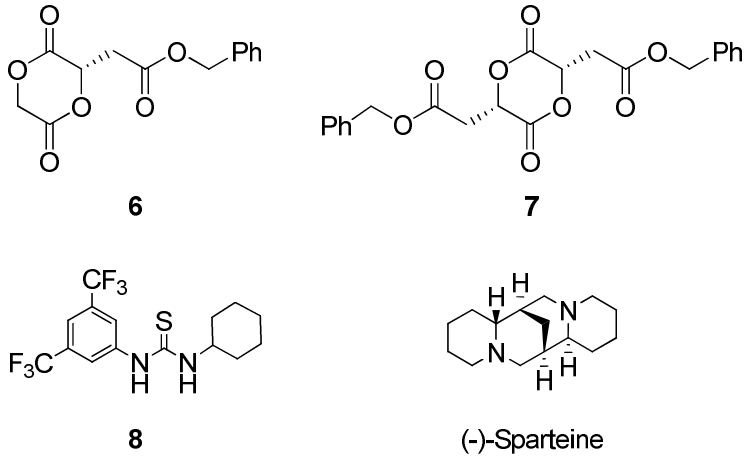

Figure 2.1. Cyclic diester monomers 3-(*S*)-[(benzyloxycarbonyl)methyl]-1,4-dioxane-2,5-dione, BMD (**6**) and 3,6-(*S*)-[di(benzyloxycarbonyl)methyl]-1,4-dioxane-2,5-dione, malide (**7**) synthesised from *L*-malic acid and 1-(3,5-bis(trifluoromethyl)phenyl)-3-cyclohexylthiourea (**8**)/(-)-sparteine organic catalysts.

Several recent advances in ROP catalysis have resulted in greatly enhanced levels of selectivity for both stereoselectivity and for ring-opening of cyclic esters in preference to transesterification side-reactions and selectivity for preferential ring-opening based on the stereochemistry of the adjacent chiral centre.[8-9] One of the most notable examples is the dual component thiourea/amine catalysts (Figure 2.1). These organic molecules exhibit exceptional selectivity towards ring-opening of lactide compared to transesterification of the polymer chain such that even at very high monomer conversions and extended reaction times, polydispersities remain ≤ 1.07. [10-11] It

was hypothesised that selective and controlled ROP of malic acid-based monomers would be possible using these highly selective catalysts to provide a potentially versatile platform for the synthesis of poly(ester)s with pendant ester functionality. Herein, the improved synthesis of 3-(*S*)-[(benzyloxycarbonyl)methyl]-1,4-dioxane-2,5-dione (BMD) and 3,6-(*S*)-[di(benzyloxycarbonyl)methyl]-1,4-dioxane-2,5-dione (malide) from commercially available *L*-malic acid is reported along with the application of organic catalysts to mediate the controlled ROP of BMD to yield copolymers consisting of glycolic acid and benzyl α-(*L*)-malate units (PBMD).

2.2 Results and Discussion

2.2.1 Synthesis of 3-(S)-[(benzyloxycarbonyl)methyl]- and 3,6-(S)-[di(benzyloxycarbonyl)methyl]-1,4-dioxane-2,5-diones, BMD and malide

The synthesis of 3-(*S*)-[(benzyloxycarbonyl)methyl]- and 3,6-(*S*)-[di(benzyloxycarbonyl)methyl]-1,4-dioxane-2,5-diones (BMD, **6**, and malide, **7**, respectively), were achieved *via* an improved synthesis of benzyl α-(*L*)-malate, **4**, from *L*-malic acid in 3 steps (Scheme 2.1). First, the reaction of *L*-malic acid, **1**, with 2,2-dimethoxypropane in the presence of catalytic *p*-toluenesulfonic acid (*p*TsOH) resulted in the selective acetonide protection of the α-hydroxy acid, **2**. Subsequent benzylation of the remaining β-carboxylic acid was achieved by reaction with benzyl bromide, **3**, followed by deprotection of the acetonide group at 40 °C in an AcOH/THF/H_2O (1:1:1) solvent mixture for 24 h resulting in benzyl α-(*L*)-malate, **4**, in a 48% yield over the 3 steps. Coupling of the resultant α-hydroxy acid with bromoacetyl bromide in the presence of NEt_3 and subsequent intramolecular cyclisation in the presence of $NaHCO_3$ through slow addition into DMF resulted in the isolation of BMD, **6**, in a 55% yield (Scheme 2.1). A *pseudo*-high dilution cyclisation technique was utilised to reduce the amount of byproduct formed such that significant pre-dilution of **5** (0.14 M) in DMF before slow injection (0.707 $mL.h^{-1}$) into a $NaHCO_3$/DMF suspension provided a substantial improvement in yield compared to previous syntheses of this monomer.[3] Retention of the stereochemistry in the synthesis of **6** from *L*-malic acid was confirmed through measurement of its specific rotation *via* polarimetry observing an $[\alpha]_D^{33}$ = -35.7° (in $CHCl_3$, c = 0.42 $g.L^{-1}$), ref $[\alpha]_D^{25}$ = -8.6° (in MeOH, c = 1.0 $g.L^{-1}$).[3]

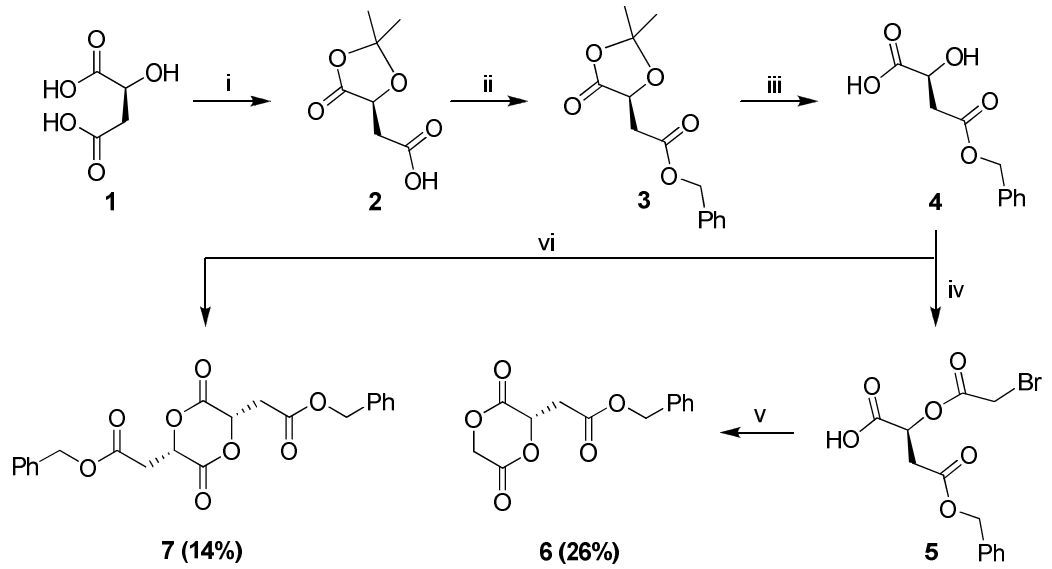

Scheme 2.1. Synthesis of 3-(*S*)-[(benzyloxycarbonyl)methyl]-1,4-dioxane-2,5-dione, **6**, and 3,6-(*S*)-[di(benzyloxycarbonyl)methyl]-1,4-dioxane-2,5-dione, **7**, from *L*-malic acid, **1**. Conditions: (i) $Me_2C(OMe)_2$, *p*TsOH; (ii) $PhCH_2Br$, NEt_3, Acetone; (iii) AcOH, THF/H_2O; (iv) $BrC(O)CH_2Br$, NEt_3, DMAP, CH_2Cl_2; (v) $NaHCO_3$, DMF; (vi) Δ, *p*TsOH, toluene (overall yield from *L*-malic acid in parentheses).

The α-hydroxy acid was additionally dimerised in refluxing toluene with catalytic *p*TsOH to yield malide, **7**, (30%, Scheme 2.1). Again, as with the synthesis of **6**, the yield of this final cyclisation step was severely hindered by the formation of undesired oligomer byproducts and transesterification. Dilute conditions (0.05 M) were employed in an attempt to increase the yield; however, this provided no considerable improvement. Despite the poor yield of the final cyclisation step, the overall synthesis of **7** provides an improvement on previously reported yields.[7] Representive ^{1}H NMR spectra of **4**, **6**, and **7** are shown in Figure 2.2. The methine proton of **4** appears at δ = 4.58 ppm, while clear signals at δ = 7.35, 5.18 and 2.99-2.90 ppm are characteristic of the benzyl group and the methylene protons of the malate unit respectively. The chemical shift of the methine proton provides simple confirmation for the formation of

both **6** and **7** as upon cyclisation the methine proton shifts downfield to δ = 5.22 and 5.45 ppm in **6** and **7** respectively while there was no significant change in the remaining chemical shifts compared to **4** (Figure 2.2).

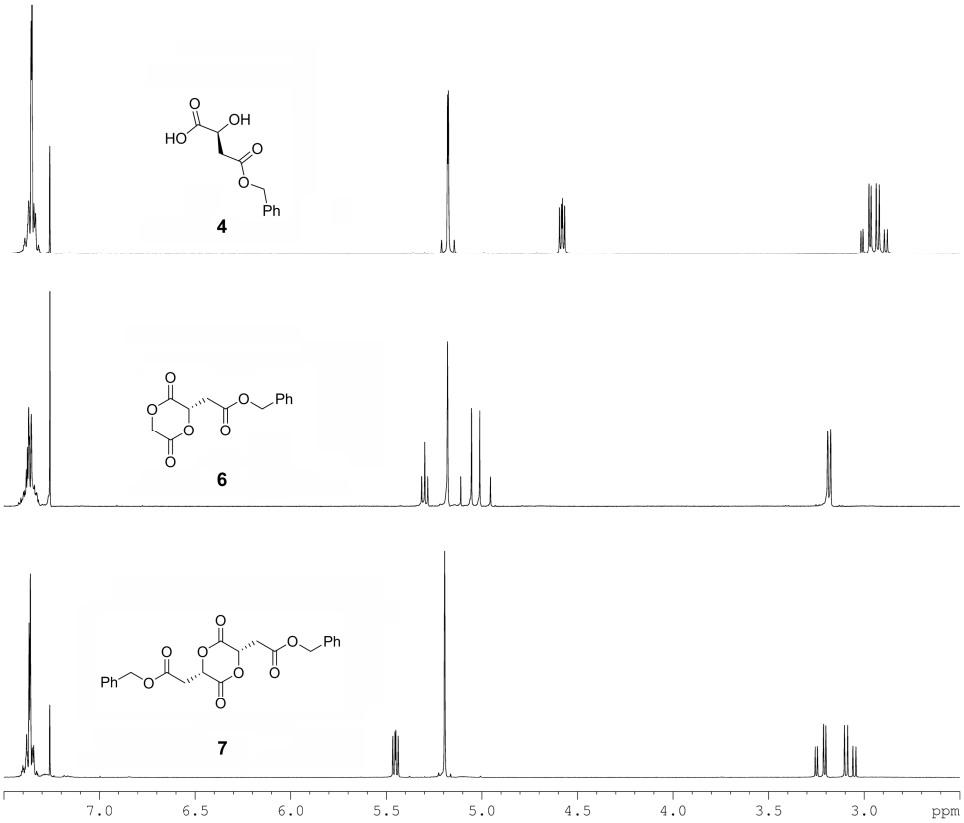

Figure 2.2. ^{1}H NMR spectrum of **4**, **6** and **7** (400 MHz; $CDCl_3$).

2.2.2 Ring-Opening Polymerisation studies of BMD

Attempts to polymerise malide, **7**, with the 1-(3,5-bis(trifluoromethyl)phenyl)-3-cyclohexylthiourea (**8**) and (-)-sparteine system did not result in the isolation of any polymeric materials, most likely a consequence of the high steric hindrance and low ring strain of the monomer.[12-13] ROP of **7** was also attempted with a variety of other different catalysts, both organic and inorganic, however resulted

in no improvement of previous reported results. As such, efforts were concentrated on the polymerisation of BMD, **6**, as the less hindered glycolic acid unit was postulated to lead to a more facile polymerisation. ROP of **6** catalysed by **8** and (-)-sparteine using a range of initiators was initially investigated at 25 °C in $CHCl_3$ solution (Scheme 2.2). ^{1}H NMR spectroscopy provided a convenient method for monitoring the progress of the polymerisation by observation of the reduction of the methylene resonance of the malate unit of the monomer at δ = 3.12 ppm and the appearance of the corresponding broad multiplet at δ = 3.08 - 2.85 ppm in PBMD. Upon completion of the allotted time, polymerisations were quenched by the removal of (-)-sparteine *via* a 1.0 M $HCl_{(aq)}$ wash and removal of **8** by its extraction into Et_2O. The polymers were precipitated into ice cold petroleum ether (b.p. 40-60 °C).

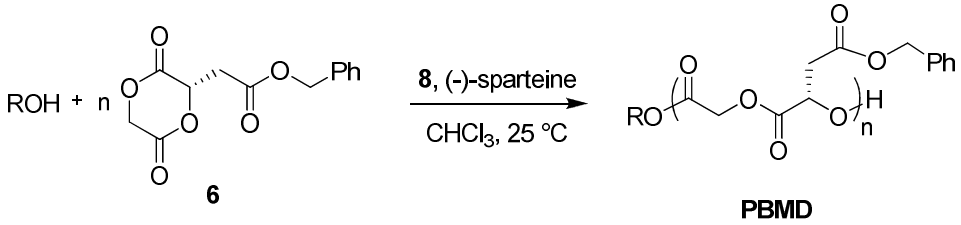

Scheme 2.2. Ring-opening polymerisation of 3-(*S*)-[(benzyloxycarbonyl)methyl]-1,4-dioxane-2,5-dione, **6**, using 1-(3,5-bis(trifluoromethyl)phenyl)-3-cyclohexylthiourea, **8**, and (-)-sparteine.

2.2.2.1 Ring-Opening Polymerisation studies of BMD – effect of temperature

Initial studies investigated the ROP of **6** under conditions previously reported for lactide ROP, initiating from *neo*-pentanol in the presence of 10 mol% **8** and 5 mol% (-)-sparteine as cocatalysts. At a monomer-to-initiator ratio of 50 ([M]/[I] = 50), the ROP of **6** achieved 79% monomer conversion after 180 min. While gel permeation chromatography (GPC) analysis of the resultant polymer indicated

that the polymerisation was well controlled with a number-average molecular weight (M_n) of 7 420 g.mol^{-1} and polydispersity (PDI) of 1.17, prolonged reaction times did not lead to increased levels of monomer conversion. Indeed exposure to increased reaction times led to a decrease in molecular weight and a broadening of the PDI consistent with the occurrence of transesterification side reactions. In an attempt to achieve higher conversions the effect of polymerisation temperature was initially investigated. Raising the temperature to 60 °C resulted in retardation of the polymerisation observing only 15% monomer conversion after 180 min. Comparison of monomer conversion *versus* time at different temperatures, 25, 35 and 45 °C, during the initial 30 min clearly demonstrated the correlation between monomer conversion and temperature in the ROP of **6** (Figure 2.3). Decreasing the ROP temperature below 25 °C was thought to provide a further improvement on monomer conversion, however, this resulted in a decrease in solubility of **6** in the $CHCl_3$ solution and as a consequence a retardation of the ROP was again observed. This observation between monomer conversion and ROP temperature was consistent with decreased ring-strain of the monomer, resulting from the increased bulk of the ring-substituents stabilising the ring-closed form relative to its linear counterpart and thus limiting the exothermicity of the ring-opening process. As the ROP of **6** is governed by thermodynamic equilibrium, this effect results in a higher critical concentration of the monomer reflected in a lower yield of the linear polymer thus the ring-opening of **6** being preferred at lower temperatures.[12-13] It was hypothesised that this observation was also partly responsible, along with steric effects, for the poor polymerisability of **7**, a consequence of the presence of the two bulky substituents.

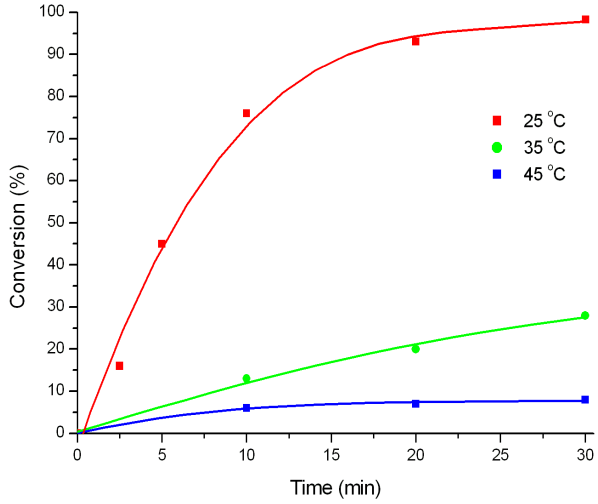

Figure 2.3. Plot of time (min) *versus* monomer conversion (measured by ^{1}H NMR spectroscopy) for the ROP of **6** ([M]/[I] = 50, $[\mathbf{6}]_0$ = 0.32 M) using 25 mol% of **8** and 5 mol% (-)-sparteine as cocatalysts and *neo*-pentanol as the initiator at a range of temperatures.

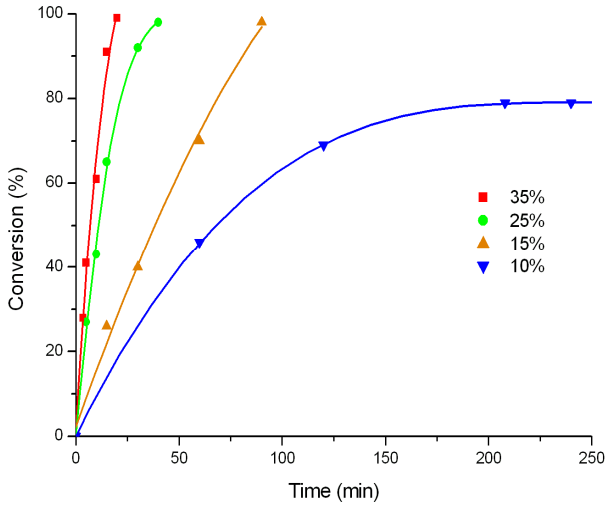

Figure 2.4. Plot of time (min) *versus* monomer conversion (measured by ^{1}H NMR spectroscopy) for the ROP of **6** ([M]/[I] = 50, $[\mathbf{6}]_0$ = 0.32 M) using varying mol% of **8** and 5 mol% (-)-sparteine as cocatalysts and *neo*-pentanol as the initiator.

2.2.2.2 Ring-Opening Polymerisation studies of BMD – effect of 1-(3,5-bis(trifluoromethyl)phenyl)-3-cyclohexylthiourea, 8, concentration

Maintaining the polymerisation temperature at 25 °C the loading of **8** was increased in an attempt to increase the selectivity for ROP over transesterification and thus achieve higher monomer conversions (Figure 2.4). To this end, employing a 15 mol% loading of **8** resulted in an increase in monomer conversion such that for a [M]/[I] = 50, 96% monomer conversion was observed after 120 min. Furthermore, high levels of control over the polymerisation resulted in a PBMD exhibiting M_n = 9 900 g.mol^{-1} and PDI = 1.16 (Figure 2.5). A further increase in loading of **8** to 25 mol% resulted in a further decrease in the time required to reach high monomer conversions such that after only 30 min PBMD with M_n = 9 500 g.mol^{-1} and PDI = 1.15 was obtained. Higher loadings of **8** (35+ mol%) decreased the polymerisation time to achieve 90+% monomer conversion further, however, resulted in a small loss of control with a broadening of PDI attributed to transesterification. Interestingly, the ROP of **6** was complete approximately four times faster (t = 30 min, monomer conversion = 92%) than the ROP of lactide (t = 120 min) under identical conditions, possibly a consequence of the reduced steric demands of the glycolic acid unit.

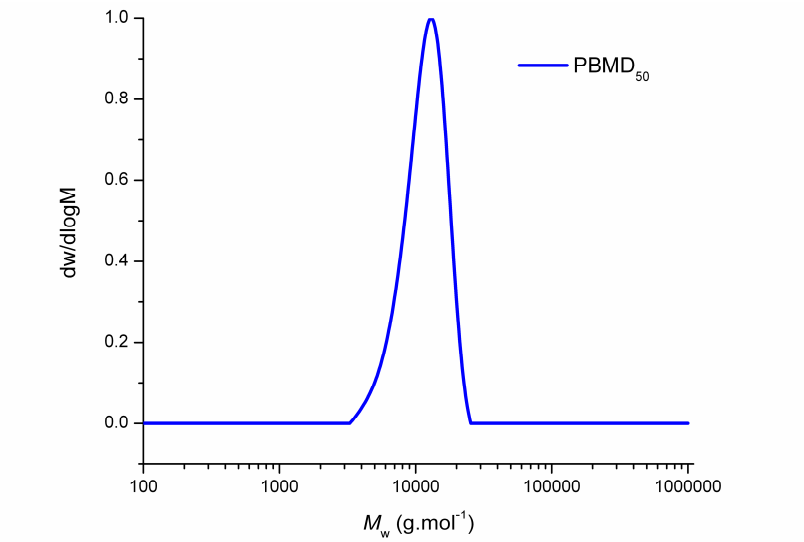

Figure 2.5. GPC trace of PBMD ([M]/[I] = 50) (M_n = 9 900 g.mol^{-1}, PDI = 1.16) prepared by ROP of **6** ([**6**]$_0$ = 0.32 M) catalysed using 15 mol% of **8** and 5 mol% (-)-sparteine as cocatalysts and *neo*-pentanol as the initiator.

2.2.2.3 Ring-Opening Polymerisation studies of BMD – PBMD control

Investigation of the polymerisation control resulted in the observation of linear correlation between M_n and monomer conversion (Figure 2.6), and between M_n and initial monomer to initiator ratio (Figure 2.7). However, notably both charts do not display a zero intercept which indicates that the rate of propagation is greater than the rate of initiation. The isolation of oligomers in attempted single turnover experiments, even in the presence of a large excess of initiator, further confirmed this hypothesis.

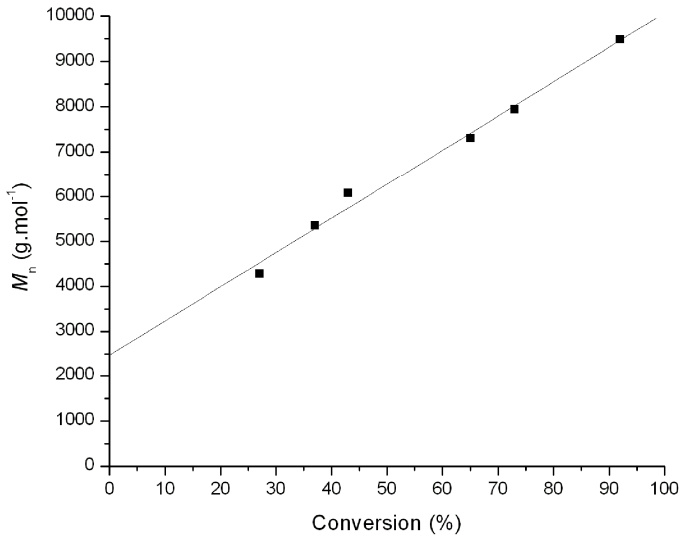

Figure 2.6. Plot of M_n *versus* monomer conversion (measured by ^{1}H NMR spectroscopy) for the ROP of **6** ([M]/[I] = 50, $[\mathbf{6}]_0$ = 0.32 M) using 25 mol% **8** and 5 mol% (-)-sparteine as cocatalysts and *neo*-pentanol as the initiator.

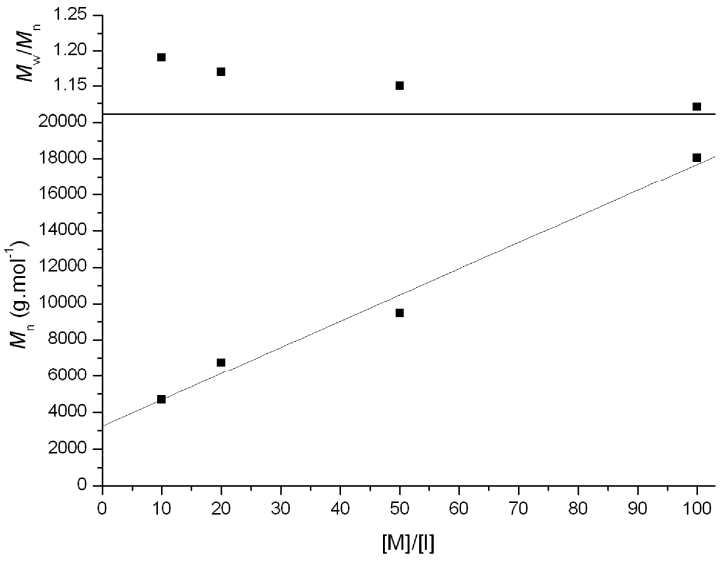

Figure 2.7. Plot of [M]/[I] *versus* M_n and PDI for ROP of **6** ($[\mathbf{6}]_0$ = 0.32 M) using 25 mol% **8** and 5 mol% (-)-sparteine as cocatalysts and *neo*-pentanol as the initiator.

Nonetheless, following standard work-up, analysis of a low degree of polymerisation (DP) PBMD ([M]/[I] = 20) with M_n = 6 750 g.mol^{-1} and PDI = 1.17 (Figure 2.8) by ^{1}H NMR spectroscopy confirmed a DP = 24 polymer based

on the integration of the methylene and *tert*-butyl *neo*-pentanyl resonances at $\delta \sim$ 3.80 and 0.90 ppm respectively against those of the main chain methine protons at δ = 5.65 – 5.54 ppm. Interestingly, the *tert*-butyl resonances of the α-chain end was assigned to two distinctive singlets at δ = 0.92 and 0.89 ppm respectively (Figure 2.9) arising from the non-selective ring-opening of the asymmetric **6** by *neo*-pentanol during the initiation step, clearly demonstrating a notable electronic difference between the two resultant chain ends. Further analysis of the PBMD by MALDI-TOF MS revealed a single distribution centered around m/z = 5394.0 corresponding to a sodium charged DP20 polymer chain with a *neo*-pentanol end group; a regular spacing equal to the molecular weight of the repeat unit of **6** (m/z = 264) demonstrates the lack of significant transesterification of the polymer chains (Figure 2.10).

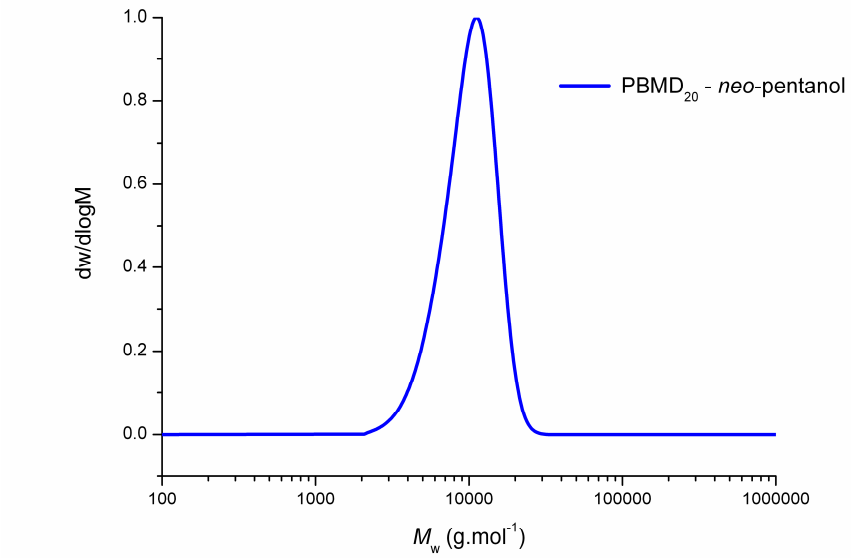

Figure 2.8. GPC trace of PBMD ([M]/[I] = 20) (M_n = 6 750 g.mol^{-1}, PDI = 1.17) prepared by ROP of **6** ([**6**]$_0$ = 0.32 M) catalysed using 25 mol% of **8** and 5 mol% (-)-sparteine as cocatalysts and *neo*-pentanol as the initiator.

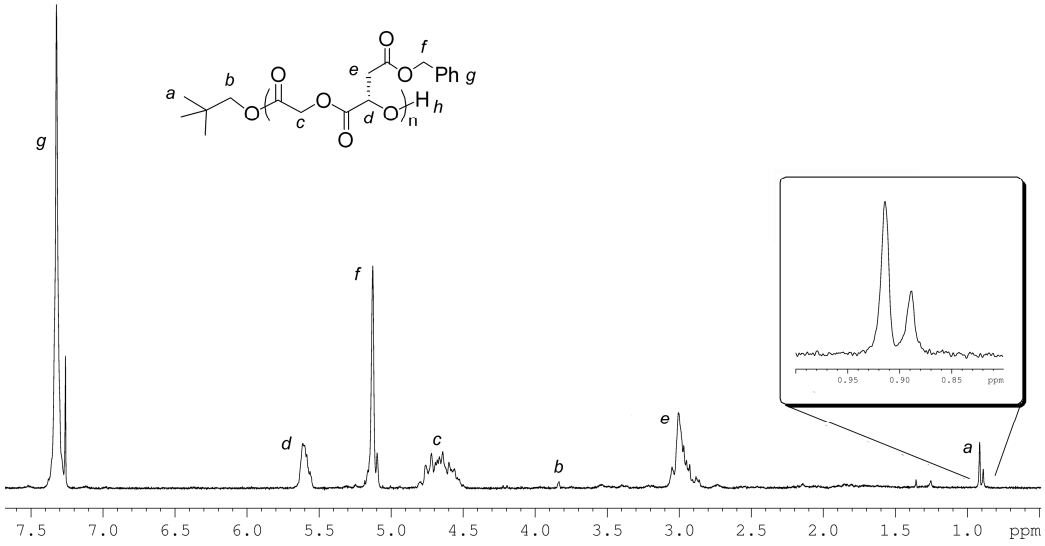

Figure 2.9. ^{1}H NMR spectrum of PBMD ([M]/[I] = 20) initiated from *neo*-pentanol (400 MHz; $CDCl_3$).

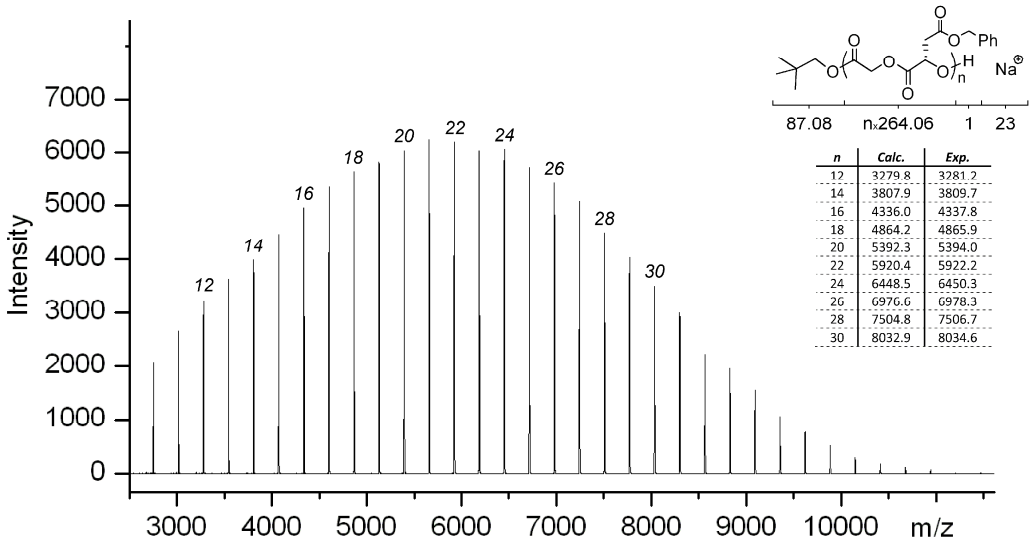

Figure 2.10. MALDI-TOF MS analysis of a PBMD ([M]/[I] = 20) initiated from *neo*-pentanol.

2.2.2.4 Ring-Opening Polymerisation studies of BMD – PBMD α-chain end characterisation

In an attempt to characterise the two different PBMD α-chain groups and thus enable estimation of the preference for ring-opening at either ester of **6**, model compounds **15** and **16** were synthesised *via* condensation reaction of glycolic acid or benzyl α-(*L*)-malate, **4**, with *neo*-pentanol and subsequent acetylation of the remaining alcohol group by treatment with acetyl chloride (Scheme 2.3). Examination of the ^{1}H NMR spectra of **15** and **16** reveal singlet resonances at δ = 0.93 and 0.90 ppm respectively, providing a good correlation to those observed for the PBMD α-chain ends (Figure 2.11). Integration of the α-chain end *tert*-butyl *neo*-pentanyl resonances from three PBMD samples reveals approximately a 2:1 ratio (glycolate:malate opening) which corresponds to a 67 +/- 1% selectivity towards the ring-opening of **6** at the least hindered glycolate ester of the ring.

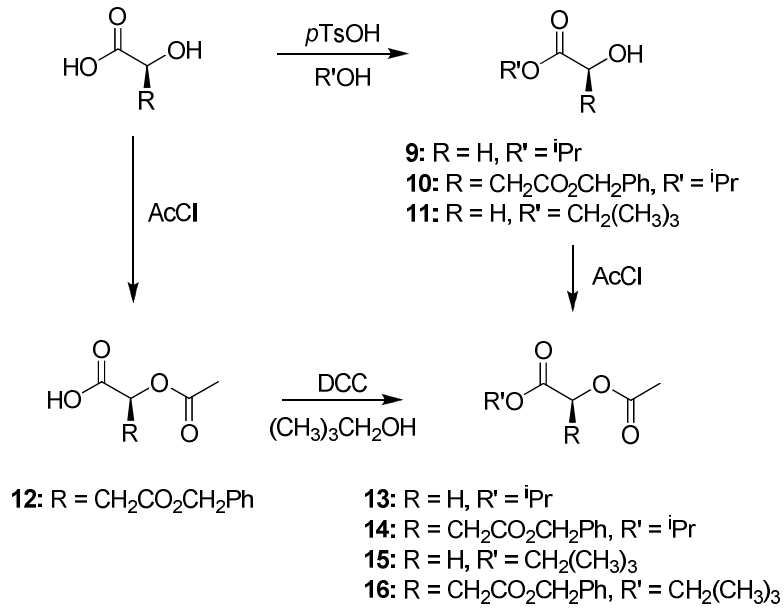

Scheme 2.3. Synthesis of glycolate, **13** and **15**, and benzyl α-(*L*)-malate, **14** and **16**, end-group models.

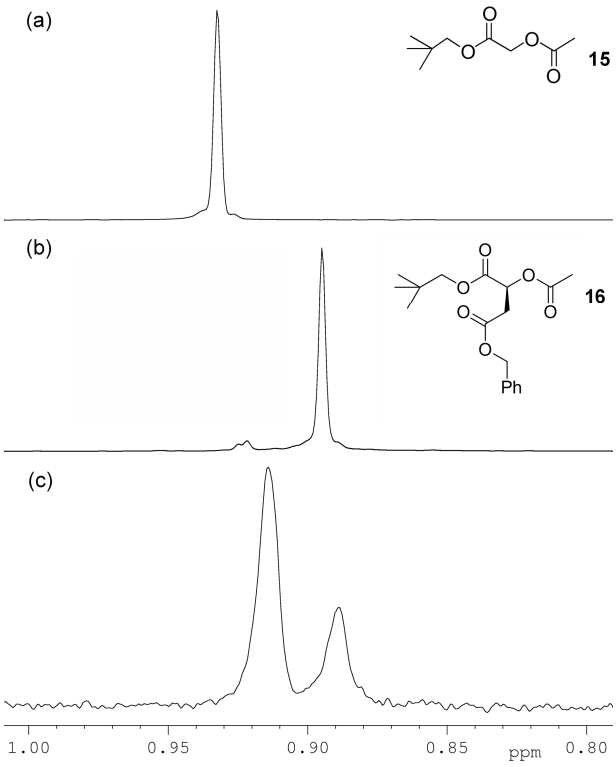

Figure 2.11. Expansion of δ = 0.80 to 1.00 ppm region of ^{1}H NMR spectra (400 MHz; $CDCl_3$) showing the *neo*-pentyl methyl resonances of (a) **15**, (b) **16** and (c) PBMD ([M]/[I] = 20) prepared by the ring-opening polymerisation of **6** initiated from *neo*-pentanol using **8**/(-)-sparteine.

2.2.2.5 Ring-Opening Polymerisation studies of BMD – initiator versatility

In order to further study the initiator efficiency, the ROP of **6** was initiated from a more sterically hindered secondary alcohol, specifically 2-propanol. Interestingly, the ROP of **6** using 2-propanol as the alcoholic initiator required increased loadings of **8**, 35 mol%, and longer reaction times to reach >90% monomer. A range of PBMD with varying [M]/[I] (Table 2.1) were prepared in a comparable manner to that previously described and again correlation of the [M]/[I] (Figure 2.12) and monomer conversion (Figure 2.13) with M_n resulted in a linear relationship with a non-zero intercept.

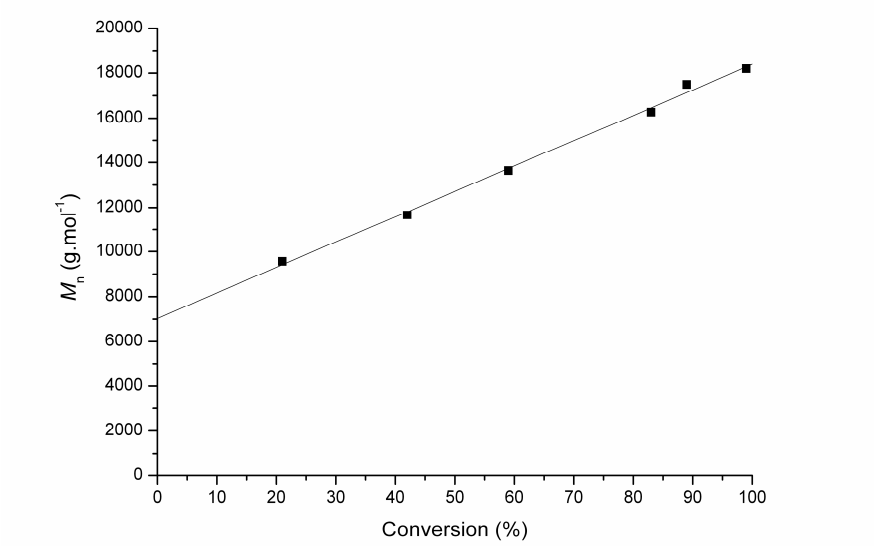

Figure 2.12. Plot of M_n *versus* monomer conversion (measured by ^{1}H NMR spectroscopy) for the ROP of **6** ([M]/[I] = 50, $[\mathbf{6}]_0$ = 0.32 M) using 35 mol% **8** and 5 mol% (-)-sparteine as cocatalysts and 2-propanol as the initiator.

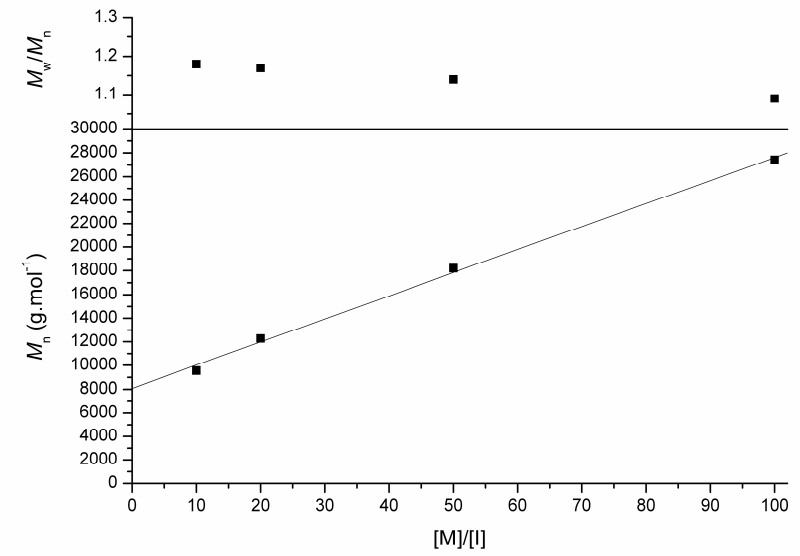

corresponding to a sodium charged DP20 polymer chain with an *iso*-propyl α-chain end (Figure 2.14).

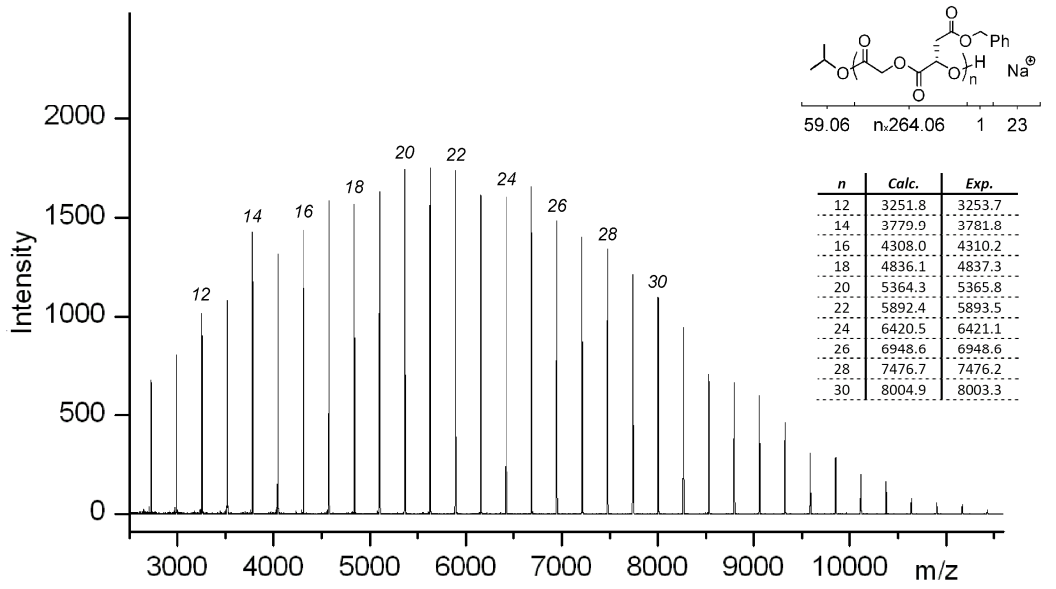

Figure 2.14. MALDI-TOF MS analysis of a PBMD ([M]/[I] = 20) initiated from 2-propanol.

Interestingly, despite the DP (measured by ^{1}H NMR spectroscopy) of the PBMDs again roughly correlating to the [M]/[I] ratio, the M_n of each polymer, as determined by GPC analysis was higher than that obtained when ROP was initiated from *neo*-pentanol (Table 2.1, Figure 2.15 and Figure 2.16). It was tentatively postulated that this discrepancy arises as a consequence of the formation of low molecular weight impurities such as cyclic oligomers occurring during the initiation period, consuming initiating alcohol but producing low molecular weight species that are indistinguishable from PBMD by ^{1}H NMR spectroscopy, thus distorting the measurement of DP with respect to GPC analysis of the polymers.

Table 2.1. Effect of [M]/[I] for *neo*-pentanol *versus* 2-propanol initiation of the ring-opening polymerisation of **6**.[a]

Initiating Alcohol	[M]/[I]	Time (min)	Monomer Conversion (%)	DP[b]	M_n[b] (g.mol^{-1})	M_n[c] (g.mol^{-1})	PDI[c]
neo-Pentanol	10	5[d]	98	13	3 520	4 700	1.19
neo-Pentanol	20	10[d]	98	24	6 420	6 750	1.17
neo-Pentanol	50	20[d]	92	43	11 440	9 490	1.15
neo-Pentanol	100	40[d]	96	-	-	18 070	1.12
2-Propanol	10	6[e]	98	12	3 230	9 530	1.17
2-Propanol	20	12[e]	97	24	6 400	11 020	1.12
2-Propanol	50	25[e]	99	41	10 880	18 200	1.14
2-Propanol	100	50[e]	97	-	-	26 050	1.11

[a] $[\mathbf{6}]_0$ = 0.32 M; 5 mol% (-)-sparteine; $CHCl_3$. [b] Determined by ^{1}H NMR Spectroscopy. [c] Determined by GPC analysis. [d] 25 mol% **8**. [e] 35 mol% **8**.

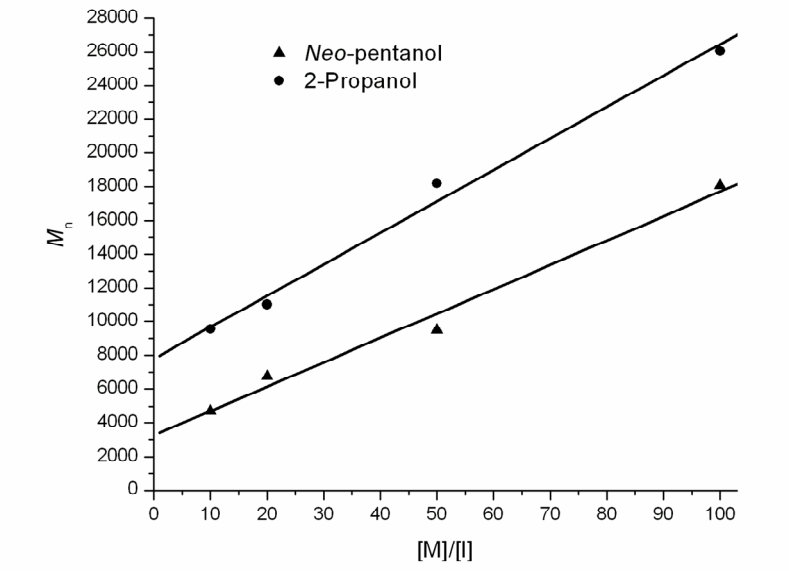

Figure 2.15. Comparison of plots of [M]/[I] *versus* M_n for ROP of **6** ($[\mathbf{6}]_0$ =0.32 M) using 25 and 35 mol% **8** and 5 mol% (-)-sparteine as cocatalysts using *neo*-pentanol (▲) and 2-propanol (●) as the initiators respectively.

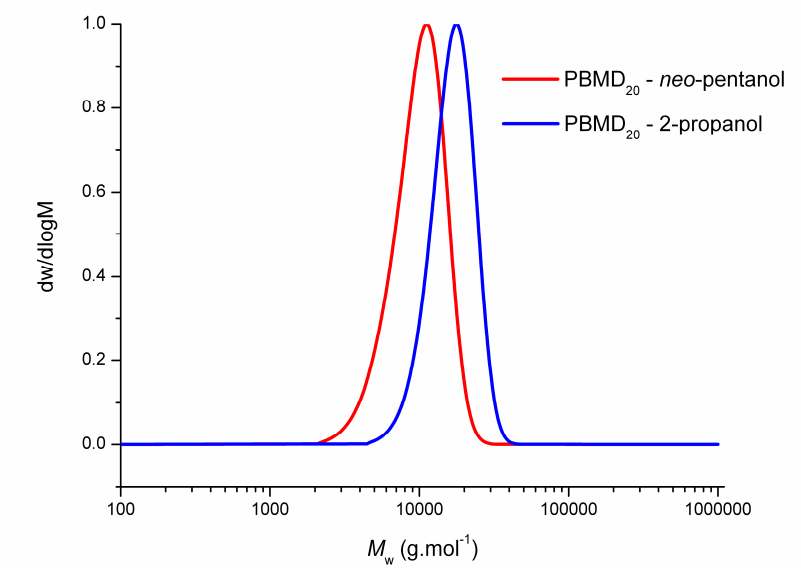

Figure 2.16. Comparison of GPC traces of PBMD ([M]/[I] = 20) initiated from *neo*-pentanol (M_n = 6 750 g.mol^{-1}, PDI = 1.17) (▬) and PBMD ([M]/[I] = 20) initiated from 2-propanol (M_n = 11 020 g.mol^{-1}, PDI = 1.12) (▬) prepared by ROP of **6** ([**6**]$_0$ = 0.32 M) catalysed using 25 and 35 mol% of **8** respectively and 5 mol% (-)-sparteine as cocatalysts

Close analysis of the ^{1}H NMR spectrum of the PBMD again revealed two α-chain end methyl resonances (from the *iso*-propyl group), a doublet at δ = 1.24 ppm and an overlapping doublet of doublets centered at δ = 1.21 ppm (Figure 2.17). Comparison of these to model compounds (Figure 2.18) suggested that, as expected, the doublet at δ = 1.24 ppm results from initial ring-opening of **6** yielding a glycolate ester whereas the overlapping doublet of doublets arises from ring-opening of the **6** generating a malate ester with the adjacent chiral centre leading to the inequivalence of the methyl resonances. Integration of these resonances suggests that initiation from 2-propanol results in a comparable selectivity to *neo*-pentanol of approximately a 69 +/- 1% toward ring-opening of **6** at the less hindered carbonyl. This suggested that the initiator efficiency relates to the molecular weight of the resultant PBMD, the unchanged distribution of glycolate ester to malate ester end groups indicates that steric effects may not be

the primary factor in determining initiator efficiency. To this end the investigations were broadened with respect to initiating alcohol.

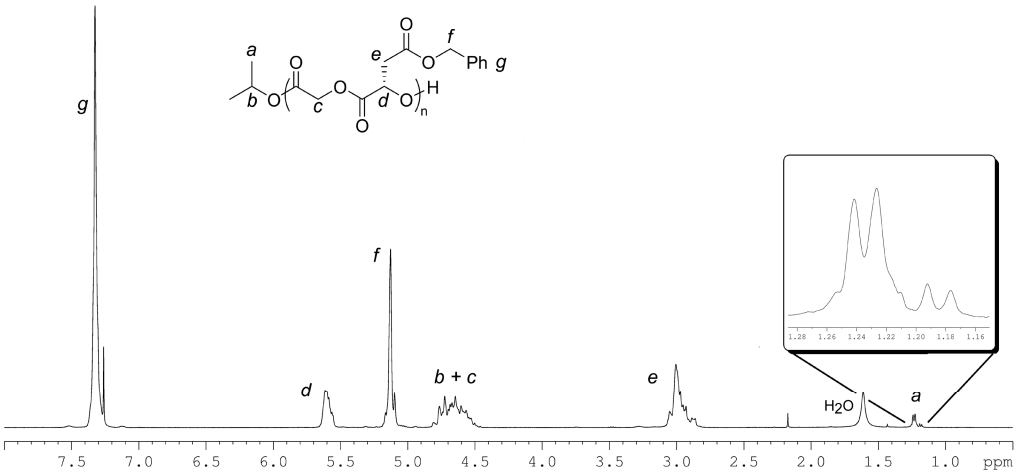

Figure 2.17. ^{1}H NMR spectrum of PBMD ([M]/[I] = 20) initiated from 2-propanol (400 MHz; $CDCl_3$).

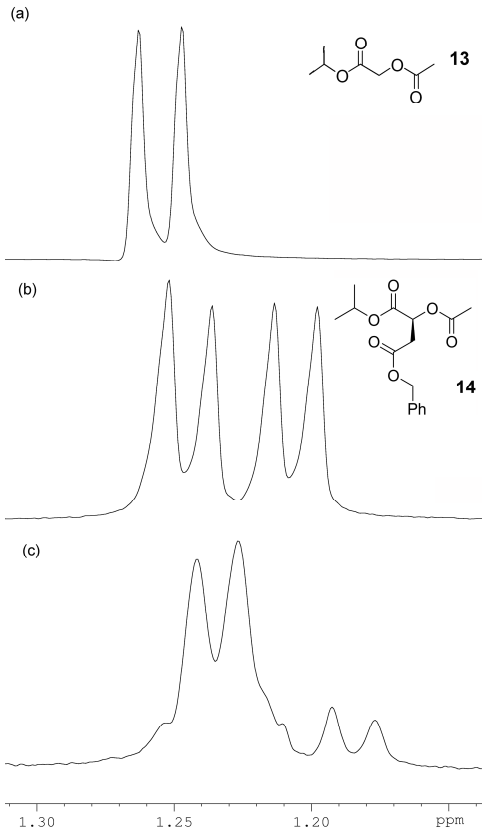

Figure 2.18. Expansion of δ = 1.14 to 1.31 ppm region of ^{1}H NMR spectra (400 MHz; $CDCl_3$) showing the *iso*-propyl methyl resonances of (a) **13**, (b) **14** and (c) PBMD prepared by the ring-opening polymerisation of **6** initiated from 2-propanol using **8**/(-)-sparteine.

Table 2.2. Effect of alcohol initiator in the ring-opening polymerisation of **6**.[a]

Initiating Alcohol	[M]/[I]	Time (min)	DP[b]	M_n[b] (g.mol^{-1})	M_n[c] (g.mol^{-1})	PDI[c]
9	20	6[d]	18	4 870	4 700	1.14
10	20	6[e]	19	5 280	5 650	1.12
Benzyl alcohol	20	8[d]	-	-	5 920	1.17
1-Phenylethanol	20	8[e]	16	4 350	6 600	1.17
neo-Pentanol	20	10[d]	24	6 420	6 750	1.17
Ethanol	20	12[d]	23	6 120	8 800	1.12
2-Propanol	20	12[e]	24	6 400	11 020	1.12
2-Butanol	20	20[e]	28	7 470	13 300	1.10
Benzyl amine	20	8[d]	-	-	7 390	1.19
1,3-Propanediol	20	8[d]	20[f]	10 640	11 380	1.14

[a] $[\mathbf{6}]_0$ = 0.32 M; 5 mol% (-)-sparteine; $CHCl_3$. [b] Determined by ^{1}H NMR Spectroscopy. [c] Determined by GPC analysis. [d] 25 mol% **8**. [e] 35 mol% **8**. [f] DP per alcohol.

Initiation of the ROP of **6** through variation of only the alcoholic initiator (Table 2.2) resulted in a significant spread of PBMD molecular weights. Initiation from benzyl alcohol, ethanol, 1-phenylethanol and 2-butanol ([M]/[I] = 20) resulted in PBMDs with molecular weights of 5 920, 8 800, 6 600 and 13 300 g.mol^{-1} respectively while maintaining low PDIs (Table 2.2). End group fidelity and the DP of the poly(ester)s was confirmed by both MALDI-TOF MS and ^{1}H NMR spectroscopy. Evidently, while the DP (measured by ^{1}H NMR spectroscopy) remains largely invariant, the M_n (determined by GPC) changes dramatically with different alcoholic initiators. These results clearly show that steric hindrance was not the major contributing factor to the correlation of PBMD molecular weight to that predicted from the monomer to initiator ratio. Comparison of a PBMD initiated from 1-phenylethanol to those initiated from ethanol and 2-

propanol revealed that despite being the most sterically hindered, initiation from 1-phenylethanol resulted in a PBMD with the lowest molecular weight (M_n = 6 600 g.mol^{-1}), believed to be a consequence of more efficient initiation resulting from the electron deficient nature of the initiator. It was believed that this initiator efficiency may also be the reason for the required increased loading of **8** and reaction times to reach >90% monomer conversion when the ROP of **6** was initiated from 2-propanol. It was further observed that a correlation between the resulting PBMD molecular weight and the pKa of the initiating alcohol was present with the pKa value of the alcohol having a strong relationship to its initiation efficiency (Figure 2.19).

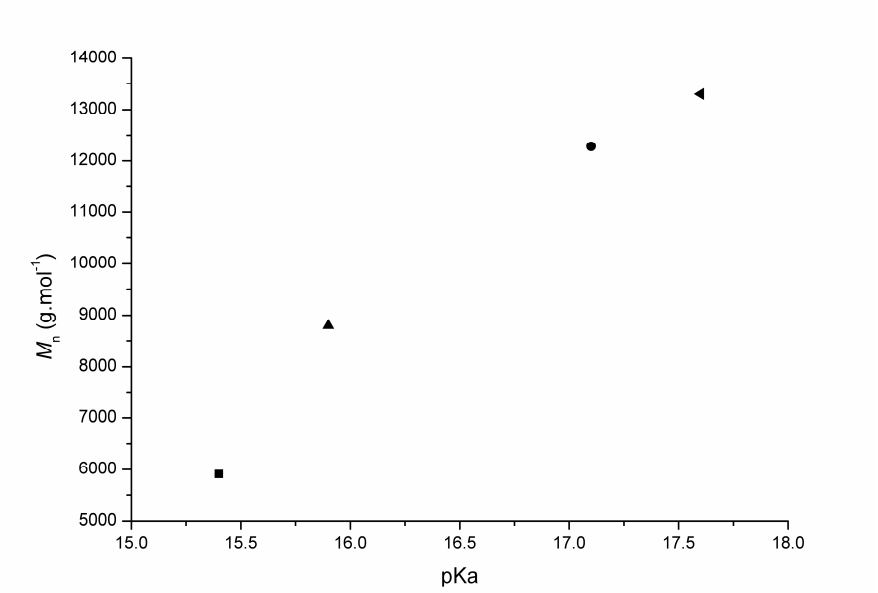

Figure 2.19. Correlation between the observed PBMD M_n (from GPC analysis) and pKa of the initiating alcohols benzyl alcohol (■), ethanol (▲), 2-propanol (●) and 2-butanol (◀) applied in the preparation of PBMD ([M]/[I] = 20).

Further attempts to optimise the initiator efficiency of the polymerisation focused on the synthesis and application of initiators that provided good models for the putative propagating species. To this end, isopropyl-2-hydroxyacetate, **9**, and 4-

benzyl-1-isopropyl 2-hydroxysuccinate, **10**, were applied to initiate the ROP of **6**. Analysis of the resultant PBMDs by GPC revealed the lowest molecular weights, correlating most closely to the DP measured by ^{1}H NMR end group analysis, while maintaining low polydispersities throughout the polymerisation. Poor initiation commonly also leads to a broadening of the PDI of the resultant polymers arising from the rapid propagation of initiated chains with new chains being initiated. In an attempt to investigate these observed effects further, a competition experiment between *neo*-pentanol and 2-propanol initiators was performed. ROP of **6** using a 1:1 molar ratio of alcohols and a target overall [M]/[alcohol] = 10 ([M]/[I] = 20 with respect to each initiating alcohol) resulted in a PBMD with a monomodal distribution with M_n = 6 780 g.mol^{-1} and PDI = 1.18 by GPC analysis, comparable to polymers obtained through initiation from *neo*-pentanol at a [M]/[I] = 20. Close analysis of the poly(ester) by ^{1}H NMR spectroscopy revealed both *neo*-pentanol and 2-propanol α-end groups in a 2:1 ratio. These data suggest that the increased initiator efficiency of *neo*-pentanol compared to 2-propanol results in the majority of the initial ring-opening of **6** occurring with *neo*-pentanol however, the increased rate of initiation of *neo*-pentanol with respect to 2-propanol and relative propagation rates of the more activated PBMD propagating ω-chain ends result in very few new PBMD chains being initiated after the primary initiation event, despite the presence of excess 2-propanol.

Further initiator versatility was investigated through preparation of a telechelic PBMD ([M]/[I] = 40) ([M]/[I] = 20 per alcohol group) by initiation from 1,3-propanediol with the polymerisation achieving 99% monomer conversion within 8 min and the resultant PBMD exhibiting M_n = 11 380 g.mol^{-1} and PDI = 1.14 as

determined by GPC analysis. The initiator tolerance of this ROP was tested with the application of benzyl amine as an initiator successfully realising a PBMD ([M]/[I] = 20) while showing no significant difference in rate or control compared to alcohols reaching 99% monomer conversion in 8 min with M_n = 7 390 g.mol^{-1} and PDI = 1.19.

2.2.2.6 Ring-Opening Polymerisation studies of BMD – Block Copolymer Formation

Further extension of this methodology was investigated to realise the synthesis of block copolymers. Primarily, the synthesis of amphiphilic poly(ethylene oxide)-*b*-PBMD block copolymers by initiation from commercially available monomethylether PEO_{2K} and PEO_{5K} (M_n ~ 2 000 and 5 000 g.mol^{-1} respectively) macroinitiators was investigated. ROP of **6** ([M]/[I] = 20) with PEO_{2K}-monomethylether (M_n = 3 400 g.mol^{-1}, PDI = 1.05) as the initiator resulted in >99% monomer conversion after 30 min. GPC analysis of the copolymer confirmed successful PBMD chain growth (PEO_{2K}-*b*-$PBMD_{20}$; M_n = 9 260 g.mol^{-1}, PDI = 1.13) (Figure 2.20). Successful block copolymer preparation was also achieved with initiation from monomethylether PEO_{5K} (M_n = 8 200 g.mol^{-1}, PDI = 1.04) realising the desired block copolymer PEO_{5K}-*b*-$PBMD_{20}$ (M_n = 12 340 g.mol^{-1}, PDI = 1.15). Chain growth of **6** ([M]/[I] = 20) from monomethylether PEO_{2K} and PEO_{5K} was also confirmed by ^{1}H NMR spectroscopy indicating the presence of both the PEO methylene and the PBMD malate resonances at δ = 3.64 ppm and 3.08 – 2.85 ppm respectively.

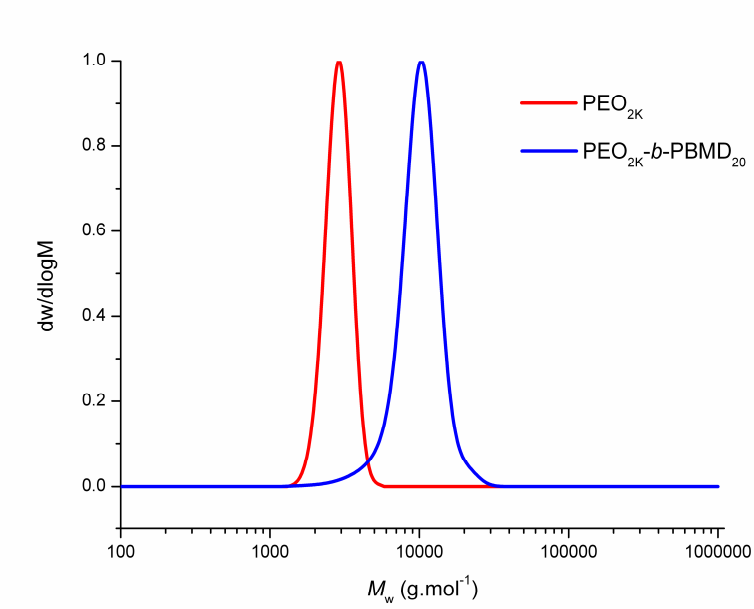

Figure 2.20. GPC traces of PEO_{2K} (M_n = 3 400 g.mol^{-1}, PDI = 1.05) (—) and PEO_{2K}-*b*-$PBMD_{20}$ (M_n = 9 260 g.mol^{-1}, PDI = 1.13) (—) prepared by ROP of **6** ([**6**]$_0$ = 0.32 M) catalysed using 25 mol% of **8** and 5 mol% (-)-sparteine as cocatalysts and monomethylether PEO_{2K} as a macroinitiator.

Block copolymers were also demonstrated to be accessible by using poly(*L*-lactide)s, PLLA, as macroinitiators for the polymerisation of **6** ([M]/[I] = 20). PLLAs ([M]/[I] = 20 and 50) were synthesised by ROP of *L*-lactide using identical conditions as described above with 35 mol% **8** and 5 mol% (-)-sparteine, initiated from *neo*-pentanol. Complete monomer conversion for [M]/[I] = 20 and 50 was achieved after 30 min and 75 min respectively. Chain growth of **6** ([M]/[I] = 20) from $PLLA_{20}$-OH was confirmed by ^{1}H NMR spectroscopy showing the presence of both the PLLA methyl and the PBMD malate resonances at δ = 1.58 and 3.08 – 2.85 ppm respectively. Additionally, GPC analysis revealed an increase in molecular weight from 8 360 g.mol^{-1} ($PLLA_{20}$-OH) to 19 080 g.mol^{-1} ($PLLA_{20}$-*b*-$PBMD_{20}$) while maintaining a low PDI (Figure 2.21). Chain growth from $PLLA_{50}$-OH (M_n = 14 020 g.mol^{-1}, PDI = 1.09) was

also achieved resulting in the successful synthesis of $PLLA_{50}$-*b*-$PBMD_{20}$ (M_n = 24 160 g.mol^{-1}, PDI = 1.07).

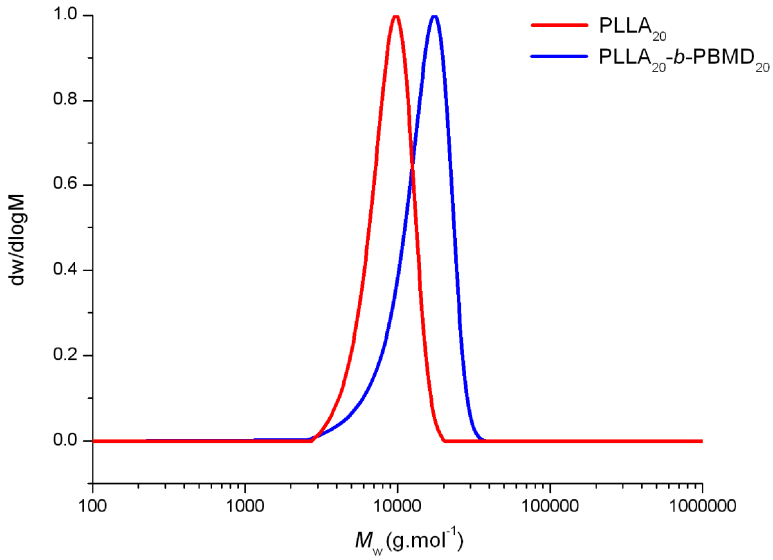

Figure 2.21. GPC traces of $PLLA_{20}$-OH (M_n = 8 360 g.mol^{-1}, PDI = 1.11) (—) and $PLLA_{20}$-*b*-$PBMD_{20}$ (M_n = 19 080 g.mol^{-1}, PDI = 1.18) (—) prepared ROP of **6** ([**6**]$_0$ = 0.32 M) catalysed using 35 mol% of **8** and 5 mol% (-)-sparteine as cocatalysts and $PLLA_{20}$-OH as a macroinitiator.

2.2.3 Deprotection of PBMD – Formation of PGMA

Deprotection of the pendant carboxylic acid groups of PBMD ([M]/[I] = 20) (M_n = 5 950 g.mol^{-1}; PDI = 1.16) was accomplished by hydrogenolysis using H_2 over Pd/C and resulted in hydrophilic poly(glycolic acid-*co*-malic acid)s (PGMA) (Scheme 2.4). Clean and complete removal of the benzyl protecting groups was deduced from the disappearance of all the aromatic and benzylic signals from both the ^{1}H (Figure 2.22) and ^{13}C NMR spectra. Further confirmation was obtained from the change in solubility of the resulting polymer from the PBMD (soluble in $CHCl_3$, insoluble in MeOH) to the PGMA (soluble in MeOH, insoluble in $CHCl_3$). This process did not result in degradation of the poly(ester) backbone, as shown by the lack of resonances associated with changes to the

electronic environment of the methine protons associated with a neighboring hydroxy proton in the ^{1}H NMR spectrum that would be apparent upon cleavage of the backbone. Furthermore, analysis of the polymer by aqueous GPC showed a single distribution with a M_n = 2 410 g.mol^{-1} and PDI = 1.12 (compared to PEG standards). It was postulated that the hydrophobic nature of the poly(ester) backbone results in tightly coiled polymers thus leading to low molecular weight values by aqueous GPC analysis.

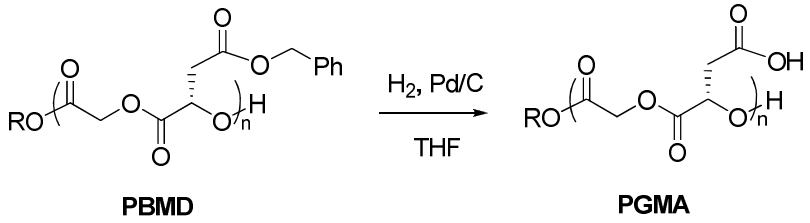

Scheme 2.4. The synthesis of poly(glycolic acid-*co*-malic acid), PGMA, from the deprotection of poly(3-(*S*)-[(benzyloxycarbonyl)methyl]-1,4-dioxane-2,5-dione), PBMD, using hydrogenolysis with H_2 and Pd/C.

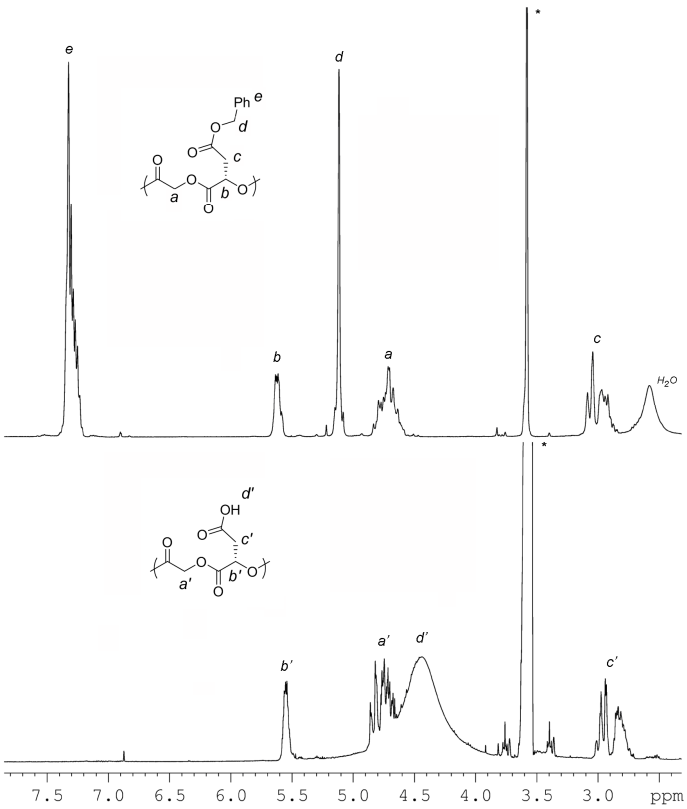

Figure 2.22. ^{1}H NMR spectra of (i) $PBMD_{20}$ and (ii) $PGMA_{20}$ (d^8-THF, 400 MHz; * indicates residual solvent signal).

2.2.4 Degradation of PGMA

Degradations were performed in H_2O on PGMA ([M]/[I] = 20) at a concentration of 0.55 mmol.L^{-1}. The degradations were monitored *via* acid-base titration using a 0.50 mmol.L^{-1} aqueous NaOH solution with four drops of a phenolphthalein in methanol solution as the pH indicator. Phenolphthalein produces a strong pink color when the pH of the solution reaches 8.2 thus providing a simple method with which to determine the extent of the degradation. Degradation was complete after six days determined when three equivalents to monomer of the aqueous NaOH solution was required to neutralise the solution. Aqueous GPC analysis provided a simple method to monitor the molecular weight loss during the degradation. The M_n gradually decreased over time along with a broadening of the PDI that plateaued after six days in agreement with the titration experiment. Examination of ^{1}H NMR spectra during the degradation in D_2O demonstrates a gradual reduction of resonances attributed to PGMA at δ = 5.93 – 5.85 and 3.32 – 3.22 ppm with a corresponding increase of new resonances at δ = 4.54 – 4.48 and 3.19 – 3.01 ppm resulting from the degradation products. Mass spectrometry of the degradation solution after six days confirmed the presence of only a range of small molecular weight degradation products including malic acid ([M]+Na = 157.01), glycolic acid dimer ([M]+Na = 157.01), malic/glycolic acid dimer ([M]+Na = 215.02) and malic acid dimer ([M]+Na = 273.02).

2.3 Conclusions

In conclusion, an improved synthesis of both BMD, **6**, and malide, **7**, monomers from *L*-malic acid has been successfully demonstrated. Homopolymerisation of **6** using the organocatalytic **8**/(-)-sparteine system enabled the synthesis of

functional poly(ester)s with pendant benzyl protected carboxylic acid groups to high monomer conversions in the absence of transesterification side reactions. The choice of initiator was demonstrated to be important such that initiating species that more closely resembled the propagating species led to lower molecular weight polymers. Nonetheless, the versatility of the polymerisation system was shown with successful initiation from a range of alcohols and amines including the use of PEO and PLLA as macroinitiators in the preparation of block copolymers. Removal of the benzyl protecting groups was successful without any polymer backbone scission to yield hydrophilic poly(ester)s and degradation studies of the resultant PGMAs in H_2O was demonstrated to occur within six days as determined by titration, aqueous GPC analysis, ^1H NMR spectroscopy and mass spectrometry. The derivation of this versatile functional poly(ester) from a biorenewable resource provides a potential route to a range of other functional poly(ester)s *via* this platform.

2.4 References

(1) Pounder, R. J.; Dove, A. P. *Polym. Chem.* **2010**, *1*, 260.

(2) Coulembier, O.; Degée, P.; Hedrick, J. L.; Dubois, P. *Prog. Polym. Sci.* **2006**, *31*, 723.

(3) Kimura, Y.; Shirotani, K.; Yamane, H.; Kitao, T. *Macromolecules* **1988**, *21*, 3338.

(4) Kimura, Y.; Shirotani, K.; Yamane, H.; Kitao, T. *Polymer* **1993**, *34*, 1741.

(5) Yamaoka, T.; Hotta, Y.; Kobayashi, K.; Kimura, Y. *Int. J. Biol. Macromol.* **1999**, *25*, 265.

(6) Lee, J.; Cho, E. C.; Cho, K. *J. Controlled Release* **2004**, *94*, 323.

(7) Ouchi, T.; Fujino, A. *Makromol. Chem.* **1989**, *190*, 1523.

(8) Dechy-Cabaret, O.; Martin-Vaca, B.; Bourissou, D. *Chem. Rev.* **2004**, *104*, 6147.

(9) Stanford, M. J.; Dove, A. P. *Chem. Soc. Rev.* **2010**, *39*, 486.

(10) Pratt, R. C.; Lohmeijer, B. G. G.; Long, D. A.; Lundberg, P. N. P.; Dove, A. P.; Li, H. B.; Wade, C. G.; Waymouth, R. M.; Hedrick, J. L. *Macromolecules* **2006**, *39*, 7863.

(11) Dove, A. P.; Pratt, R. C.; Lohmeijer, B. G. G.; Waymouth, R. M.; Hedrick, J. L. *J. Am. Chem. Soc.* **2005**, *127*, 13798.

(12) Jing, F.; Hillmyer, M. A. *J. Am. Chem. Soc.* **2008**, *130*, 13826.

(13) Allinger, N. L.; Zalkow, V. *J. Org. Chem.* **1960**, *25*, 701.

Chapter 3 - Mechanistic studies into the ring-opening polymerisation of an *O*-carboxyanhydride monomer derived from malic acid.

3.1 Introduction

The ring-opening polymerisation of difunctionalised cyclic diester monomers such as 3,6-(*S*)-[di(benzyloxycarbonyl)methyl]-1,4-dioxane-2,5-dione (malide) provides a significant challenge, largely a consequence of the high steric hindrance and low ring strain of the monomer. Along with providing significantly reduced accessibility to the ester moieties of cyclic diester monomers, the increased steric bulk of the ring-substituents also results in stabilisation of the ring-closed form relative to its linear counterpart and thus limiting the exothermicity of the ring-opening process.[1-2] As ROP is governed by thermodynamic equilibrium, this effect results in a higher critical concentration of the monomer reflected in a lower yield of the linear polymer thus severely hindering ring-opening. Recent developments have realised the synthesis and ROP of 1,3-dioxolane-2,5-diones that provide activated equivalents of cyclic diesters resulting in the simple preparation of analogous poly(ester)s. Recently Bourissou and coworkers reported the synthesis and ROP of 5-(*S*)-methyl-1,3-dioxolane-2,4-dione (*L*-lacOCA) the activated *O*-carboxyanhydride equivalent of *L*-lactide from *L*-lithium lactate and diphosgene (Scheme 3.1). ROP of *L*-lacOCA mediated by 4-dimethylaminopyridine (DMAP) at 25 °C resulted in well-defined poly(*L*-lactide) (PLLA) in minutes (*e.g* [M]/[I] = 20; M_n = 2 110 g.mol^{-1}; PDI = 1.20). Unlike all other functional cyclic ester monomers, the polymerisation of *O*-carboxyanhydrides is not complicated by reduced polymerisation activity resulting from steric crowding as the polymerisation is entropically driven through the liberation of CO_2 during the process rather than being enthalpically driven through the release of ring strain.[3] Bourissou, Martin-Vaca and coworkers also reported the synthesis and ROP of *L*-gluOCA (**XXXII**) *via* similar procedures as *L*-lacOCA from *O*-benzyl-*L*-glutamic acid realising a well-defined

functional poly(ester) mediated with DMAP at 25 °C in minutes (*e.g* [M]/[I] = 20; M_n = 3 500 g.mol^{-1}; PDI = 1.19) (Scheme 3.1 and 3.2).[4]

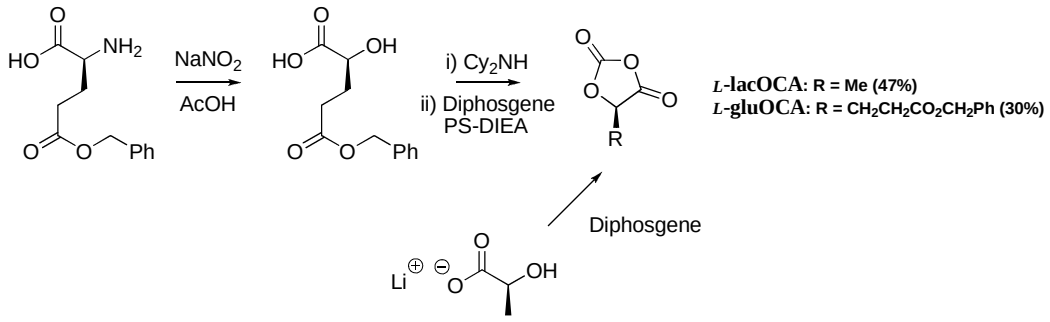

Scheme 3.1. The synthesis of functional 1,3-dioxolane-2,5-diones *L*-lacOCA and *L*-gluOCA (**XXXII**) with overall yield in parentheses.

As well as its homopolymerisation, *L*-gluOCA was also successfully copolymerised with *L*-lacOCA resulting in the controlled synthesis of statistical and block copolymers that were capable of subsequent deprotection through hydrogenolysis providing polyesters suitable for possible post-polymerisation modifications (Scheme 3.2).[4] Interestingly, *L*-gluOCA proved slightly more reactive than *L*-lacOCA which was a marked contrast to the pronounced deactivation resulting from the introduction of pendant functional groups to 1,4-dioxane-2,5-diones.

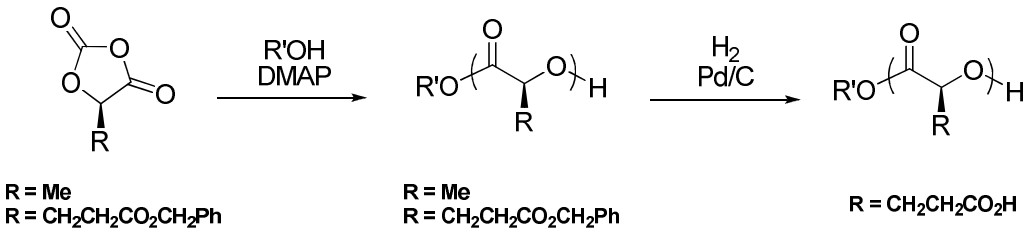

Scheme 3.2. ROP of functional 1,3-dioxolane-2,5-diones and subsequent deprotection.

A detailed computational investigation comparing the DMAP-catalysed ROP of both lactide and lacOCA has been reported. In both cases it was predicted that the base activation of the initiating/propagating alcohol was much more energetically favourable than the nucelophilic activation of the monomers. The key role of multiple hydrogen bonding was evidenced, as well as the possibility of DMAP acting as a bifunctional catalyst (Figure 3.1). Comparison of anhydrides and *O*-carboxyanhydrides suggested that competition between nucleophilic and basic pathways is governed by subtle effects, such as the tertiary/primary class of the alcohol and the cyclic/acyclic nature of the substrate.[5]

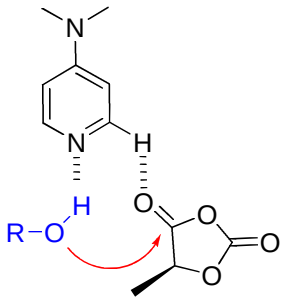

Figure 3.1. DMAP acting as a possible bifunctional catalyst in the ROP of *L*-lacOCA.

This work is focused on the ROP of monomers derived from malic acid. Given the low reactivity of malide towards ROP, it was hypothesised that the chemistry employed in the synthesis and ROP of previously reported functional 1,3-dioxolane-2,5-diones could be applied in preparation of novel monomers from malic acid. Herein the synthesis and ROP of 5-(*S*)- and 5-(*R*)-[(benzyloxycarbonyl)methyl]-1,3-dioxolane-2,4-diones (*L*-malOCA, ***L*-17** and *D*-malOCA, ***D*-17**, respectively) from commercially available *L*- and *D*-malic acid respectively is reported providing the activated equivalents of previously reported

3,6-(*S*)-[di(benzyloxycarbonyl)methyl]-1,4-dioxane-2,5-dione (**XX**, malide). Investigation into application of pyridine based catalysts to mediate the controlled ROP of both enantiopure malOCAs resulting in poly(benzyl α-malate) (PBMA) capable of deprotection to yield the highly desirable hydrophilic poly(malic acid) (PMA) was undertaken.

3.2 Results and Discussion

3.2.1 Synthesis of 5-(S)- and 5-(R)-[(benzyloxycarbonyl)methyl]-1,3-dioxolane-2,4-dione, L-malOCA and D-malOCA

The synthesis of 5-(*S*)-[(benzyloxycarbonyl)methyl]-1,3-dioxolane-2,4-dione (*L*-malOCA, ***L*-17**) was achieved using β-benzyl α-(*L*)-malate, **4**, which in turn was realised *via* the improved synthesis discussed in chapter 2 from *L*-malic acid in 3 steps in a 48% yield (Scheme 3.3). The procedure was also successfully applied to *D*-malic acid in the synthesis of the β-benzyl α-(*D*)-malate enantiomer (*D*-malOCA, ***D*-17**) in comparable yields. Intramolecular cyclisation of each enantiomer of **4** with diphosgene in the presence of catalytic activated carbon in dry THF resulted in the isolation of both ***L*-17** and ***D*-17** in 68% and 65% yields respectively (Scheme 3.3).

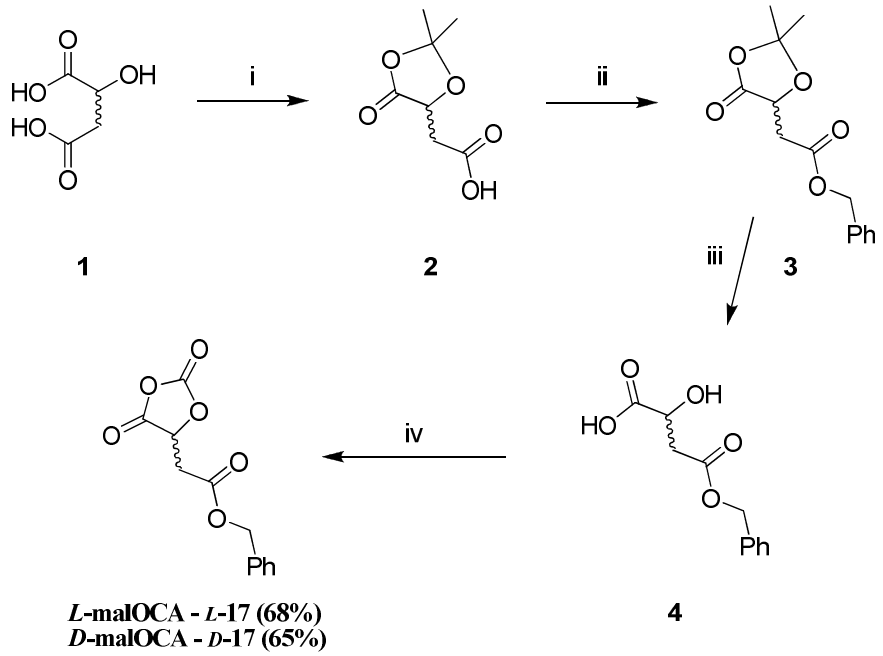

Scheme 3.3. Synthesis of 5-(*S*)- and 5-(*R*)-[(benzyloxycarbonyl)methyl]-1,3-dioxolane-2,4-dione, ***L*-17** and ***D*-17**, from *L*- and *D*-malic acid respectively, **1**. Conditions: (i) $Me_2C(OMe)_2$, *p*TsOH; (ii) $PhCH_2Br$, NEt_3, Acetone; (iii) AcOH, THF/H_2O; (iv) Diphosgene, activated carbon, THF.

Representative ^{1}H NMR spectra of **4** and *L*-malOCA are shown in Figure 3.2. The methine proton of **4** appears as at δ = 4.58 ppm, while clear signals at δ = 7.35, 5.18 and 2.99 - 2.90 ppm are characteristic of the benzyl group and the methylene protons of the malate unit respectively. The chemical shift of the methine proton provides simple confirmation of formation of **17** with a distinctive downfield shift of the methine proton shifts to δ = 5.09 ppm upon cyclisation. No significant change in the remaining chemical shifts compared to **4** (Figure 3.2) are observed. Retention of the stereochemistry in the synthesis of both *L*- and *D*-malOCA from malic acid was confirmed through measurement of their specific rotation *via* polarimetry observing $[\alpha]_D^{33}$ values of -21.9° (in $CHCl_3$, c = 5.96 g.L^{-1}) and +20.9° (in $CHCl_3$, c = 5.98 g.L^{-1}) respectively.

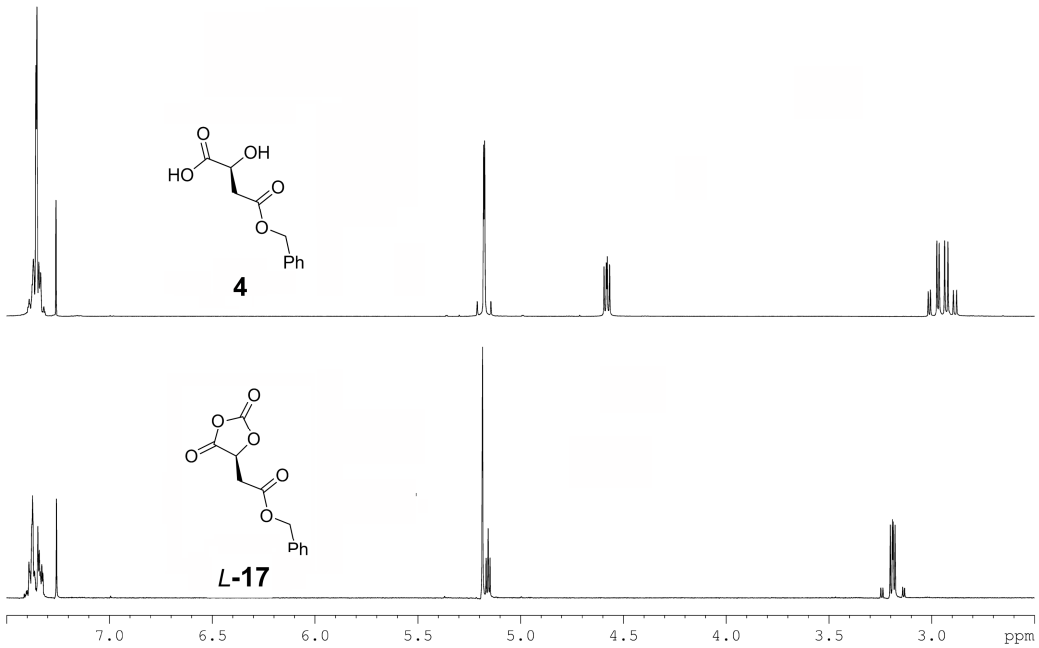

Figure 3.2. ^{1}H NMR spectrum of **4** and ***L*-17** (400 MHz; $CDCl_3$).

3.2.2 Ring-Opening Polymerisation studies of L-malOCA – 4-dimethylaminopyridine (DMAP)

As previously described, *L*-malOCA provides an activated equivalent of 3,6-(*S*)-[di(benzyloxycarbonyl)methyl]-1,4-dioxane-2,5-dione (*L*-malide), providing an analogous route into poly(benzyl α-(*L*)-malate) (P(*L*-BMA)). DMAP was initially applied as a catalyst in the investigation of the ROP of ***L*-17** at 25 °C in CH_2Cl_2 solution, conditions successfully applied to the ROP of *L*-lacOCA and *L*-gluOCA (Scheme 3.4). ^{1}H NMR spectroscopy provided a convenient method for monitoring the progress of the polymerisation by observation of the reduction of the methine resonance at δ = 5.09 ppm and the methylene resonance of the malate unit at δ = 3.13 ppm of the monomer and the appearance of the corresponding broad multiplets at δ = 5.61 – 5.51 and 3.05 – 2.78 ppm respectively in P(*L*-BMA). Upon completion of the allotted time, polymerisations were quenched *via* a 1.0 M $HCl_{(aq)}$ wash to remove DMAP. The polymers were subsequently precipitated into ice cold petroleum ether (b.p. 40-60 °C).

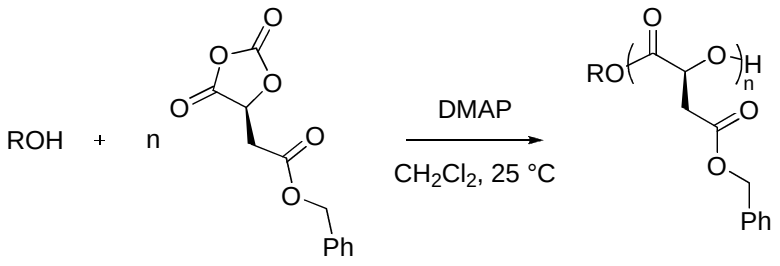

***L*-17** **P(*L*-BMA)**

Scheme 3.4. Ring-opening polymerisation of 5-(*S*)-[(benzyloxycarbonyl)methyl]-1,3-dioxolane-2,4-dione, ***L*-17**, using DMAP.

Initial studies investigated the ROP of ***L*-17** with initiation from *neo*-pentanol in the presence of DMAP as catalyst at a 1:1 ratio to initiating alcohol. At a

monomer-to-initiator ratio of 20 ([M]/[I] = 20), the ROP of ***L*-17** achieved >90% monomer conversion after only one minute with GPC analysis of the resultant P(*L*-BMA)$_{20}$ indicating that the polymerisation was well controlled, displaying a number-average molecular weight (M_n) of 3 730 g.mol^{-1} with a polydispersity (PDI) of 1.19 (Figure 3.3).

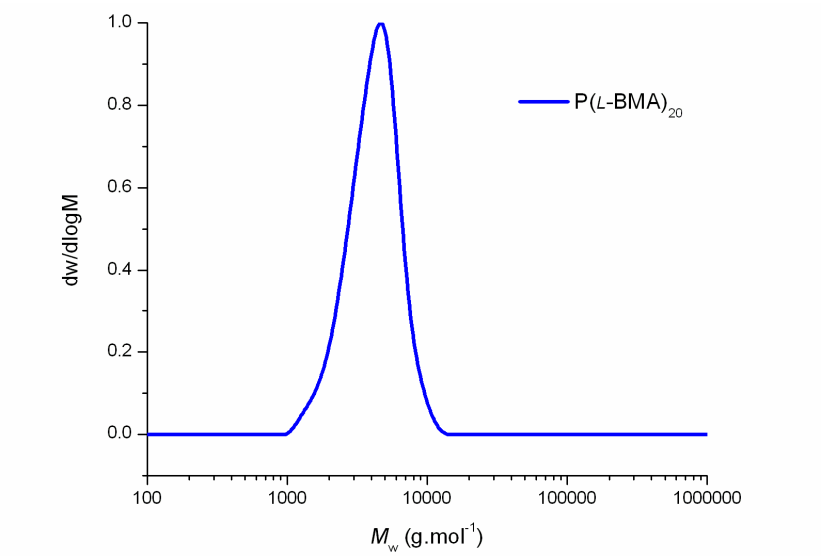

Figure 3.3. GPC trace of P(*L*-BMA)$_{20}$ (M_n = 3 727 g.mol^{-1}, PDI = 1.19) prepared by ROP of ***L*-17** ([***L*-17**]$_0$ = 0.32 M) catalysed with 5 mol% DMAP using *neo*-pentanol as the initiator.

Investigation of the 'living' characteristics of the polymerisation resulted in the observation of a linear correlation between M_n and initial monomer to initiator ratio (Figure 3.4), however, a plot of M_n *versus* monomer conversion was unachievable as a consequence of the high rate of the ROP. Further confirmation of the 'living' characteristics of the ROP was obtained through a second-feed experiment in which to a P(*L*-BMA) macroinitiator initiated from *neo*-pentanol ([M]/[I] = 20) (M_n = 3 730 g.mol^{-1}; PDI = 1.19), the further ROP of ***L*-17** ([M]/[I] = 20) enabled a chain extended P(*L*-BMA)$_{40}$ to be isolated that exhibited a double molecular weight (M_n = 7 390 g.mol^{-1}) while maintaining a low PDI of 1.20.

Leaving the resultant P(*L*-BMA)$_{40}$ for 2 h (24 times longer than required to reach >90% monomer conversion) in the presence of DMAP resulted in negligible changes in both the molecular weight (M_n = 7 050 g.mol^{-1}) and polydispersity (PDI = 1.19) suggesting that transesterification side reactions were minimal despite full monomer consumption (Figure 3.5).

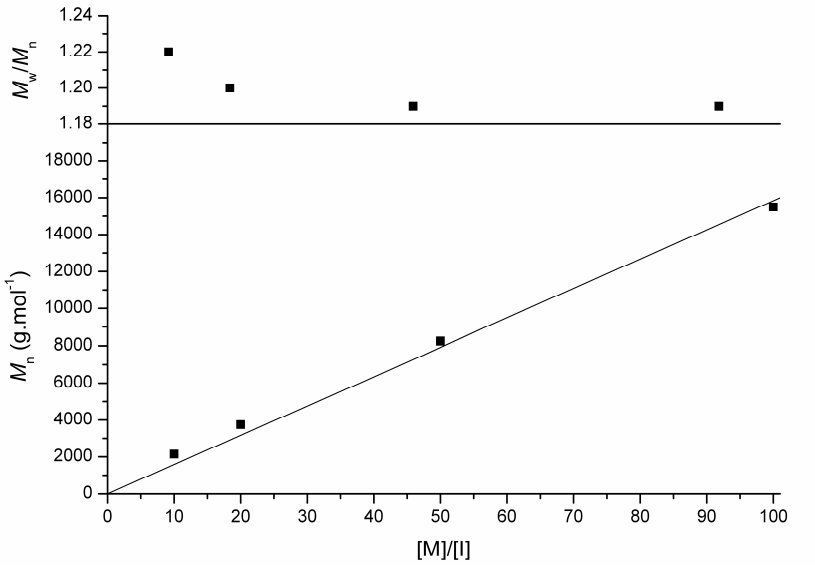

Figure 3.4. Plot of [M]/[I] *versus* M_n and PDI for ROP of ***L*-17** ([***L*-17**]$_0$ = 0.32 M) using 5 mol% DMAP as the catalyst and *neo*-pentanol as the initiator at a ratio of 1:1.

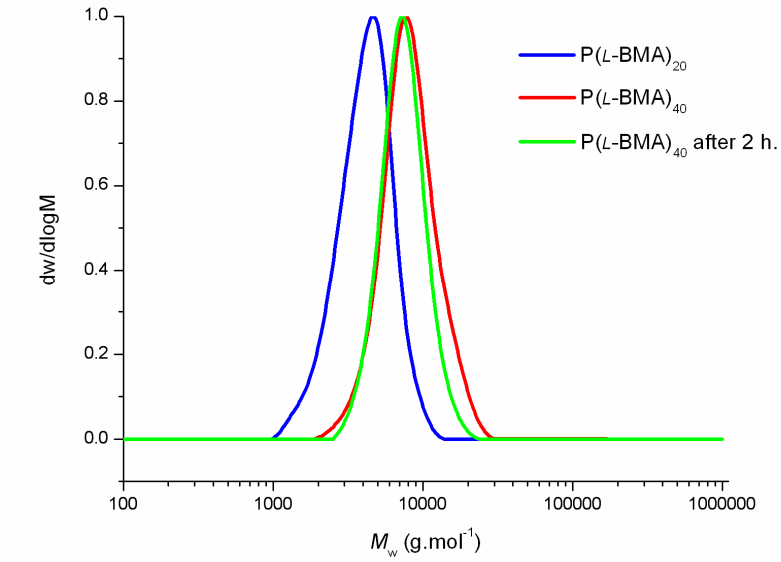

Figure 3.5. GPC traces of P(*L*-BMA)$_{20}$ (M_n = 3 730 g.mol^{-1}, PDI = 1.19) (—), P(*L*-BMA)$_{40}$ (M_n = 7 390 g.mol^{-1}, PDI = 1.20) (—) and P(*L*-BMA)$_{40}$ (M_n = 7 050 g.mol^{-1}, PDI = 1.19) (—) after 2 h prepared by ROP of ***L*-17** ([***L*-17**]$_0$ = 0.32 M) catalysed with 5 mol% DMAP using *neo*-pentanol as the initiator.

^{1}H NMR spectroscopy of a P(*L*-BMA) ([M]/[I] = 20; M_n = 4 210 g.mol^{-1}; PDI = 1.22) confirmed a DP = 23 polymer based on the integration of the *tert*-butyl *neo*-pentanyl resonances at δ = 0.87 ppm against those of the main chain methine protons at δ = 5.55 ppm (Figure 3.6). Further analysis of the polymer by MALDI-TOF MS revealed a single distribution centered around m/z = 4234.3 which corresponds to a sodium charged DP20 polymer chain with a *neo*-pentanol end group; a regular spacing equal to the molecular weight of the repeat unit of benzyl α-(*L*)-malate (m/z = 206) demonstrates the lack of significant transesterification of the polymer chains (Figure 3.7).

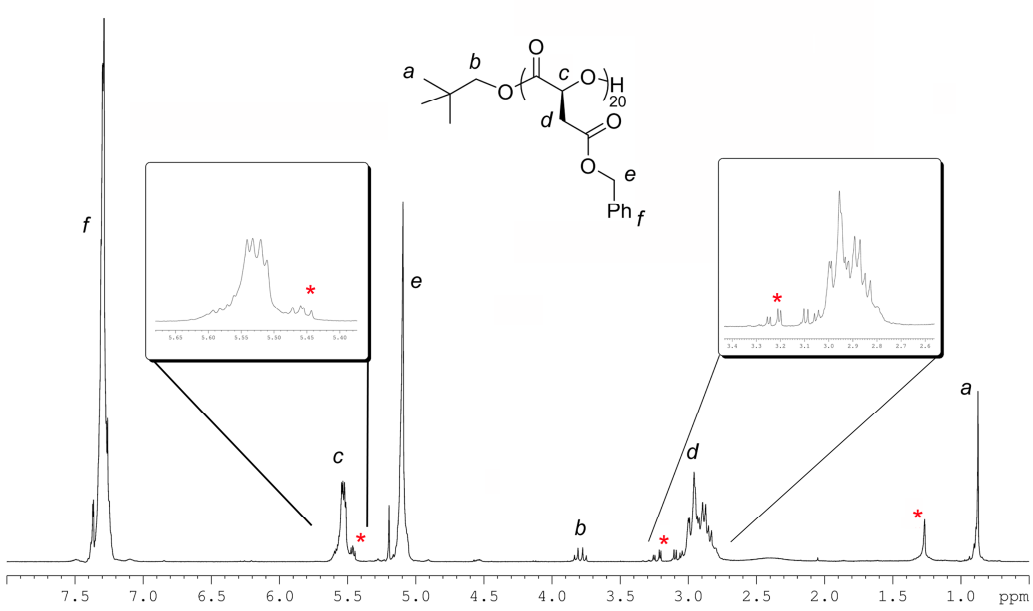

Figure 3.6. ^{1}H NMR spectrum of a P(*L*-BMA)$_{20}$ (M_n = 4 210 g.mol^{-1}, PDI = 1.22) prepared by ROP of ***L*-17** ([***L*-17**]$_0$ = 0.32 M) catalysed with 5 mol% DMAP using *neo*-pentanol as the initiator and the presence of impurities (*) (400 MHz; $CDCl_3$).

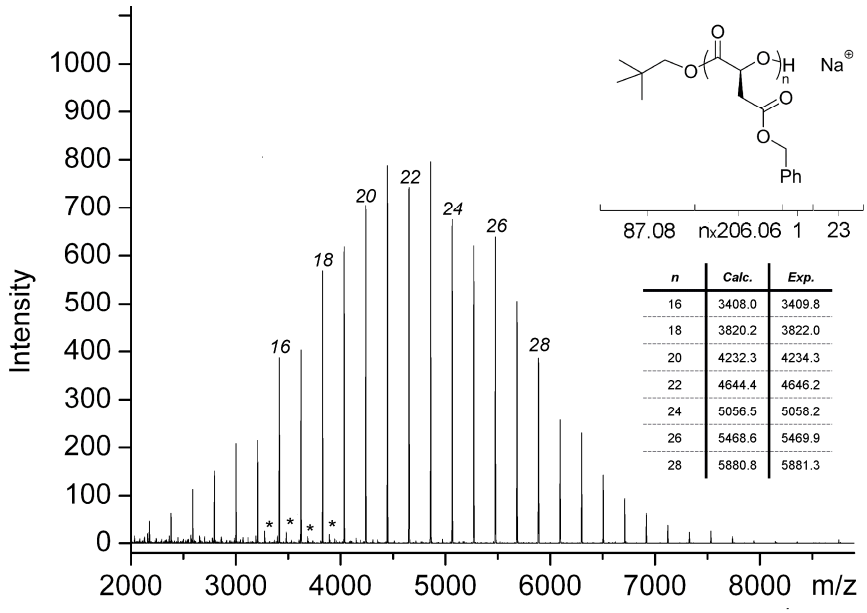

Figure 3.7. MALDI-TOF MS analysis of a P(*L*-BMA)$_{20}$ (M_n = 4 210 g.mol^{-1}, PDI = 1.22) prepared by ROP of ***L*-17** ([***L*-17**]$_0$ = 0.32 M) catalysed with 5 mol% DMAP using *neo*-pentanol as the initiator and the presence of impurities (*****).

Despite the successful and controlled polymerisation of ***L*-17** under these conditions, the formation of side products were clearly observed in both the ^{1}H NMR and MALDI-TOF MS spectra of the polymers. ^{1}H NMR spectroscopy reveals similar resonances to that of the targeted P(*L*-BMA) with signals at δ = 5.49 and 3.08 ppm suggesting the presence of both the methine and malate chemical environments (Figure 3.6, *). Comparison of integrals attributed to the impurity and that of the desired P(*L*-BMA) suggest that the polymer was ~95% pure. MALDI-TOF-MS also confirmed the presence of side products with the major byproduct distribution possessing a lower molecular weight distribution with a regular spacing equal to the molecular weight of the benzyl α-(*L*)-malate repeat unit (m/z = 206) (Figure 3.7, *). Initially, removal of these side products was thought to be successful through precipitation into ice cold acidified methanol as confirmed from ^{1}H NMR spectroscopy with the absence of the

signals at both δ = 5.49 and 3.08 ppm (Figure 3.8). Analysis *via* MALDI-TOF MS indicated that precipitation had successfully removed the majority of the smaller molecular weight species, however, the larger main side product distribution remained (Figure 3.9). Although precipitation resulted in the isolation of cleaner P(*L*-BMA) it also had a significant detrimental effect on the yield, decreasing to 19%.

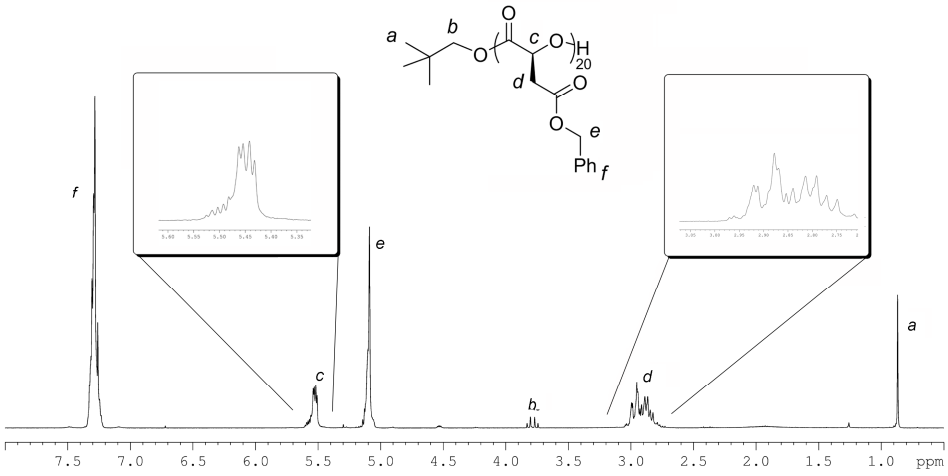

Figure 3.8. ^{1}H NMR spectrum of a P(*L*-BMA)$_{20}$ (M_n = 4 210 g.mol^{-1}, PDI = 1.22) prepared by ROP of ***L*-17** ([***L*-17**]$_0$ = 0.32 M) catalysed with 5 mol% DMAP using *neo*-pentanol as the initiator after precipitation into ice cold acidified methanol (400 MHz; $CDCl_3$).

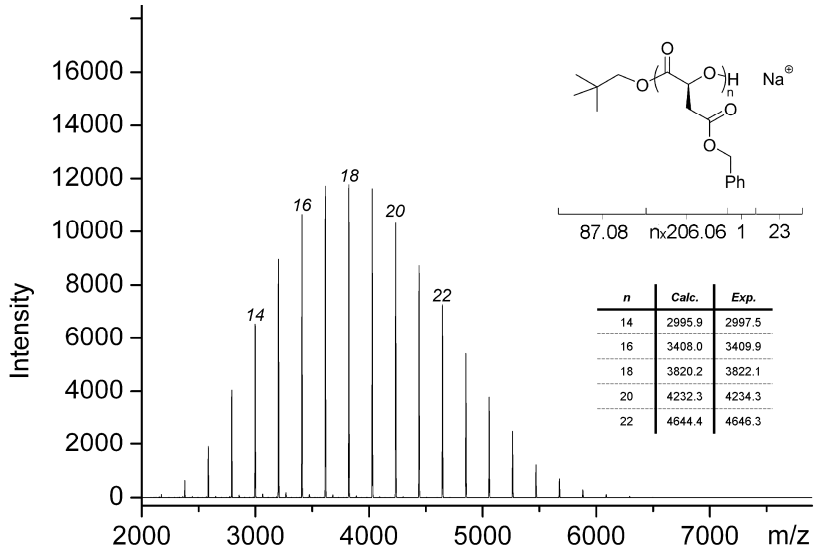

Figure 3.9. MALDI-TOF MS analysis of a P(*L*-BMA)$_{20}$ (M_n = 4 210 g.mol^{-1}, PDI = 1.22) prepared by ROP of ***L*-17** ([***L*-17**]$_0$ = 0.32 M) catalysed with 5 mol% DMAP using *neo*-pentanol as the initiator after precipitation into ice cold acidified methanol.

3.2.3 Ring-Opening Polymerisation studies of L-malOCA – mechanistic studies

Thin-layer chromatography of a P(*L*-BMA) ([M]/[I] = 20) prepared using DMAP revealed two products that were successfully separated *via* column chromatography using a EtOAc:Hexanes (50:50) solvent system; A further product(s) remained on the baseline. P(*L*-BMA)$_{20}$ was isolated, R_f value = 0.8, and was verified *via* ^{1}H NMR spectroscopy and MALDI-TOF MS analysis confirming end-group fidelity with the major peak at m/z = 4234.8 corresponding to a sodium charged DP20 polymer chain with a *neo*-pentanol end group possessing a regular spacing of 206, equal to that of benzyl α-(*L*)-malate, demonstrating that no significant transesterification of the polymer chains occurred during the purification process (Figure 3.10). Importantly, GPC analysis also demonstrated no significant change in the P(*L*-BMA)$_{20}$ upon column chromatography. ^{1}H NMR spectroscopy and MALDI-TOF MS analysis of the second product, R_f value = 0.3, indicated a polymer resembling P(*L*-BMA) with a single distribution with the major peak at m/z = 4918.1, m/z = 272 higher than that of P(*L*-BMA), with a regular spacing equal to the molecular weight of benzyl α-(*L*)-malate (m/z = 206) (Figure 3.11). The observed mass increase from MALDI-TOF MS analysis suggested the presence of a single molecule of *L*-malOCA (m/z = 250, *i.e.* the repeat unit + CO_2) and an additional sodium atom (m/z = 23) to an already sodium charged P(*L*-BMA) initiated from *neo*-pentanol.

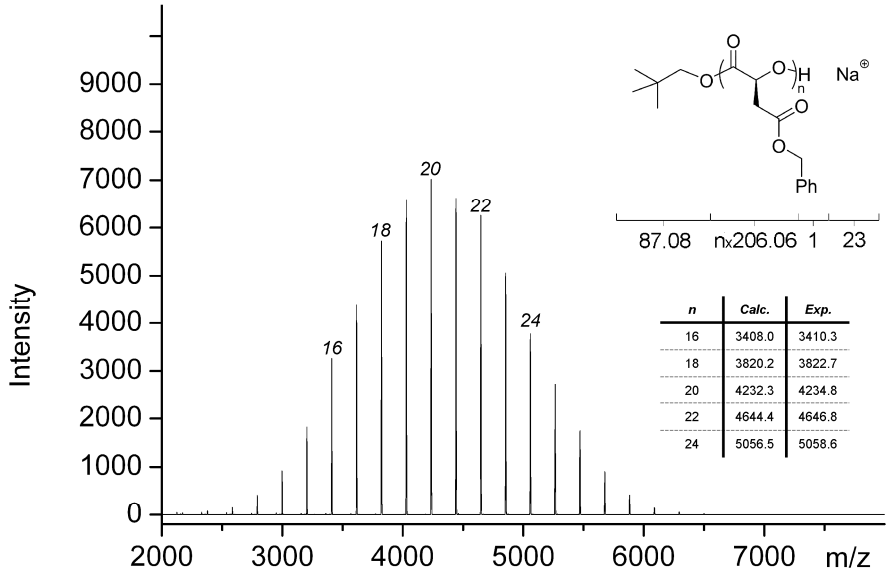

Figure 3.10. MALDI-TOF MS analysis of a P(*L*-BMA)$_{20}$ (M_n = 3 860 g.mol^{-1}, PDI = 1.10) prepared by ROP of ***L*-17** ([***L*-17**]$_0$ = 0.32 M) catalysed with 5 mol% DMAP using *neo*-pentanol as the initiator purified *via* column chromatography using EtOAc:Hexanes (50:50), R_f value of 0.8.

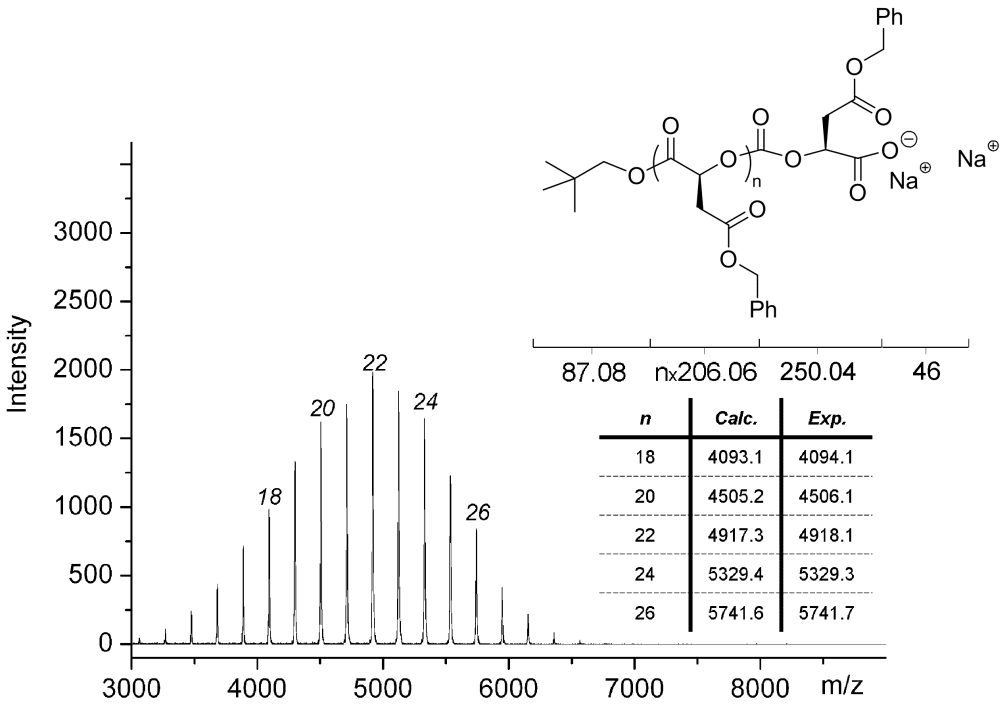

Figure 3.11. MALDI-TOF MS analysis of the impurity prepared during the ROP of ***L*-17** ([***L*-17**]$_0$ = 0.32 M) catalysed with 5 mol% DMAP using *neo*-pentanol as the initiator purified *via* column chromatography using EtOAc:Hexanes (50:50), R_f value of 0.3.

^{1}H NMR spectroscopy confirmed the presence of a *neo*-pentyl ester end group implying that initiation had proceeded through the expected mechanism. The presence of an additional sodium ion is indicative of a carboxylic acid group that must be present at the ω-chain end. It is proposed that this would result from a mis-insertion step whereby the active propagating P(*L*-BMA) end group attacks the 2-position of the OCA ring, rather than at the expected 5-position, resulting in a carbonate linkage and an inactive carboxylic acid ω-chain end group, incapable of further propagation (Scheme 3.5).

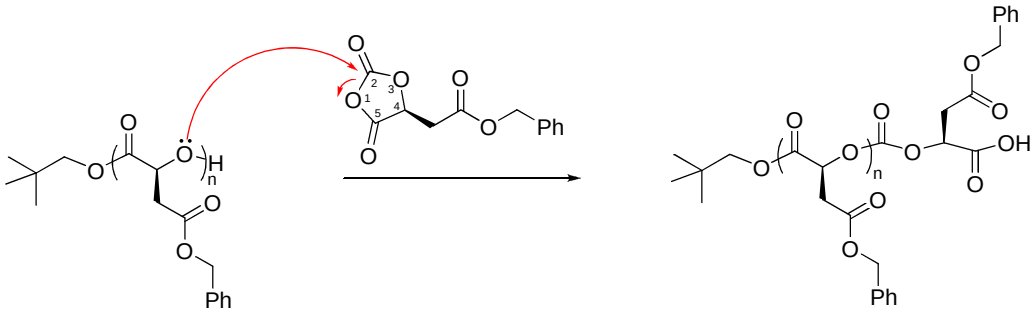

Scheme 3.5. Structure of the side product formation from the mis-insertion of ***L*-17** at the 2-position of the *O*-carboxyanhydride during the ROP.

In the presence of excess cationisation salt, the carboxylic acid ω-chain end group of this P(*L*-BMA) enables the presence of two sodium atoms present in the MALDI-TOF MS analysis, whereby one sodium atom is present as the salt of the carboxylic acid ω-chain end group while the other provides the charge for the P(*L*-BMA) species. Confirmation of this was achieved through variation of the cationisation salt used in the MALDI-TOF MS process. Changing the cationisation salt from sodium trifluoroacetate (NaTFA) to lithium chloride (LiCl) resulted in the observation of a shift in the major peak of this P(*L*-BMA) species from m/z = 4918.1 to m/z = 4886.5 respectively corresponding to a difference of m/z = 32, equal to the difference in mass between two sodium

atoms and two lithium atoms (Figure 3.12). This confirms the proposed structure for this side product possessing a major peak at 4918.1 m/z ([M]/[I] = 22 + 2Na) in MALDI-TOF MS analysis.

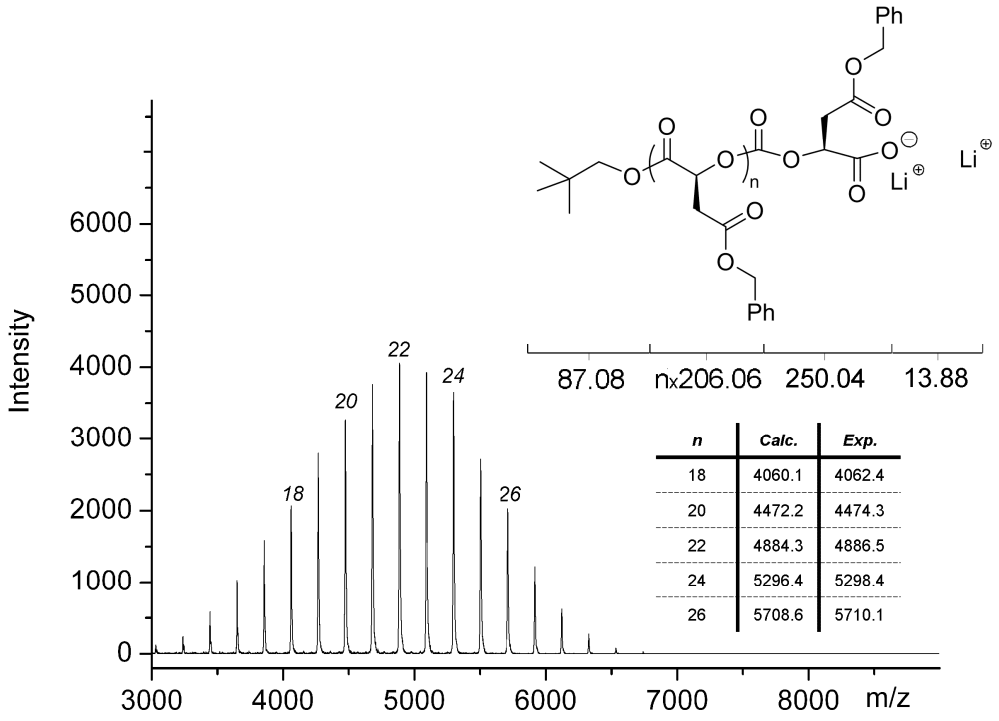

n	Calc.	Exp.
18	4060.1	4062.4
20	4472.2	4474.3
22	4884.3	4886.5
24	5296.4	5298.4
26	5708.6	5710.1

Figure 3.12. MALDI-TOF MS analysis of the impurity prepared during the ROP of ***L*-17** ($[\boldsymbol{L}\text{-}\mathbf{17}]_0$ = 0.32 M) catalysed with 5 mol% DMAP using *neo*-pentanol as the initiator purified *via* column chromatography using LiCl as the cationisation salt.

In order to investigate the origin of the impurities observed in the ^{1}H NMR spectrum of the polymers, further studies were conducted. It was postulated that the formation of these side products was a result of the acidic nature of the methine proton in ***L*-17** making it susceptible to deprotonation by DMAP leading to the synthesis of the observed side products. Interestingly, the previously reported ROPs of both *L*-lacOCA and *L*-gluOCA under identical conditions resulted in no side product formation despite the similar structures of ***L*-17** and *L*-gluOCA (Figure 3.13).[3-4] The only subtle difference between the two monomers

is the proximity of the pendant benzyl α-(*L*)-malate group in ***L*-17** possessing one less methylene group between it and the *O*-carboxyanhydride ring compared to that in *L*-gluOCA.

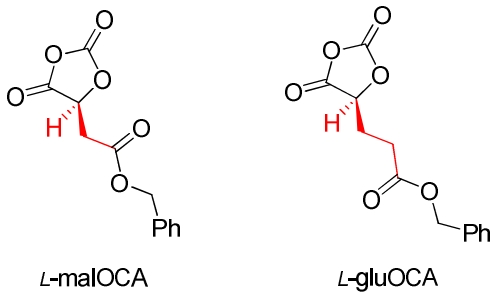

Figure 3.13. Structures of *L*-malOCA, ***L*-17**, and *L*-gluOCA.

Computational investigation into the ROP mechanism of lacOCA catalysed with DMAP involved two possible mechanisms being studied; "nucleophilic" (Scheme 3.6a) and "general-base" catalysis (Scheme 3.6c), of which the latter proved much more energetically favourable.[5] It was further suggested that subtle effects can have significant affects on the competition between these two mechanistic pathways. By analogy to the ROP of structurally related *N*-carboxyanhydride monomers, it is also possible for ROP to occur *via* a "basic" mechanism, in which the DMAP deprotonates the methine proton to create an anionic cyclic anhydride species that attacks a new monomer to result in a ketone linkage in the polymer (Scheme 3.6b) as previously proposed by Kricheldorf *et al.* in the pyridine catalysed ROP of lacOCA.[6] The ROP of ***L*-17** could proceed *via* any of these possible mechanisms thus potentially resulting in a range of impurities. The proximity of the pendant benzyl α-(*L*)-malate group to the *O*-carboxyanhydride is postulated to have a significant effect on the acidity of the methine proton in the ring resulting in an increase in the pKa of the methine

proton of ***L*-17**, compared to *L*-gluOCA, thus making it more susceptible to deprotonation under the basic ROP conditions.

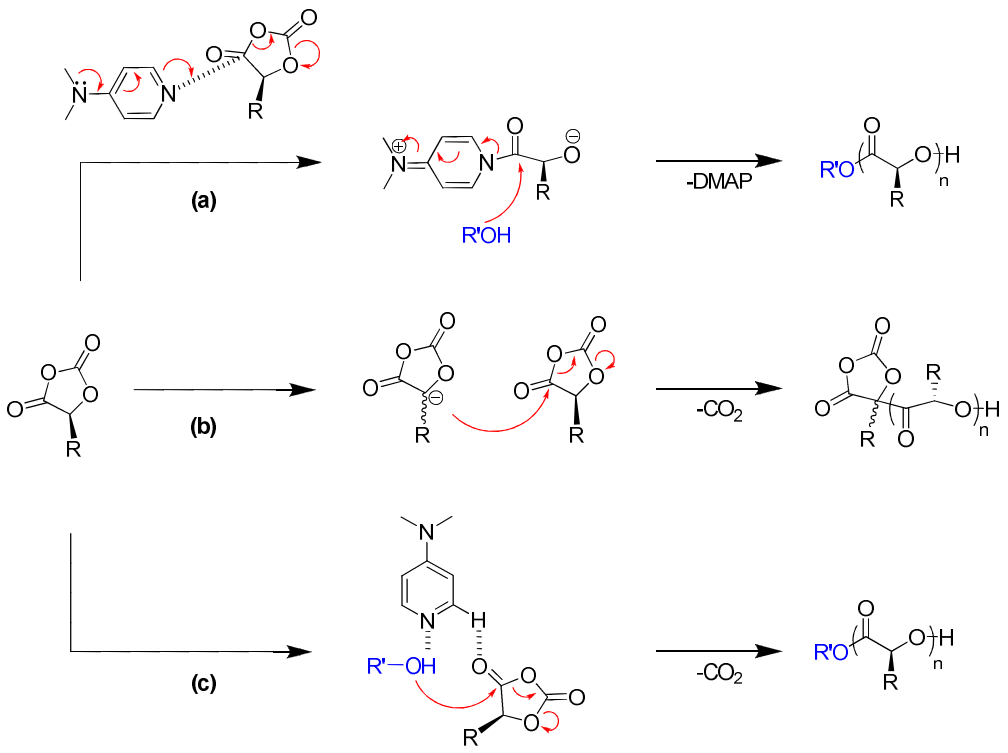

Scheme 3.6. The three different possible mechanisms in the ROP of ***L*-17**; (a) nucleophilic, (b) basic and (c) general-base catalysis.

To investigate the potential for ***L*-17** to react directly with DMAP, the ROP of ***L*-17** was repeated under identical conditions to those described previously in the absence of an alcohol initiator. ^{1}H NMR spectroscopy confirmed consumption of ***L*-17** ([***L*-17**]/[DMAP] = 20) after 5 min resulting in at least three different sets of resonances between δ = 5.61 – 5.30 and 3.33 – 2.60 ppm. The broad resonances at δ = 5.45 – 5.40 and 2.90 – 2.60 ppm are comparable to the signals present in the DMAP catalysed ROP of ***L*-17**. Furthermore, the resonances at δ = 5.37 – 5.30 and 3.15 – 2.90 ppm correlate closely to the impurities observed under standard ROP conditions (Figure 3.14). A comparable reaction with *neo*-pentanol

(5 mol%) and ***L*-17** in the absence of DMAP displayed no conversion of monomer.

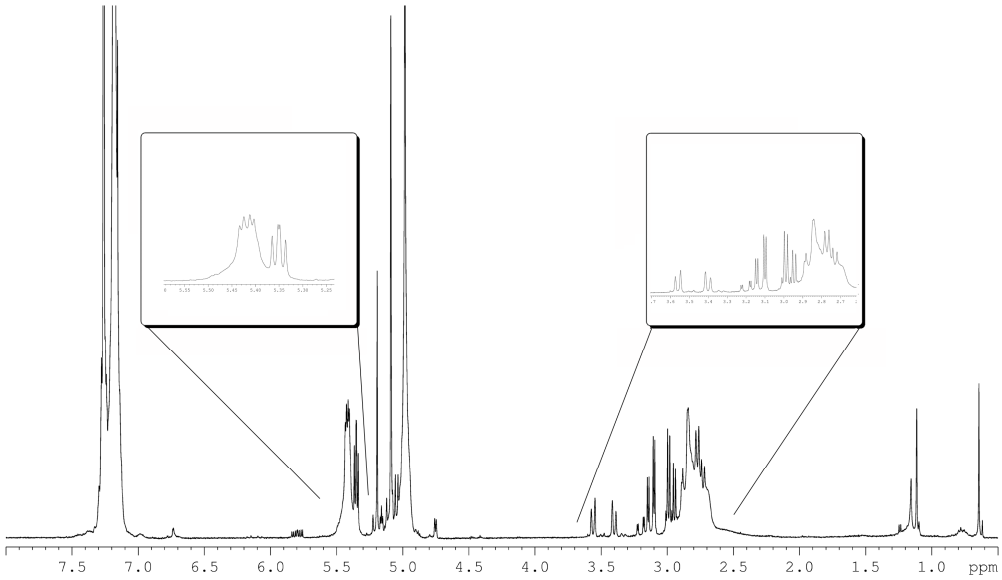

Figure 3.14. ^{1}H NMR spectrum of the products resulting from the reaction between DMAP (5 mol%) and ***L*-17** ($[\boldsymbol{L}\text{-}\mathbf{17}]_0$ = 0.32 M) in the absence of an alcoholic initiator (400 MHz; $CDCl_3$).

Close analysis of the MALDI-TOF MS spectra analysed in reflector mode (NaTFA cationisation salt; Figure 3.15A) observed three polymeric distributions, each displaying regular spacings equal to the molecular weight of the benzyl α-(*L*)-malate repeat unit (m/z = 206). The major distribution has a molecular weight that after subtraction of the sodium charge, is exactly divisible by the repeat unit. The second distribution is spaced from the first by m/z = 22, which corresponds to the replacement of a proton with a sodium ion. The final distribution is m/z = 62 greater than the most intense distribution which corresponds to the addition of CO_2 and H_2O. This latter distribution is perhaps the most simple to assign as the product of DMAP initiation according to the "nucleophilic" mechanism with chain growth terminated by a mis-insertion. After the aqueous acid work-up this

leaves carboxylic acid groups on both chain ends, comparable to that described previously (Scheme 3.7).

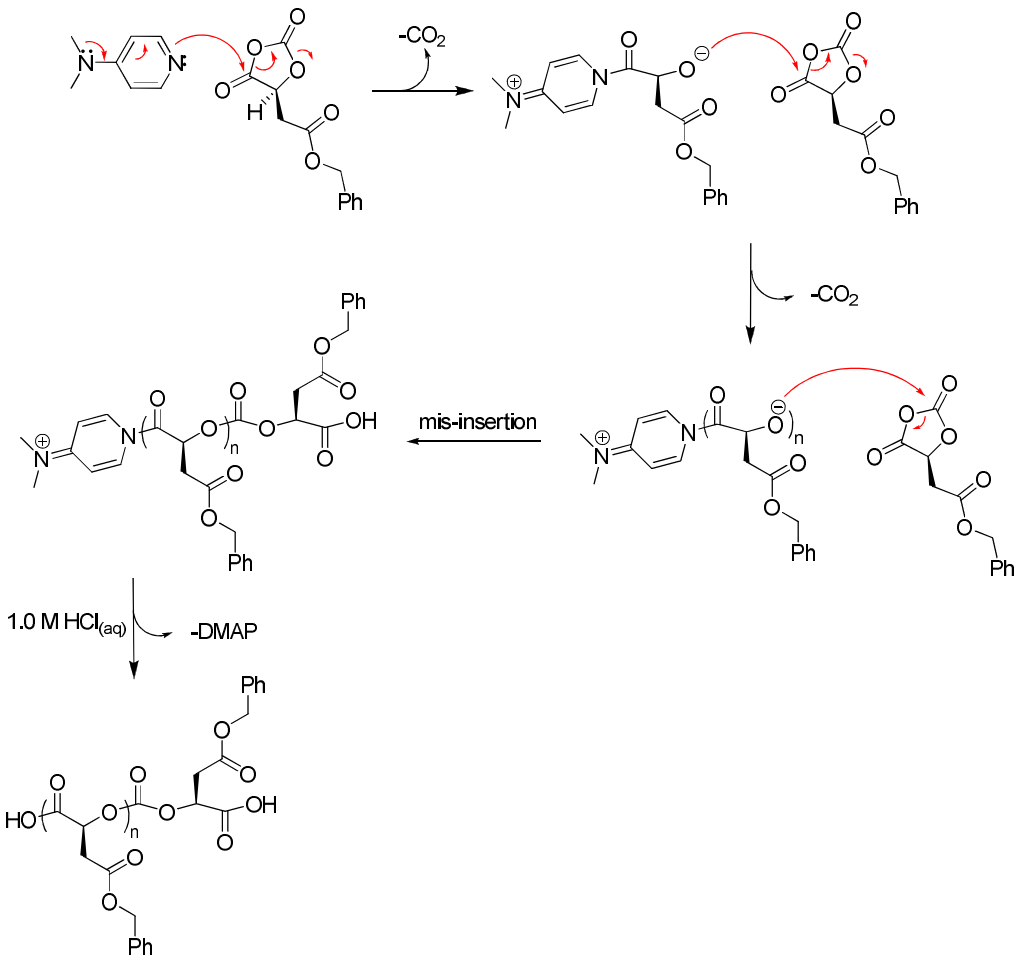

Scheme 3.7. The proposed nucleophilic mechanism for the reaction between DMAP (5 mol%) and ***L*-17** ($[\boldsymbol{L}\text{-}\mathbf{17}]_0$ = 0.32 M) in the absence of an alcoholic initiator.

Assignment of both other species is less clear. As with the previous example, confirmation of the presence of a second metal atom was obtained through variation of the cationisation salt. Measurement of the MALDI-TOF MS of the same polymer using KI in preference to NaTFA, resulted in the observation of species with differences corresponding to the replacement of 1 and 2 sodium ions with potassium, confirming the assignment (Figure 3.15B). As both species are

singly charged, one of the sodium ions provides the overall counterion, but the other must be incorporated in the polymer. To further investigate these observations, MALDI-TOF MS spectra were collected in linear mode to ascertain if these species result from the formation of a metastable ion in the MALDI-TOF MS from fragmentation of the generated parent ion during the flight path in the field free region between the ion source and detector.[7] The formation the postsource metastable ion in the field free region results in all of the species having the same velocity that in linear mode, despite their different molecular weights, are detected at the same time and hence demonstrate identical molecular weights. In reflector mode however, ions are decelerated partway through their flight and then reaccelerated in a different direction by a 'mirror' toward the second detector thus providing enhanced resolution capable of distinguishing between the species resulting from the postsource fragmentation. Analysis of this polymer in linear mode (Figure 3.16) reveals a marked change in the intensities of the distributions corresponding to the polymer species with one and two sodium atoms respectively. Additionally, their intensity is related to the laser power used to ionise the samples such that lower laser power leads to an increased intensity of the 2 sodium-containing species, which indicates that this species is indeed a metastable ion formed during the MALDI-TOF MS analysis.

Several mechanistic rationalisations for these observations exist. The possibility exists of a zwitterionic polymerisation to yield a cyclic polymer in a similar manner to that described by Hedrick, Waymouth and coworkers in the *N*-heterocyclic carbene mediated ROP of lactide.[8-10] However, the presence of the metastable species combined with the lack of a clearly assignable ^{1}H NMR spectrum makes this unlikely. While the presence of some of these species can not be ruled out from this evidence, it is postulated that the high pKa of DMAP

in combination with the increased acidity of the methine proton of the monomer are more likely to lead to ROP of ***L*-17** *via* the "basic" mechanism. Termination of the resulting polymer through back-biting at the monomer unit located at the α-chain end of the polymer with attack at the 5-position would lead to loss of CO_2, that after protonation would provide a cyclic polymer with an identical molecular mass to that observed (Scheme 3.8, **A**). Again however, a simple ^{1}H NMR spectrum would be expected. Additionally, the final cyclisation could occur by ring-opening at the 2-position of the OCA α-chain end, again resulting in a cyclic P(*L*-BMA) however introducing a carbonate linkage and a single pendant carboxylic acid group (Scheme 3.8, **B**). It is hypothesised that CO_2 is lost by decarboxylation of the unstable β-keto acid present in this species during ionisation resulting in a metastable species capable of supporting a second sodium ion while also possessing an overall sodium counterion (Scheme 3.8, **C**).

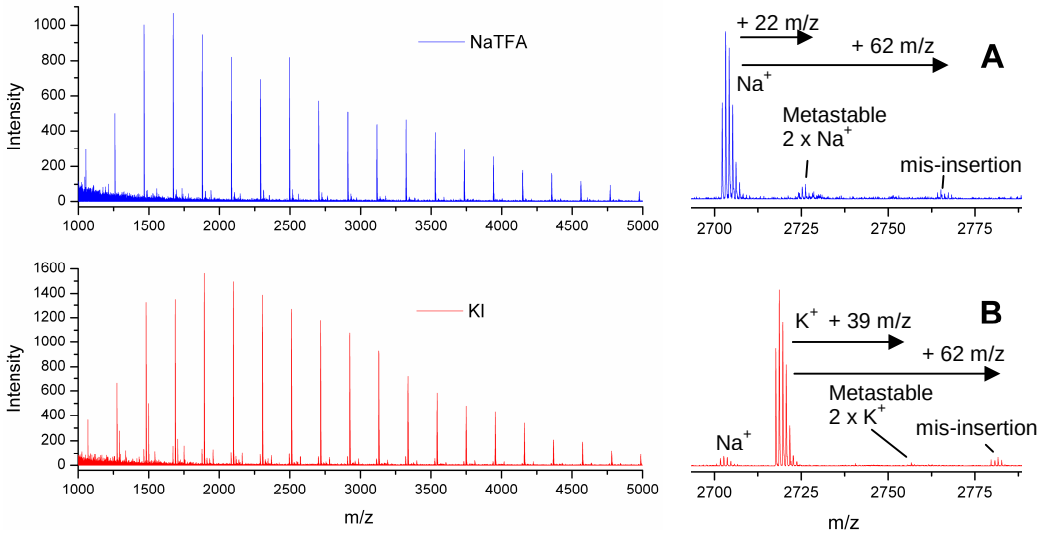

Figure 3.15. MALDI-TOF MS analysis (reflector mode) of the products resulting from the reaction between DMAP (5 mol%) and ***L*-17** ($[\textbf{\textit{L}}\textbf{-17}]_0$ = 0.32 M) in the absence of an alcoholic initiator using NaTFA (—) and KI (—) as the cationisation salts.

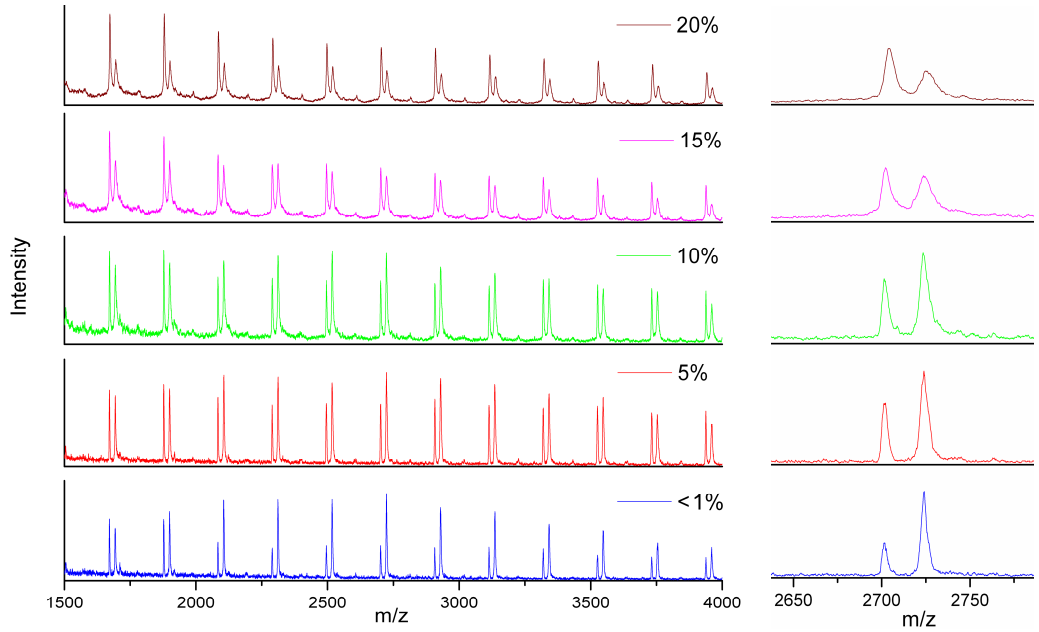

Figure 3.16. MALDI-TOF MS analysis (linear mode) of the products resulting from the reaction between DMAP (5 mol%) and ***L*-17** ($[\boldsymbol{L}\textbf{-17}]_0$ = 0.32 M) in the absence of an alcoholic initiator using NaTFA as the cationisation salt at varying laser powers; 20% (—), 15% (—), 10% (—), 5% (—) and <1% (—).

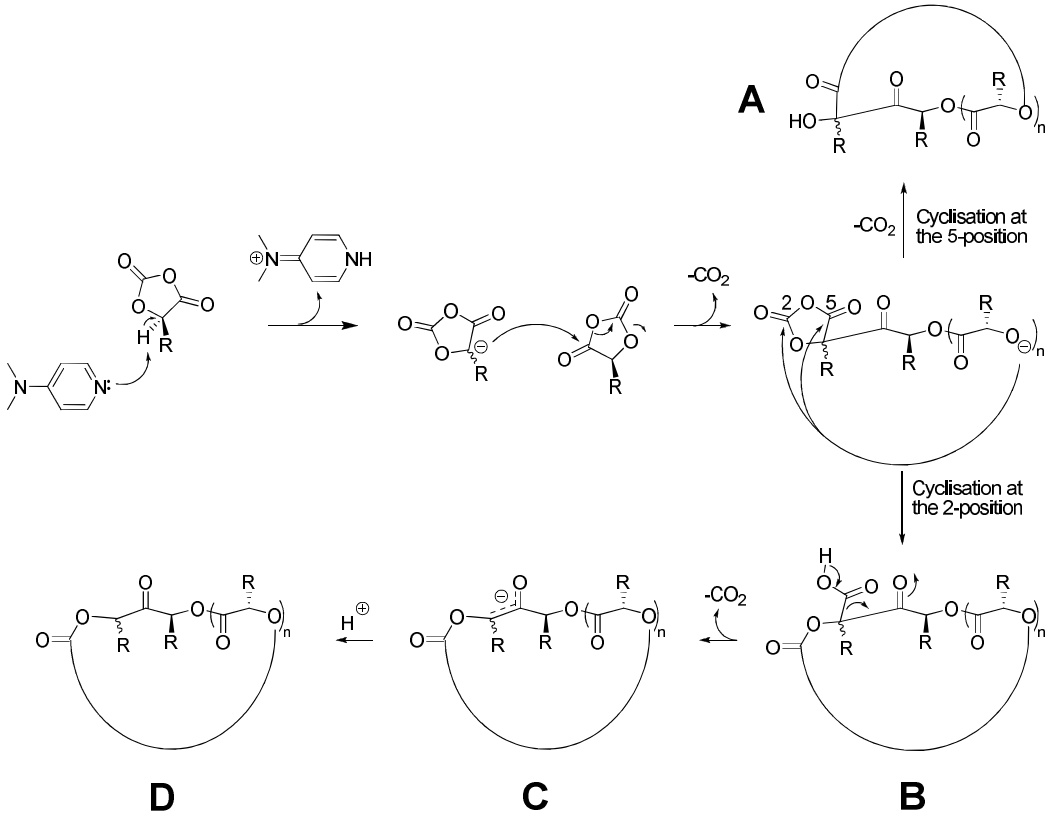

Scheme 3.8. The proposed mechanism for the reaction between DMAP (5 mol%) and ***L*-17** ($[\boldsymbol{L}\textbf{-17}]_0$ = 0.32 M) in the absence of an alcoholic initiator along with the postulated structures (**A – D**) observed *via* MALDI-TOF MS analysis.

To further support this hypothesis, ROP of ***L*-17** with pyridine was studied. If the observed species were a result of the "basic" mechanism, the significantly lower pKa of pyridine (5.3) would prevent deprotonation of ***L*-17** thus eliminating the formation of this product. Consequently, the ROP of ***L*-17** ([***L*-17**]/[pyridine] = 20) was performed in the absence of an alcohol initiator. After a significantly longer reaction time (30 h) ^{1}H NMR spectroscopy confirmed complete consumption of ***L*-17** with a greatly simplified spectrum displaying resonances at δ = 7.37 – 7.20, 5.52 – 5.49, 5.09 and 3.01 – 2.80 ppm (Figure 3.17). MALDI-TOF MS analysis confirmed a single distribution with different molecular weights to those observed when DMAP was applied as the catalyst (Figure 3.18). The mass of the peaks observed in the MALDI-TOF MS spectrum were in agreement with a singly sodium charged P(*L*-BMA) resulting from ROP *via* the "nucleophilic" mechanism whereby pyridine attacks ***L*-17** at the 5-position enabling a zwitterionic polymerisation of ***L*-17** to proceed. Upon quenching the polymerisation by washing with aqueous acid, the acylpyridinium α-chain end group is removed to yield a carboxylic acid group (Scheme 3.9). It is believed that any chain termination occurring *via* ring-opening of ***L*-17** at the 2-position resulting in a carbonate linkage that upon quenching would result in both a carboxylic acid α- and ω-chain end group is removed during workup attributing to the observed low molecular weight of the isolated P(*L*-BMA).

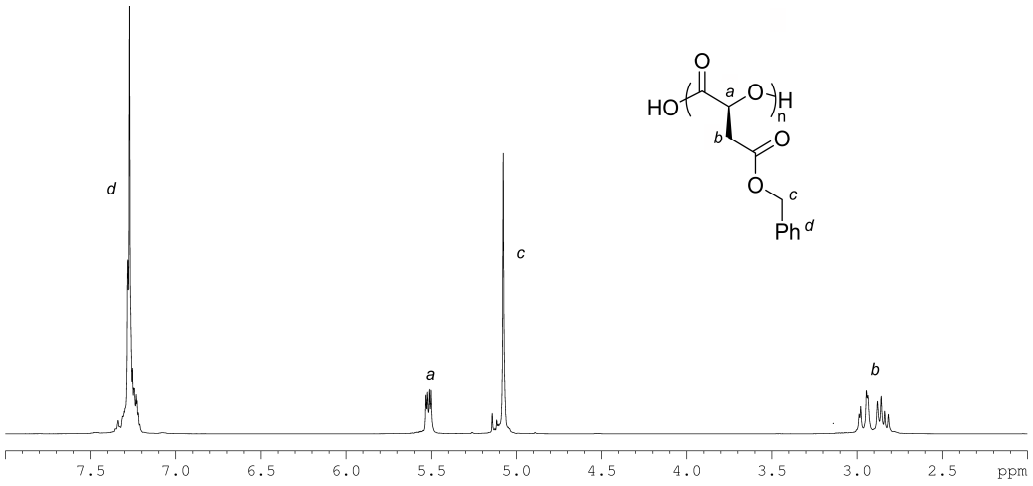

Figure 3.17. ^{1}H NMR spectrum of the product resulting from the reaction between pyridine (5 mol%) and ***L*-17** ([***L*-17**]$_0$ = 0.32 M) in the absence of an alcoholic initiator (400 MHz; $CDCl_3$).

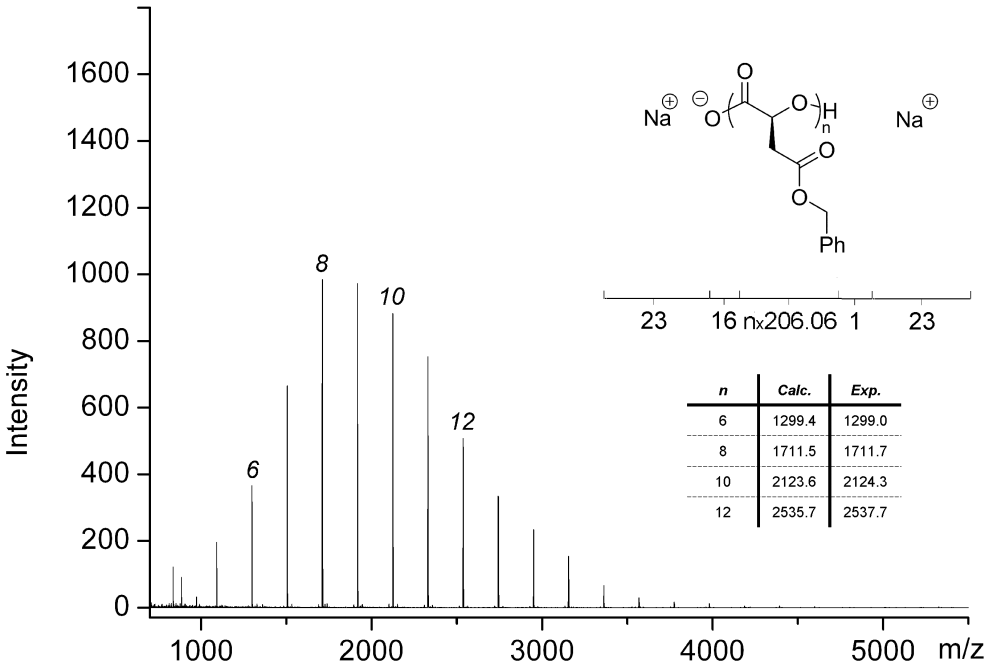

n	Calc.	Exp.
6	1299.4	1299.0
8	1711.5	1711.7
10	2123.6	2124.3
12	2535.7	2537.7

Figure 3.18. MALDI-TOF MS analysis of the product resulting from the reaction between pyridine (5 mol%) and ***L*-17** ([***L*-17**]$_0$ = 0.32 M) in the absence of an alcoholic initiator.

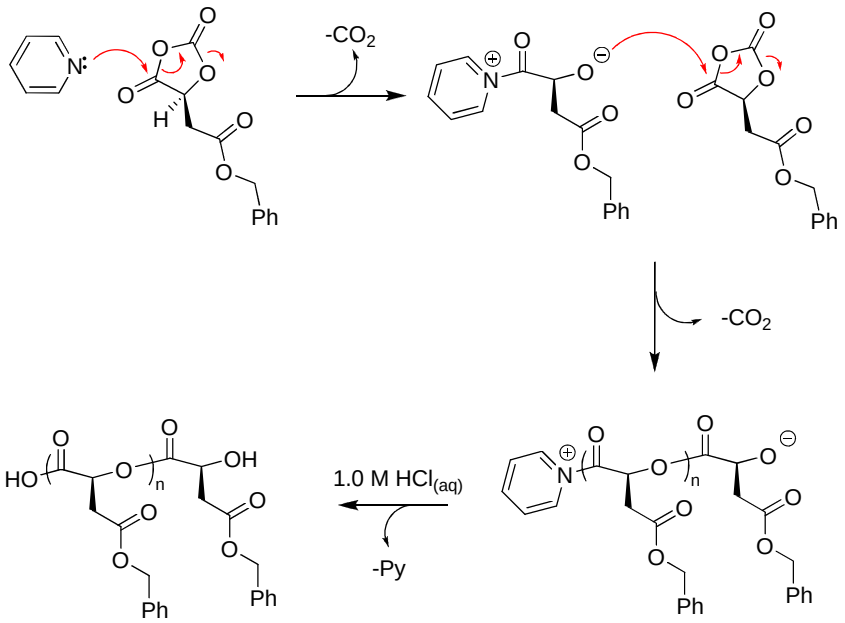

Scheme 3.9. The proposed nucleophilic mechanism for the reaction between pyridine (5 mol%) and ***L*-17** ([***L*-17**]$_0$ = 0.32 M) in the absence of an alcoholic initiator.

3.2.3.1 Ring-Opening Polymerisation studies of L-malOCA – pyridine

As the application of pyridine to mediate the ROP of ***L*-17** was shown to reduce the side product formation (in comparison to the DMAP catalysed polymerisation), it was further investigated as a catalyst for the ROP of ***L*-17** ([M]/[I] = 20) in the presence of *neo*-pentanol at a ratio of 1:1 to catalyst. The polymerisation proceeded considerably slower than that catalysed by DMAP achieving 93% monomer conversion after 435 min with GPC analysis of the resultant P(*L*-BMA) indicating that the polymerisation was well controlled resulting in a polymer displaying a number-average molecular weight of 2 100 g.mol^{-1} with a polydispersity of 1.13 (Figure 3.19).

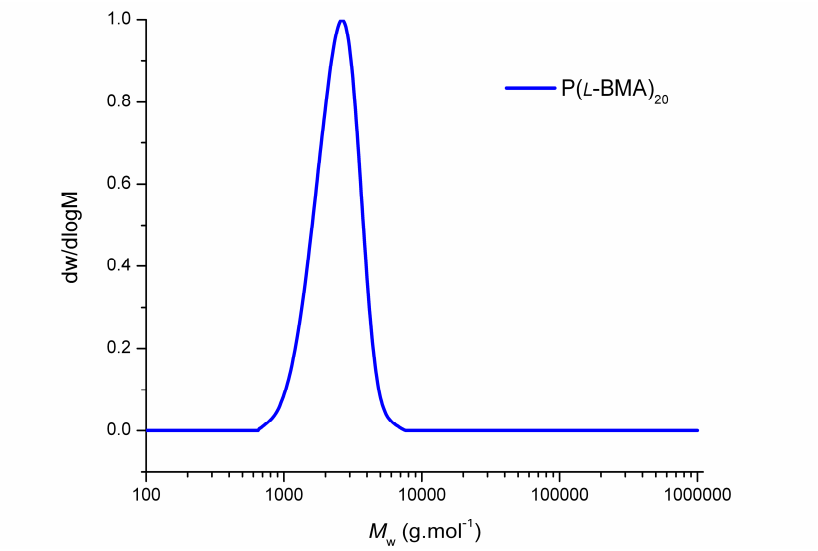

Figure 3.19. GPC trace of P(*L*-BMA) ([M]/[I] = 20) (M_n = 2 100 g.mol^{-1}, PDI = 1.13) prepared by ROP of ***L*-17** ([***L*-17**]$_0$ = 0.32 M) catalysed with 5 mol% pyridine using *neo*-pentanol as the initiator.

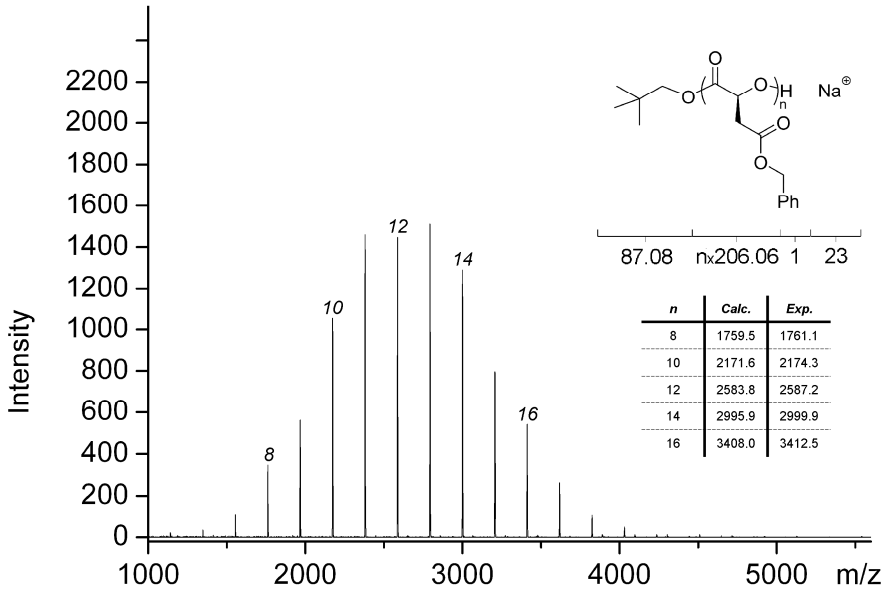

Figure 3.20. MALDI-TOF MS analysis of a P(*L*-BMA) ([M]/[I] = 20) (M_n = 2 100 g.mol^{-1}, PDI = 1.13) prepared by ROP of ***L*-17** ([***L*-17**]$_0$ = 0.32 M) catalysed with 5 mol% pyridine using *neo*-pentanol as the initiator.

Both ^{1}H NMR spectroscopy and MALDI-TOF MS analysis confirmed that no side products were present. Despite this positive result, ^{1}H NMR spectroscopy,

GPC and MALDI-TOF analysis all suggested the DP of the resulting P(*L*-BMA) was close to 12, significantly lower than the targeted [M]/[I] = 20 (Figure 3.20). This lower than expected DP and molecular weight of P(*L*-BMA) was not observed when the ROP of ***L*-17** was catalysed with DMAP. It was hypothesised that while the low pKa of pyridine successfully enabled the ROP of ***L*-17** to proceed without interactions with the acidic methine proton, it also results in a change of the polymerisation mechanism that is not observed when catalysed with DMAP.

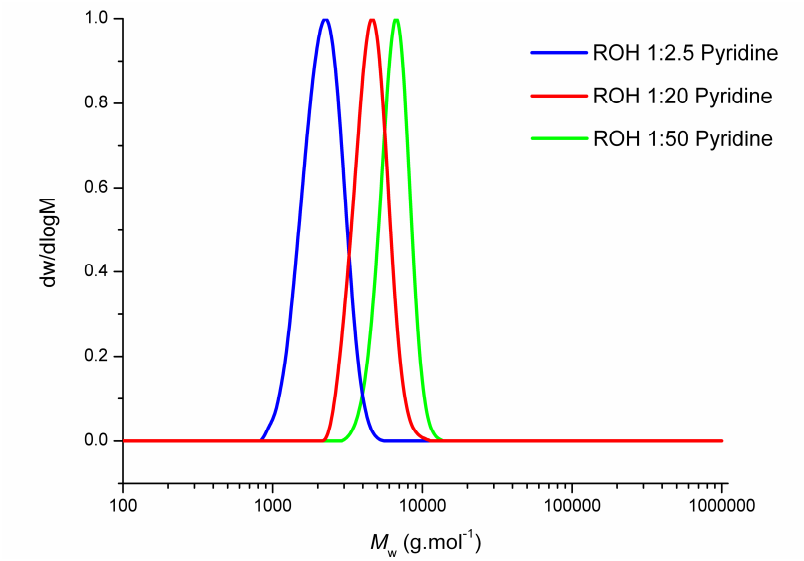

Figure 3.21. GPC traces of P(*L*-BMA) ([M]/[I] = 50) (M_n = 2 040 g.mol^{-1}, PDI = 1.09), (M_n = 4 170 g.mol^{-1}, PDI = 1.06) and (M_n = 6 010 g.mol^{-1}, PDI = 1.05) prepared by ROP of ***L*-17** ([***L*-17**]$_0$ = 0.32 M) using 2.5:1(—), 20:1 (—) and 50:1 (—) pyridine to alcohol ratio respectively using *neo*-pentanol as the initiator.

The resulting P(*L*-BMA) molecular parameters were shown to have a significant dependence on the concentration of the pyridine catalyst demonstrated through variation of the pyridine to *neo*-pentanol molar ratio in the ROP of ***L*-17** ([M]/[I] = 20). Increasing the pyridine concentration resulted in an increase in the

molecular weight of the P(*L*-BMA) obtained and therefore enabled the targeted [M]/[I] to be reached. However, along with the increase in P(*L*-BMA) molecular weight, increasing the pyridine concentration resulted in the appearance of the side product visible by MALDI-TOF MS analysis while ^{1}H NMR spectroscopy remained clear of any side product formation at all pyridine concentrations. Increasing the ratio of pyridine to *neo*-pentanol from 1:1 up to 20:1 resulted in the molecular weight of P(*L*-BMA) increasing from 2 100 to 2 710 g.mol^{-1} respectively while maintaining a low polydispersity of 1.09. This increase in molecular weight was also observed *via* MALDI-TOF MS analysis with the main distribution centered around m/z = 3408.9 corresponding to a DP of 16 compared to m/z = 2584.2 (DP = 12) resulting when pyridine was applied in a 1:1 ratio with *neo*-pentanol. This dependence of molecular weight on pyridine concentration was observed to a greater extent when targeting a P(*L*-BMA) with [M]/[I] = 50. A catalyst-to-*neo*-pentanol ratio of 2.5:1 realised a P(*L*-BMA) displaying a molecular weight of 2 040 g.mol^{-1} with a polydispersity of 1.09 that upon increasing the ratio to 20:1 and further 50:1 realised P(*L*-BMA)s with M_n = 4 170 g.mol^{-1}, PDI = 1.06 and M_n = 6 010 g.mol^{-1}, PDI = 1.05 respectively (Figure 3.21). This was again further confirmed *via* MALDI-TOF MS analysis of the respective P(*L*-BMA)s with the main distributions centered around m/z = 2585.1 (DP = 12) (M_n = 2 340 g.mol^{-1}, PDI = 1.06), m/z = 4645.9 (DP = 22) (M_n = 3 930 g.mol^{-1}, PDI = 1.16) and m/z = 6707.4 (DP = 32) (M_n = 6 200 g.mol^{-1}, PDI = 1.08) at ratios of 2.5:1, 20:1 and 50:1 respectively (Figure 3.22).

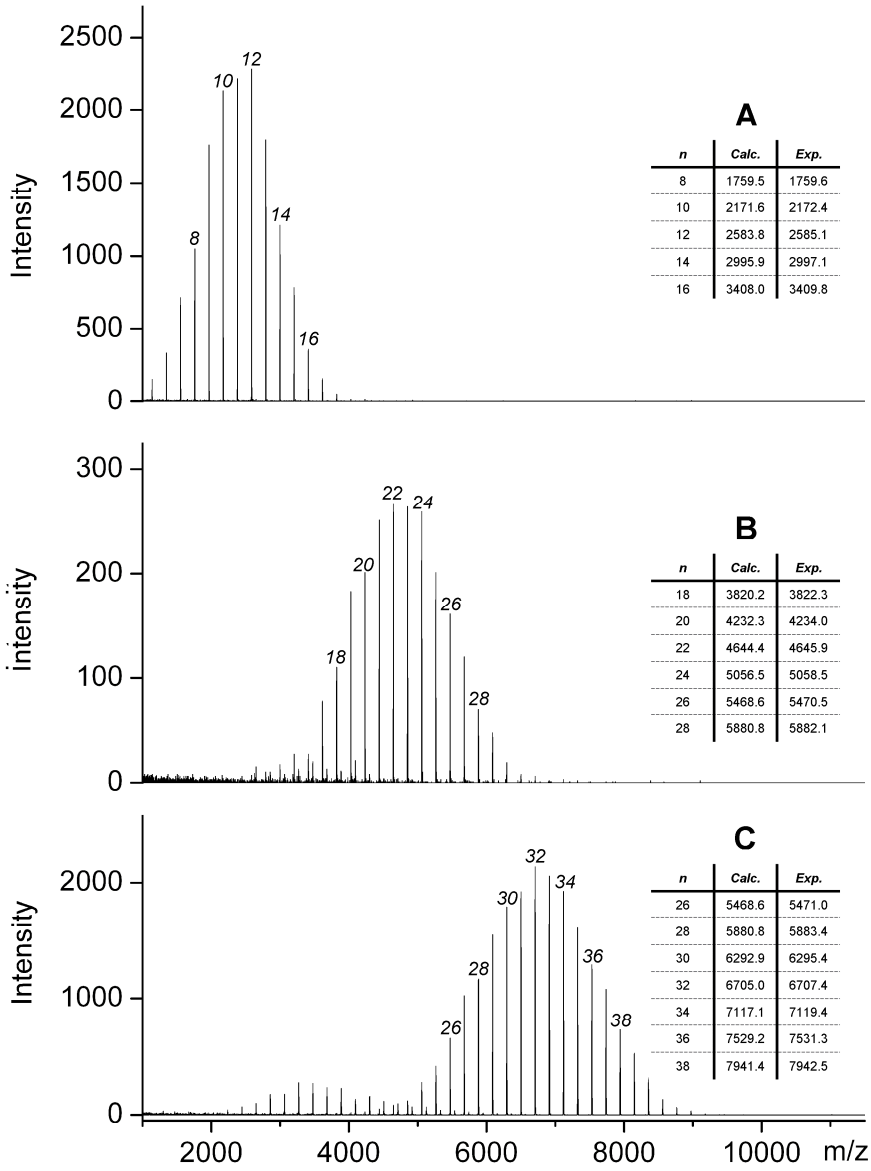

Figure 3.22. MALDI-TOF MS analysis of P(*L*-BMA)s ([M]/[I] = 50) prepared by ROP of ***L*-17** ([***L*-17**]$_0$ = 0.32 M) catalysed with pyridine at; 2.5:1 to *neo*-pentanol (**A**), 20:1 to *neo*-pentanol (**B**) and 50:1 to *neo*-pentanol (**C**).

Further inspection of the ^{1}H NMR spectra measured during the polymerisation revealed notable differences in the chemical shift of the *neo*-pentyl group of the initiating/propagating species (Figure 3.23). During the initial stages of the ROP of ***L*-17** with a high pyridine concentration (50:1 pyridine-to-alcohol ratio), the *neo*-pentyl group is observed as a singlet at δ = 0.86 ppm throughout the

polymerisation (Figure 3.23a and b). Notably however, at lower pyridine concentration (2.5:1 pyridine-to-alcohol ratio) this resonance is observed to change during the polymerisation. Whilst in the latter stages of the polymerisation the resonance is observed as a singlet at δ = 0.86 ppm (Figure 3.23c), in the initial stages, multiple resonances between δ = 0.94 – 0.84 ppm are observed (Figure 3.23d). These observations indicate that at high pyridine concentrations, initiation is efficient whereas low pyridine concentrations lead to inefficient initiation.

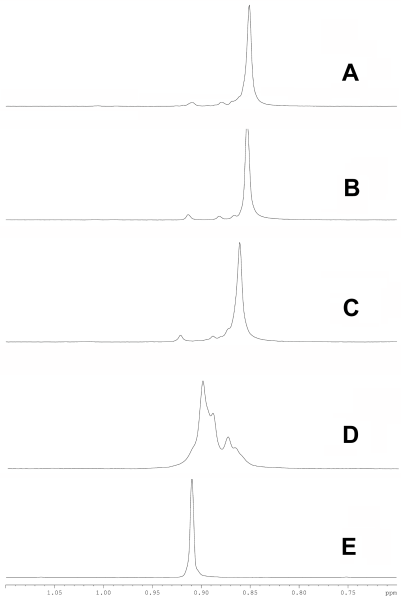

Figure 3.23. Expansion of δ = 1.10 to 0.70 ppm region of ^{1}H NMR spectra (400 MHz; $CDCl_3$) showing the *neo*-pentyl resonances of P(*L*-BMA) ([M]/[I] = 50) prepared by the ROP of ***L*-17** ($[\boldsymbol{L}\textbf{-17}]_0$ = 0.32 M) initiated from *neo*-pentanol catalysed with pyridine at; 50:1 to *neo*-pentanol at high monomer conversion (**A**), 50:1 to *neo*-pentanol at low monomer conversion (**B**), 2.5:1 to *neo*-pentanol at high monomer conversion (**C**), 2.5:1 to *neo*-pentanol at low monomer conversion (**D**), and *neo*-pentanol (**E**).

It is postulated that these observations may be the result of a competing ROP mechanism that results from a pKa dependant equilibrium (Scheme 3.10A) between free pyridine/alcohol and a pyridine-alcohol adduct required for

"general-base" catalysed ROP (Scheme 3.10B). In accordance with Le Chatelier's principle, higher concentrations of pyridine will result in the equilibrium lying towards pyridine-alcohol adduct, thus enabling all alcohol molecules to efficiently initiate/propagate ROP. Conversely, at low pyridine concentrations the equilibrium will lie towards the free species resulting in an increased probability of the occurrence of side reactions resulting from nucleophilic attack of pyridine on the monomer (Scheme 3.10C).

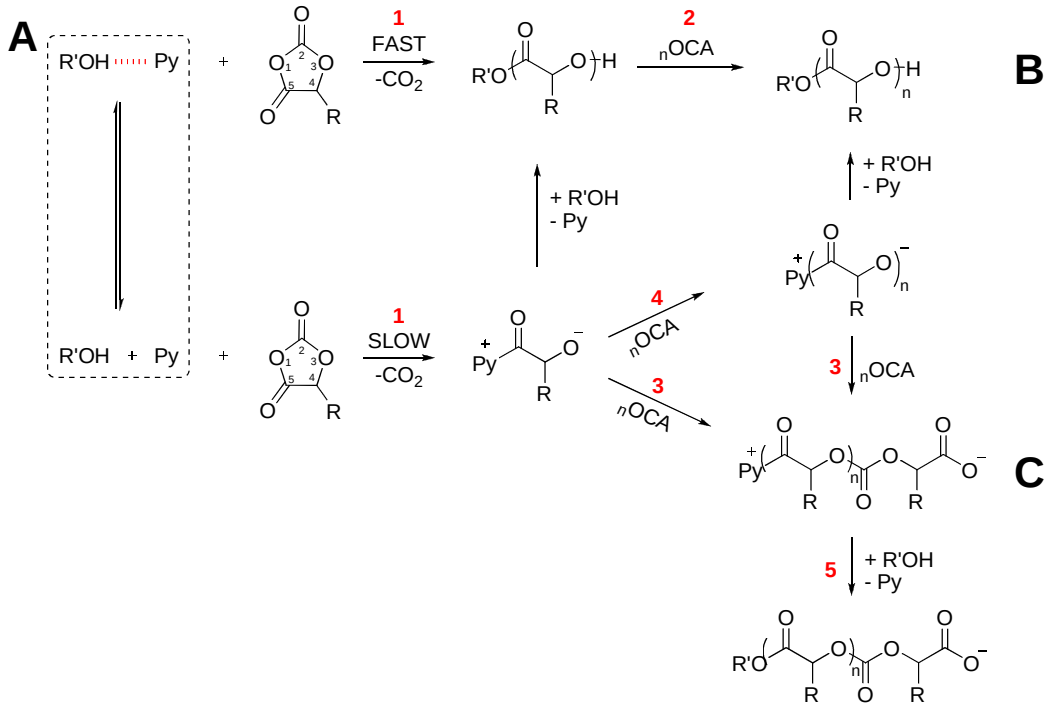

Scheme 3.10. The proposed mechanisms for the ROP of ***L*-17** ($[\boldsymbol{L}\textbf{-17}]_0$ = 0.32 M) with pyridine in the presence of an alcoholic initiator; (**A**) pKa dependant equilibrium, (**B**) general-base catalysis and (**C**) nucleophilic.

As previously outlined, "general-base" catalysed ring-opening is believed to be preferred at the 5-position of the OCA ring thus, after loss of CO_2, presents an alcohol group capable of propagating the polymerisation reaction (Scheme 3.10, **1**, **2** and **4**). Any ring-opening event to occur at the 2-position of the OCA ring

(Scheme 3.10, **3**) would result in the formation of a carbonate linkage and an ω-carboxylic acid chain end, incapable of propagating ROP; selection is governed by subtle electronic effects. Ring-opening of the monomer by the pyridine/alcohol adduct is expected to result in a chain extended alcohol whereas ring-opening of the monomer by nucleophilic attack of pyridine will result in an acylpyridinium α-chain end group that can transesterify with either the initiating alcohol or the propagating end group of another polymeric species capable of propagation. If however, the more nucleophilic acylpyridinium zwitterion displays an increased probability of ring-opening at the 2-position, oligomeric species with carboxylic acid end groups would result (Scheme 3.10, **5**). Experimentally, these are likely to be removed upon quenching and workup of the polymerisation, accounting for the consumption of monomer and alcohol during the polymerisation.

While higher pyridine concentrations would also be expected to lead to increased free pyridine that may also participate in "nucleophilic" ROP, the increased likelihood of alcohol being involved in a pyridine/alcohol adduct reduces the probability that the alcohol will be consumed by this mechanism. Indeed, increasing the pyridine concentration in the ROP of ***L*-17** also led to the observation of low molecular weight polymer species by MALDI-TOF MS that correspond to polymer chains with a *neo*-pentyl ester α-chain end and the 'mis-inserted' carboxylate ω-chain end. It is also worthy of note that the ROP of ***L*-17** was observed to proceed 5 times slower in the absence of an alcoholic initiator than in an identical reaction with added alcohol, thus confirming that the "general–base" mechanism proceeds at a greatly increased rate than that of the "nucleophilic" mechanism.

3.2.4 Ring-Opening Polymerisation studies of L-malOCA – catalyst variation

These observations, in addition to the long reaction times of pyridine led to the investigation of further variation of the pyridine catalyst. It was postulated that a catalyst with a pKa value between that of pyridine and DMAP may enable the polymerisation of ***L*-17** to proceed without interaction between the catalyst and the acidic methine proton as well as preventing the mechanistic issues observed with pyridine by driving the pKa dependant equilibrium toward the general-base catalysis mechanism. Three *para*-substituted pyridines were investigated as catalysts in the ROP of ***L*-17** with pKa values of their respective conjugative acids ranging from 8.8 to 6.0 (Figure 3.24).

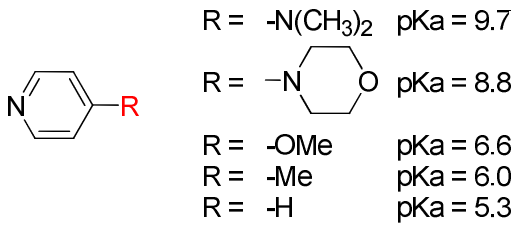

Figure 3.24. The *para*-substituted pyridine catalysts applied to the ROP of ***L*-17**.[11-14]

3.2.4.1 Ring-Opening Polymerisation studies of L-malOCA – 4-methylpyridine

As a consequence of the introduction of the unusual observations in the ROP of ***L*-17** catalysed by pyridine, attributed to its low pKa value and nucleophilicity, 4-methylpyridine (pKa = 6.0) was investigated as a catalyst. The ROP of ***L*-17** ([M]/[I] = 20) was performed with 4-methylpyridine at a 1:1 ratio to *neo*-pentanol. It was noted that the polymerisation rate, as with pyridine, was greatly reduced, in line with the lower pKa of the catalyst. Here, the polymerisation achieved 95% monomer conversion after 160 min. GPC analysis of the resultant P(*L*-BMA) indicated that the polymerisation was well controlled with a number

average molecular weight of 2 950 g.mol^{-1} and a polydispersity of 1.12 similar to that achieved with pyridine (Figure 3.25). As with the ROP of ***L*-17** catalysed by pyridine, the molecular weight was lower than targeted and was further confirmed *via* MALDI-TOF MS analysis with the main distribution centered around m/z = 3409.8 (DP = 16) (Figure 3.26). However, unlike the pyridine-catalysed ROP, even at a ratio of 1:1 with *neo*-pentanol, side product formation was present, observed by MALDI-TOF MS analysis, although no side product was observed *via* ^{1}H NMR spectroscopy. The molecular weight of the resulting P(*L*-BMA)s, as with pyridine, could be increased with increasing 4-methylpyridine concentration while maintaining no ^{1}H NMR visible impurity. These data suggest that 4-methylpyridine is behaving in a very similar manner to pyridine and therefore the ROP of ***L*-17** is hindered with the same problems. As a result, 4-methylpyridine provides little improvement to pyridine and was not further investigated.

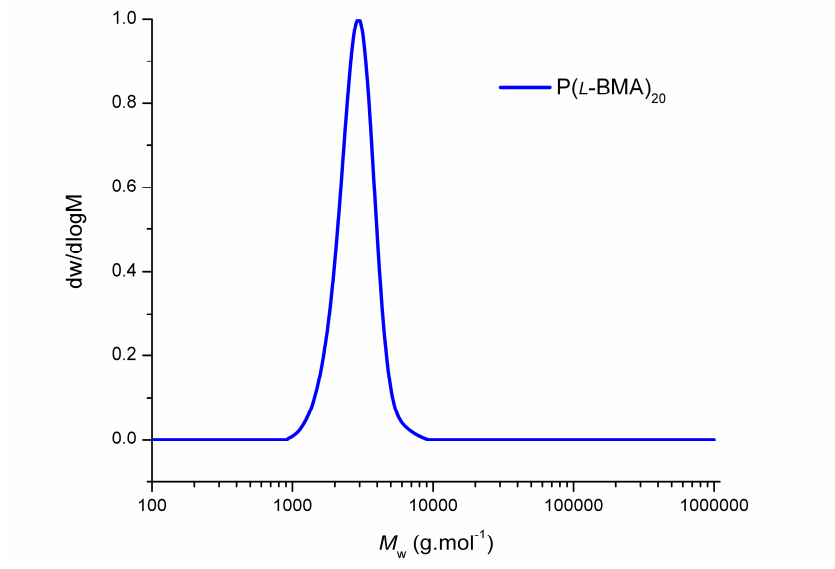

Figure 3.25. GPC trace of P(*L*-BMA) ([M]/[I] = 20) (M_n = 2 950 g.mol^{-1}, PDI = 1.12) prepared by ROP of ***L*-17** ([***L*-17**]$_0$ = 0.32 M) catalysed with 4-methylpyridine using *neo*-pentanol as the initiator.

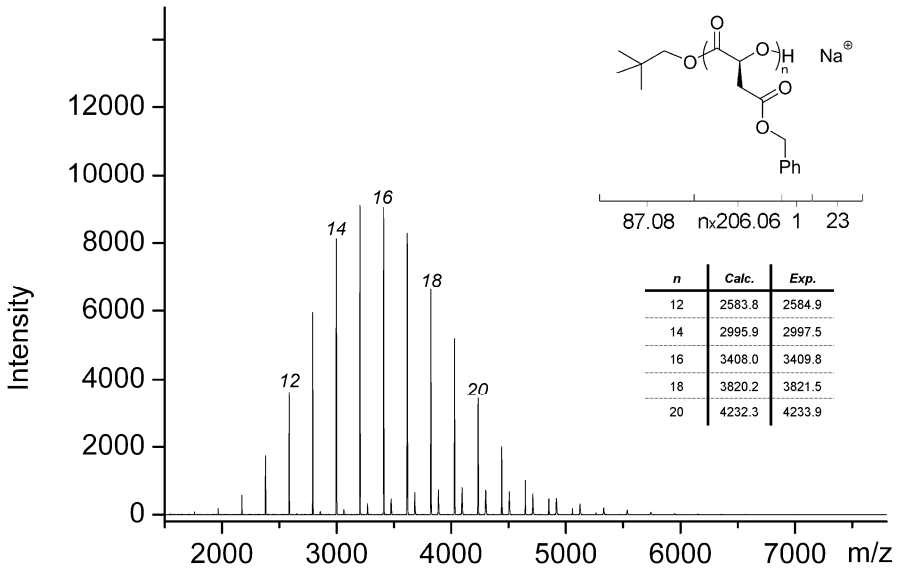

Figure 3.26. MALDI-TOF MS analysis of a P(*L*-BMA) ([M]/[I] = 20) (M_n = 2 950 g.mol^{-1}, PDI = 1.12) prepared by ROP of ***L*-17** ([***L*-17**]$_0$ = 0.32 M) catalysed with 5 mol% 4-methylpyridine using *neo*-pentanol as the initiator.

3.2.4.2 Ring-Opening Polymerisation studies of L-malOCA – 4-methoxypyridine

Further increase of the pKa value of the pyridine catalyst was achieved by the application of 4-methoxypyridine (pKa = 6.6) for the ROP of ***L*-17**. The ROP of ***L*-17** ([M]/[I] = 20) was performed with 4-methoxypyridine at a 1:1 ratio to *neo*-pentanol. Monomer conversion reached 95% after 90 min with GPC analysis of the resultant P(*L*-BMA) indicating the polymerisation was well controlled displaying a number average molecular weight of 3 860 g.mol^{-1} with a polydispersity of 1.10 (Figure 3.27).

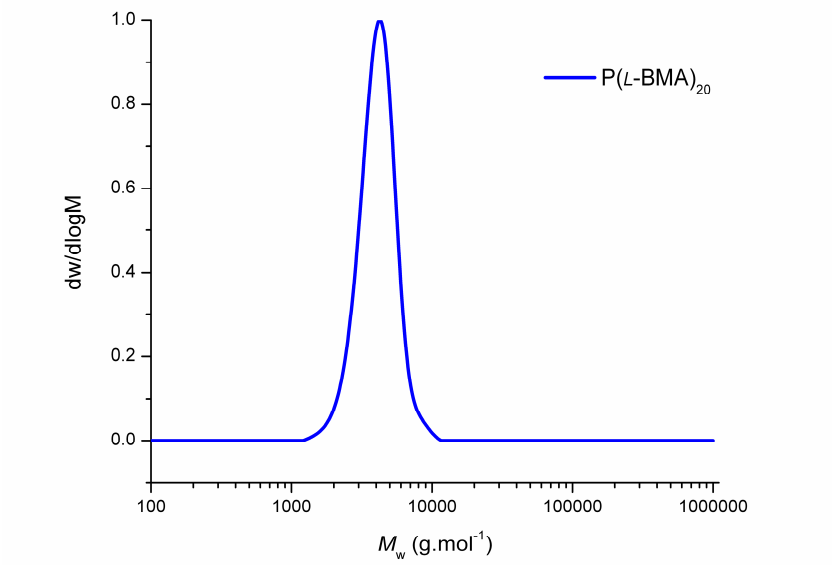

Figure 3.27. GPC trace of P(*L*-BMA) ([M]/[I] = 20) (M_n = 3 860 g.mol^{-1}, PDI = 1.10) prepared by ROP of ***L*-17** ([***L*-17**]$_0$ = 0.32 M) catalysed with 4-methoxypyridine using *neo*-pentanol as the initiator.

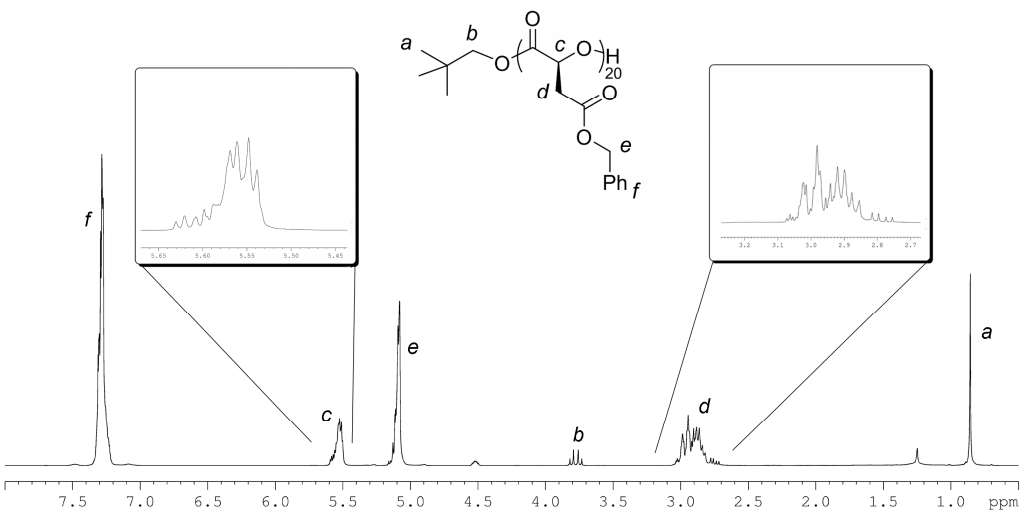

Figure 3.28. ^{1}H NMR spectrum of a P(*L*-BMA) ([M]/[I] = 20) (M_n = 3 860 g.mol^{-1}, PDI = 1.10) prepared by ROP of ***L*-17** ([***L*-17**]$_0$ = 0.32 M) catalysed with 5 mol% 4-methoxypyridine using *neo*-pentanol as the initiator (400 MHz; $CDCl_3$).

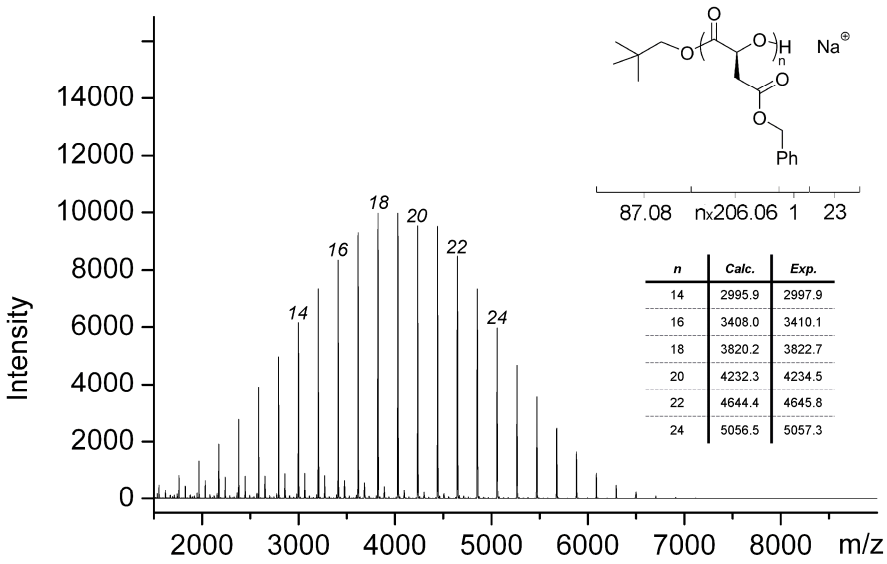

Figure 3.29. MALDI-TOF MS analysis of a P(*L*-BMA) ([M]/[I] = 20) (M_n = 3 860 g.mol^{-1}, PDI = 1.10) prepared by ROP of ***L*-17** ([***L*-17**]$_0$ = 0.32 M) catalysed with 5 mol% 4-methoxypyridine using *neo*-pentanol as the initiator.

^{1}H NMR spectroscopy confirmed the targeted [M]/[I] = 20 and, as with pyridine and 4-methylpyridine, confirmed the absence of any side product formation that was visible when the ROP was catalysed with DMAP (Figure 3.28). MALDI-TOF MS analysis indicated a main distribution centered around m/z = 4234.5 corresponding to a DP of 20 that provided an improvement on the low molecular weight P(*L*-BMA)s obtained from catalysis with 4-methylpyridine and pyridine. Unfortunately, the impurity visible *via* MALDI-TOF MS analysis was still present, however; analysis indicated that this was the only impurity present providing a much cleaner P(*L*-BMA) with the predictable molecular weight from the [M]/[I] ratio (Figure 3.29).

3.2.4.3 Ring-Opening Polymerisation studies of L-malOCA – 4-morpholinopyridine

4-Morpholinopyridine (pKa = 8.8) was also examined as a catalyst for the ROP of ***L*-17** ([M]/[I] = 20) initiating from *neo*-pentanol at a catalyst-to-initiator ratio of 1:1. The polymerisation proceeded slower than the polymerisation catalysed by DMAP, achieving 94% monomer conversion (determined by ^{1}H NMR spectroscopy) after 60 min with GPC analysis of the resultant P(*L*-BMA)$_{20}$ which indicates that the polymerisation was well controlled displaying a molecular weight of 3 870 g.mol^{-1} with a PDI of 1.14 (Figure 3.30). However, both ^{1}H NMR spectroscopy (Figure 3.31) and MALDI-TOF MS (Figure 3.32) analysis indicated that some side products were present providing no improvement to the DMAP catalysed ROP suggesting that the pKa of the pyridine was too high.

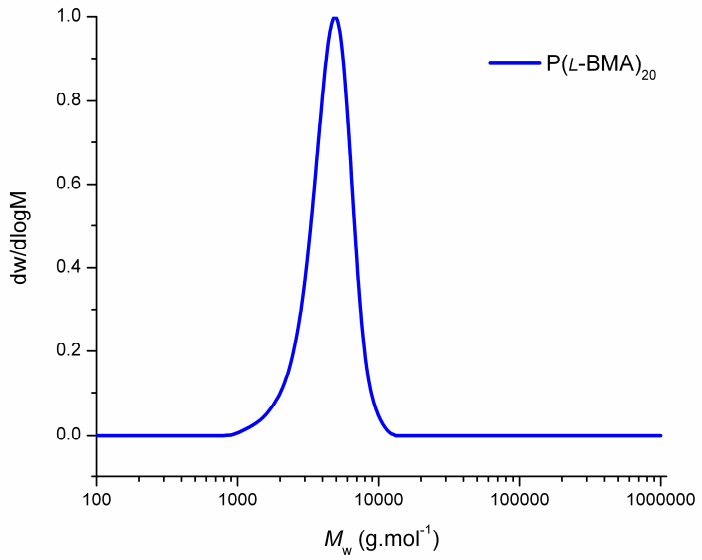

Figure 3.30. GPC trace of P(*L*-BMA) ([M]/[I] = 20) (M_n = 3 870 g.mol^{-1}, PDI = 1.14) prepared by ROP of ***L*-17** ([***L*-17**]$_0$ = 0.32 M) catalysed with 5 mol% 4-morpholinopyridine using *neo*-pentanol as the initiator.

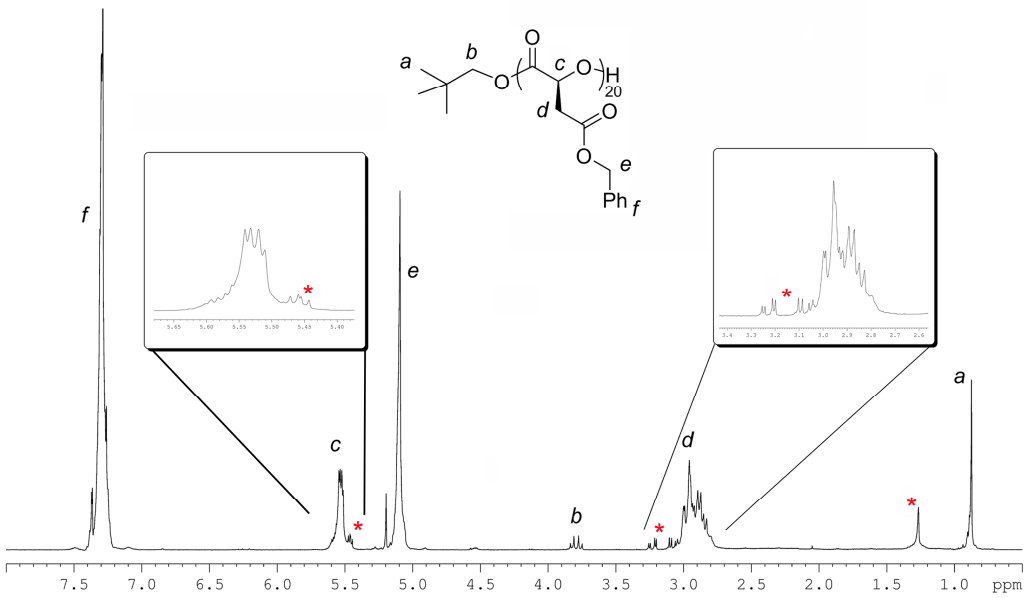

Figure 3.31. ^{1}H NMR spectrum of a P(*L*-BMA) ([M]/[I] = 20) (M_n = 3 870 g.mol^{-1}, PDI = 1.14) prepared by ROP of ***L*-17** ([***L*-17**]$_0$ = 0.32 M) catalysed with 5 mol% 4-morpholinopyridine using *neo*-pentanol as the initiator and the presence of impurities (*) (400 MHz; $CDCl_3$).

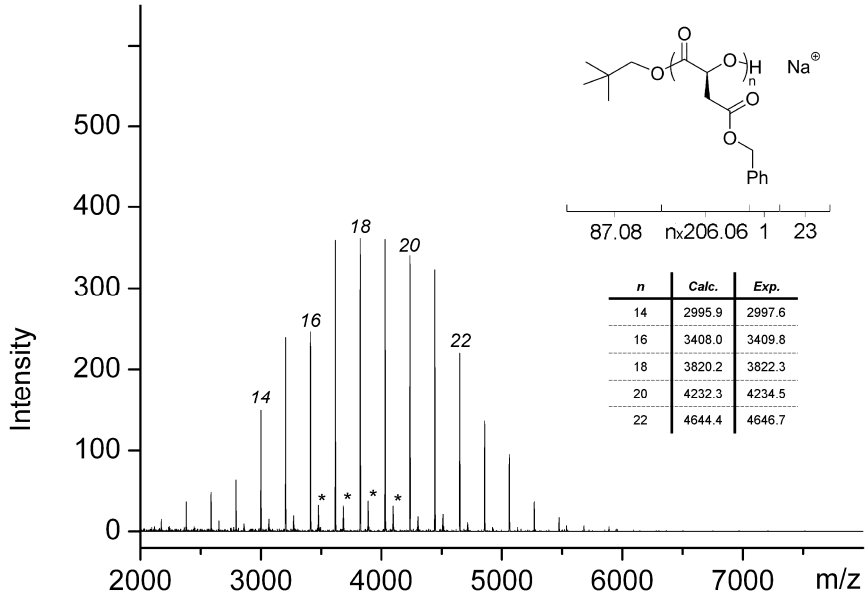

Figure 3.32. MALDI-TOF MS analysis of a P(*L*-BMA) ([M]/[I] = 20) (M_n = 3 870 g.mol^{-1}, PDI = 1.14) prepared by ROP of ***L*-17** ([***L*-17**]$_0$ = 0.32 M) catalysed with 5 mol% 4-morpholinopyridine using *neo*-pentanol as the initiator and the presence of impurities (*****).

Overall, 4-methoxypyridine provided the greatest levels of control over the other *para*-substituted pyridine catalysts investigated in the ROP of ***L*-17** enabling the successful preparation of P(*L*-BMA) (Table 3.1). Subsequent purification *via* column chromatography as previously described realised clean P(*L*-BMA)s and thus this system was used in preparation of all further polymers. This investigation demonstrated that the ROP of ***L*-17** displayed a strong dependence on the pKa of the ROP catalyst resulting in a significant effect on both the polymerisation time and mechanism along with side product formation. Furthermore, the side product observed in the MALDI-TOF MS analysis of all the P(*L*-BMA)s prepared with the range of pyridine based catalysts all correlated to the species isolated from column chromatography described earlier.

Table 3.1. Catalyst variation for the ROP of ***L*-17** targeted at [M]/[I] = 20.[a]

Amine Catalyst	**pKa**	**Time (min)**	M_n[c] **(g.mol^{-1})**	M_w/M_n[c]	**DP**[b]	**Impurity?**	
						^{1}H NMR[b]	**MS**[d]
DMAP	9.7	5	3 730	1.19	23	✓	✓
4-Morpholinopyridine	8.8	60	3 870	1.14	19	✓	✓
4-Methoxypyridine	6.6	90	3 860	1.10	22	×	✓
4-Methylpyridine	6.0	160	2 950	1.12	17	×	×[e]
Pyridine	5.3	435	2 100	1.13	16	×	×[e]

[a] $[\boldsymbol{L}\text{-}\mathbf{17}]_0$ = 0.32 M; 5 mol% amine catalyst, 25 °C. [b] Determined by ^{1}H NMR Spectroscopy. [c] Determined by GPC analysis. [d] Determined by MALDI-TOF MS. [e] at low catalyst concentration.

3.2.5 Ring-Opening Polymerisation studies of L-malOCA – detailed investigation of 4-methoxypyridine catalysis

Further investigation into the ROP of ***L*-17** with 4-methoxypyridine resulted in the observation of 'living' characteristics. A linear relationship between M_n and initial monomer to initiator ratio (Figure 3.33) was demonstrated and, as a consequence of the decreased rate of polymerisation compared to DMAP, also between M_n and monomer conversion (Figure 3.34). Further confirmation of the 'living' characteristics of the ROP catalysed with 4-methoxypyridine was obtained through a second-feed experiment in which to a P(*L*-BMA)$_{20}$ macroinitiator initiated from *neo*-pentanol ([M]/[I] = 20) (M_n = 3 860 g.mol^{-1}; PDI = 1.10), the further ROP of ***L*-17** ([M]/[I] = 20) enabled a chain extended P(*L*-BMA)$_{40}$ to be isolated that exhibited a double molecular weight (M_n = 7 760 g.mol^{-1}) while maintaining a low PDI of 1.12 (Figure 3.35). Leaving the resultant P(*L*-BMA)$_{40}$ for 8 h (5 times longer than required to reach >90% monomer conversion) in the presence of 4-methoxypyridine resulted in negligible changes in both the molecular weight (M_n = 8 030 g.mol^{-1}) and polydispersity (PDI = 1.11) suggesting that transesterification side reactions were minimal despite full monomer consumption (Figure 3.35).

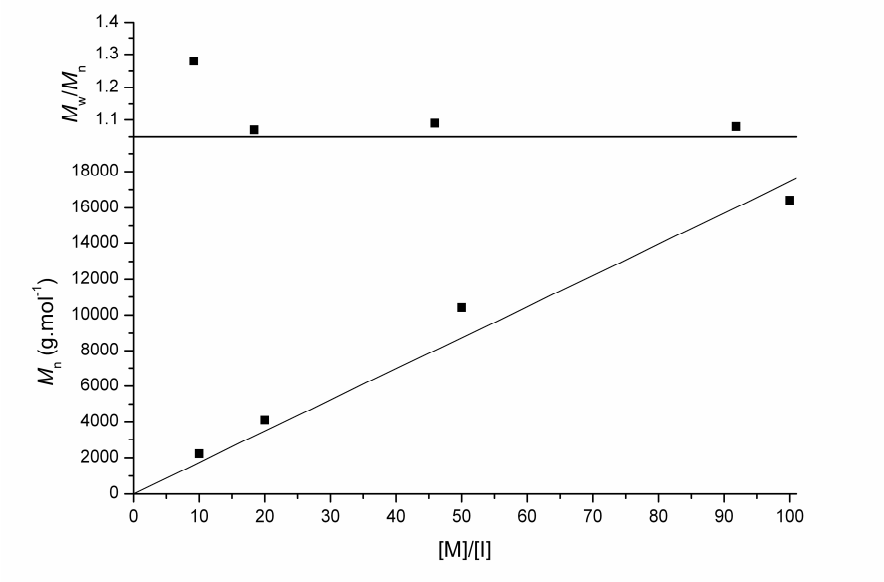

Figure 3.33. Plot of [M]/[I] *versus* M_n and PDI for ROP of ***L*-17** ([***L*-17**]$_0$ = 0.32 M) using 5 mol% 4-methoxypyridine and *neo*-pentanol as the initiator at a ratio of 1:1.

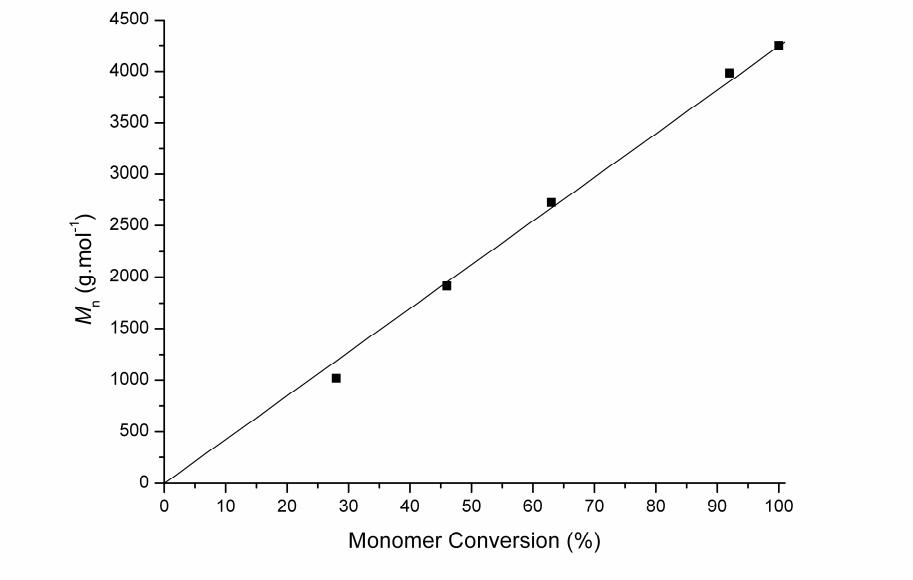

Figure 3.34. Plot of monomer conversion *versus* M_n and PDI for ROP of ***L*-17** ([***L*-17**]$_0$ = 0.32 M) using 5 mol% 4-methoxypyridine and *neo*-pentanol as the initiator at a ratio of 1:1.

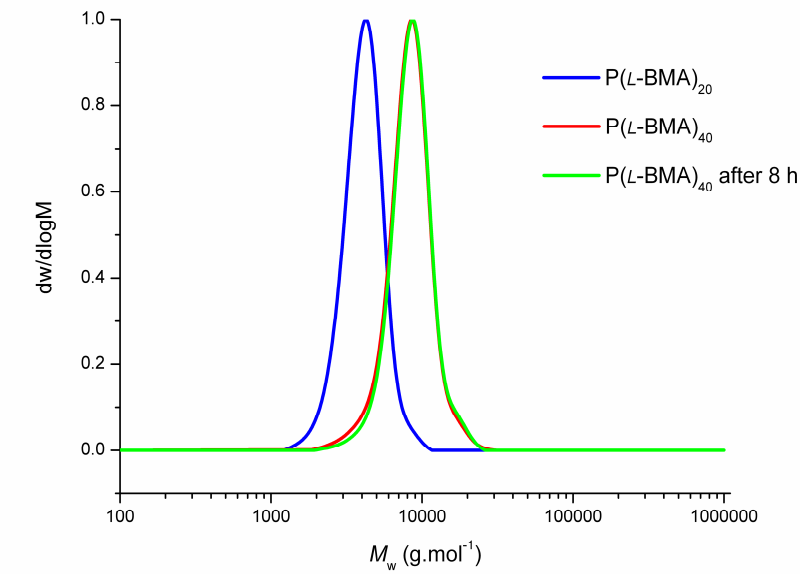

Figure 3.35. GPC traces of P(*L*-BMA)$_{20}$ (M_n = 3 860 g.mol^{-1}, PDI = 1.10) (—), P(*L*-BMA)$_{40}$ (M_n = 7 760 g.mol^{-1}, PDI = 1.12) (—) and P(*L*-BMA)$_{40}$ (M_n = 8 030 g.mol^{-1}, PDI = 1.11) (—) after 8 h prepared by ROP of ***L*-17** ([***L*-17**]$_0$ = 0.32 M) catalysed with 4-methoxypyridine using *neo*-pentanol as the initiator.

3.2.5.1 Ring-Opening Polymerisation studies of D-malOCA – 4-methoxypyridine

As described earlier, the synthetic methodology applied in the synthesis of *L*-malOCA, ***L*-17**, was also successfully employed to the other enantiomer yielding *D*-malOCA, ***D*-17**, in comparable yields from *D*-malic acid. The ROP of ***D*-17** ([M]/[I] = 20) was undertaken through application of the optimum ROP conditions using 4-methoxypyridine as the ROP catalyst at a 1:1 ratio to *neo*-pentanol. As expected, there was no significant difference in time to reach >90% monomer conversion compared with ***L*-17** (90 min) with GPC analysis confirming the controlled preparation of P(*D*-BMA)$_{20}$ observing a molecular weight of 3 820 g.mol^{-1} and a PDI of 1.09 (Figure 3.36). ^{1}H NMR spectroscopy and MALDI-TOF MS analysis confirmed end group fidelity revealing the main distribution around m/z = 4440.6 corresponding to a sodium charged DP21

polymer chain with a *neo*-pentanol end group; a regular spacing equal to the molecular weight of the repeat unit of benzyl α-(*D*)-malate (m/z = 206) demonstrates the lack of significant transesterification of the polymer chains. As with the ROP of ***L*-17** using 4-methoxypyridine, the impurity visible by MALDI-TOF MS analysis remained and was successfully removed *via* column chromatography using identical conditions yielding pure P(*D*-BMA)$_{20}$ (Figure 3.37).

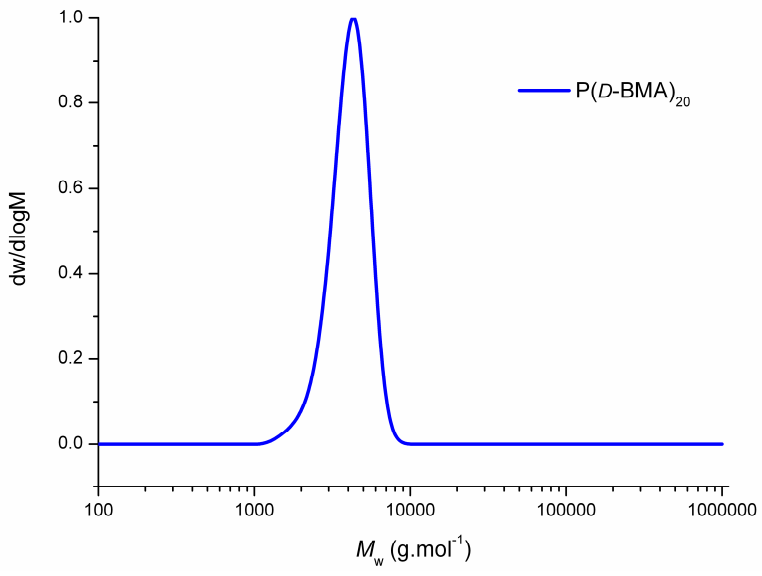

Figure 3.36. GPC trace of P(*D*-BMA) ([M]/[I] = 20) (M_n = 3 820 g.mol^{-1}, PDI = 1.09) prepared by ROP of ***D*-17** ([***D*-17**]$_0$ = 0.32 M) catalysed with 4-methoxypyridine using *neo*-pentanol as the initiator.

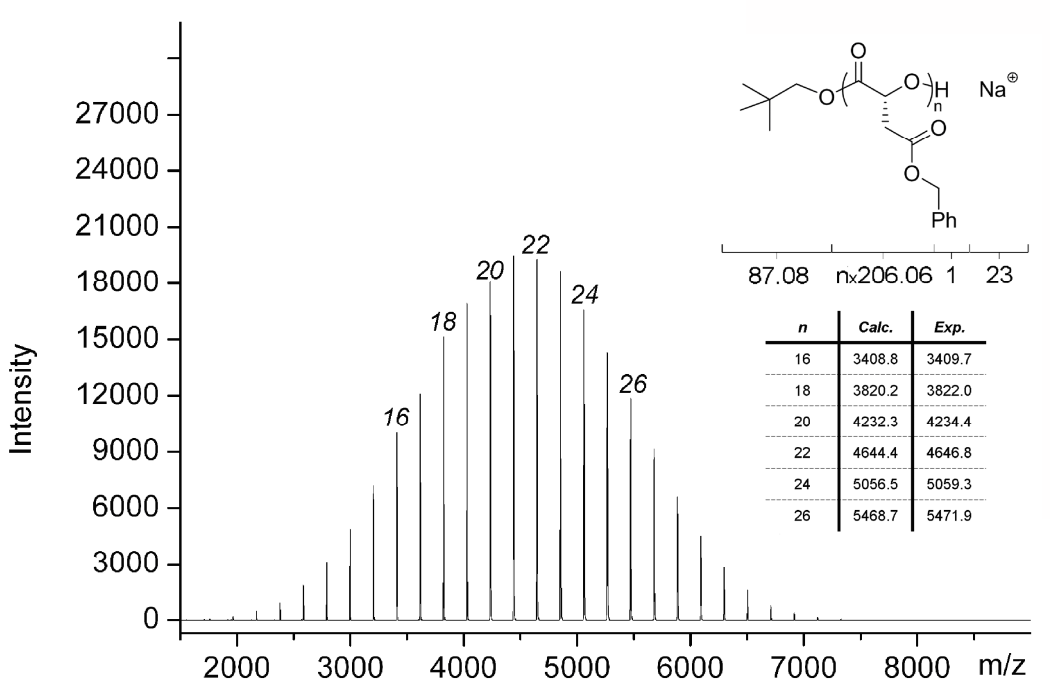

Figure 3.37. MALDI-TOF MS analysis of a P(*D*-BMA) ([M]/[I] = 20) (M_n = 3 820 g.mol^{-1}, PDI = 1.09) prepared by ROP of ***D*-17** ([***D*-17**]$_0$ = 0.32 M) catalysed with 5 mol% 4-methoxypyridine using *neo*-pentanol as the initiator.

3.2.5.2 Ring-Opening Polymerisation studies of L-malOCA – Block Copolymer Formation

Further extension of this methodology was investigated to enable the synthesis of block copolymers. Primarily, the synthesis of amphiphilic poly(ethylene oxide)-*b*-P(*L*-BMA) block copolymers by initiation from commercially available MeO-PEO$_{5K}$-OH or MeO-PEO$_{10K}$-OH (M_n ~ 5 000 and 10 000 g.mol^{-1} respectively) macroinitiators was investigated catalysed by 4-methoxypyridine. ROP of ***L*-17** ([M]/[I] = 20) with MeO-PEO$_{5K}$-OH (M_n = 8 200 g.mol^{-1}, PDI = 1.04) as the initiator resulted in >99% monomer conversion after 225 min. GPC analysis of the block copolymer confirmed P(*L*-BMA) chain growth (PEO$_{5K}$-*b*-P(*L*-BMA)$_{20}$; M_n = 11 540 g.mol^{-1}, PDI = 1.18). Successful block copolymer preparation was also achieved with initiation from MeO-PEO$_{10K}$-OH (M_n = 16 270 g.mol^{-1}, PDI =

1.03) realising the desired block copolymer PEO_{10K}-*b*-P(*L*-BMA)$_{20}$ (M_n = 19 440 g.mol^{-1}, PDI = 1.03) (Figure 3.38). ^{1}H NMR spectroscopy confirmed the presence of PEO, methine and malate units at δ = 5.55, 3.62, and 3.05 – 2.78 ppm respectively at the expected ratio.

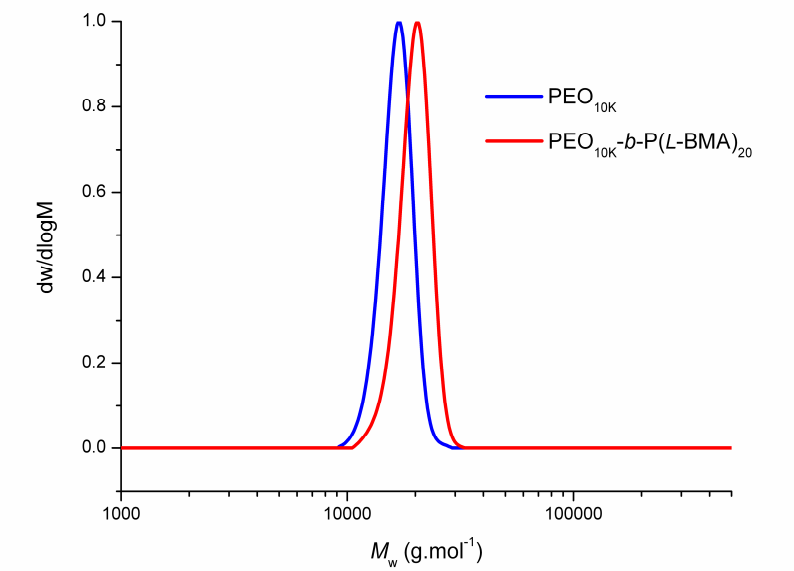

Figure 3.38. GPC traces of PEO_{10K}-*b*-P(*L*-BMA)$_{20}$ (M_n = 19 440 g.mol^{-1}, PDI = 1.03) (—) prepared by ROP of ***L*-17** ([M]/[I] = 20) ([***L*-17**]$_0$ = 0.32 M) catalysed with 4-methoxypyridine using MeO-PEO_{10K}-OH (M_n = 16 270 g.mol^{-1}, PDI = 1.03) (—) as the macroinitiator.

Block copolymers were also demonstrated to be accessible with poly(*L*-lactide), PLLA, prepared from poly(*L*-lactide) as a macroinitiator for the polymerisation of ***L*-17** ([M]/[I] = 20). PLLAs ([M]/[I] = 20 and 50) were synthesised by ROP of *L*-lacOCA using identical conditions as described above with 4-methoxypyridine, initiated from *neo*-pentanol. Complete monomer conversion for [M]/[I] = 20 and 50 was achieved after 60 min and 150 min respectively. Chain growth of ***L*-17** ([M]/[I] = 20) from the two PLLA-OH macroinitiators was confirmed by ^{1}H NMR spectroscopy showing the presence of both the lactide methyl and malate

resonances at δ = 1.58 and 3.08 – 2.85 ppm respectively. Additionally, GPC analysis revealed an increase in molecular weight from 2 640 g.mol^{-1} (PLLA$_{20}$-OH) to 5 890 g.mol^{-1} (PLLA$_{20}$-*b*-P(*L*-BMA)$_{20}$) with a low PDI being maintained. Chain growth from PLLA$_{50}$-OH (M_n = 7 680 g.mol^{-1}, PDI = 1.06) was also achieved resulting in the successful synthesis of PLLA$_{50}$-*b*-P(*L*-BMA)$_{20}$ (M_n = 10 850 g.mol^{-1}, PDI = 1.05) (Figure 3.39).

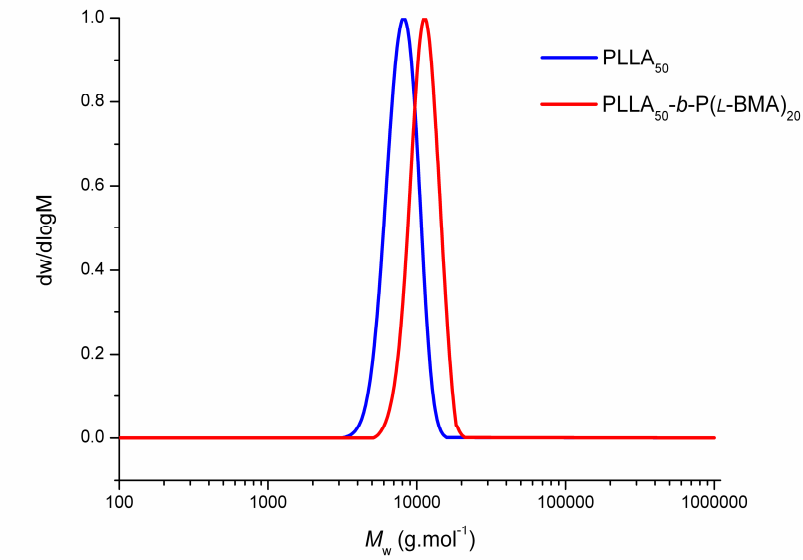

Figure 3.39. GPC traces of PLLA$_{50}$-*b*-P(*L*-BMA)$_{20}$ (M_n = 10 850 g.mol^{-1}, PDI = 1.05) (—) prepared by ROP of ***L*-17** ([M]/[I] = 20) ([***L*-17**]$_0$ = 0.32 M) catalysed with 4-methoxypyridine using PLLA$_{50}$-OH (M_n = 7 680 g.mol^{-1}, PDI = 1.06) (—) as the macroinitiator.

3.2.6 Deprotection of P(L-BMA) – Formation of PMA

Deprotection of the pendant carboxylic acid groups of P(*L*-BMA)$_{20}$ (M_n = 3 860 g.mol^{-1}, PDI = 1.10) was accomplished by hydrogenolysis using H_2 over Pd/C and resulted in hydrophilic poly(*L*-malic acid) (PMA) in 15 min at 40 °C (Scheme 3.11). Clean and complete removal of the benzyl protecting groups was deduced from the disappearance of all of the aromatic and benzylic signals from both the ^{1}H (Figure 3.40) and ^{13}C NMR spectra. Further confirmation was

obtained from the change in solubility of the resulting polymer from the P(*L*-BMA)$_{20}$ (soluble in $CHCl_3$, insoluble in MeOH) to the PMA_{20} (soluble in MeOH, insoluble in $CHCl_3$). This process did not result in degradation of the poly(ester) backbone, as shown by lack of resonances associated with changes to the electronic environment of the methine protons associated with a neighbouring hydroxyl proton in the ^1H NMR spectrum that would be apparent upon cleavage of the backbone. Electrospray MS provided additional confirmation of deprotection through observation of PMA_{20} as a doubly charged species (Figure 3.41a) with the major peak at m/z = 1203.5 that upon deconvolution (Figure 3.41b) resulted in a major peak at m/z = 2408.3 equal to the desired PMA_{20} along with additional peaks correlating to singly (m/z = 2430.2) (Figure 3.42c) and doubly (m/z = 2452.1) (Figure 3.42d) sodium charged PMA_{20}. A lower molecular weight species was also present at m/z = 2390.2 matching ring closure of the PMA_{20} end group resulting in the loss of a molecule of H_2O (Figure 3.42a). Additional analysis of both P(*L*-BMA)$_{20}$ and PMA_{20} by GPC using a 0.1 M citric acid in THF solution as the eluent exhibited distributions with (M_n = 4 980 g.mol^{-1}; PDI = 1.06) and (M_n = 1 100 g.mol^{-1}; PDI = 1.10) respectively (compared to poly(styrene) standards) (Figure 3.43). A small molecular weight tail was observed on the GPC trace of PMA_{20} that was believed to be the result of a small amount of degradation occurring under the analysis conditions. It is postulated that the significant molecular weight difference observed between P(*L*-BMA)$_{20}$ and PMA_{20} *via* GPC analysis is a result of interactions between the PMA_{20} and the eluent solvent system resulting in tightly coiled polymers thus leading to low observed molecular weight values.

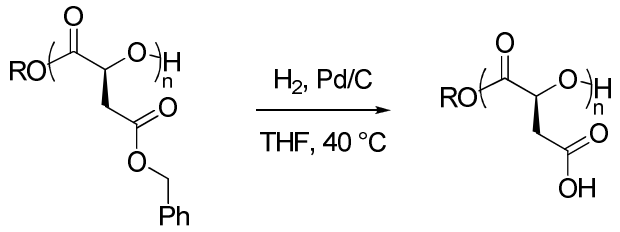

P(*L*-BMA) **PMA**

Scheme 3.11. Deprotection of poly(benzyl α-(*L*)-malate), P(*L*-BMA), using hydrogenolysis to yield PMA.

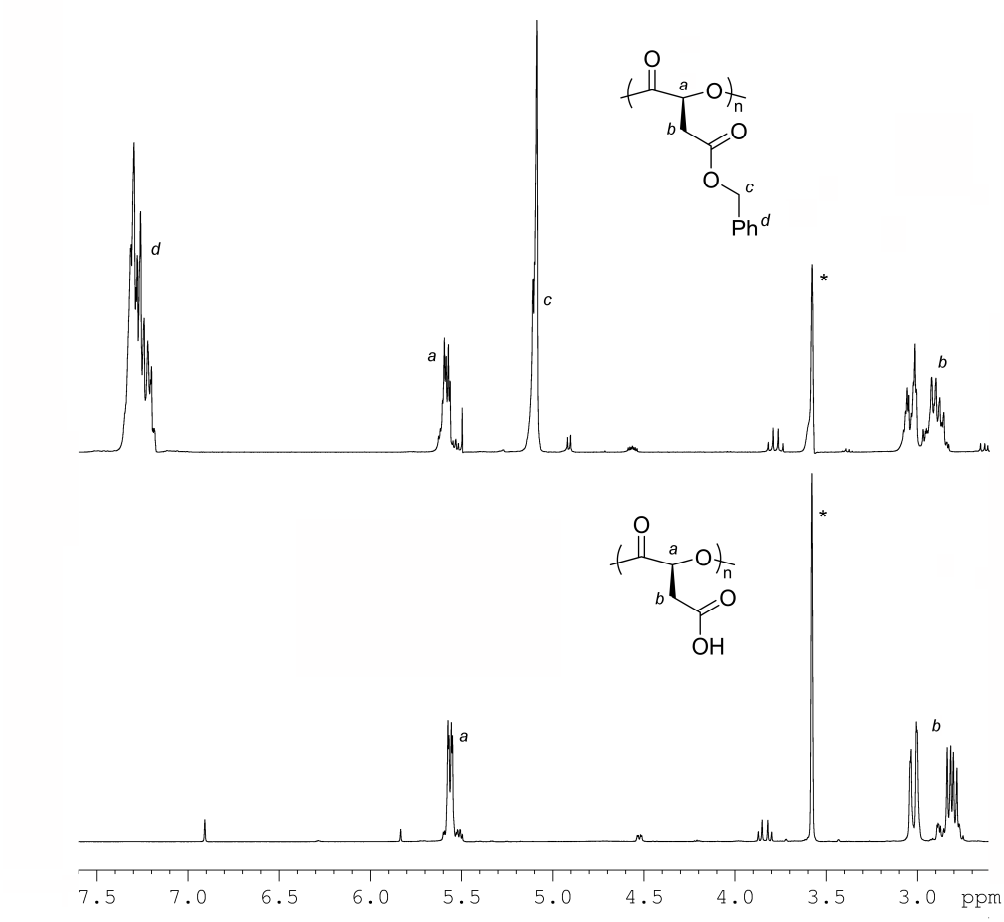

Figure 3.40. ^{1}H NMR spectra of (i) P(*L*-BMA)$_{20}$ and (ii) PMA$_{20}$ (d^{8}-THF, 400 MHz; * indicates residual solvent signal).

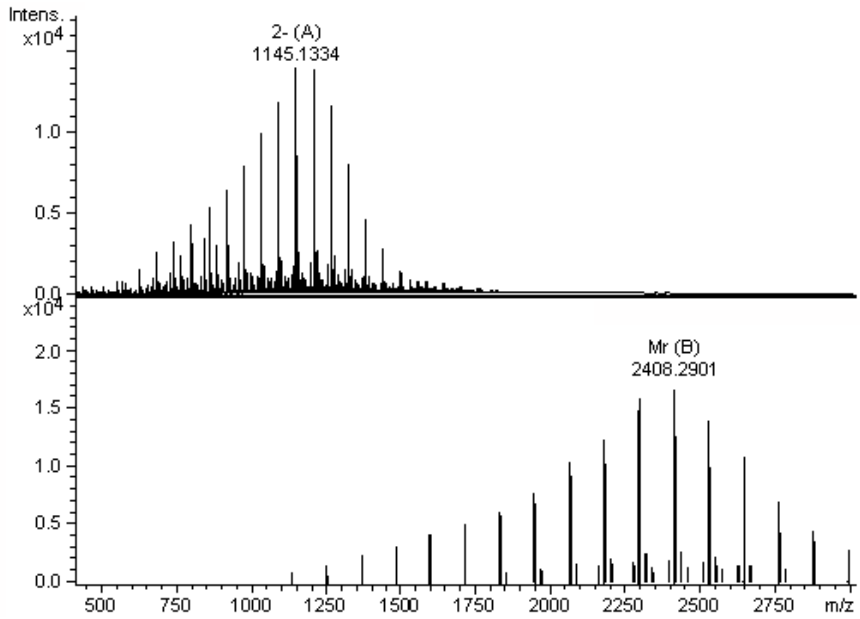

Figure 3.41. ESI MS raw data (A) and deconvoluted (B) analysis of a PMA ([M]/[I] = 20) (M_n = 1 100 g.mol^{-1}; PDI = 1.10) prepared through the hydrogenation of P(*L*-BMA)$_{20}$ prepared by ROP of ***L*-17** ([***L*-17**]$_0$ = 0.32 M) catalysed with 5 mol% pyridine using *neo*-pentanol as the initiator.

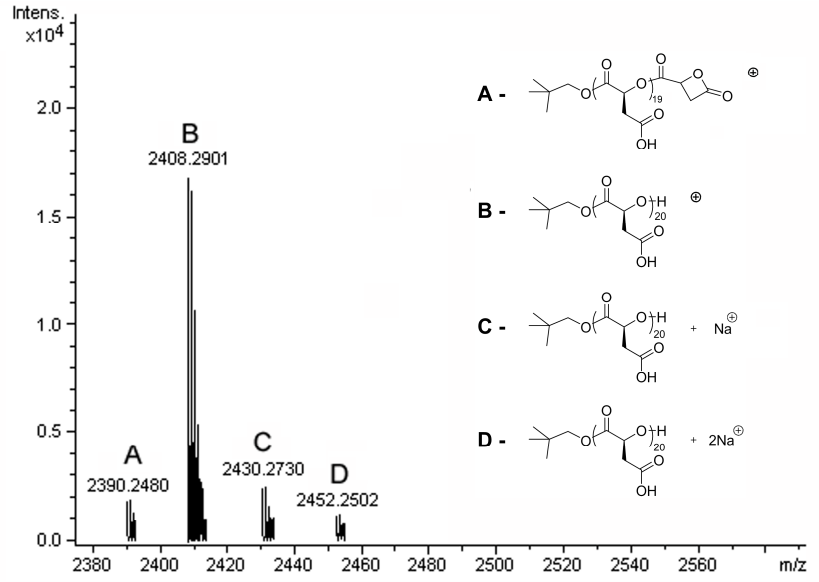

Figure 3.42. ESI MS zoom of deconvoluted analysis of PMA ([M]/[I] = 20) (M_n = 1 100 g.mol^{-1}; PDI = 1.10) prepared through the hydrogenation of a P(*L*-BMA)$_{20}$ prepared by ROP of ***L*-17** ([***L*-17**]$_0$ = 0.32 M) catalysed with 5 mol% pyridine using *neo*-pentanol as the initiator.

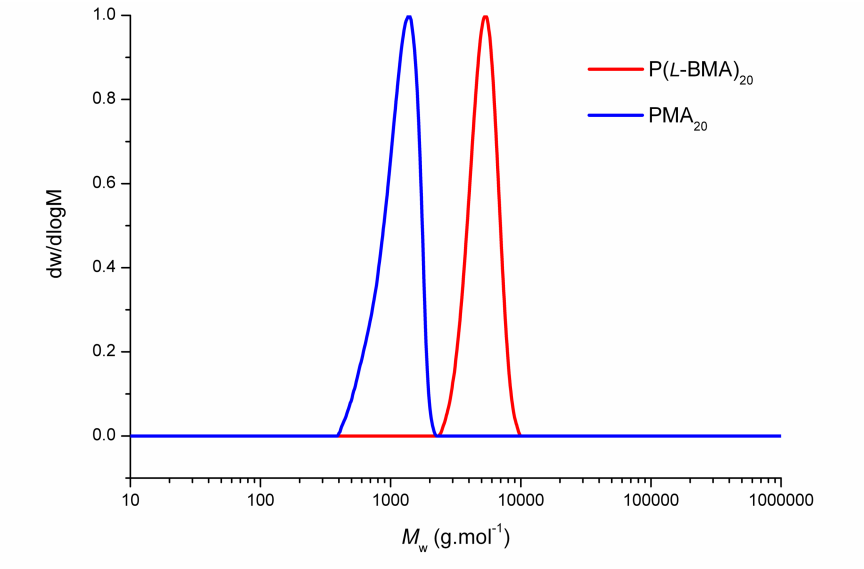

Figure 3.43. GPC traces of P(*L*-BMA)$_{20}$ (M_n = 4 980 g.mol^{-1}, PDI = 1.06) (—) and PMA$_{20}$ (M_n = 1 100 g.mol^{-1}, PDI = 1.10) (—) prepared by ROP of ***L*-17** ([***L*-17**]$_0$ = 0.32 M) catalysed with 4-methoxypyridine using *neo*-pentanol as the initiator and subsequent hydrogenolysis using H_2 and Pd/C (GPC values using 0.1 M citric acid in THF eluent compared to poly(styrene) standards).

3.2.7 Degradation of PMA

Thermal degradation of both P(*L*-BMA)$_{20}$ and PMA$_{20}$ was studied using thermogravimetric analysis (TGA). Significant differences in the temperature at which the polymers degraded was observed (Figure 3.44). While both poly(ester)s fully degraded within a reasonably short temperature range, P(*L*-BMA)$_{20}$ was stable up to 280 °C whereas PMA$_{20}$ began degrade at a significantly lower temperature, ~ 180 °C. It is believed that the pendant carboxylic acid groups of PMA$_{20}$ facilitated the degradation of PMA$_{20}$ in an auto-catalytic process.

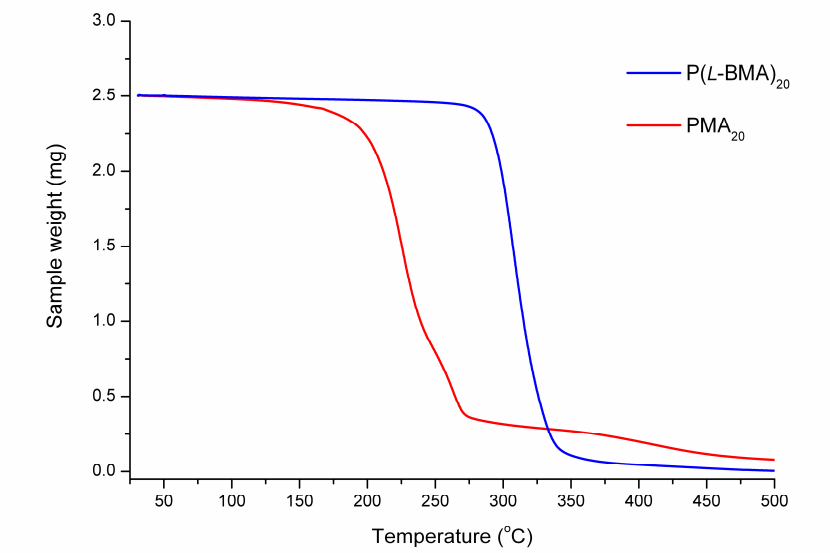

Figure 3.44. TGA analysis of both P(*L*-BMA)$_{20}$ (M_n = 4 980 g.mol^{-1}, PDI = 1.06) (▬) and PMA$_{20}$ (M_n = 1 100 g.mol^{-1}, PDI = 1.10) (▬) from 25 to 500 °C.

Hydrolytic degradations were performed in H_2O at room temperature on a PMA ([M]/[I] = 15) at a concentration of 0.48 mmol.L^{-1}. The degradations were monitored *via* acid-base titration using a 0.45 mmol.L^{-1} aqueous NaOH solution with four drops of a phenolphthalein pH indicator in methanol solution. Degradation was complete after 10 days determined when two equivalents of the NaOH solution was required to neutralise the reaction. Examination of ^{1}H NMR spectra during the degradation in D_2O demonstrates a gradual reduction of resonances attributed to PMA$_{15}$ at δ = 5.67 and 3.17 – 2.96 ppm with a corresponding increase of new resonances at δ = 4.53 and 2.93 – 2.76 ppm respectively resulting from the degradation products. Electrospray (ESI) MS provided a useful method to monitor the molecular weight loss during the PMA degradation. Significant molecular weight loss was observed early in the degradation after 30 h that subsequently continued at a slower rate realising near complete degradation to *L*-malic acid (m/z = 133.0) after 7 days with the final oligomers requiring an additional 3 days to fully degrade (Figure 3.45). Attempts

to monitor this degradation *via* GPC analysis failed as a consequence of the rapid initial weight loss of the degradation, confirmed through ESI MS, along with the presence of citric acid in the GPC solvent system that resulted in a DRI response that overlapped with the degradation products thus making accurate calculations of molecular weight and PDI impossible.

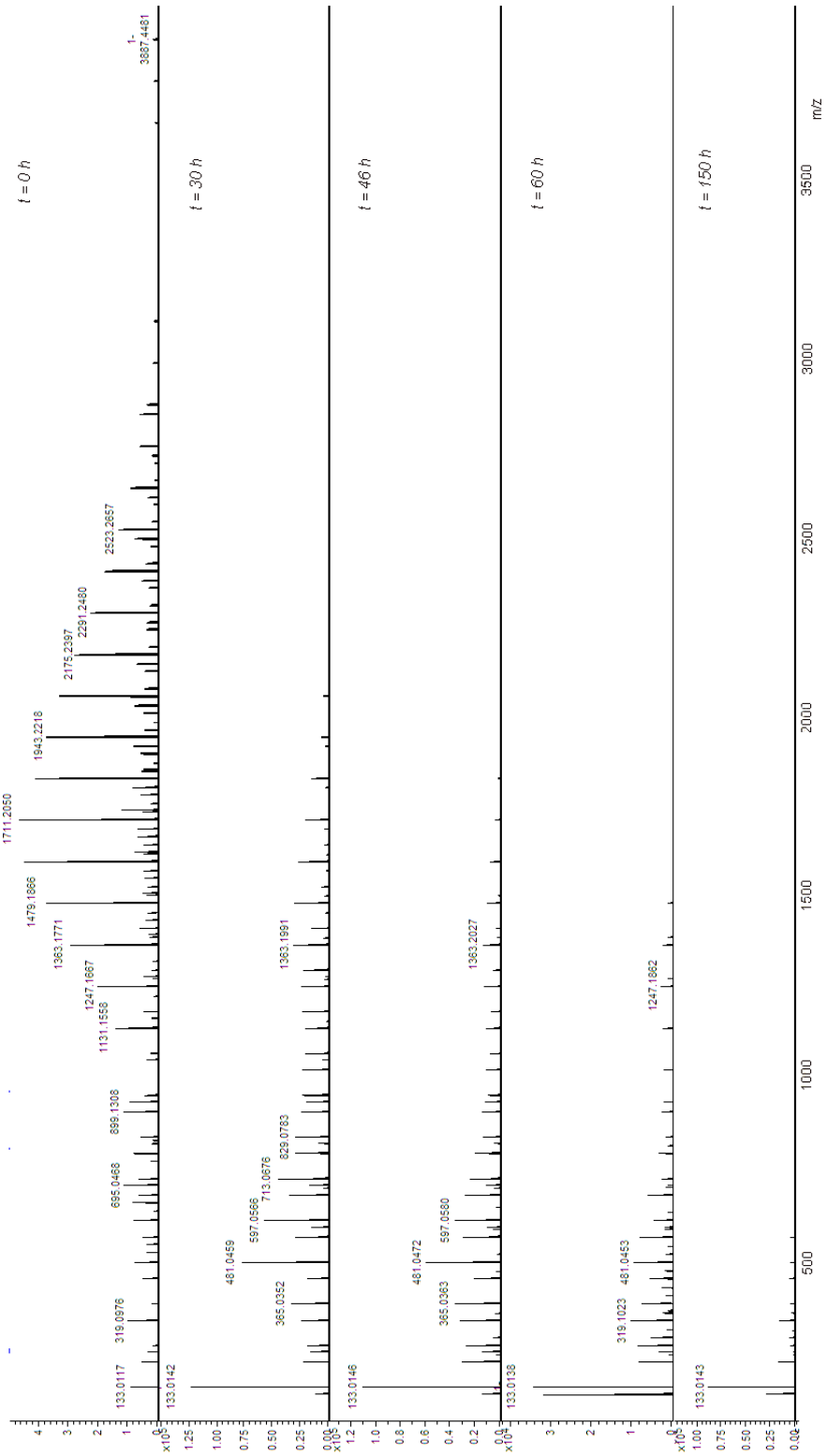

Figure 3.45. ESI MS analysis of the degradation of PMA ([M]/[I] = 15) ([PMA_{15}]$_0$ = 0.36 mmol.L^{-1}) in H_2O at room temperature.

3.3 Conclusions

In conclusion, the novel synthesis of *L*-malOCA and *D*-malOCA, ***L*-17** and ***D*-17**, from *L*- and *D*-malic acid respectively has been demonstrated. Homopolymerisation of ***L*-17** catalysed with a range of pyridine based catalysts enabled the synthesis of functional poly(ester)s with pendant benzyl protected carboxylic acid groups to high monomer conversions in the absence of transesterification side reactions. The choice of ROP catalyst was demonstrated to have a significant effect on the amount of side products produced with their removal shown to be successful *via* column chromatography. The versatility of the polymerisation system was shown through the successful initiation from alcohols including PEO and PLLA as macroinitiators in the preparation of block copolymers. Removal of the benzyl protecting groups was successful without any polymer backbone scission to yield hydrophilic poly(ester)s and degradation studies of the resultant PMA_{15} in H_2O was demonstrated to occur fully within 10 days as determined by titration, ^1H NMR and mass spectrometry. The derivation of this versatile functional poly(ester) from a biorenewable resource provides a potential route to a range of other functional poly(ester)s *via* this platform.

3.4 References

(1) Jing, F.; Hillmyer, M. A. *J. Am. Chem. Soc.* **2008**, *130*, 13826.

(2) Allinger, N. L.; Zalkow, V. *J. Org. Chem.* **1960**, *25*, 701.

(3) Thillaye du Boullay, O.; Marchal, E.; Martin-Vaca, B.; Cossio, F. P.; Bourissou, D. *J. Am. Chem. Soc.* **2006**, *128*, 16442.

(4) Thillaye du Boullay, O.; Bonduelle, C.; Martin-Vaca, B.; Bourissou, D. *Chem. Commun.* **2008**, 1786.

(5) Bonduelle, C.; Martín-Vaca, B.; Cossío, Fernando P.; Bourissou, D. *Chem. Eur. J.* **2008**, *14*, 5304.

(6) Kricheldorf, H. R.; Jonte, J. M. *Polym. Bull.* **1983**, *9*, 276.

(7) Li, Y.; Hoskins, J. N.; Sreerama, S. G.; Grayson, S. M. *Macromolecules* **2010**, *43*, 6225.

(8) Jeong, W.; Shin, E. J.; Culkin, D. A.; Hedrick, J. L.; Waymouth, R. M. *J. Am. Chem. Soc.* **2009**, *131*, 4884.

(9) Culkin, D.; Jeong, W.; Csihony, S.; Gomez, E.; Balsara, N.; Hedrick, J.; Waymouth, R. *Angew. Chem. Int. Ed.* **2007**, *46*, 2627.

(10) Jeong, W.; Hedrick, J. L.; Waymouth, R. M. *J. Am. Chem. Soc.* **2007**, *129*, 8414.

(11) *Handbook of chemistry and physics*; 54th ED ed., 1973 - 1974.

(12) Albert, A.; Phillips, J. N. *J. Chem. Soc.* **1956**, 1294.

(13) Brown, H. C.; Mihm, X. R. *J. Am. Chem. Soc.* **1955**, *77*, 1723.

(14) Bunting, J. W.; Toth, A.; Heo, C. K. M.; Moors, R. G. *J. Am. Chem. Soc.* **1990**, *112*, 8878.

Chapter 4 - Synthesis and micellisation of novel degradable amphiphilic block copolymers of poly(ethylene oxide) and poly(benzyl α-malate).

4.1 Introduction

Over the past few decades amphiphilic block copolymers have received special attention as a consequence of their ability to act as building blocks in supramolecular chemistry realising highly ordered self-assembled structures.[1-5] Molecular self-assembly is a powerful approach for fabricating novel supramolecular architectures.[6-7] Generally, self-organisation is driven by weak, non-covalent interactions (hydrogen bonds, Van der Waals interactions). In the case of amphiphilic block copolymers, self-assembly is driven by the hydrophobic effect whereby the selective solvation of the hydrophilic block in aqueous solution drives the polymers to arrange in a manner that most effectively reduces the free energy, *i.e* whereby the hydrophilic blocks are solvated in the aqueous phase and the hydrophobic blocks are protected in the core of the particle.[6] The dimensions of the resultant self-assembled particles are largely controlled by the molecular weight of the polymer blocks whereas the mole fraction of the blocks has a significant effect on the morphology of the resultant particles.[8-9]

The biocompatibility and biodegradability of amphiphilic poly(ethylene oxide)-*b*-poly(lactide) (PEO-*b*-PLA) or poly(ethylene oxide)-*b*-poly(lactide)-*co*-poly(glycolide) (PEO-*b*-PLGA) block-copolymer micelles has resulted in them being extensively studied as drug carriers.[10-15] Most drugs have a hydrophobic character and are thus easily incorporated into micelles by simple physical entrapment, through dialysis or by an oil/water emulsion method, resulting in greatly increased solubility of the hydrophobic drug in aqueous media. The ability of PEO-*b*-poly(ester) micelles to encapsulate hydrophobic drugs as well as their biodegradability and biocompatibility make these highly attractive systems and thus have been extensively studied.[10,16-17]

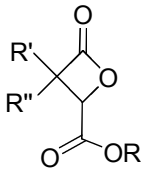

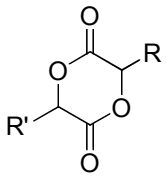

LXXII: R = CH_2Ph, R' = H, R'' = H
LXXVI: R = $(CH_2)_3CH_3$, R' = H, R'' = H
LXXVII: R = $(CH_2)_3CH_3$, R' = Me, R'' = H
LXXVIII: R = $(CH_2)_5CH_3$, R' = H, R'' = H
LXXIX: R = $CH_2CH_2C(CH_3)_3$, R' = H, R'' = H
XCVI: R = CH_2Ph, R' = Me, R'' = H

III: R = $(CH_2)_5CH_3$, R' = $(CH_2)_5CH_3$
VI: R = $(CH_2)_5CH_3$, R' = Me
XVIII: R = $CH_2C(O)OCH_2Ph$, R' = H
XXIV: R = $(CH_2)_2C(O)OCH_2Ph$, R' = Me

Figure 4.1. Structures of benzyl β-malolactone (MLABz, **LXXII**), butyl malolactonate (**LXXVI**), butyl 3-methylmalolactonate (**LXXVII**), hexyl malolactonate (**LXXVIII**), neohexyl malolactonate (**LXXIX**) and (*R*,*S*)-4-benzyloxycarbonyl-3,3-dimethyl-2-oxetanone (**XCVI**), 3,6-di-*n*-hexyl- (diHLA, **III**), 3-methyl-6-*n*-hexyl- (mHLA, **VI**), 3-(*S*)-[(benzyloxycarbonyl)methyl]-1,4-dioxane-2,5-diones (BMD, **XVIII**) and benzyl-3-(5-methyl-3,6-dioxo-1,4-dioxan-2-yl)propanoate (mBzCLA, **XXIV**).

While the application of PLA or PLGA in the core of micelles has been utilised in biodegradable and biocompatible drug delivery systems they do have potential drawbacks resulting from their lack of functionality. As a consequence, several reports of benzyl β-malolactone (MLABz, **LXXII**) (Figure 4.1) capable of realising poly(MLABz), the structural isomer of PBMA described in chapter 3, has been applied in polymeric micelle preparation. Poly(MLABz) is often applied as the hydrophilic component of amphiphilic block copolymer with other hydrophobic poly(ester)s due to its readily accessibility to water soluble poly(β-malic acid) (PMA) through hydrogenolysis. An example of this involved the preparation of a telechelic ABA triblock poly(εCL-*co*-MLABz-*co*-εCL) that upon hydrogenolysis of the MLABz groups realised an amphiphilic triblock poly(εCL-*co*-MLA-*co*-εCL) that was shown to self-assemble into 'flower' micelles in pure water by UV spectroscopy with pyrene.[18] Other work has involved the grafting of poly(MLABz) to chitosan that after subsequent hydrogenolysis yielded

amphiphilic chitosan derivatives capable of self-assembly in water resulting in nanoparticles with average hydrodynamic diameters of 190 – 350 nm capable of incorporating paclitaxel.[19] Poly(MLABz) has been further applied as a macroinitiator in the ROP of benzyl β-malolactone (MLABz, **LXXVI**) and butyl 3-methylmalolactonate (**LXXVII**) along with copolymerisation of hexyl malolactonate (**LXXVIII**) and neohexyl malolactonate (**LXXIX**) with MLABz that upon deprotection yields amphiphilic block and statistical copolymers. Self-assembly of these in water realised nanoparticles with average hydrodynamic diameters between 35 to 171 nm with the physical characteristics dependant on block chain lengths and chemical structure of the hydrophobic components.[20-21] This technique has been further applied in the hydrogenolysis of (*R*,*S*)-4-benzyloxycarbonyl-3,3-dimethyl-2-oxetanone (**XCVI**) groups (Figure 4.1) incorporated into an ABA telechelic PLLA-*b*-poly(**XCVI**-*co*-β-BL)-*b*-PLLA to realise the respective amphiphilic triblock copolymer that, after self-assembly at low temperatures (4 °C), yielded 'flower' type micelles with microgelation occurring at 25 °C and dissolution of the microgel at 40 °C.[22]

3-(*S*)-[(Benzyloxycarbonyl)methyl]-1,4-dioxane-2,5-dione (BMD, **XVIII**) (Figure 4.1), structurally similar to both MLABz and (*R*,*S*)-4-benzyloxycarbonyl-3,3-dimethyl-2-oxetanone, has been incorporated (3 – 9%) into a PEO-*b*-poly(DLLA-*co*-BMD) capable of self-assembly. Subsequent deprotection of the BMD groups in the hydrophobic core to malic acid units was demonstrated to dramatically increase the drug loading efficiency of papaverine resulting from hydrogen bonding between the carboxylic acid groups and the drug.[23] Möller *et al.* have recently reported the use of benzyl-3-(5-methyl-3,6-dioxo-1,4-dioxan-2-yl)propanoate (**XXIV**), along with MLABz, 3,6-di-*n*-hexyl-1,4-dioxane-2,5-

dione (**III**) and 3-methyl-6-*n*-hexyl-1,4-dioxane-2,5-dione (**IV**) (Figure 4.1) in the preparation of a range of novel degradable nanoparticles. These polymeric micelles consisted of hydrophilic coronas of either PEO, PMA or PmCLA with the latter two resulting from the deprotection of poly(MLABz) and poly(**XXIV**) respectively and hydrophobic cores of either PLA, poly(**III**) or poly(**IV**) all possessing average hydrodynamic diameters below 100 nm and low CMC values between 5 x 10^{-3} and 100 x 10^{-3} g.L^{-1}.[24]

As discussed in chapter 3, the synthesis and ring-opening polymerisation (ROP) of novel *O*-carboxyanhydrides 5-(*S*)-[(benzyloxycarbonyl)methyl]-1,3-dioxolane-2,4-dione (*L*-malOCA, ***L*-17**) and 5-(*R*)-[(benzyloxycarbonyl)methyl]-1,3-dioxolane-2,4-dione (*D*-malOCA, ***D*-17**) from *L*- and *D*-malic acid respectively was reported to realise the functional poly(ester)s, poly(benzyl α-(*L*)-malate), P(*L*-BMA), and poly(benzyl α-(*D*)-malate), P(*D*-BMA). Herein, the synthesis and characterisation of novel amphiphilic PEO-*b*-PBMA block copolymers using ***L*-17** and ***D*-17** synthesised from commercially available *L*- and *D*-malic acid respectively is reported. Self-assembly of these leading to a variation in both size dimensions and stability of the micelles tunable through variation of both the hydrophobic and hydrophilic block lengths is also investigated. The accessibility of enantiopure PEO-*b*-P(*L*-BMA) and PEO-*b*-P(*D*-BMA) also led to the investigation of the formation of polymeric micelles with enhanced stabilisation through stereocomplex interactions of the PBMA chains in the hydrophobic core.

4.2 Results and Discussion

4.2.1 Synthesis of enantiomerically pure PEO_x-b-P(L-BMA)$_n$ and PEO_x-b-P(D-BMA)$_n$

The synthesis of amphiphilic PEO-*b*-PBMA diblock copolymers was achieved *via* the initiation of ROP of ***L*-17** and ***D*-17** from commercially available monomethylether PEO homopolymers, catalysed with 4-methoxypyridine (Scheme 4.1). ROP of ***L*-17** and ***D*-18** at different monomer-to-initiator ratios from monomethylether PEO macroinitiators with different degrees of polymerisation was investigated at 25 °C in a $CHCl_3$ solution. Upon completion of the allotted time, polymerisations were quenched by removal of 4-methoxypyridine *via* precipitation of the polymerisation solution into ice cold petroleum ether (b.p. 40-60 °C).

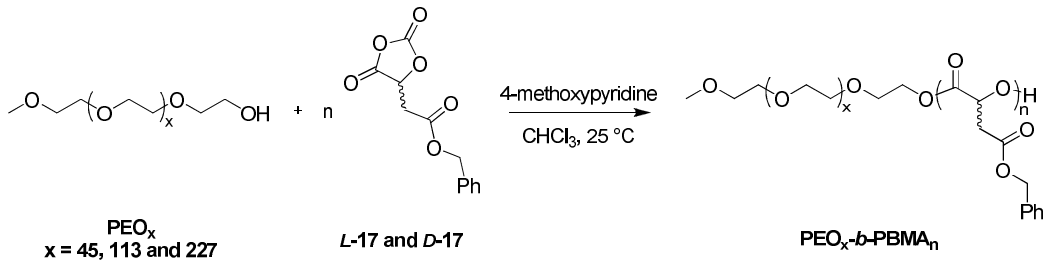

Scheme 4.1. Ring-opening polymerisation of 5-(*S*)- and 5-(*R*)-[(benzyloxycarbonyl)methyl]-1,3-dioxolane-2,4-dione, ***L*-17** and ***D*-17,** with initiation from different monomethylether PEO macroinitiators using 4-methoxypyridine.

^{1}H NMR spectroscopy provided a convenient method for monitoring the progress of the polymerisation by observation of the reduction of the methine resonance at δ = 5.09 ppm and the methylene resonance of the malate unit at δ = 3.13 ppm of the monomer and the appearance of the corresponding broad multiplets at δ = 5.61 – 5.51 and 3.05 – 2.78 ppm respectively in PBMA. The MeO-PEO-OH

macroinitiator enabled simple calculation of the degree of polymerisation (DP) by comparison of the methylene resonance of the repeating ethylene glycol unit at δ = 3.62 ppm and the methylene resonance in PBMA at δ = 3.05 – 2.78 (Figure 4.2). The molecular weight and DP were controlled by adjusting the monomer-to-initiator ([M]/[I]) ratio. GPC analysis of the block copolymers confirmed PBMA chain growth from the MeO-PEO-OH macroinitiators with an increase in retention time upon block copolymer formation whereby chain growth of a P(*L*-BMA) ([M]/[I] = 25) was successful from MeO-PEO_{5K}-OH (M_n = 7 530 g.mol^{-1}, PDI = 1.03) resulting in the preparation of PEO_{5K}-*b*-P(*L*-BMA)$_{25}$ (M_n = 16 940 g.mol^{-1}, PDI = 1.03) (Figure 4.3). A range of amphiphilic block copolymers were prepared through variation of both PEO and PBMA chain lengths *via* alteration of the [M]/[I] and selection of different molecular weight macroinitiators along with choice of enantiomer of the monomer (Table 4.1).

Table 4.1. Polymerisation data for the chain extension of MeO-PEO-OH of different molecular weights with PBMA at different monomer-to-initiator ratios through the ROP of either ***L*-17** or ***D*-17**.[a]

MeO-PEO-OH	[M]/[I] (17 enantiomer)	DP[b]	M_n[b] (g.mol^{-1})	M_n[c] (g.mol^{-1})	M_w/M_n[c]
2K	-	-	2 290	2 790	1.04
2K	5 (*L*)	5	3 320	3 850	1.04
5K	-	-	5 690	7 530	1.03
5K	10 (*L*)	10	7 750	9 400	1.04
5K	10 (*D*)	9	7 540	8 950	1.03
5K	25 (*L*)	25	10 840	16 940	1.03
5K	40 (*L*)	37	13 310	20 410	1.03
10K	-	-	11 030	16 270	1.03
10K	20 (*L*)	23	15 770	19 440	1.03

[a] [***L*-17**]$_0$ = 0.32 M; 5 mol% 4-methoxypyridine; $CHCl_3$; 25 °C. [b] Determined by ^{1}H NMR Spectroscopy. [c] Determined by GPC analysis.

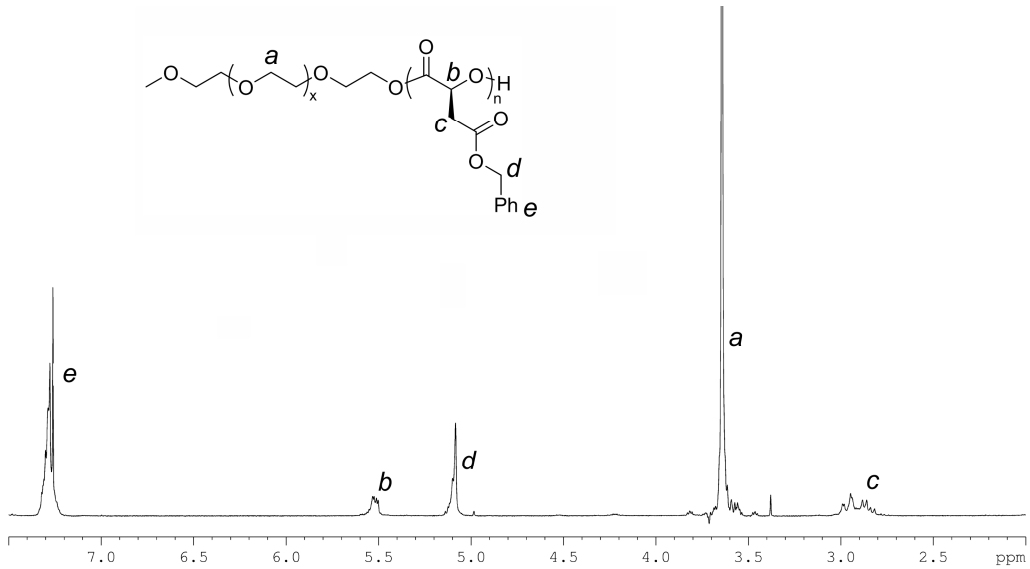

Figure 4.2. ^{1}H NMR spectrum of a PEO_{5K}-*b*-P(*L*-BMA)$_{25}$ (M_n = 16 940 g.mol^{-1}, PDI = 1.03) prepared by ROP of ***L*-17** ([***L*-17**]$_0$ = 0.32 M) catalysed with 5 mol% 4-methoxypyridine using MeO-PEO_{5K}-OH as the macroinitiator (400 MHz; $CDCl_3$).

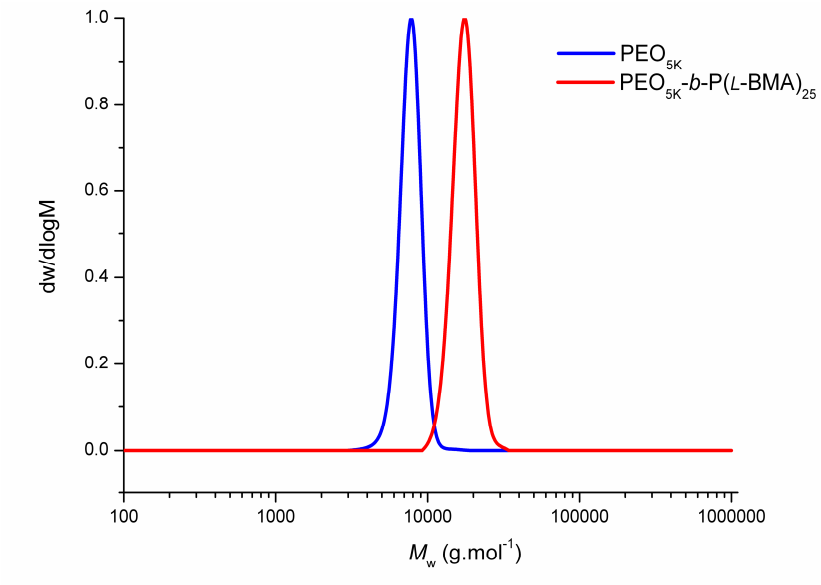

Figure 4.3. GPC traces of PEO$_{5K}$-*b*-P(*L*-BMA)$_{25}$ (M_n = 16 940 g.mol^{-1}, PDI = 1.03) (—) prepared by ROP of ***L*-17** from MeO-PEO$_{5K}$-OH (M_n = 7 530 g.mol^{-1}, PDI = 1.03) (—).

4.2.2 Preparation of PEO$_x$-b-P(L-BMA)$_n$ micelles

The amphiphilic nature of the PEO$_x$-*b*-PBMA$_n$ copolymers, consisting of hydrophobic PBMA and hydrophilic PEO segments, provides the opportunity to form polymeric micelles in water possessing a PBMA core and a PEO corona. It was postulated that self-assembly of these amphiphilic block copolymers would realise micellar morphologies as a consequence of both the molecular weight ratio between the hydrophilic and hydrophobic blocks and their relative chain lengths.[8-9,25] Two methods were investigated for micellar organisation; the first being direct dissolution and the second the solvent switch method. These two techniques were compared in the self-assembly of PEO$_{5K}$-*b*-P(*L*-BMA)$_{25}$. As a consequence of the water solubility of this block copolymer (resulting from the relatively short hydrophobic P(*L*-BMA) segment) the direct dissolution technique could be successfully applied. Here the amphiphilic diblock PEO$_{5K}$-*b*-P(*L*-BMA)$_{25}$ was dissolved in nanopure water at a total concentration of 0.3 mg.mL^{-1}

at 25 °C. Analysis of the resultant micelles using dynamic light scattering (DLS) confirmed the presence of micelles with average solution hydrodynamic diameters, D_h of 33 ± 7 nm (Figure 4.4) and larger structures with D_h = 133 ± 19 nm. The second procedure for self-assembly was through the solvent switch method. Here the PEO_{5K}-*b*-P(*L*-BMA)$_{25}$ was dissolved in THF, a good solvent for both blocks, at a concentration of 1 mg.mL^{-1}, before a double volume of deionised water was added dropwise to the stirred THF solution at 25 °C at a rate of *ca.* 10 mL.h^{-1}. The resulting solution was dialysed against nanopure water (molecular weight cut-off (MWCO) = 3.5 kDa) for 3 days to yield a micelle solution concentration of ~0.3 mg.mL^{-1}. Analysis of the solution *via* DLS confirmed the presence of polymeric micelles with a number based average solution hydrodynamic diameter (D_h) of 18 ± 1 nm (Figure 4.4). Interestingly, these micelles, along with all other micelles prepared in this study, showed larger species in both the volume and intensity based average solution hydrodynamic diameters attributed to micelle aggregation from favorable interactions of the neutral PEO coronas. To ensure these observations of micelle formation were a result of the preparation methods a sample of the linear PEO_{5K}-*b*-P(*L*-BMA)$_{25}$ dissolved in THF was subjected to DLS analysis. This analysis indicated a significantly lower average solution hydrodynamic diameter of D_h = 4 ± 1 nm (Figure 4.4) which is indicative of a unimolecular chain size and thus confirms self-assembly occurred during the micellisation process. In addition to DLS analysis, the micelles prepared *via* the solvent switch method were characterised by deposition onto a carbon surface, stained with 2% uranyl acetate solution, and imaged using transmission electron microscopy (TEM); by this method, the micelle diameters were determined to be D_{av} = 19 ± 5 nm (Figure 4.5).

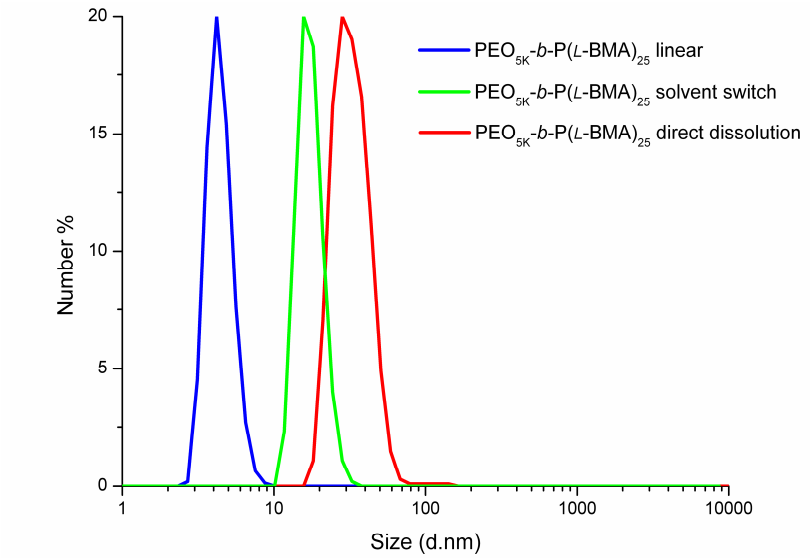

Figure 4.4. DLS data for micelles prepared using PEO_{5K}-*b*-P(*L*-BMA)$_{25}$ *via* direct dissolution (D_h = 33 ± 7 nm) (▬) and solvent switch (D_h = 18 ± 1 nm) (▬) methods along with the linear PEO_{5K}-*b*-P(*L*-BMA)$_{25}$ precursor in THF (D_h = 4 ± 1 nm) (▬).

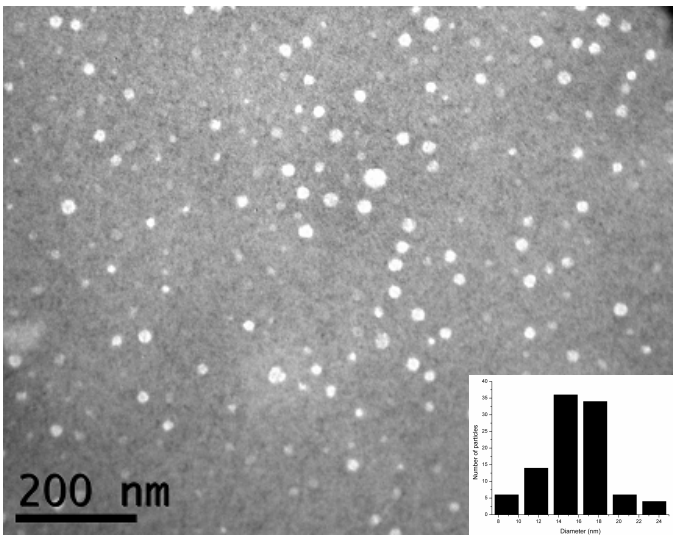

Figure 4.5. TEM image of the micelles prepared from PEO_{5K}-*b*-P(*L*-BMA)$_{25}$ (D_{av} = 16 ± 5 nm) *via* the solvent switch method. Scale bar shown is 200 nm. Samples were stained with uranyl acetate (2% solution), drop deposited onto a carbon-coated copper grid and allowed to dry under ambient conditions. Inset: TEM size distribution histogram.

4.2.2.1 Investigation of the hydrophobic P(L-BMA)$_n$ chain length on the dimensions and stability of PEO$_{5K}$-b-P(L-BMA)$_n$ micelles

The effect of the hydrophobic P(*L*-BMA) chain length on the dimensions of the resulting self-assembled PEO$_{5K}$-P(*L*-BMA)$_n$ polymeric micelles was investigated using three different molecular weight amphiphilic block copolymers initiated from MeO-PEO$_{5K}$-OH with varying hydrophobic P(*L*-BMA) chain lengths ([M]/[I] = 10, 25 and 40) (Table 4.2). GPC analysis of the block copolymers confirmed P(*L*-BMA) chain growth from the MeO-PEO$_{5K}$-OH (M_n = 7 530 g.mol^{-1}, PDI = 1.03) with increased retention time upon block copolymer formation resulting in block copolymers with M_n of 9 400, 16 940 and 20 412 g.mol^{-1} and PDI of 1.04, 1.03 and 1.03 for [M]/[I] of 10, 25 and 40 respectively (Figure 4.6). ^{1}H NMR spectroscopy provided evidence of the end group fidelity and thus confirmed the targeted [M]/[I]. Preparation of amphiphilic block copolymers with larger P(*L*-BMA) chains ([M]/[I] > 50) resulted in the observation of two species by GPC analysis that could not be separated. It is postulated that the other species may occur as a result of poor initiation from the monomethylether PEO macroinitiator, in turn resulting from the polymer coiling in $CHCl_3$ during the ROP thus reducing the accessibility of the alcohol chain end.

Table 4.2. Polymerisation data for the chain extension of MeO-PEO$_{5K}$-OH with P(*L*-BMA) at [M]/[I] = 10, 25 and 40 through the ROP of ***L*-17**[a] and characterisation data of the resulting micelles.

Polymer	M_n[b] (g.mol^{-1})	M_n[c] (g.mol^{-1})	M_w/M_n[c]	DLS of micelle, D_h[d] (nm)	TEM of micelle, D_{av}[e] (nm)
PEO$_{5K}$-*b*-P(*L*-BMA)$_{10}$	7 060	9 400	1.04	18 ± 1	16 ± 6
PEO$_{5K}$-*b*-P(*L*-BMA)$_{25}$	10 150	16 940	1.03	18 ± 1	16 ± 5
PEO$_{5K}$-*b*-P(*L*-BMA)$_{40}$	13 240	20 410	1.03	22 ± 1	19 ± 5

[a] [***L*-17**]$_0$ = 0.32 M; 5 mol% 4-methoxypyridine; $CHCl_3$; 25 °C. [b] Determined by ^{1}H NMR Spectroscopy. [c] Determined by GPC analysis. [d] Number-averaged hydrodynamic diameters in aqueous solution by DLS. [e] Average diameters were measured by TEM, calculated from the values for 100 particles.

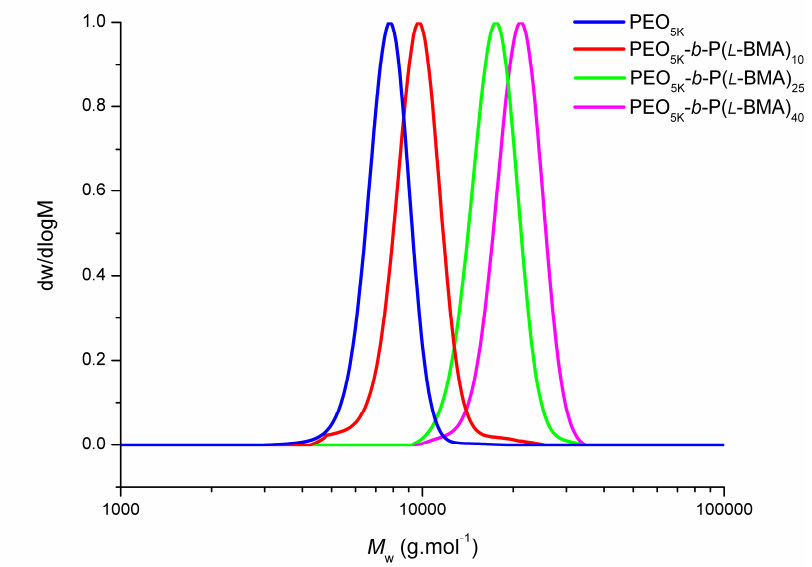

Figure 4.6. GPC traces of PEO$_{5K}$-*b*-P(*L*-BMA)$_{10}$ (M_n = 9 400 g.mol^{-1}, PDI = 1.04) (—), PEO$_{5K}$-*b*-P(*L*-BMA)$_{25}$ (M_n = 16 940 g.mol^{-1}, PDI = 1.03) (—) and PEO$_{5K}$-*b*-P(*L*-BMA)$_{40}$ (M_n = 20 412 g.mol^{-1}, PDI = 1.03) (—) prepared by ROP of ***L*-17** from MeO-PEO$_{5K}$-OH (M_n = 7 530 g.mol^{-1}, PDI = 1.03) (—).

Self-assembly of each of these amphiphilic block copolymers using the solvent switch method previously described resulted in polymeric micelles with comparable average solution hydrodynamic diameters. The PEO$_{5K}$-*b*-P(*L*-BMA)$_{40}$ micelle exhibited a D_h = 22 ± 1 nm while both PEO$_{5K}$-*b*-P(*L*-BMA)$_{10}$ and PEO$_{5K}$-

b-P(*L*-BMA)$_{25}$ were slightly smaller with diameters of D_h = 18 ± 1 nm (Figure 4.7). This result is in agreement with that reported previously with PEO-*b*-PLA micelles that possessed the greatest proportion of lactide units resulting in larger average solution hydrodynamic diameters.[12,26] TEM analysis further confirmed the presence of well-defined spherical micelles with diameters of D_{av} = 16 ± 6 (Figure 4.8), 16 ± 5 nm (Figure 4.5) and 19 ± 5 nm (Figure 4.9) for [M]/[I] = 10, 25 and 40 respectively providing good agreement with DLS analysis. Despite the PEO$_{5K}$-*b*-P(*L*-BMA)$_{40}$ block copolymer possessing a higher hydrophobic molecular weight ratio, only micelles were observed demonstrating that the resulting micellar morphologies are not only dependant on the molecular weight ratio between the hydrophilic and hydrophobic blocks but also on the relative chain lengths of each of these blocks.[8-9,25]

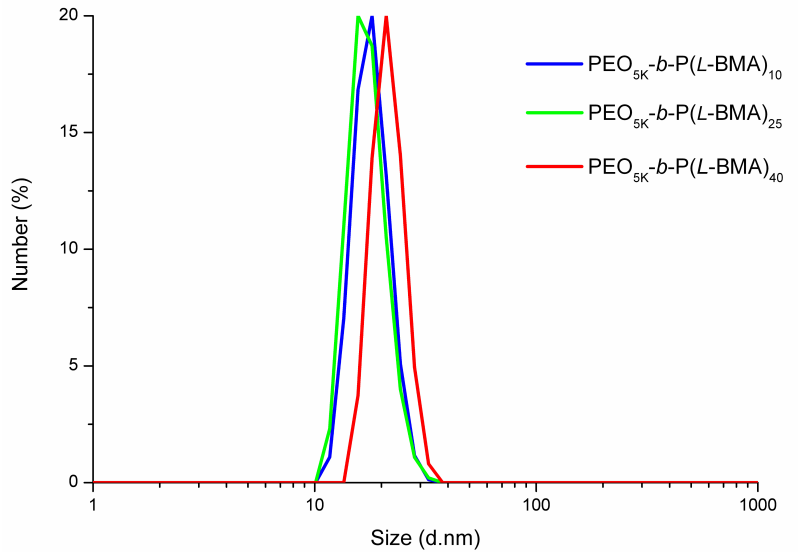

Figure 4.7. DLS data for micelles prepared from PEO$_{5K}$-*b*-P(*L*-BMA)$_{10}$ (D_h = 18 ± 7 nm) (—), PEO$_{5K}$-*b*-P(*L*-BMA)$_{25}$ (D_h = 18 ± 1 nm) (—) and PEO$_{5K}$-*b*-P(*L*-BMA)$_{40}$ (D_h = 22 ± 1 nm) (—) *via* the solvent switch method.

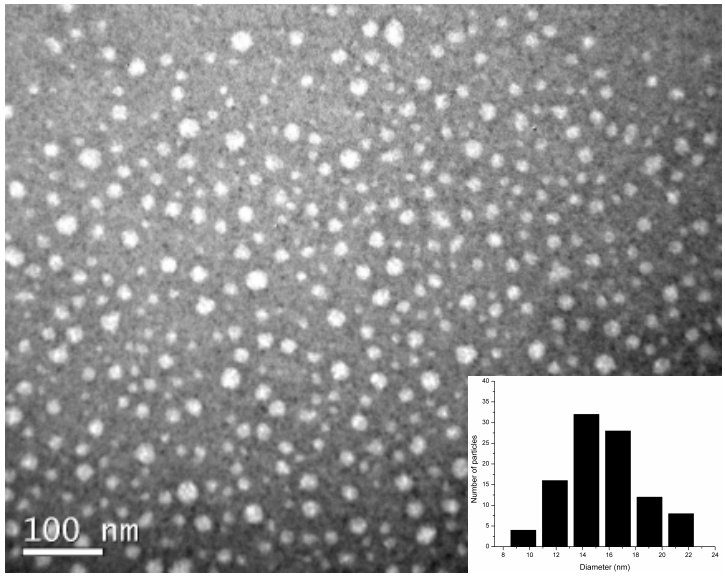

Figure 4.8. TEM image of the micelles prepared from PEO_{5K}-*b*-P(*L*-BMA)$_{10}$ (D_{av} = 16 ± 5 nm) *via* the solvent switch method. Scale bar shown is 100 nm. Samples were stained with uranyl acetate (2% solution), drop deposited onto a carbon-coated copper grid and allowed to dry under ambient conditions. Inset: TEM size distribution histogram.

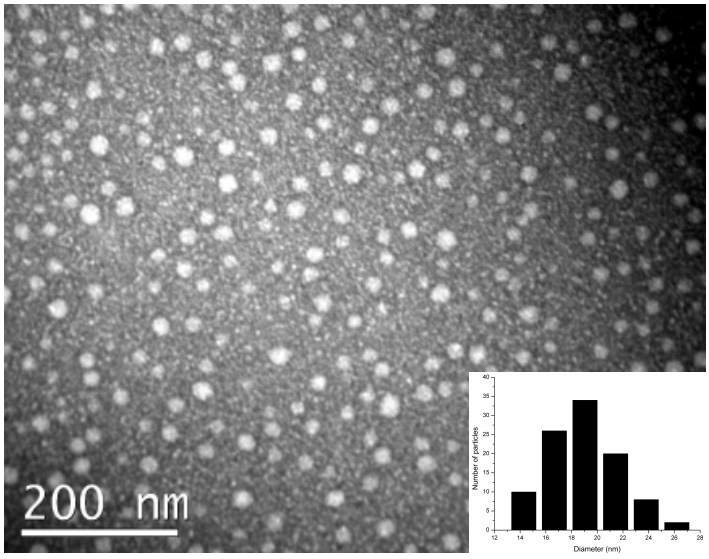

Figure 4.9. TEM image of the micelles prepared from PEO_{5K}-*b*-P(*L*-BMA)$_{40}$ (D_{av} = 19 ± 5 nm) the solvent switch method. Scale bar shown is 200 nm. Samples were stained with uranyl acetate (2% solution), drop deposited onto a carbon-coated copper grid and allowed to dry under ambient conditions. Inset: TEM size distribution histogram.

In addition, investigation into the effect of the hydrophobic P(*L*-BMA) chain length on the stabilisation of the resulting micelles was undertaken. The critical micelle concentration (CMC) of the micelles provides a simple procedure to quantify stability enabling comparison between different nanostructures. CMCs were determined by fluorescence spectroscopy using pyrene as a fluorescent probe. Pyrene is hydrophobic and exhibits low solubility in water (6×10^{-7} $mol.L^{-1}$) such that as its environment changes from polar to non-polar, its absorption, emission and excitation spectra are altered. An absorption peak at 335 nm shifts to 338 nm when pyrene shifts from an aqueous environment to being trapped in the hydrophobic core of micelles.[27] Comparison of the intensity ratio of the absorption peaks (I_{338}/I_{335}) and concentration of the micelle solution enables precise determination of the CMC value from the intersection of the two straight lines (inflection point) that result in this plot, the base line and the rapidly rising I_{338}/I_{335} line. CMC measurements were achieved through preparation of an acetone solution of pyrene at 6×10^{-5} $mol.L^{-1}$ of which 0.05 mL was removed and left for the acetone to fully evaporate. A solution of the micelles (5 mL) at different concentrations (from 0.3 to 0.0003 $mg.mL^{-1}$) were added to the pyrene to result in a pyrene concentration of 6×10^{-7} $mol.L^{-1}$. The solution was left to stir for two days to ensure equilibrium before being analysed using fluorescence spectroscopy.

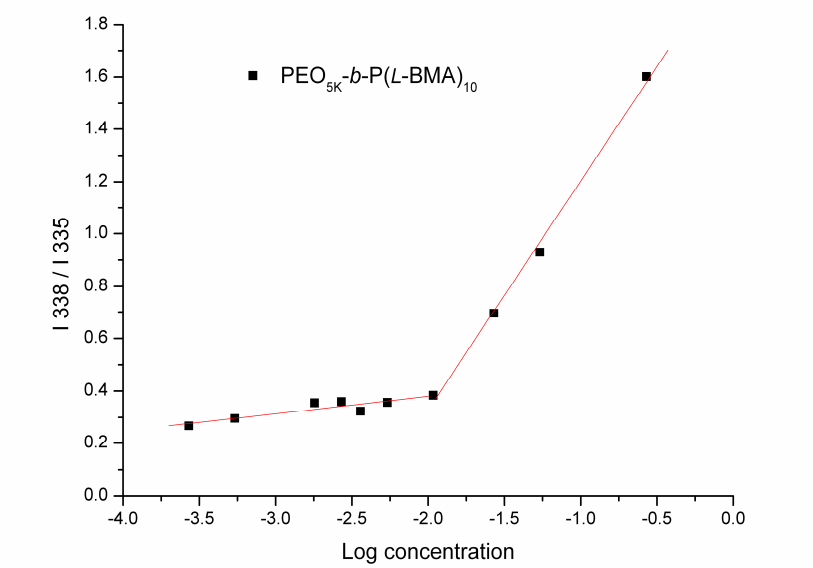

Figure 4.10. Concentration dependence of pyrene I_{338}/I_{335} intensity ratio for PEO_{5K}-*b*-P(*L*-BMA)$_{10}$ micelles in water at room temperature. (Diblock: M_n = 9 400 g.mol^{-1}, PDI = 1.04; and [pyrene]$_0$ = 6 x 10^{-7} M). Inflection point at 1.23 x 10^{-2} g.L^{-1}.

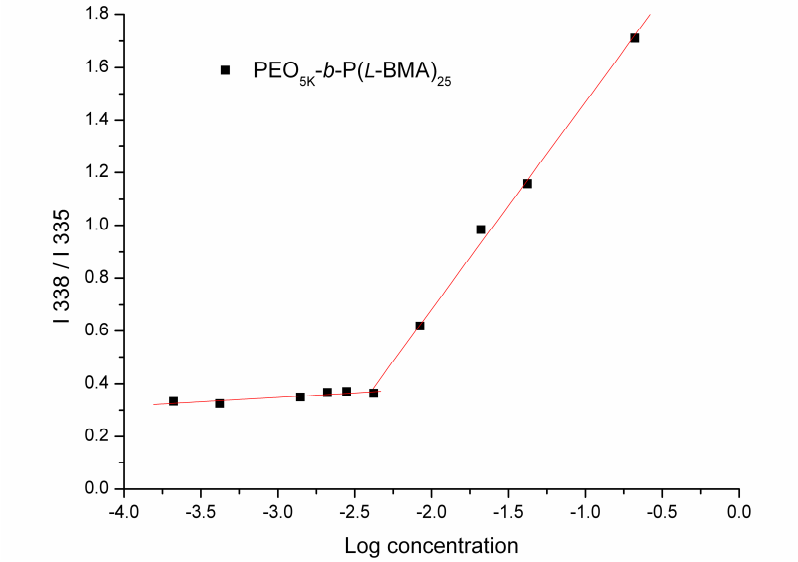

Figure 4.11. Concentration dependence of pyrene I_{338}/I_{335} intensity ratio for PEO_{5K}-*b*-P(*L*-BMA)$_{25}$ micelles in water at room temperature. (Diblock: M_n = 16 940 g.mol^{-1}, PDI = 1.03; and [pyrene]$_0$ = 6 x 10^{-7} M). Inflection point at 3.61 x 10^{-3} g.L^{-1}.

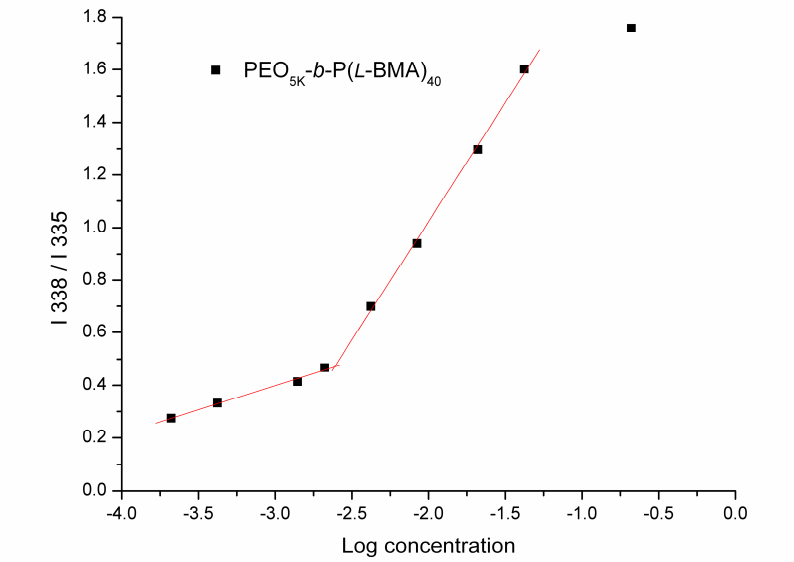

Figure 4.12. Concentration dependence of pyrene I_{338}/I_{335} intensity ratio for PEO_{5K}-*b*-P(*L*-BMA)$_{40}$ micelles in water at room temperature. (Diblock: M_n = 20 412 g.mol^{-1}, PDI = 1.03; and [pyrene]$_0$ = 6 x 10^{-7} M). Inflection point at 2.33 x 10^{-3} g.L^{-1}.

All samples of polymeric micelles exhibited low CMC values below 1.25 x 10^{-2} g.L^{-1} (Figure 4.10, 4.11 and 4.12) which indicates that they possess high thermodynamic stabilities, potentially enabling their application as novel biodegradable drug delivery systems in dilute conditions. As expected the micelle CMC values decreased with increasing length of the hydrophobic P(*L*-BMA) chain resulting in an increase in thermodynamic stability attributed to the enhanced hydrophobic interactions in the micelle core. A relationship between the weight ratio of the P(*L*-BMA) block and the respective micelle CMC value was observed with increasing weight ratio of P(*L*-BMA) from 28% ([M]/[I] = 10) to 50% ([M]/[I] = 25) and 62% ([M]/[I] = 40) resulting in decreasing CMC values from 1.23 x 10^{-2} g.L^{-1}, 3.61 x 10^{-3} g.L^{-1} and 2.33 x 10^{-3} g.L^{-1} respectively (Figure 4.13). These data show that the CMC of these micelles can be tailored

through variation of the monomer-to-initiator ratio in the initial amphiphilic block copolymer synthesis.

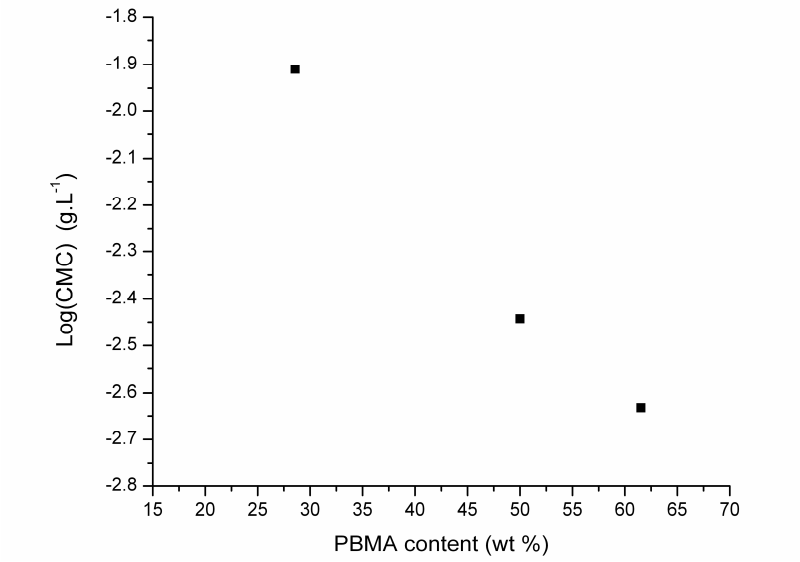

Figure 4.13. Plot of P(*L*-BMA) content *versus* log(CMC) for different sized PEO_{5K}-*b*-P(*L*-BMA)$_n$ prepared from the ROP of ***L*-17** ([***L*-17**]$_0$ = 0.32 M) using 4-methoxypyridine as the catalyst and MeO-PEO_{5K}-OH as the macroinitiator at varying [M]/[I].

4.2.2.2 Investigation of the overall molecular weight of PEO_x-b-P(L-BMA)$_n$ copolymers on the dimensions and stability of the resulting micelles

The effect of the overall molecular weight of the linear PEO_x-*b*-P(*L*-BMA)$_n$ on the physical dimensions and stability of the resulting self-assembled polymeric micelles was also investigated by the preparation and self-assembly of three amphiphilic block copolymers with different molecular weights while maintaining comparable P(*L*-BMA) to PEO weight ratios of ~28%. Three different MeO-PEO-OH with different molecular weights (M_w = 2 000, 5 000 and 10 000 g.mol^{-1}) were applied as macroinitiators for the ROP of ***L*-17** at different monomer-to-initiator ratios of 5, 10 and 20 respectively realising PEO_x-*b*-P(*L*-BMA)$_n$ with overall molecular weights of ~ 3 000, 7 000 and 14 100 g.mol^{-1}

(Table 4.3). The PEO_{5K}-*b*-P(*L*-BMA)$_{10}$ was prepared and characterised as previously described. GPC analysis of the other two block copolymers confirmed P(*L*-BMA) chain growth from the MeO-PEO-OH macroinitiators with an increase in retention time upon block copolymer formation to PEO_{2K}-*b*-P(*L*-BMA)$_5$ (M_n = 3 850 g.mol^{-1}, PDI = 1.04) and PEO_{10K}-*b*-P(*L*-BMA)$_{20}$ (M_n = 19 440 g.mol^{-1}, PDI = 1.03) from MeO-PEO_{2K}-OH (M_n = 2 790 g.mol^{-1}, PDI = 1.04) and MeO-PEO_{10K}-OH (M_n = 16 270 g.mol^{-1}, PDI = 1.03) respectively (Figure 4.14). ^{1}H NMR spectroscopy provided confirmation of the end group fidelity of the block copolymers, confirming the targeted [M]/[I].

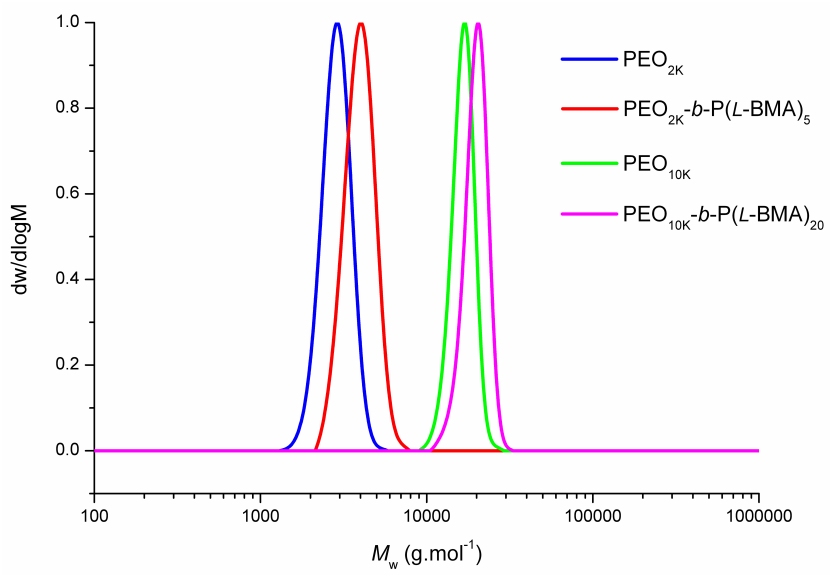

Figure 4.14. GPC traces of PEO_{2K}-*b*-P(*L*-BMA)$_5$ (M_n = 3 850 g.mol^{-1}, PDI = 1.04) (—) and PEO_{10K}-*b*-P(*L*-BMA)$_{20}$ (M_n = 19 440 g.mol^{-1}, PDI = 1.03) (—) prepared by ROP of ***L*-17** from MeO-PEO_{2K}-OH (M_n = 2 790 g.mol^{-1}, PDI = 1.04) (—) and MeO-PEO_{10K}-OH (M_n = 16 270 g.mol^{-1}, PDI = 1.03) (—) respectively.

Table 4.3. Polymerisation data for the chain extension of MeO-PEO_{2K}-OH, MeO-PEO_{5K}-OH and MeO-PEO_{10K}-OH with P(*L*-BMA) at [M]/[I] = 5, 10 and 20 respectively through the ROP of ***L*-17**[a] and characterisation data of the resulting micelles.

Polymer	M_n[b] (g.mol^{-1})	M_n[c] (g.mol^{-1})	M_w/M_n[c]	DLS of micelle, D_h[d] (nm)	TEM of micelle, D_{av}[e] (nm)
PEO_{2K}-*b*-P(*L*-BMA)$_5$	3 030	3 850	1.04	13 ± 1	13 ± 5
PEO_{5K}-*b*-P(*L*-BMA)$_{10}$	7 060	9 400	1.04	18 ± 1	19 ± 6
PEO_{10K}-*b*-P(*L*-BMA)$_{20}$	14 120	19 440	1.03	24 ± 1	20 ± 6

[a] [***L*-17**]$_0$ = 0.32 M; 5 mol% 4-methoxypyridine; $CHCl_3$; 25 °C. [b] Determined by ^{1}H NMR Spectroscopy. [c] Determined by GPC analysis. [d] Number-averaged hydrodynamic diameters in aqueous solution by DLS. [e] Average diameters were measured by TEM, calculated from the values for 100 particles.

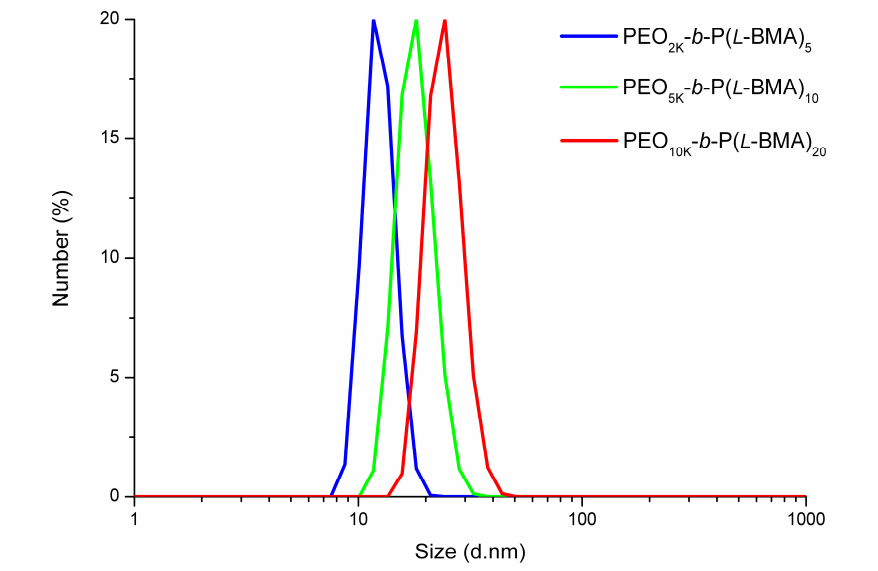

Figure 4.15. DLS data for micelles prepared from PEO_{2K}-*b*-P(*L*-BMA)$_5$ (D_h = 13 ± 1 nm) (—), PEO_{5K}-*b*-P(*L*-BMA)$_{10}$ (D_h = 18 ± 1 nm) (—) and PEO_{10K}-*b*-P(*L*-BMA)$_{20}$ (D_h = 24 ± 1 nm) (—) *via* the solvent switch method.

Self-assembly of these amphiphilic block copolymers resulted in micelles with significantly different average solution hydrodynamic diameters *via* DLS analysis, as expected from the difference in overall molecular weight of the linear block copolymer precursors (Table 4.2). As described previously, the average solution hydrodynamic diameter of the PEO_{5K}-*b*-P(*L*-BMA)$_{10}$ micelles was D_h = 18 ± 1 nm. Self-assembly of PEO_{10K}-*b*-P(*L*-BMA)$_{20}$ resulted in polymeric micelles with a larger diameter of D_h = 24 ± 1 nm, as a consequence of the overall molecular weight being double that of PEO_{5k}-*b*-P(*L*-BMA)$_{10}$. The same trend was observed with the PEO_{2K}-*b*-P(*L*-BMA)$_5$ micelles, observing a decrease in the average solution hydrodynamic diameter to D_h = 13 ± 1 nm (Figure 4.15). TEM analysis confirmed the presence of well-defined spherical micelles in good agreement with the DLS analysis along with correlation between linear block copolymer precursor molecular weight and the resulting micelle diameter increasing from D_{av} = 13 ± 5 nm (Figure 4.16), D_{av} = 19 ± 6 nm (Figure 4.8) and D_{av} = 20 ± 6 nm (Figure 4.17) for PEO_{2K}-*b*-P(*L*-BMA)$_5$, PEO_{5K}-*b*-P(*L*-BMA)$_{10}$ and PEO_{10K}-*b*-P(*L*-BMA)$_{20}$ respectively.

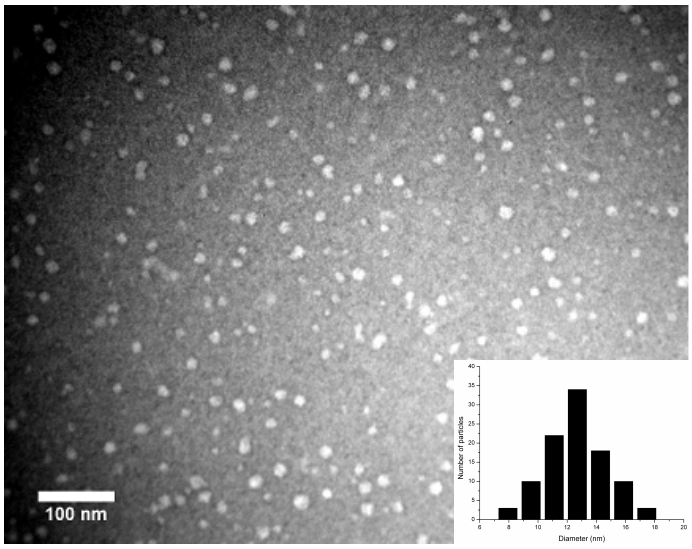

Figure 4.16. TEM image of the micelles prepared from PEO_{2K}-*b*-P(*L*-BMA)$_5$ (D_{av} = 13 ± 5 nm) *via* the solvent switch method. Scale bar shown is 100 nm. Samples were stained with uranyl acetate (2% solution), drop deposited onto a carbon-coated copper grid and allowed to dry under ambient conditions. Inset: TEM size distribution histogram.

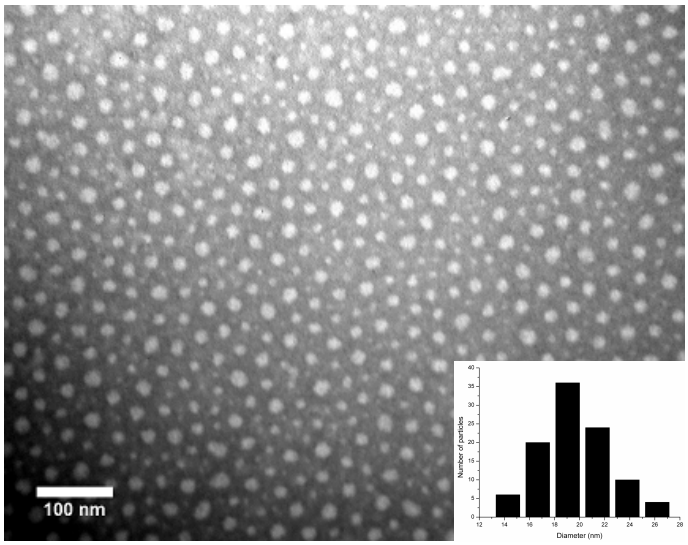

Figure 4.17. TEM image of the micelles prepared from PEO_{10K}-*b*-P(*L*-BMA)$_{40}$ (D_{av} = 20 ± 6 nm) *via* the solvent switch method. Scale bar shown is 100 nm. Samples were stained with uranyl acetate (2% solution), drop deposited onto a carbon-coated copper grid and allowed to dry under ambient conditions. Inset: TEM size distribution histogram.

Further to these investigations, calculation of the CMC values of the polymeric micelles was undertaken to determine whether the molecular weight of the linear amphiphilic block copolymer precursor had an effect on the stabilisation of the micelles. The CMC values of these micelles were determined as before *via* fluorescence spectroscopic analysis using pyrene as a probe at different micelle solution concentrations.

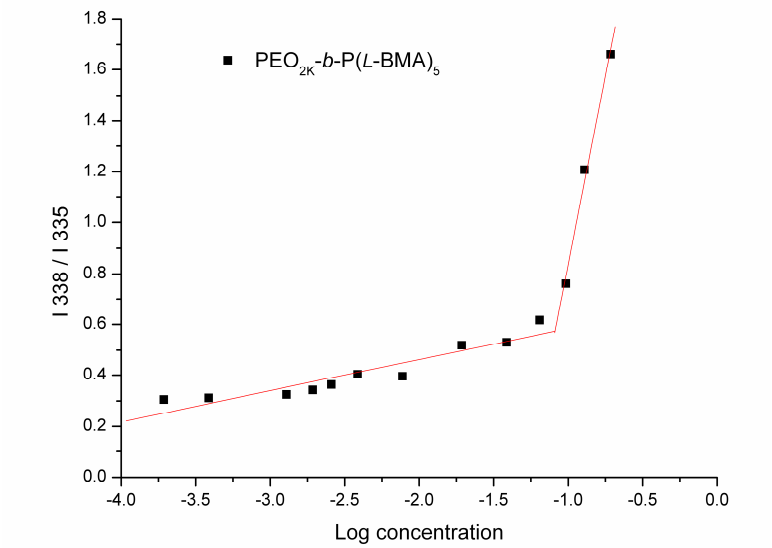

Figure 4.18. Concentration dependence of pyrene I_{338}/I_{335} intensity ratio for PEO_{2K}-*b*-P(*L*-BMA)$_5$ micelles in water at room temperature. (Diblock: M_n = 3 850 g.mol^{-1}, PDI = 1.04; and [pyrene]$_0$ = 6 x 10^{-7} M). Inflection point at 6.16 x 10^{-2} g.L^{-1}.

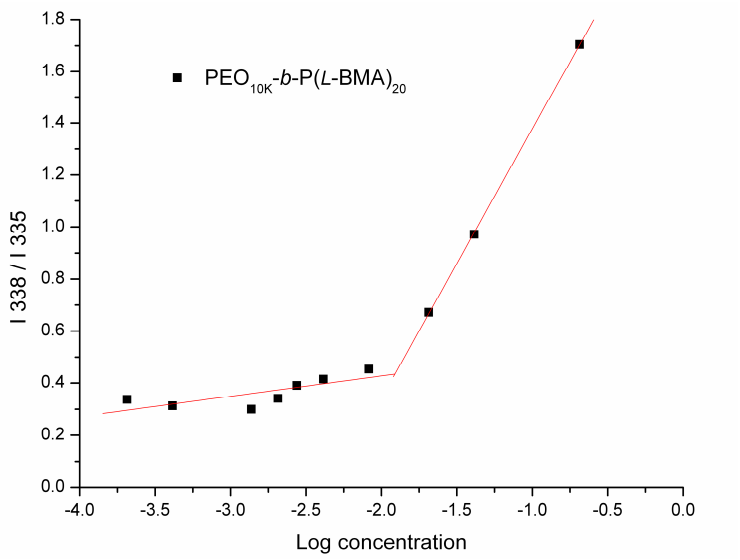

Figure 4.19. Concentration dependence of pyrene I_{338}/I_{335} intensity ratio for PEO_{10K}-*b*-P(*L*-BMA)$_{20}$ micelles in water at room temperature. (Diblock: M_n = 19 440 g.mol^{-1}, PDI = 1.03; and [pyrene]$_0$ = 6 x 10^{-7} M). Inflection point at 1.00 x 10^{-2} g.L^{-1}.

As determined earlier, PEO_{5K}-*b*-P(*L*-BMA)$_{10}$ micelles display a low CMC of 1.23 x 10^{-2} g.L^{-1} (Figure 4.10). Micelles prepared using PEO_{2K}-*b*-P(*L*-BMA)$_5$ exhibited a CMC value of 6.16 x 10^{-2} g.L^{-1}, considerably higher than all other polymeric micelles investigated in this study (Figure 4.18). The short hydrophobic P(*L*-BMA) chain of PEO_{2K}-*b*-P(*L*-BMA)$_5$ does not provide enough hydrophobic interactions in the micelle core to stabilise the polymeric micelle in aqueous conditions therefore exhibiting a low thermodynamic stability compared to amphiphilic block copolymers with longer P(*L*-BMA) chains. On the other hand, self-assembly of PEO_{10K}-*b*-P(*L*-BMA)$_{20}$ with its significantly larger molecular weight resulted in micelles with a higher thermodynamic stability than that of PEO_{5K}-*b*-P(*L*-BMA)$_{10}$ micelles displaying a CMC value of 1.00 x 10^{-2} g.L^{-1} (Figure 4.19). As a consequence of their stability in dilute aqueous conditions, both PEO_{5K}-*b*-P(*L*-BMA)$_{10}$ and PEO_{10K}-*b*-P(*L*-BMA)$_{20}$ polymeric micelles are promising candidates as a possible novel drug carriers.

4.2.3 Investigation into stereocomplex formation between P(L-BMA) and P(D-BMA)

While polymeric micelles are relatively stable in an aqueous environment, they remain equilibrium systems held together through hydrophobic effects and hence are readily disrupted *via* changes in conditions such as dilution, ultrasound, heat or changes in pH.[28-30] For example, micelles prepared from PEO-*b*-PDLLA have been shown to dissociate after intravenous injection and are rapidly excreted in urine.[31] Although instability of particles under certain conditions is a useful property and has been exploited in many ways;[32-34] for other applications it is necessary for the particles to have much greater stability, especially *in vivo*, to meet requirements such as long circulation times, accumulation at targeted sites and controlled drug release. Strategies to increase the stability of polymeric micelles generally rely on chemical cross-linking of either the core[35-38] or shell[39-42] to produce more robust nanoparticles. While this technique successfully facilitates the preparation of stable particles it can also lead to a reduction in encapsulation efficiency, hydrophilicity and/or biodegradability. As an alternative to this stabilising process, enhanced stability can also be achieved from dynamic polymer-polymer interactions such as polyelectrolyte,[43-46] stereocomplexation,[26] and hydrogen bonding[47] in both the core and shell of polymeric micelles.

As a consequence of the ready availability of enantiopure lactide, much research has been directed toward the investigation of stereocomplex formation between stereoregular chains of poly(lactide)s and poly(lactic acid)s prepared from optically pure monomer sources with retention of chirality during the polymerisation process.[48-51] When poly(*L*-LA) (PLLA) and poly(*D*-LA) (PDLA) are present in a system, various types of crystallites can be formed, when these crystallites compose of solely PLLA or PDLA they are identified as 'homo-

crystallites' prepared through homo-crystallisation. However, when both enantiopure polymer chains are present three types of crystallites can be formed from either packing side by side, randomly and a mixture of the two, all demonstrating stronger interactions compared to homo-crystallites.[48] Ikada and Tsuji *et al.* in 1987 reported the first investigation into the stereocomplex formation between PLLA and PDLA. Using an equimolar blend of both homochiral polymers they demonstrated a positive shift in the melting temperature (T_m) of 50 °C to 230 °C indicative of stereocomplex formation, measured *via* differential scanning calorimetry (DSC) analysis, compared to ~180 °C observed for the enantiopure poly(ester)s.[52] Application of this interaction was first employed in micelle stabilisation by Leroux *et al.* with micelles from an equimolar blend of PEO-*b*-PLLA and PEO-*b*-PDLA. The resultant stereocomplex micelles had kinetic stability and redispersion properties superior to micelles formed with isotactic or racemic polymers alone.[53] Other groups have utilised stereocomplex interactions between homochiral PLA in the stabilisation of polymeric micelles with hydrophilic segments including PEO,[26,54-56] poly(*N*-isopropylacylamide) (PNIPAM)[57] and poly(N-isopropylacrylamide-*co*-2-hydroxyethylmethacrylate.[58]

In addition to synthesising a range of novel amphiphilic PEO-*b*-PBMA copolymers and their subsequent successful self-assembly, investigation into stabilisation of these polymeric micelles through stereocomplexation between enantiopure P(*L*-BMA) and P(*D*-BMA) chains in the hydrophobic core as reported with structurally similar PLLA and PDLA was undertaken. Stereocomplex formation between ***L*-17** and ***D*-17** was initially investigated using melting point analysis. The stereocomplexed sample was prepared using an

equimolar mixture of ***L*-17** and ***D*-17** that was recrystallised in diethylether to realise the desired stereocomplex crystallised product (***SC*-17**). Melting point determination of ***L*-17**, ***D*-17** and ***SC*-17** showed that going from the optically pure samples to the stereocomplexed mixture resulted in a 26 °C increase from 52 – 56 °C to 80 – 81 °C respectively. This result indicated that the two enantiomers may be forming a racemic stereocomplex that exhibits a synergistic stability toward temperature. DSC analysis provides another simple technique to identify the presence of stereocomplexation in a polymer mixture through observation of an increase in the melting temperature (T_m) going from enantiopure polymers to a stereocomplexed polymer mixture. P(*L*-BMA)s with different molecular weights ([M]/[I] = 10, 20 and 40) prepared through initiation from *neo*-pentanol were examined using DSC analysis from -40 to 200 °C (10 °C.min^{-1}). While all three P(*L*-BMA)s demonstrated clear glass transition temperatures (T_g) (~ 10 °C), a T_m was not observed (Figure 4.20). Applying temperatures above 250 °C resulted in degradation of the P(*L*-BMA)s evidenced by rapid loss of molecular weight loss with onset at 280 °C *via* thermogravimetric analysis (TGA) (Figure 4.21). Combination of equimolar blends of these polymers with analogous P(*D*-BMA) resulted in no significant change observed in either DSC or TGA analysis.

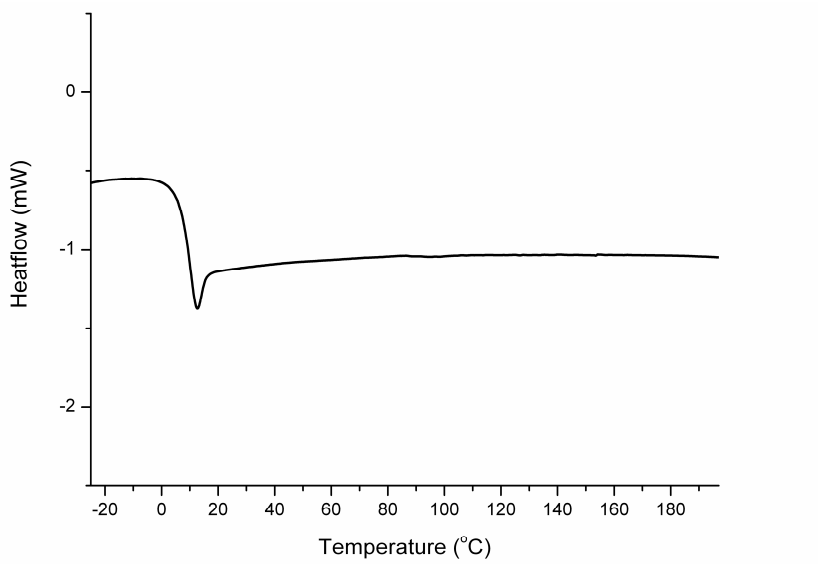

Figure 4.20. DSC thermogram of P(*L*-BMA)$_{20}$ (M_n = 3 860 g.mol^{-1}, PDI = 1.10) from -20 to 200 °C.

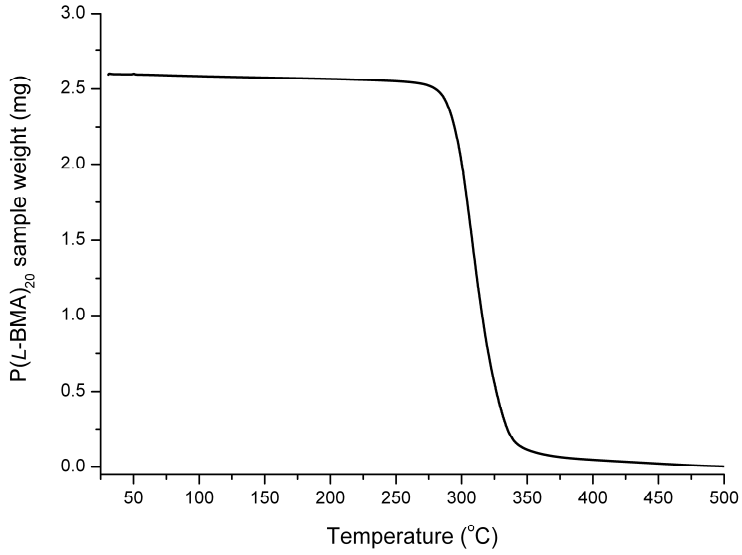

Figure 4.21. TGA analysis of P(*L*-BMA)$_{20}$ (M_n = 3 860 g.mol^{-1}, PDI = 1.10) from 25 to 500 °C.

4.2.3.1 Investigation into stereocomplexed micelles of PEO$_{5K}$-b-P(L-BMA)$_{10}$ and PEO$_{5K}$-b-P(D-BMA)$_{10}$ copolymers on the dimensions and stability

Despite no T_m values being observed for the PBMA homopolymers, comparison of the melting points of ***L*-17**, ***D*-17** and ***SC*-17** suggest stereocomplexation could occur. Investigation into the utilisation of this interaction toward the stabilisation

of micelles was attempted through the preparation of a polymeric micelle using an equimolar blend of enantiopure amphiphilic block copolymers. As has been observed in stereocomplexed micelles of PEO-*b*-PLA, stereocomplexation in the hydrophobic core leads to changes in the physical dimensions along with enhanced stability to realise stable biodegradable micelles without the use of undesirable cross-linking techniques. This interaction was investigated using PEO_{5K}-*b*-P(*L*-BMA)$_{10}$ and PEO_{5K}-*b*-P(*D*-BMA)$_{10}$. PEO_{5K}-*b*-P(*D*-BMA)$_{10}$ (M_n = 8 950 g.mol^{-1}, PDI = 1.03) was prepared in an identical manner as PEO_{5K}-*b*-P(*L*-BMA)$_{10}$ using ***D*-17** rather than ***L*-17** and through self-assembly, analogous to before, of an equimolar mixture of both these enantiopure amphiphilic block copolymers realised the respective stereocomplexed micelle (Table 4.4).

Table 4.4. Polymerisation data for the chain extension of MeO-PEO_{5K}-OH with P(*L*-BMA) and P(*D*-BMA) at [M]/[I] = 10 through the ROP of ***L*-17** and ***D*-17** respectively[a] and characterisation data of the resulting enantiopure and stereocomplexed micelles.

Polymer	M_n[b] (g.mol^{-1})	M_n[c] (g.mol^{-1})	M_w/M_n[c]	DLS of micelle, D_h[d] (nm)	TEM of micelle, D_{av}[e] (nm)
PEO_{5K}-*b*-P(*L*-BMA)$_{10}$	7 060	9 400	1.04	18 ± 1	16 ± 6
PEO_{5K}-*b*-P(*D*-BMA)$_{10}$	7 060	8 950	1.03	19 ± 1	16 ± 4
PEO_{5K}-*b*-P(*L*-BMA)$_{10}$ + PEO_{5K}-*b*-P(*D*-BMA)$_{10}$	-	-	-	23 ± 1	18 ± 5

[a] [***L*-17**]$_0$ + [***D*-17**]$_0$ = 0.32 M; 5 mol% 4-methoxypyridine; $CHCl_3$; 25 °C. [b] Determined by ^{1}H NMR Spectroscopy. [c] Determined by GPC analysis. [d] Number-averaged hydrodynamic diameters in aqueous solution by DLS. [e] Average diameters were measured by TEM, calculated from the values for 100 particles.

DLS measurements show that the two enantiopure PEO_{5K}-*b*-P(*L*-BMA)$_{10}$ and PEO_{5K}-*b*-P(*D*-BMA)$_{10}$ micelles exhibit similar particle sizes around 18 ± 1 nm whereas the stereocomplexed micelles exhibit a larger average hydrodynamic solution diameter of 23 ± 1 nm (Figure 4.22). It is postulated that within the enantiopure micelles the PBMA chains may be random coils with little or no beneficial interaction occurring between neighbouring chains. However, in the stereocomplexed micelle it is envisaged that a varying degree of interdigitation between chains upon formation of a stereocomplex prevents the polymer chains from collapsing leading to a larger particle size.

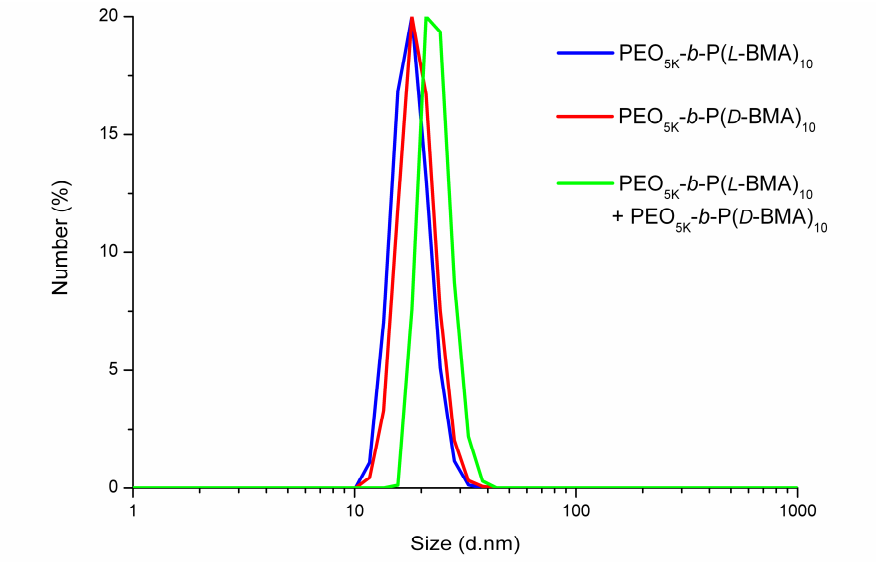

Figure 4.22. DLS data for micelles prepared from PEO_{5K}-*b*-P(*L*-BMA)$_{10}$ (D_h = 18 ± 1 nm) (▬), PEO_{5K}-*b*-P(*D*-BMA)$_{10}$ (D_h = 19 ± 1 nm) (▬) and PEO_{5K}-*b*-P(*L*-BMA)$_{10}$ + PEO_{5K}-*b*-P(*D*-BMA)$_{10}$ equimolar mixed system (D_h = 23 ± 1 nm) (▬) *via* the solvent switch method.

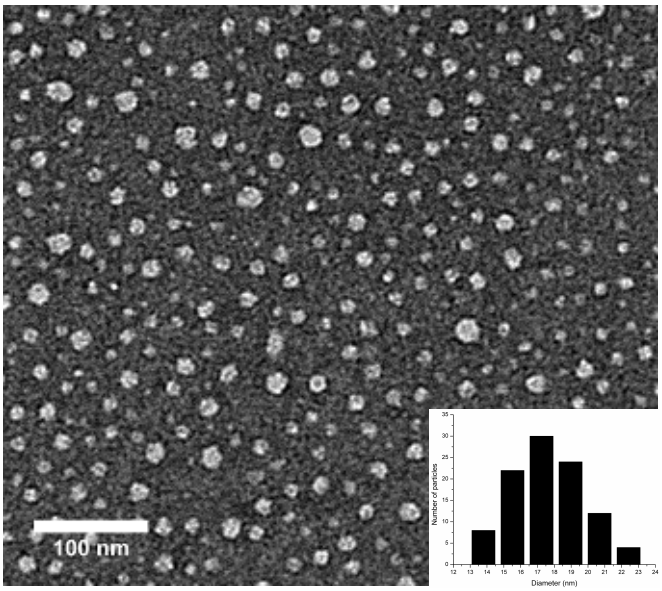

Figure 4.23. TEM image of the stereocomplexed micelles prepared from an equimolar mixture of PEO_{5K}-*b*-P(*L*-BMA)$_{10}$ and PEO_{5K}-*b*-P(*D*-BMA)$_{10}$ (D_{av} = 18 ± 5 nm) *via* the solvent switch method. Scale bar shown is 100 nm. Samples were stained with uranyl acetate (2% solution), drop deposited onto a carbon-coated copper grid and allowed to dry under ambient conditions. Inset: TEM size distribution histogram.

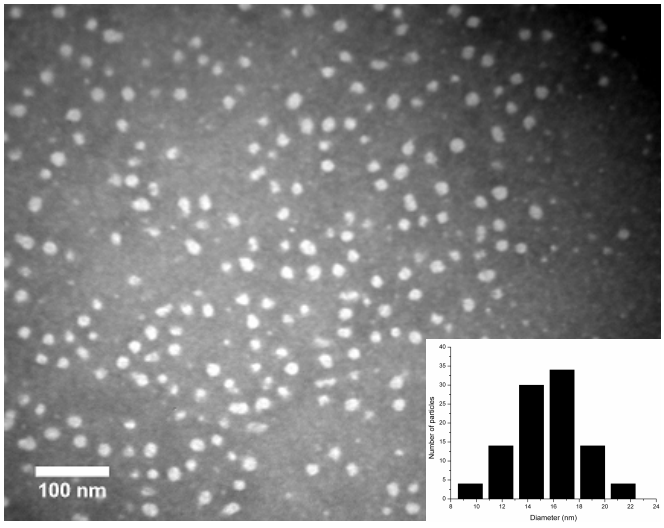

Figure 4.24. TEM image of the micelles prepared from PEO_{5K}-*b*-P(*D*-BMA)$_{10}$ (D_{av} = 16 ± 4 nm) *via* the solvent switch method. Scale bar shown is 100 nm. Samples were stained with uranyl acetate (2% solution), drop deposited onto a carbon-coated copper grid and allowed to dry under ambient conditions. Inset: TEM size distribution histogram.

In other systems, there is quite often a difference seen between light scattering and microscopy data, and the same is true in these examples. TEM analysis confirmed the presence of well-defined spherical micelles resulting from both the enantiopure PEO_{5K}-*b*-P(*D*-BMA)$_{10}$ and stereocomplexed micelles. In correlation with DLS analysis, the stereocomplexed micelle observed an increase in the diameter of D_{av} = 18 ± 5 nm (Figure 4.23) compared to the enantiopure PEO_{5K}-*b*-P(*L*-BMA)$_{10}$ and PEO_{5K}-*b*-P(*D*-BMA)$_{10}$ micelles exhibiting comparable diameters of D_{av} = 16 ± 6 nm (Figure 4.8) and D_{av} = 16 ± 4 nm (Figure 4.24) respectively.

Additional evidence suggesting for the presence of interactions between the enantiopure PBMA chains in the hydrophobic core of the stereocomplexed micelle was obtained through calculation of the CMC using fluorescence spectroscopy with pyrene as a probe. The stereocomplexed micelle exhibited enhanced stability in aqueous conditions with a CMC value of 5.53 x 10^{-3} g.L^{-1} (Figure 4.25) significantly lower than both enantiopure PEO_{5K}-*b*-P(*L*-BMA)$_{10}$ (Figure 4.10) and PEO_{5K}-*b*-P(*D*-BMA)$_{10}$ (Figure 4.26) micelles with CMC values of 1.23 x 10^{-2} g.L^{-1} and 9.78 x 10^{-3} g.L^{-1} respectively. This decrease in the CMC value of the stereocomplexed micelles is of similar magnitude to that observed upon stereocomplexation in PLA-*b*-PEO micelle systems.[26, 53]

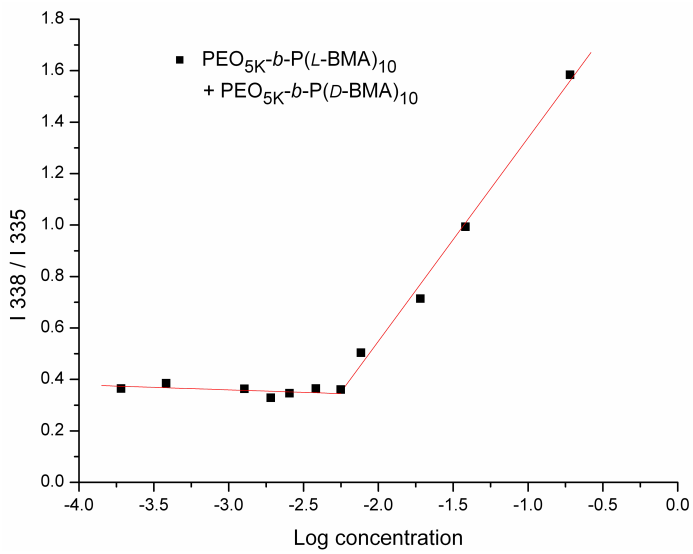

Figure 4.25. Concentration dependence of pyrene I_{338}/I_{335} intensity ratio for an equimolar mixture of PEO_{5K}-*b*-P(*L*-BMA)$_{10}$ and PEO_{5K}-*b*-P(*D*-BMA)$_{10}$ stereocomplexed micelles in water at room temperature. (Diblocks: M_n = 9 400 g.mol^{-1}, PDI = 1.04 (L) and M_n = 8 950 g.mol^{-1}, PDI = 1.03 (D); and [pyrene]$_0$ = 6 x 10^{-7} M). Inflection point at 5.53 x 10^{-3} g.L^{-1}.

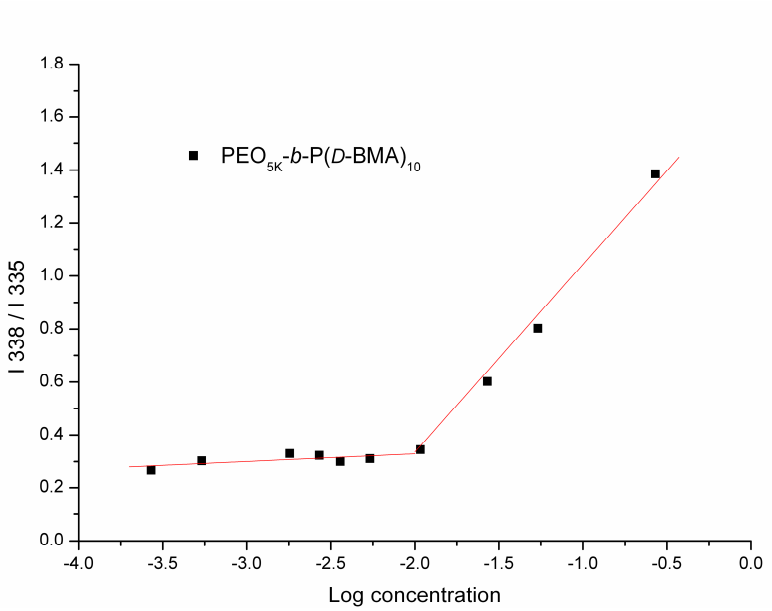

Figure 4.26. Concentration dependence of pyrene I_{338}/I_{335} intensity ratio for PEO_{5K}-*b*-P(*D*-BMA)$_{10}$ micelles in water at room temperature. (Diblock: M_n = 8 950 g.mol^{-1}, PDI = 1.03; and [pyrene]$_0$ = 6 x 10^{-7} M). Inflection point at 9.78 x 10^{-3} g.L^{-1}.

Further evidence for stereocomplexation was obtained through redispersion experiments comparing both the stereocomplexed and homochiral micelles. A sample of the micelle solutions (3 mL) were freeze dried and then subsequently redispersed through addition of water (3 mL). DLS analysis observed no change in the number-average solution hydrodynamic diameter for the stereocomplexed micelle upon redispersion maintaining a D_h of 30 nm resulting from the enhanced stabilisation in the hydrophobic core (Figure 4.27). However, the homochiral observed significant changes in the micelles structures with an increase in D_h from 23 ± 3 nm to 107 ± 13 nm. The pre-redispersion D_h values of the micelles were larger than previously described due to favourable aggregation occurring over time between the neutrally charged PEO coronas of the polymeric micelles.

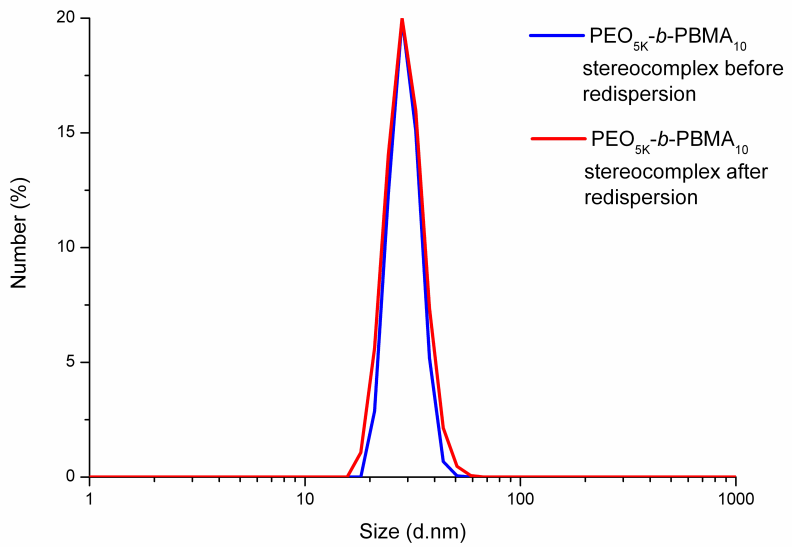

Figure 4.27. DLS data for stereocomplex micelles from a PEO_{5K}-*b*-P(*L*-BMA)$_{10}$ + PEO_{5K}-*b*-P(*D*-BMA)$_{10}$ equimolar mixed system before redispersion (D_h = 30 ± 3 nm) (—) and after (D_h = 30 ± 5 nm) (—).

These data along with DLS and TEM analysis suggest that an equimolar mixture of enantiopure PEO_{5K}-*b*-P(*L*-BMA)$_{10}$ and PEO_{5K}-*b*-P(*D*-BMA)$_{10}$ is capable of

realising polymeric micelles through self-assembly exhibiting different physical dimensions and enhanced stability in aqueous conditions compared to their enantiopure derivatives.

All of the polymeric micelles prepared in this investigation showed good long term stability in aqueous conditions with no significant changes in the average solution hydrodynamic diameters measured *via* DLS analysis after two months.

4.3 Conclusions

In conclusion, the preparation and self-assembly of a range of amphiphilic PEO_x-*b*-$PBMA_n$ block copolymers using *L*-malOCA, ***L*-17**, and *D*-malOCA, ***D*-17**, prepared from *L*- and *D*-malic acid respectively has been demonstrated. The resulting polymeric micelles consisted of a hydrophilic PEO corona and a hydrophobic PBMA core. Through variation of PEO and PBMA block lengths it was determined that the physical dimensions and stability of the resulting micelles could be tuned, as evidenced by DLS analysis, TEM analysis and CMC calculations using fluorescence microscopy with pyrene as the probe. As a consequence of the accessibility to enantiopure PBMA blocks, a stereocomplexed micelle was prepared *via* self-assembly of an equimolar mixture of enantiopure PEO_{5K}-*b*-P(*L*-BMA)$_{10}$ and PEO_{5K}-*b*-P(*D*-BMA)$_{10}$. Evidence from DLS and TEM analysis along with CMC calculations suggest favorable stereocomplexation interactions are present in the hydrophobic core of the micelle resulting in different physical dimensions and enhanced stabilities compared to micelles prepared from both enantiopure PEO_{5K}-*b*-P(*L*-BMA)$_{10}$ and PEO_{5K}-*b*-P(*D*-BMA)$_{10}$. All of the polymeric micelles prepared in this investigation showed good long term stability in aqueous conditions with many

of them exhibiting low CMC values providing promising candidates as novel drug carriers.

4.4 References

(1) Förster, S.; Antonietti, M. *Adv. Mater.* **1998**, *10*, 195.

(2) Alexandridis, P. *Curr. Opin. Colloid Interface Sci.* **1996**, *1*, 490.

(3) van Hest, J. C. M.; Delnoye, D. A. P.; Baars, M. W. P. L.; van Genderen, M. H. P.; Meijer, E. W. *Science* **1995**, *268*, 1592.

(4) Jenekhe, S. A.; Chen, X. L. *Science* **1999**, *283*, 372.

(5) Kukula, H.; Schlaad, H.; Antonietti, M.; Förster, S. *J. Am. Chem. Soc.* **2002**, *124*, 1658.

(6) Zhang, S. *Nat. Biotechnol.* **2003**, *21*, 1171.

(7) Rösler, A.; Vandermeulen, G. W. M.; Klok, H.-A. *Adv. Drug. Del. Rev.* **2001**, *53*, 95.

(8) O'Reilly, R. K.; Hawker, C. J.; Wooley, K. L. *Chem. Soc. Rev.* **2006**, *35*, 1068.

(9) Stubenrauch, K.; Moitzi, C.; Fritz, G.; Glatter, O.; Trimmel, G.; Stelzer, F. *Macromolecules* **2006**, *39*, 5865.

(10) Kataoka, K.; Harada, A.; Nagasaki, Y. *Adv. Drug. Del. Rev.* **2001**, *47*, 113.

(11) Lin, W.-J.; Juang, L.-W.; Lin, C.-C. *Pharm. Res.* **2003**, *20*, 668.

(12) Riley, T.; Stolnik, S.; Heald, C. R.; Xiong, C. D.; Garnett, M. C.; Illum, L.; Davis, S. S.; Purkiss, S. C.; Barlow, R. J.; Gellert, P. R. *Langmuir* **2001**, *17*, 3168.

(13) Yasugi, K.; Nagasaki, Y.; Kato, M.; Kataoka, K. *J. Controlled Release* **1999**, *62*, 89.

(14) Yoo, H. S.; Park, T. G. *J. Controlled Release* **2001**, *70*, 63.

(15) Zhang, X.; Li, Y.; Chen, X.; Wang, X.; Xu, X.; Liang, Q.; Hu, J.; Jing, X. *Biomaterials* **2005**, *26*, 2121.

(16) Otsuka, H.; Nagasaki, Y.; Kataoka, K. *Adv. Drug. Del. Rev.* **2003**, *55*, 403.

(17) Liggins, R. T.; Burt, H. M. *Adv. Drug. Del. Rev.* **2002**, *54*, 191.

(18) Coulembier, O.; Degee, P.; Dubois, P. *Macromol. Chem. Phys.* **2006**, *207*, 484.

(19) Zhao, Z. M.; He, M.; Yin, L. C.; Bao, J. M.; Shi, L. L.; Wang, B. Q.; Tang, C.; Yin, C. H. *Biomacromolecules* **2009**, *10*, 565.

(20) Cammas-Marion, S.; Bear, M. M.; Harada, A.; Guerin, P.; Kataoka, K. *Macromol. Chem. Phys.* **2000**, *201*, 355.

(21) Cammas-Marion, S.; Guerin, P. *Macromol. Symp.* **2000**, *153*, 167.

(22) Coulembier, O.; Mespouille, L.; Hedrick, J. L.; Waymouth, R. M.; Dubois, P. *Macromolecules* **2006**, *39*, 4001.

(23) Lee, J.; Cho, E. C.; Cho, K. *J. Controlled Release* **2004**, *94*, 323.

(24) Nottelet, B.; Tommaso, C. D.; Mondon, K.; Gurny, R.; Möller, M. *J. Polym. Sci., Part A: Polym. Chem.* **2010**, *48*, 3244.

(25) Blanazs, A.; Armes, S. P.; Ryan, A. J. *Macromol. Rapid Commun.* **2009**, *30*, 267.

(26) Chen, L.; Xie, Z.; Hu, J.; Chen, X.; Jing, X. *J. Nano Res.* **2007**, *9*, 777.

(27) Wilhelm, M.; Zhao, C. L.; Wang, Y.; Xu, R.; Winnik, M. A.; Mura, J. L.; Riess, G.; Croucher, M. D. *Macromolecules* **1991**, *24*, 1033.

(28) Huang, X.; Du, F.; Cheng, J.; Dong, Y.; Liang, D.; Ji, S.; Lin, S.-S.; Li, Z. *Macromolecules* **2009**, *42*, 783.

(29) Magnusson, J. P.; Khan, A.; Pasparakis, G.; Saeed, A. O.; Wang, W.; Alexander, C. *J. Am. Chem. Soc.* **2008**, *130*, 10852.

(30) Zhao, Y.; Bertrand, J.; Tong, X.; Zhao, Y. *Langmuir* **2009**, *25*, 13151.

(31) Burt, H. M.; Zhang, X.; Toleikis, P.; Embree, L.; Hunter, W. L. *Colloids Surf., B* **1999**, *16*, 161.

(32) Sallach, R. E.; Wei, M.; Biswas, N.; Conticello, V. P.; Lecommandoux, S.; Dluhy, R. A.; Chaikof, E. L. *J. Am. Chem. Soc.* **2006**, *128*, 12014.

(33) Kim, B. S.; Lee, H.; Min, Y. H.; Poon, Z.; Hammond, P. T. *Chem. Commun.* **2009**, 4194.

(34) Kazunori, K.; Glenn S, K.; Masayuki, Y.; Teruo, O.; Yasuhisa, S. *J. Controlled Release* **1993**, *24*, 119.

(35) O'Reilly, R. K.; Joralemon, M. J.; Hawker, C. J.; Wooley, K. L. *New. J. Chem.* **2007**, *31*, 718.

(36) Henselwood, F.; Liu, G. *Macromolecules* **1997**, *30*, 488.

(37) Wegrzyn, J. K.; Stephan, T.; Lau, R.; Grubbs, R. B. *J. Polym. Sci., Part A: Polym. Chem.* **2005**, *43*, 2977.

(38) Rheingans, O.; Hugenberg, N.; Harris, J. R.; Fischer, K.; Maskos, M. *Macromolecules* **2000**, *33*, 4780.

(39) Thurmond, K. B.; Kowalewski, T.; Wooley, K. L. *J. Am. Chem. Soc.* **1997**, *119*, 6656.

(40) Read, E. S.; Armes, S. P. *Chem. Commun.* **2007**, 3021.

(41) Jiang, X.; Ge, Z.; Xu, J.; Liu, H.; Liu, S. *Biomacromolecules* **2007**, *8*, 3184.

(42) Wang, X.; Liu, K.; Arsenault, A. C.; Rider, D. A.; Ozin, G. A.; Winnik, M. A.; Manners, I. *J. Am. Chem. Soc.* **2007**, *129*, 5630.

(43) Harada, A.; Kataoka, K. *Macromolecules* **1995**, *28*, 5294.

(44) Kakizawa, Y.; Kataoka, K. *Adv. Drug. Del. Rev.* **2002**, *54*, 203.

(45) Lavasanifar, A.; Samuel, J.; Kwon, G. S. *Adv. Drug. Del. Rev.* **2002**, *54*, 169.

(46) Weaver, J. V. M.; Tang, Y. Q.; Liu, S. Y.; Iddon, P. D.; Grigg, R.; Billingham, N. C.; Armes, S. P.; Hunter, R.; Rannard, S. P. *Angew. Chem., Int. Ed.* **2004**, *43*, 1389.

(47) Lee, S. C.; Lee, H. J. *Langmuir* **2006**, *23*, 488.

(48) Tsuji, H. *Macromol. Biosci.* **2005**, *5*, 569.

(49) Lee, W.-K.; Iwata, T.; Gardella, J. A. *Langmuir* **2005**, *21*, 11180.

(50) Kim, S. H.; Nederberg, F.; Zhang, L.; Wade, C. G.; Waymouth, R. M.; Hedrick, J. L. *Nano Lett.* **2007**, *8*, 294.

(51) Spasova, M.; Mespouille, L.; Coulembier, O.; Paneva, D.; Manolova, N.; Rashkov, I.; Dubois, P. *Biomacromolecules* **2009**, *10*, 1217.

(52) Ikada, Y.; Jamshidi, K.; Tsuji, H.; Hyon, S. H. *Macromolecules* **1987**, *20*, 904.

(53) Kang, N.; Perron, M.-È.; Prud'homme, R. E.; Zhang, Y.; Gaucher, G.; Leroux, J.-C. *Nano Lett.* **2005**, *5*, 315.

(54) Nederberg, F.; Appel, E.; Tan, J. P. K.; Kim, S. H.; Fukushima, K.; Sly, J.; Miller, R. D.; Waymouth, R. M.; Yang, Y. Y.; Hedrick, J. L. *Biomacromolecules* **2009**, *10*, 1460.

(55) Lim, D. W.; Park, T. G. *J. Appl. Polym. Sci.* **2000**, *75*, 1615.

(56) Bishara, A.; Kricheldorf, H. R.; Domb, A. J. *Macromol. Symp.* **2005**, *225*,17.

(57) Kim, S. H.; Tan, J. P. K.; Nederberg, F.; Fukushima, K.; Yang, Y. Y.; Waymouth, R. M.; Hedrick, J. L. *Macromolecules* **2008**, *42*, 25.

(58) Hu, J. L.; Han, Y. D.; Zhuang, X. L.; Chen, X. S.; Li, Y. S.; Jing, X. B. *Nanotechnology* **2007**, *18*.

Chapter 5 - Conclusions

5.1 Conclusions

The synthesis of poly(ester)s by the ROP of monomers derived from malic acid has been reported. Initial studies focused on the synthesis of both 3-(*S*)-[(benzyloxycarbonyl)methyl]- and 3-(*S*)-[di(benzyloxycarbonyl)methyl]-1,4-dioxane-2,5-diones (BMD, **6**, and malide, **7**, respectively) from *L*-malic acid; Improved syntheses of both monomers were reported. Homopolymerisation of BMD using the selective organocatalytic 1-(3,5-bis(trifluoromethyl)phenyl)-3-cyclohexylthiourea (**8**) and (-)-sparteine system was successful enabling the synthesis of functional poly(ester)s (PBMD) with pendant benzyl protected carboxylic acid groups in the absence of transesterification side reactions. The choice of initiator was determined to be an important factor in controlling the resulting PBMD molecular weight such that a more electron deficient initiating species resulted in lower molecular weights PBMDs. The versatility of the polymerisation system was demonstrated through successful initiation from a range of alcohols and amines including the use of PEO and PLLA as macroinitiators. Deprotection of the benzyl protecting groups to side chain carboxylic acids proceeded without any polymer backbone scission realising hydrophilic poly(glycolic acid-*co*-malic acid)s (PGMA) that completely degraded in H_2O after six days determined by titration, aqueous GPC analysis, ^{1}H NMR and mass spectrometry.

Attempts to polymerise malide with the **8**/(-)-sparteine system did not result in the isolation of any polymeric materials, postulated to be a consequence of the high steric hindrance and low ring strain of the monomer. Consequently, in an attempt to obtain analogous poly(ester)s, the synthesis of 5-(*S*)- and 5-(*R*)-[(benzyloxycarbonyl)methyl]-1,3-dioxolane-2,4-diones (*L*-malOCA, ***L*-17** and *D*-

malOCA, ***D*-17**, respectively) from *L*- and *D*-malic acid respectively was demonstrated, providing activated equivalents of malide that was able to be polymerised. Controlled ROP of *L*-malOCA and *D*-malOCA catalysed with a range of pyridine based catalysts realised functional poly(benzyl α-malate)s (PBMA) with pendant benzyl protected carboxylic acid groups in the absence of transesterification side reactions. The choice of pyridine catalyst had a significant effect on the amount of side products produced such that 4-methoxypyridine was found to provide PBMAs with the least amount of side product that was subsequently successful removed *via* column chromatography. Hydrogenolysis of the pendant benzyl protecting groups proceeded without any polymer backbone scission realising hydrophilic poly(malic acid)s (PMA) with complete degradation in H_2O occurring within 10 days as determined by titration, ^{1}H NMR and mass spectrometry. The derivation of both PBMD and PBMA from a biorenewable resource provides a potential route to functional poly(ester)s *via* this platform.

Both *L*-malOCA and *D*-malOCA were further applied in the synthesis of a range of novel amphiphilic PEO_x-*b*-$PBMA_n$ block copolymers. Subsequent self assembly of these block copolymers realised polymeric micelles consisting of a hydrophilic PEO corona and a hydrophobic PBMA core. Variation of the PEO and PBMA block lengths significantly affected the physical dimensions and stability of the resulting micelles evidenced by DLS analysis, TEM analysis and CMC calculations using fluorescence microscopy such that increasing the overall molecular weight of the amphiphilic block copolymer along with increasing the hydrophobic block length realised polymeric micelles with larger diameter and lower CMC values. As a consequence of the accessibility to enantiopure PBMA blocks, a stereocomplexed micelle was prepared *via* self-assembly of an

equimolar mixture of enantiopure PEO_{5K}-*b*-P(*L*-BMA)$_{10}$ and PEO_{5K}-*b*-P(*D*-BMA)$_{10}$. DLS and TEM analysis revealed an increase in the diameters of the polymeric micelles that along with CMC calculations demonstrating a value half of that of the homochiral micelles suggested that stereocomplexation was occurring in the hydrophobic core of the micelle. All the polymeric micelles prepared in this investigation showed good long term stability in aqueous conditions with many of them exhibiting low CMC values providing promising candidates as novel drug carriers.

Chapter 6 - Experimental

6.1 Materials

L-lactide was purified by recrystallisation from dry dichloromethane and sublimation (x2). Chloroform and (-)-sparteine was dried over CaH_2, distilled, degassed and stored under a nitrogen atmosphere. All alcohol and amine initiators were dried over suitable dry agents and were distilled, degassed and/or sublimed as required. Triethylamine, acetone and benzylamine were dried and stored over 4Å molecular sieves. 1-(3,5-bis(trifluoromethyl)phenyl)-3-cyclohexylthiourea (**8**) was prepared as previously reported.[1] Compounds **2** to **7** and **9** to **18** were prepared using modified literature procedures.[2-4] All other chemicals and solvents were obtained from Aldrich and used as received.

6.2 General Considerations

All manipulations were performed under moisture- and oxygen-free conditions either in a nitrogen-filled glovebox or by standard Schlenk techniques. Gel-permeation chromatography (GPC) was used to determine the molecular weights and polydispersities of the synthesised polymers. GPC in THF was conducted on a system comprised of a Varian 390-LC-Multi detector suite fitted with differential refractive index (DRI), light scattering (LS) and ultra-violet (UV) detectors equipped with a guard column (Varian Polymer Laboratories PLGel 5 µM, 50 × 7.5 mm) and two mixed D columns (Varian Polymer Laboratories PLGel 5 µM, 300 × 7.5 mm). The mobile phase was tetrahydrofuran with 5% triethylamine eluent at a flow rate of 1.0 $mL.min^{-1}$, and samples were calibrated against Varian Polymer laboratories Easi-Vials linear poly(styrene) standards (162-2.4 × 10^5 $g.mol^{-1}$) using Cirrus v3.3. GPC in aqueous media was conducted on a system comprised of a Varian 390-LC-Multi detector suite fitted with

differential refractive index (DRI), viscometer (VIS) and ultra-violet (UV) detectors equipped with a guard column (Varian Polymer Laboratories PL aquagel-OH Guard 8 µM, 50 × 7.5 mm), two Varian Polymer Laboratories PL-aquagel-OH 30 8 µM, 300 × 7.5 mm columns and one Varian Polymer Laboratories PL-aquagel-OH 40 8 µM, 300 × 7.5 mm column. The mobile phase was an aqueous solution containing 2 L of H_2O, 34 g of sodium nitrate and 3.12 g of sodium phosphate monobasic dehydrate that was adjusted to pH 8.2 with a 1.0 M $NaOH_{(aq)}$ solution. The eluent flow rate was 1.0 $mL.min^{-1}$ and samples were calibrated against Varian Polymer laboratories Easi-Vials linear poly(ethylene glycol) standards (106-9.1 × 10^5 $g.mol^{-1}$) using Cirrus v3.3. ^1H and ^{13}C NMR spectra were recorded on a Bruker DPX-300, DPX-400, AC400, or DRX-500 spectrometer at 293 K unless stated otherwise. Chemical shifts are reported as δ in parts per million (ppm) and referenced to the chemical shift of the residual solvent resonances ($CDCl_3$ ^1H: δ = 7.26 ppm; ^{13}C δ = 77.16 ppm). Mass spectra were acquired by MALDI-TOF (matrix-assisted laser desorption and ionisation time-of-flight) mass spectrometry using a Bruker Daltonics Ultraflex II MALDI-TOF mass spectrometer, equipped with a nitrogen laser delivering 2 ns laser pulses at 337 nm with positive ion TOF detection performed using an accelerating voltage of 25 kV. Solutions of trans-2-[3-(4-*tert*-butylphenyl)-2-methyl-2-propy-lidene]malonitrile (DCTB) as matrix (0.3 µL of a 10 $g.L^{-1}$ acetone solution), sodium trifluoroacetate as cationisation salt (0.3 µL of a 10 $g.L^{-1}$ acetone solution), and analyte (0.3 µL of a 1 $g.L^{-1}$ DCM solution) were applied sequentially to the target followed by solvent evaporation to prepare a thin matrix/analyte film. The samples were measured in linear ion mode (unless stated differently) and calibrated by comparison to 2 × 10^3 and 5 × 10^3 $g.mol^{-1}$ monomethylether poly(ethylene oxide) standards. Low resolution mass spectra

were recorded on an Esquire 2000 platform with electrospray ionisation. High resolution mass spectra were recorded on a Bruker UHR-Q-TOF MaXis with electrospray ionisation. Elemental analyses were performed in duplicate by Warwick Analytical Services. Average solution hydrodynamic diameters (D_h) and size distributions of the PEO-*b*-PBMA micelles in aqueous solution were determined by dynamic light scattering (DLS). The DLS measurements were taken on a Malvern Nano S Zetasizer Nano Series instrument operating at 25 °C with a 635-nm laser module using a cumulants fit analysis method. All determinations were made in triplicate (with 12 runs recorded). Transmission electron microscopy (TEM) samples were prepared by drop deposition and dried *via* blotching onto copper/carbon grids that had been treated with oxygen plasma to increase the surface hydrophilicity. The particles were stained using a dilute 5% solution of uranyl acetate and examined with a transmission electron microscope (JEOL TEM-1200), operating at 100 kV. Micrographs were collected at magnifications varying from 80K to 120K and calibrated digitally. Histograms of number-average particle diameters (D_{av}) and standard deviations were generated from the analysis of a minimum of 100 particles from at least three different micrographs. Critical micelle concentration determinations were performed using fluorescence spectroscopy on a Cary Eclipse single-beam Perkin-Elmer LS55 fluorometer. Specific rotation measurements for **6**, ***L*-17** and ***D*-17** were recorded in $CHCl_3$ on a Perkin-Elmer 241 polarimeter using a sodium source ($\lambda = 589$ nm) and a 1 cm rotation cell.

6.3 Experimental details for Chapter 2

6.3.1 Synthesis of 2-[2,2-dimethyl-5-oxo-1,3-dioxolan-4-yl]acetic acid (2)[5]

To a mixture of *L*-malic acid (20 g, 0.15 mol) and 2,2-dimethoxypropane (74 mL, 0.60 mol) in a Schlenk tube under nitrogen was added *p*-toluenesulfonic acid monohydrate (0.29 g, 1.5 mmol) and the solution was stirred at room temperature for 3.5 h. H_2O (100 mL) containing $NaHCO_3$ (0.13 g, 1.5 mmol) was added to the solution and the aqueous layer was separated and extracted with DCM (5 x 100 mL). The combined organic layers were dried with $NaSO_4$, filtered and the solvent removed under reduced pressure. The resulting solid was recrystallised from Et_2O yielding a white solid (16.89 g, 97 mmol, 65%). Data was in accordance with that previously reported.[5]

^{1}H NMR ($CDCl_3$, 400.0 MHz): δ = 11.02 (1H, s, -COO*H*), 4.71 (1H, ABX, $^3J_{A\text{-}X}$ = 6.53 Hz, $^3J_{B\text{-}X}$ = 3.76 Hz, -C*H*CO-), 3.00 (1H, ABX, $^2J_{A\text{-}B}$ = 17.32 Hz, $^3J_{B\text{-}X}$ = 3.76 Hz, -CH_2COOH), 2.86 (1H, ABX, $^2J_{A\text{-}B}$ = 17.32 Hz, $^3J_{A\text{-}X}$ = 6.53 Hz, -CH_2COOH), 1.62 (3H, s, -CH_3), 1.57 (3H, s, -CH_3).

^{13}C NMR ($CDCl_3$, 100.0 MHz): δ = 175.1 (-*C*OOH), 171.9 (-*C*OO-), 111.4 (-*C*(CH_3)$_2$), 70.4 (-*C*HCOO-), 36.0 (-*C*H_2COOH), 26.8 (-*C*H_3), 25.8 (-*C*H_3).

6.3.2 Synthesis of 2-[2,2-dimethyl-5-oxo-1,3-dioxolan-4-yl]acetic acid benzyl ester (3)[6]

To a solution of **2** (10 g, 61 mmol) in dry acetone under nitrogen was added dry NEt_3 (10.2 mL, 73 mmol) followed by benzyl bromide (8.9 mL, 75 mmol). The solution was refluxed for 60 h at 50 °C before being cooled to room temperature. The solids were removed by filtration and washed with acetone before the volatile organic solvents were removed under reduced pressure. The resulting

residue was dissolved in EtOAc (300 mL) and H_2O (150 mL). The aqueous layer was further extracted with EtOAc (2 x 100 mL) before the combined organic layers were dried with $MgSO_4$, filtered and reduced *in vacuo*. The resultant solid was recrystallised from Et_2O to yield white crystals (12.14 g, 46 mmol, 80%). Data was in accordance with that previously reported.[6]

^{1}H NMR ($CDCl_3$, 400.0 MHz): δ = 7.36 (5H, m, -C$H_{aromatic}$), 5.20 and 5.16 (2H, AB, $^2J_{A\text{-}B}$ = 12.30 Hz, -CH_2Ar), 4.74 (1H, ABX, $^3J_{A\text{-}X}$ = 6.53 Hz, $^3J_{B\text{-}X}$ = 3.77 Hz, -C*H*COO-), 2.98 (1H, ABX, $^2J_{A\text{-}B}$ = 16.94 Hz, $^3J_{B\text{-}X}$ = 3.77 Hz, -CH_2COOCH$_2$Ar), 2.84 (1H, ABX, $^2J_{A\text{-}B}$ = 16.94 Hz, $^3J_{A\text{-}X}$ = 6.53 Hz, -CH_2COOCH$_2$Ar), 1.58 (3H, s, -CH_3), 1.56 (3H, s, -CH_3).

^{13}C{^{1}H} NMR ($CDCl_3$, 100.0 MHz): δ = 169.1 (-*C*OO-), 135.3 (-$C_{ipso\text{-}aromatic}$), 128.6 (-*C*H$_{meta\text{-}aromatic}$), 128.5 (-*C*H$_{para\text{-}aromatic}$), 128.4 (-*C*H$_{ortho\text{-}aromatic}$), 111.2 (-*C*(CH$_3$)$_2$), 70.7 (-*C*HCOO-), 67.0 (-*C*H$_2$Ar), 36.3 (-*C*H$_2$COOCH$_2$Ar), 26.7 (-*C*H$_3$), 25.9 (-*C*H$_3$).

6.3.3 Synthesis of 2-hydroxy-succinic acid 4-benzyl ester (4)[7]

A solution of **3** (20.47 g, 77 mmol) was dissolved in AcOH/THF/H_2O (1:1:1) (300 mL) and heated for 24 h at 40 °C. The solvent was removed under reduced pressure and the resulting colorless oil was freeze dried to yield a white solid (16.02 g, 72 mmol, 92%). Data was in accordance with that previously reported.[8]

^{1}H NMR ($CDCl_3$, 400.0 MHz): δ = 7.35 (5H, m, -C$H_{aromatic}$), 5.20 and 5.16 (2H, AB, $^2J_{A\text{-}B}$ = 12.30 Hz, -CH_2Ar), 4.58 (1H, ABX, $^3J_{A\text{-}X}$ = 6.55 Hz, $^3J_{B\text{-}X}$ = 4.56 Hz, -C*H*COO-), 2.99 (1H, ABX, $^2J_{A\text{-}B}$ = 16.94 Hz, $^3J_{B\text{-}X}$ = 4.56 Hz, -CH_2COOCH$_2$Ar), 2.90 (1H, ABX, $^2J_{A\text{-}B}$ = 16.94 Hz, $^3J_{A\text{-}X}$ = 6.55 Hz, -CH_2COOCH$_2$Ar).

$^{13}C\{^{1}H\}$ NMR ($CDCl_3$, 100.0 MHz): δ = 176.8 (-*C*OOH), 171.0 (-*C*OO-), 135.1 (-$C_{ipso\text{-}aromatic}$), 128.7 (-*C*$H_{meta\text{-}aromatic}$), 128.5 (-*C*$H_{para\text{-}aromatic}$), 128.4 (-*C*$H_{ortho\text{-}aromatic}$), 67.0 (-*C*$H_2$Ar), 67.0 (-*C*HCOO-), 38.2 (-*C*H_2COOCH_2Ar).

6.3.4 Synthesis of 2-(2-bromo-acetoxy)-succinic acid 4-benzyl ester (5)[9]

A solution of α-hydroxy acid, **4**, (6.6 g, 0.029 mol) and NEt_3 (4.1 mL, 29 mmol) in CH_2Cl_2 (200 mL) was added to a solution of bromoacetyl bromide (2.56 mL, 29 mmol) and DMAP (0.36 g, 29 mmol) in CH_2Cl_2 (125 mL) at 0 °C. The resulting solution was stirred at room temperature for 16 h under a nitrogen atmosphere. The reaction was then concentrated *in vacuo* and the salts were precipitated out with the addition of Et_2O (150 mL). After filtration, the solvent was evaporated yielding the product as an orange oil that was used as obtained without further purification (9.87 g, 29 mmol, 97%). Data was in accordance with that previously reported.[10]

^{1}H NMR ($CDCl_3$, 400.0 MHz): δ = 7.30-7.19 (5H, m, -C*H*$_{aromatic}$), 5.48 (1H, t, $^{3}J_{H\text{-}H}$ = 6.03 Hz, -HOOCC*H*OCO-), 5.20 and 5.16 (2H, AB, $^{2}J_{A\text{-}B}$ = 12.18 Hz, -C*H*$_2$Ar), 3.86 and 3.82 (2H, AB, $^{2}J_{A\text{-}B}$ = 13.07 Hz, -COC*H*$_2$Br); 3.02 (2H, d, $^{3}J_{H\text{-}H}$ = 6.03 Hz, -C*H*$_2$COOCH_2Ar).

$^{13}C\{^{1}H\}$ NMR ($CDCl_3$, 100.0 MHz): δ = 173.3 (-*C*OOH), 168.5 (-CH$_2$*C*OOCH_2Ar), 166.2 (-*C*OOCH_2Br), 135.0 (-$C_{ipso\text{-}aromatic}$), 128.6 (-*C*$H_{meta\text{-}aromatic}$), 128.5 (-*C*$H_{para\text{-}aromatic}$), 128.4 (-*C*$H_{ortho\text{-}aromatic}$), 69.0 (-*C*HCOO-), 66.9 (-*C*H_2Ar), 35.5 (-*C*H_2COOCH_2Ar), 24.8 (-*C*OOCH_2Br).

6.3.5 Synthesis of 3-(S)-[(benzyloxycarbonyl)methyl]-1,4-dioxane-2,5-dione (6)[11]

To a vigorously stirred solution of $NaHCO_3$ (0.73 g, 8.7 mmol) in DMF (200 mL) at room temperature was added **5** (2.0 g, 5.8 mmol) in DMF (40 mL) *via* a syringe pump over 28 h. The solution was then filtered and the DMF removed in *vacuo*. The residual salts were precipitated by addition of EtOAc and filtered before the solution was concentrated *in vacuo*. The resulting brown solid was washed with hexane (200 mL) followed by MeOH (100 mL) before being recrystallised from 2-propanol to yield white needles that were dried over 4Å molecular sieves in CH_2Cl_2 solution (0.84 g, 3.2 mmol, 55%). Data was in accordance with that previously reported.[10]

^{1}H NMR ($CDCl_3$, 400.0 MHz): δ = 7.32-7.19 (5H, m, -C*H*$_{aromatic}$), 5.22 (1H, t, $^3J_{H\text{-}H}$ = 4.68 Hz, -C*H*CH_2COOCH_2Ar), 5.11 (2H, s, -C*H*$_2$Ar), 5.08 and 4.98 (2H, AB, $^2J_{A\text{-}B}$ = 16.83 Hz, -COOC*H*$_2$COO-), 3.12 (2H, d, $^3J_{H\text{-}H}$ = 4.68 Hz, -CHC*H*$_2$COOCH$_2$Ar).

^{13}C{^{1}H} NMR ($CDCl_3$, 100.0 MHz): δ = 169.0 (-CH*C*OOCH$_2$-), 164.7 (-CH$_2$*C*OOCH$_2$Ar), 162.8 (-CH$_2$*C*OOCH-), 134.6 (-*C*$_{ipso\text{-}aromatic}$), 128.8 (-*C*H$_{meta\text{-}aromatic}$), 128.7 (-*C*H$_{para\text{-}aromatic}$), 128.4 (-*C*H$_{ortho\text{-}aromatic}$), 72.0 (-C*H*COO-), 67.6 (-*C*H$_2$Ar), 65.5 (-COO*C*H$_2$COO-), 36.4 (-*C*H$_2$COOCH$_2$Ar).

6.3.6 Synthesis of 3,6-(S)-[di(benzyloxycarbonyl)methyl]-1,4-dioxane-2,5-dione (7)[12]

A solution of **4** (5.6 g, 25 mmol) and *p*-toluenesulfonic acid monohydrate (0.48 g, 2.5 mmol) in toluene (500 mL) was heated to reflux for 50 h with the resulting water formed continuously removed *via* Dean-Stark apparatus. The solution was

then concentrated *in vacuo* and the resulting crude solid purified by column chromatography (Hex 3:1 EtOAc) followed by washing with diethyl ether to yield a white solid (1.57 g, 3.8 mmol, 30%). Data was in accordance with that previously reported.[8]

^{1}H NMR ($CDCl_3$, 400.0 MHz): δ = 7.37 (5H, m, -C$H_{aromatic}$), 5.45 (1H, ABX, $^{3}J_{A\text{-}X}$ = 6.53 Hz, $^{3}J_{B\text{-}X}$ = 4.79 Hz, -C*H*COO-), 5.19 (2H, s, -CH_2Ar), 3.23 (1H, ABX, $^{2}J_{A\text{-}B}$ = 17.57 Hz, $^{3}J_{B\text{-}X}$ = 4.79 Hz, -CH_2COOCH_2Ar), 3.07 (1H, ABX, $^{2}J_{A\text{-}B}$ = 17.57 Hz, $^{3}J_{A\text{-}X}$ = 6.53 Hz, -CH_2COOCH_2Ar).

^{13}C{^{1}H} NMR ($CDCl_3$, 100.0 MHz): δ = 168.5 (-CH*C*OOCH-), 164.9 (-CH_2*C*OOCH_2Ar), 135.0 (-*C*$_{ipso\text{-}aromatic}$), 128.7 (-*C*H$_{meta\text{-}aromatic}$), 128.6 (-*C*H$_{para\text{-}aromatic}$), 128.4 (-*C*H$_{ortho\text{-}aromatic}$), 72.6 (-C*H*COO-), 67.5 (-*C*H_2Ar), 35.7 (-*C*H_2COOCH_2Ar).

6.3.7 General procedure for polymerisation of 6 ([M]/[I] = 20)

A solution of **8** (0.01 g, 0.027 mmol, 25 mol%), (-)-sparteine (0.99 µL, 0.004 mmol, 5 mol%) and initiator (0.0044 mmol, 1 equiv) was added to **6** (23 mg, 0.087 mmol, 20 equiv) in $CHCl_3$ (0.3 mL). The solution was left to stir at room temperature for the allotted time period before being diluted with DCM (4 mL), washed with cold 2.0 M $HCl_{(aq)}$ (2 x 5 mL) and brine (5 mL). The organic layer was dried over $MgSO_4$, filtered and concentrated *in vacuo*. The excess thiourea was then removed by washing with Et_2O and the PBMD was precipitated into ice cold petroleum ether (b.p. 40-60 °C) to yield pure PBMD as a white solid (0.022 g, 0.0042 mmol, 96%).

^{1}H NMR ($CDCl_3$, 400.0 MHz): δ = 7.40 – 7.25 (100H, m, -C$H_{aromatic}$), 5.65 – 5.54 (20H, m, -C*H*COO-), 5.15 – 5.11 (40H, m, -CH_2Ar), 4.82 – 4.49 (40H, m, -

COC*H*$_2$OCOCH-), 3.83 – 3.80 (2H, m, -C*H*$_2$(CH$_3$)$_3$), 3.08 – 2.85 (40H, m, -C*H*$_2$COOCH$_2$Ar), 0.92 and 0.89 (9H, s, -CH$_2$(C*H*$_3$)$_3$). GPC (THF, RI): M_n (PDI) = 6 750 g.mol^{-1} (1.17) (initiation from 2,2-dimethyl-1-propanol).

6.3.8 General procedure for the deprotection of PBMD ([M]/[I] = 20)

A balloon of H_2 was bubbled through a suspension of PBMD (0.05 g, 0.0095 mmol) and Pd/C (0.01 g, 10 wt. % loading) in THF (20 mL) for 15 min. The solution was then filtered to remove Pd/C and concentrated *in vacuo*. The PGMA was extracted into MeOH and concentrated *in vacuo* to yield the desired product as a colorless oil (0.024 g, 0.006 mmol, 73%).

^{1}H NMR (d^8-THF, 400.0 MHz): δ = 5.60 – 5.55 (20H, m, -C*H*COO-), 4.44 (20H, br s, -COO*H*), 4.86 – 4.64 (40H, m, -COC*H*$_2$OCOCH-), 3.03 – 2.70 (40H, m, -C*H*$_2$COOCH$_2$Ar), 0.9 (9H, s, -CH$_2$(C*H*$_3$)$_3$).

^{13}C{^{1}H} NMR (d^8-THF, 100.0 MHz): δ = 170.6 (-*C*OOCH$_2$C(CH$_3$)$_3$), 168.7 (-CH*C*OOCH$_2$-), 167.2 (-CH$_2$*C*OOH), 70.3 (-CH$_2$COO*C*HCOO-), 61.5 (-*C*H$_2$COOCHCOO-), 36.2 (-*C*H$_2$COOH). GPC (H_2O, RI): M_n (PDI) = 2 410 g.mol^{-1} (1.08).

6.3.9 General procedure for the degradation of PGMA ([M]/[I] = 20)

PGMA (14.5 mg, 0.0042 mmol) was dissolved in H_2O (7.5 mL) and monitored *via* acid-base titration of a sample (0.2 mL) with an aqueous NaOH solution (0.50 mmol.L^{-1}) using phenolphthalein as a pH indicator, ^{1}H NMR spectroscopy in D_2O and GPC analysis.

6.3.10 Synthesis of isopropyl 2-hydroxyacetate (9)[2]

Glycolic acid (12.5 g, 164 mmol) was dissolved in 2-propanol (50 mL) containing *p*-toluenesulfonic acid (0.125 g, 0.657 mmol). The solution was refluxed overnight in a Soxhlet extractor containing 4 Å molecular sieves. After cooling, the reaction was poured into 10% Na_2CO_3 and extracted into CH_2Cl_2. The organic layer was washed with brine and dried over $MgSO_4$. The solution was concentrated *in vacuo* to yield the desired product as a colorless oil which was further purified by distillation (60 °C, 0.025 mm Hg) (11.3 g, 95.2 mmol, 58%).

^{1}H NMR ($CDCl_3$, 400.0 MHz): δ = 5.12 (1H, sept, $^3J_{H\text{-}H}$ = 6.27 Hz, -COOC*H*$(CH_3)_2$), 4.10 (2H, s, -COOC*H*$_2$OH), 1.27 (6H, d, $^3J_{H\text{-}H}$ = 6.27 Hz, -COOCH(C*H*$_3)_2$).

^{13}C{^{1}H} NMR ($CDCl_3$, 100.0 MHz): δ = 172.9 (-*C*OOCH$(CH_3)_2$), 69.5 (-COO*C*H$(CH_3)_2$), 60.8 (-COO*C*H$_2$OH), 21.8 (-COOCH(*C*H$_3)_2$).

ESI-MS: obs, 119.09 m/z; Calc for $C_5H_{11}O_3$, 119.14 m/z.

Elemental Analysis: Calculated (Found) C: 50.8 (50.85); H: 8.5 (8.65).

6.3.11 Synthesis of neopentyl 2-hydroxyacetate (11)[2]

A solution of glycolic acid (12.5 g, 164 mmol), 2,2-dimethyl-1-propanol (15.9 g, 180 mmol) and *p*-toluenesulfonic acid (0.125 g, 0.657 mmol) in THF (50 mL) was refluxed overnight in a Soxhlet extractor containing 4 Å molecular sieves. After cooling, the reaction was poured into 10% Na_2CO_3 and extracted into CH_2Cl_2. The organic layer was washed with brine and dried over $MgSO_4$. The solution was concentrated *in vacuo* to yield the desired product as a colorless oil

which was further purified by distillation (60 °C, 0.027 mm Hg) (10.2 g, 69.8 mmol, 42%).

^{1}H NMR ($CDCl_3$, 400.0 MHz): δ = 4.18 (2H, s, -COOCH_2OH), 3.90 (2H, s, -COOCH_2C(CH_3)$_3$), 0.94 (9H, s, -COOCH_2C(CH_3)$_3$).

^{13}C{^{1}H} NMR ($CDCl_3$, 100.0 MHz): δ = 173.6 (-*C*OOCH_2C(CH_3)$_3$), 74.7 (-COO*C*H_2OH), 60.5 (-COO*C*H_2C(CH_3)$_3$), 31.4 (-COOCH_2*C*(CH_3)$_3$), 26.3 (-*C*OOCH_2C(*C*H_3)$_3$).

ESI-MS: obs, 147.01 m/z ([MH]$^+$); Calc for $C_7H_{15}O_3$, 147.10 m/z.

Elemental Analysis: Calculated (Found) C: 57.5 (57.0); H: 9.65 (9.8).

6.3.12 Synthesis of isopropyl 2-acetoxyacetate (13)[3]

A mixture of **9** (0.61 g, 5.16 mmol) and acetyl chloride (1.0 mL, 14.1 mmol) was stirred at room temperature for 2 h. The resulting solution was reduced under vacuum before the oily residue was extracted with CH_2Cl_2 (100 mL). The combined organic extracts were dried over $MgSO_4$ and concentrated *in vacuo* to yield **13** as a colorless oil (0.52 g, 3.25 mmol, 64%).

^{1}H NMR ($CDCl_3$, 400.0 MHz): δ = 5.08 (1H, sept, $^{3}J_{H\text{-}H}$ = 6.27 Hz, -COOC*H*(CH_3)$_2$), 4.55 (2H, s, -COOCH_2OCOCH_3), 2.15 (3H, s, -COOCH_2OCOCH_3), 1.26 (6H, d, $^{3}J_{H\text{-}H}$ = 6.27 Hz, -COOCH(CH_3)$_2$).

^{13}C{^{1}H} NMR ($CDCl_3$, 100.0 MHz): δ = 170.4 (-*C*OOCH_2OCOCH_3), 167.4 (-COOCH_2O*C*OCH_3), 69.3 (-COO*C*H(CH_3)$_2$), 61.0 (-COO*C*H_2OCOCH_3), 21.7 (-COOCH(*C*H_3)$_2$), 18.4 (-COOCH_2OCO*C*H_3).

ESI-MS: obs, 161.21 m/z ([MH]$^+$); Calc for $C_7H_{13}O_4$, 161.08 m/z.

Elemental Analysis: Calculated (Found) C: 52.5 (52.2); H: 7.55 (7.5).

6.3.13 Synthesis of neopentyl 2-acetoxyacetate (15)[3]

This compound was synthesised using the same procedure as described for **13** using **11** (3.46 g, 23.7mmol) and acetyl chloride (3.5 mL, 49.2 mmol); (1.87 g, 9.94 mmol, 41%).

^{1}H NMR ($CDCl_3$, 400.0 MHz): δ = 4.63 (2H, s, -COOCH_2OCOCH$_3$), 3.86 (2H, s, -COOCH_2C(CH$_3$)$_3$), 2.16 (3H, s, -COOCH$_2$OCOCH_3), 0.93 (9H, s, -COOCH$_2$C(CH_3)$_3$).

^{13}C{^{1}H} NMR ($CDCl_3$, 100.0 MHz): δ = 170.4 (-*C*OOCH$_2$C(CH$_3$)$_3$), 168.0 (-COOCH$_2$O*C*OCH$_3$), 74.5 (-COO*C*H$_2$OCOCH$_3$), 60.7 (-COO*C*H$_2$C(CH$_3$)$_3$), 31.4 (-COOCH$_2$*C*(CH$_3$)$_3$), 26.3 (-*C*OOCH$_2$C(*C*H$_3$)$_3$), 20.5 (-COOCH$_2$OCO*C*H$_3$).

ESI-MS: obs, 188.94 m/z ([MH]$^+$); Calc for $C_9H_{17}O_4$, 189.11 m/z.

Elemental Analysis: Calculated (Found) C: 57.4 (57.3); H: 8.6 (8.7).

6.3.14 Synthesis of 4-benzyl 1-isopropyl 2-hydroxysuccinate (10)[2]

This compound was synthesised using the same procedure as described for **9** from **4** (2.5 g, 11.2 mmol), *p*-toluenesulfonic acid (0.02 g, 0.105 mmol) and 2-propanol (50 mL); (1.51 g, 5.67 mmol, 51%).

^{1}H NMR ($CDCl_3$, 400.0 MHz): δ = 7.35 (5H, m, -C$H_{aromatic}$), 5.15 (2H, s, -CH_2Ar), 5.09 (1H, sept, $^{3}J_{H\text{-}H}$ = 6.27 Hz, -COOCH(CH$_3$)$_2$), 4.46 (1H, ABX, $^{3}J_{A\text{-}X}$ = 5.99 Hz, $^{3}J_{B\text{-}X}$ = 4.54 Hz, -CHCOO-), 2.89 (1H, ABX, $^{2}J_{A\text{-}B}$ = 16.57 Hz, $^{3}J_{B\text{-}X}$ = 4.54 Hz, -CH_2COOCH$_2$Ar), 2.82 (1H, ABX, $^{2}J_{A\text{-}B}$ = 16.57 Hz, $^{3}J_{A\text{-}X}$ = 5.99 Hz, -CH_2COOCH$_2$Ar), 1.26 and 1.21 (6H, d, $^{3}J_{H\text{-}H}$ = 6.27 Hz, -COOCH(CH_3)$_2$).

^{13}C{^{1}H} NMR ($CDCl_3$, 100.0 MHz): δ = 172.9 (-*C*OOCH(CH$_3$)$_2$), 170.3 (-CH$_2$*C*OOCH$_2$Ar), 135.5 (-$C_{ipso\ aromatic}$), 128.6 (-*C*H$_{meta\text{-}aromatic}$), 128.4 (-*C*H$_{para\text{-}}$

$_{aromatic}$), 128.3 (-*C*H$_{ortho\text{-}aromatic}$), 70.1 (-COO*C*H(CH$_3$)$_2$), 67.3 (-*C*HCOO-), 66.8 (-C*H*$_2$Ar), 38.8 (-*C*H$_2$COOCH$_2$Ar), 21.7 (-COOCH(*C*H$_3$)$_2$).

ESI-MS: obs, 267.04 m/z ([MH]$^+$); Calc for $C_{14}H_{19}O_5$, 267.12 m/z.

Elemental Analysis: Calculated (Found) C: 63.15 (62.); H: 6.8 (6.8).

6.3.15 Synthesis of 4-benzyl 1-isopropyl 2-acetoxysuccinate (14)[3]

This compound was synthesised using the same procedure as described for **13** from **10** (0.60 g, 2.25 mmol) and acetyl chloride (1.0 mL, 14.1 mmol); (0.53 g, 1.72 mmol, 76%).

^{1}H NMR (CDCl$_3$, 400.0 MHz): δ = 7.35 (5H, m, -C*H*$_{aromatic}$), 5.43 (1H, t, $^3J_{H\text{-}H}$ = 6.27 Hz, -C*H*COO-), 5.18 and 5.14 (2H, AB, $^2J_{A\text{-}B}$ = 12.36 Hz, -C*H*$_2$Ar), 5.04 (1H, sept, $^3J_{H\text{-}H}$ = 6.49 Hz, -COOC*H*(CH$_3$)$_2$), 2.91 (2H, d, $^3J_{H\text{-}H}$ = 6.27 Hz, -C*H*$_2$COOCH$_2$Ar), 2.08 (3H, s, -CHOCOC*H*$_3$), 1.25 and 1.20 (6H, d, $^3J_{H\text{-}H}$ = 6.49 Hz, -COOCH(C*H*$_3$)$_2$).

^{13}C{^{1}H} NMR (CDCl$_3$, 100.0 MHz): δ = 170.0 (-*C*OOCH(CH$_3$)$_2$), 169.0 (-CH$_2$*C*OOCH$_2$Ar), 168.3 (-CHO*C*OCH$_3$), 135.4 (-*C*$_{ipso\ aromatic}$), 128.6 (-*C*H$_{meta\text{-}aromatic}$), 128.5 (-*C*H$_{para\text{-}aromatic}$), 128.4 (-*C*H$_{ortho\text{-}aromatic}$), 69.8 (-COO*C*H(CH$_3$)$_2$), 68.5 (-*C*HCOO-), 66.9 (-C*H*$_2$Ar), 36.2 (-*C*H$_2$COOCH$_2$Ar), 21.6 (-COOCH(*C*H$_3$)$_2$), 20.2 (-CHOCO*C*H$_3$).

ESI-MS: obs, 309.10 m/z ([MH]$^+$); Calc for $C_{16}H_{21}O_6$, 309.13 m/z.

Elemental Analysis: Calculated (Found) C: 62.3 (62.0); H: 6.5 (6.7).

6.3.16 Synthesis of 2-acetoxy-4-(benzyloxy)-4-oxobutanoic acid (12)[3]

This compound was synthesised using the same procedure as described for **13** from **4** (0.61 g, 2.72 mmol) and acetyl chloride (3.0 mL, 42.2 mmol); (0.54 g, 2.03 mmol, 75%).

^{1}H NMR ($CDCl_3$, 400.0 MHz): δ = 7.36 (5H, m, -C*H*$_{aromatic}$), 5.53 (1H, t, $^{3}J_{H\text{-}H}$ = 6.07 Hz, -C*H*COO-), 5.19 and 5.15 (2H, AB, $^{2}J_{A\text{-}B}$ = 12.41 Hz, -CH_2Ar), 2.95 (2H, d, $^{3}J_{H\text{-}H}$ = 6.07 Hz, -CH_2COOCH_2Ar), 2.09 (3H, s, -CHOCOCH_3).

^{13}C{^{1}H} NMR ($CDCl_3$, 100.0 MHz): δ = 175.7 (-*C*OOH), 170.0 (-CH$_2$*C*OOCH$_2$Ar), 169.0 (-CHO*C*OCH$_3$), 135.3 (-*C*$_{ipso\ aromatic}$), 128.6 (-*C*H$_{meta\text{-}aromatic}$), 128.5 (-*C*H$_{para\text{-}aromatic}$), 128.4 (-*C*H$_{ortho\text{-}aromatic}$), 67.8 (-*C*HCOO-), 67.1 (-*C*H$_2$Ar), 36.0 (-*C*H$_2$COOCH$_2$Ar), 20.5 (-CHOCO*C*H$_3$).

ESI-MS: obs, 289.1 m/z ([MNa]$^+$); Calc for $C_{13}H_{14}O_6Na$, 289.07 m/z.

Elemental Analysis [M + ½ H_2O]: Calculated (Found) C: 56.7 (56.4); H: 5.5 (5.3).

6.3.17 Synthesis of 4-benzyl 1-neopentyl 2-acetoxysuccinate (16)[4]

To a solution of **12** (0.57 g, 2.12 mmol), DMAP (0.026 g, 0.21 mmol) and 2,2-dimethyl-1-propanol (0.17 g, 1.88 mmol) in CH_2Cl_2 (25 mL) was added dropwise to a solution of DCC (0.44 g, 2.12 mmol) in CH_2Cl_2 (25 mL). The resulting solution was stirred at room temperature overnight. DCU was removed by filtration and the solution was concentrated *in vacuo*. The product was extracted into EtOAc (3 x 100 mL), filtered and reduced under vacuum to yield the desired product as a brown oil (0.35 g, 1.04 mmol, 49%).

^{1}H NMR ($CDCl_3$, 400.0 MHz): δ = 7.33 (5H, m, -C*H*$_{aromatic}$), 5.53 (1H, t, $^{3}J_{H\text{-}H}$ = 6.05 Hz, -C*H*COO-), 5.13 (2H, AB, $^{2}J_{A\text{-}B}$ = 12.35 Hz, -CH_2Ar), 3.81 (2H, AB,

$^{2}J_{A\text{-}B}$ = 10.53 Hz, -COOC*H*$_2$C(CH$_3$)$_3$), 2.87 (2H, d, $^{3}J_{H\text{-}H}$ = 6.05 Hz, -C*H*$_2$COOCH$_2$Ar), 2.02 (3H, s, -CHOCOC*H*$_3$), 0.90 (9H, s, -COOCH$_2$C(C*H*$_3$)$_3$).

^{13}C{^{1}H} NMR (CDCl$_3$, 100.0 MHz): δ = 171.4 (-*C*OOCH$_2$C(CH$_3$)$_3$), 169.2 (-CH$_2$*C*OOCH$_2$Ar), 168.9 (-CHO*C*OCH$_3$), 135.4 (-*C*$_{ipso\ aromatic}$), 128.6 (-*C*H$_{meta\text{-}aromatic}$), 128.5 (-*C*H$_{para\text{-}aromatic}$), 128.4 (-*C*H$_{ortho\text{-}aromatic}$), 68.3 (-*C*HCOO-), 66.8 (-*C*H$_2$Ar), 60.4 (-COO*C*H$_2$C(CH$_3$)$_3$), 36.5 (-*C*H$_2$COOCH$_2$Ar), 31.9 (-COOCH$_2$*C*(CH$_3$)$_3$), 26.3 (-COOCH$_2$C(*C*H$_3$)$_3$), 20.6 (-CHOCO*C*H$_3$).

ESI-MS: obs, 359.1 m/z ([MNa]$^{+}$); Calc for C$_{18}$H$_{24}$O$_6$Na, 359.15 m/z.

Elemental Analysis: Calculated (Found) C: 64.3 (64.4); H: 7.2 (7.3).

6.4 Experimental details for Chapter 3

6.4.1 General Considerations

Compounds 2, 3 and 4 were prepared as reported in experimental details for chapter 2.

6.4.2 Synthesis of 5-(S)- and 5-(R)-[(benzyloxycarbonyl)methyl]-1,3-dioxolane-2,4-diones, (L- and D-17)[13]

To a suspension of α-hydroxy acid, **4**, (4.78 g, 0.021 mol, 1 equiv) in dry THF (150 mL) was added diphosgene (3.1 mL, 0.026 mol, 1.2 equiv) under a nitrogen atmosphere. The resulting mixture was then treated with activated carbon and left to stir at room temperature for 18 h. The solution was then filtered off the activated carbon and concentrated in *vacuo*. The resulting residue was washed with pentanes (2 x 100 mL) and recrystallised from Et_2O/petroleum ether (b.p. 40-60 °C) and dried over 4Å molecular sieves to yield ***L*-17** a white solid. (3.62 g, 14.3 mmol 68%) (Yield = 65% for ***D*-17**).

^{1}H NMR ($CDCl_3$, 400 MHz): δ = 7.42-7.33 (5H, m, -C$H_{aromatic}$); 5.14 (2H, s, -CH_2Ar); 5.09 (1H, ABX, $^3J_{A\text{-}X}$ = 4.02 Hz, $^3J_{B\text{-}X}$ = 3.58 Hz, -CHCH_2COOCH_2Ar); 3.22 (1H, ABX, $^2J_{A\text{-}B}$ = 18.28 Hz, $^3J_{A\text{-}X}$ = 4.02 Hz, -CH_2COOCH_2Ar), 3.16 (1H, ABX, $^2J_{A\text{-}B}$ = 18.28 Hz, $^3J_{B\text{-}X}$ = 3.58 Hz, -CH_2COOCH_2Ar).

^{13}C NMR ($CDCl_3$, 400 MHz): δ = 167.8 (-CH_2*C*OOCH_2Ar); 166.7 (-OCOO*C*OCH-); 145.4 (-O*C*OOCOCH-); 134.4 (-$C_{ipso\ aromatic}$); 128.9 (-$C_{meta\ aromatic}$); 128.8 (-$C_{para\ aromatic}$); 128.7 (-$C_{ortho\ aromatic}$); 75.0 (-OCOOCO*C*H-); 68.2 (-*C*H_2Ar); 34.4 (-CH*C*H_2COOCH_2Ar).

Elemental Analysis: Calculated (Found) C: 57.6 (57.2); H: 4.0 (4.1).

6.4.3 General procedure for polymerisation of 17 ([M]/[I] = 20)

A solution of amine catalyst (1 equiv) and *neo*-pentanol (0.88 mg, 0.01 mmol, 1 equiv) was added to **17** (50 mg, 0.2 mmol, 20 equiv) in $CHCl_3$ (0.3 mL). The solution was left to stir at room temperature for the allotted time period before being diluted with DCM (4 mL), washed with cold 2.0 M $HCl_{(aq)}$ (2 x 5 mL) and brine (5 mL). The organic layer was dried over $MgSO_4$, filtered and concentrated *in vacuo*. The PBMA was precipitated into ice cold petroleum ether (b.p. 40-60 °C) to yield $PBMA_{20}$ as a tacky solid (0.021 g, 0.005 mmol, 50%).

^{1}H NMR ($CDCl_3$, 400.0 MHz): δ = 7.42 – 7.20 (100H, m, -C*H*$_{aromatic}$), 5.61 – 5.51 (20H, m, -C*H*COO-), 5.17 – 5.04 (40H, m, -C*H*$_2$Ar), 3.81 and 3.77 (2H, AB, $^2J_{A\text{-}B}$ = 7.05 Hz,-C*H*$_2$(CH_3)$_3$), 3.05 – 2.78 (40H, m, -C*H*$_2$COOCH_2Ar), 0.89 (9H, s, -CH_2(C*H*$_3$)$_3$). GPC (THF, RI): M_n (PDI) = 3 860 g.mol^{-1} (1.10) using 4-methoxypyridine as the ROP catalyst.

6.4.4 General procedure for the deprotection of PBMA ([M]/[I] = 20)

A balloon of H_2 was bubbled through a suspension of PBMA (0.05 g, 0.0095 mmol) and Pd/C (0.01 g, 10 wt. % loading) in THF (20 mL) for 15 min. The solution was then filtered to remove Pd/C and concentrated *in vacuo*. The PMA was extracted into MeOH and concentrated *in vacuo* to yield the desired product as a colorless oil (0.027 g, 0.012 mmol, 96%).

^{1}H NMR (d^8-THF, 400.0 MHz): δ = 5.60 – 5.53 (20H, m, -C*H*COO-), 3.03 – 2.76 (40H, m, -C*H*$_2$COOCH_2Ar), 3.84 (2H, m, -C*H*$_2$(CH_3)$_3$), 0.9 (9H, s, -CH_2(C*H*$_3$)$_3$).

$^{13}C\{^{1}H\}$ NMR (d^8-THF, 100.0 MHz): δ = 170.4 (-O(CO)CHO(*C*O)-), 168.4 (-CH_2*C*OOH), 70.6 (-O(CO)*C*HO(CO)-), 36.2 (-*C*H_2COOH). GPC (THF (0.1 M citric acid), RI): M_n (PDI) = 1 100 g.mol^{-1} (1.10).

6.4.5 General procedure for the degradation of the PMA ([M]/[I] = 15)

PMA (56 mg, 0.0306 mmol) was dissolved in H_2O (64 mL) and monitored *via* acid-base titration of a sample (0.2 mL) with an aqueous NaOH solution (0.45 mmol.L^{-1}) using phenolphthalein as a pH indicator, ^{1}H NMR spectroscopy in D_2O and ESI-MS analysis.

6.5 Experimental details for Chapter 4

6.5.1 General Considerations

Compounds ***L*-17** and ***D*-17** were prepared as reported in experimental details for chapter 3.

6.5.2 General procedure for preparation of PEO-b-PBMA ([M]/[I] = 25)

A solution of 4-methoxypyridine (4.8 μL, 0.048 mmol, 1 equiv) and MeO-PEO_{5K}-OH macroinitiator (0.24 g, 0.048 mmol, 1 equiv) was added to **17** (300 mg, 1,2 mmol, 25 equiv) in $CHCl_3$ (3.75 mL). The solution was left to stir at room temperature for the allotted time period before being precipitated into ice cold petroleum ether (b.p. 40-60 °C) to yield PEO_{5K}-*b*-$PBMA_{25}$ as a white solid (0.39 g, 0.038 mmol, 82%).

^{1}H NMR ($CDCl_3$, 400 MHz): δ = 7.35 - 7.21 (125H, m, -C$H_{aromatic}$), 5.58 – 5.50 (25H, m, -C*H*COO-), 5.13 – 5.05 (50H, m, -CH_2Ar), 3.67 – 3.53 (454H, s, -O(C*H*2)$_2$O-), 3.03 – 2.80 (50H, m, -CH_2COOCH_2Ar).

GPC (THF, RI): M_n (PDI) = 16 940 g.mol^{-1} (1.03) for PEO_{5K}-*b*-P(*L*-BMA)$_{25}$.

6.5.3 General procedure for preparation of PEO-b-PBMA polymeric micelles

Deionised water (60 mL) was added dropwise to a solution of PEO_{5K}-*b*-$PBMA_{25}$ (30 mg, 0.0028 mmol) (M_n = 16 940 g.mol^{-1}, PDI = 1.03) in HPLC grade THF (30 mL) at 25 °C *via* a metering pump at a rate of 10 mL.h^{-1}. After the addition of water was complete, the micelle solution was transferred to a presoaked dialysis membrane tubes (MWCO = 3.5 kDa) and dialysed against nanopure water for 3 days with 5 water changes. The final volume of PEO_{5K}-*b*-$PBMA_{25}$ was 100 mL

affording a polymer concentration of *ca.* 0.3 mg.mL^{-1}. D_h (DLS) = 18 ± 1 nm; D_{av} (TEM) = 16 ± 5 nm; CMC (Fluorescence microscopy) = 3.61 x 10^{-3} g.L^{-1}.

6.5.4 General procedure for CMC determination of polymeric micelles[14]

0.05 mL of an acetone solution of pyrene at 6 x 10^{-5} mol.L^{-1} was placed into ten 5 mL volumetic flasks and all left to allow the acetone to fully evaporate. Solutions of the polymeric micelles (5 mL) at different concentrations (from 0.3 to 0.0003 mg.mL^{-1}) were added to the volumetic flasks resulting in a pyrene concentration of 6 x 10^{-7} mol.L^{-1}. The solutions were left to stir for two days to ensure equilibrium before being analysed using fluorescence spectroscopy.

6.6 References

(1) Pratt, R. C.; Lohmeijer, B. G. G.; Long, D. A.; Lundberg, P. N. P.; Dove, A. P.; Li, H. B.; Wade, C. G.; Waymouth, R. M.; Hedrick, J. L. *Macromolecules* **2006**, *39*, 7863.

(2) Tays, K.; Atkinson, J. *Synthetic Commun.* **1998**, *28*, 903.

(3) Athanasellis, G.; Detsi, A.; Prousis, K.; Igglessi-Markopoulou, O.; Markopoulos, J. *Synthesis* **2003**, 2015.

(4) Reina, J. J.; Rojo, J. *Tetrahedron Lett.* **2006**, *47*, 2475.

(5) Denmark, S. E.; Yang, S.-M. *J. Am. Chem. Soc.* **2004**, *126*, 12432.

(6) Barrish, J. C.; Lee, H. L.; Mitt, T.; Pizzolato, G.; Baggiolini, E. G.; Uskokovic, M. R. *J. Org. Chem.* **1988**, *53*, 4282.

(7) Du, W.; Hong, L.; Yao, T.; Yang, X.; He, Q.; Yang, B.; Hu, Y. *Bioorg. Med. Chem.* **2007**, *15*, 6323.

(8) Ouchi, T.; Fujino, A. *Makromol. Chem.* **1989**, *190*, 1523.

(9) Leemhuis, M.; van Nostrum, C. F.; Kruijtzer, J. A. W.; Zhong, Z. Y.; ten Breteler, M. R.; Dijkstra, P. J.; Feijen, J.; Hennink, W. E. *Macromolecules* **2006**, *39*, 3500.

(10) Kimura, Y.; Shirotani, K.; Yamane, H.; Kitao, T. *Macromolecules* **1988**, *21*, 3338.

(11) Marcincinova-Benabdillah, K.; Boustta, M.; Coudane, J.; Vert, M. *Biomacromolecules* **2001**, *2*, 1279.

(12) Trimaille, T.; Moller, M.; Gurny, R. *J. Polym. Sci., Part A: Polym. Chem.* **2004**, *42*, 4379.

(13) Tang, L.; Deng, L. *J. Am. Chem. Soc.* **2002**, *124*, 2870.

(14) Wilhelm, M.; Zhao, C. L.; Wang, Y.; Xu, R.; Winnik, M. A.; Mura, J. L.; Riess, G.; Croucher, M. D. *Macromolecules* **1991**, *24*, 1033.

Appendices

7.1 Additional DLS data for chapter 4

7.2 PEO_{5K}-b-P(L-BMA)$_{10}$ polymeric micelles

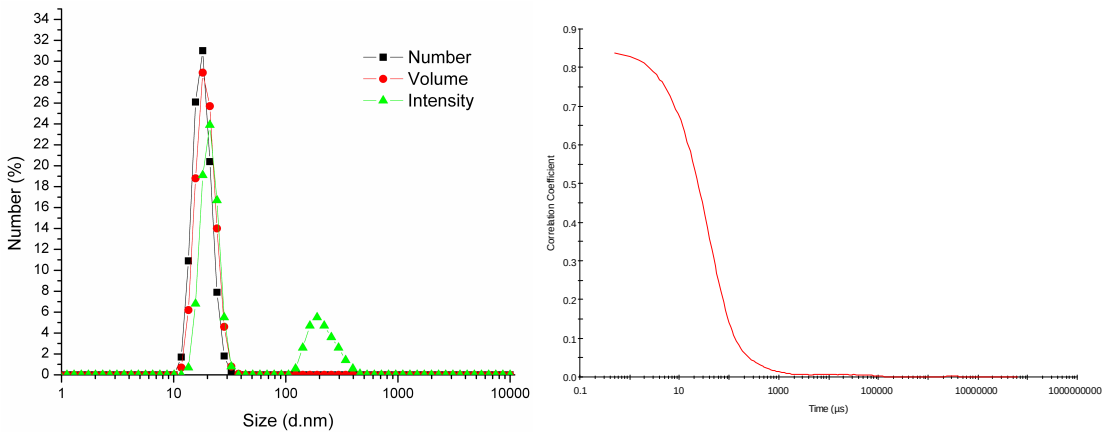

7.3 PEO_{5K}-b-P(L-BMA)$_{25}$ polymeric micelles

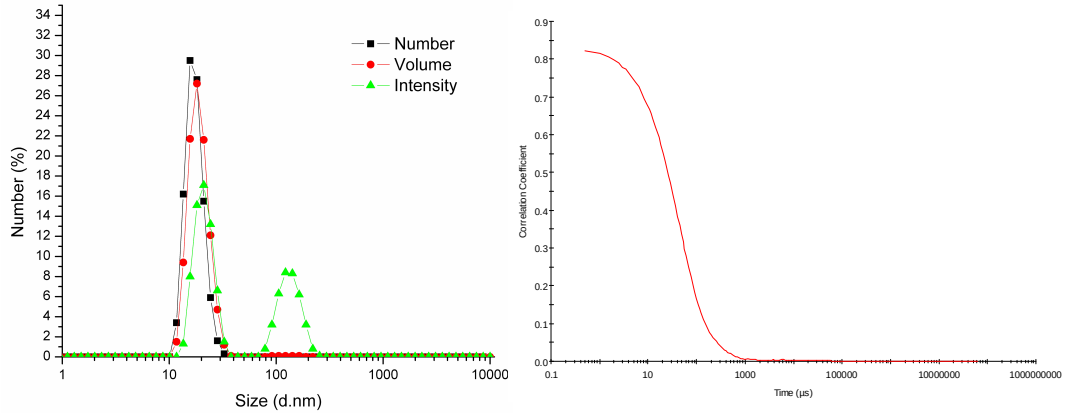

7.3 PEO_{5K}-b-P(L-BMA)$_{40}$ polymeric micelles

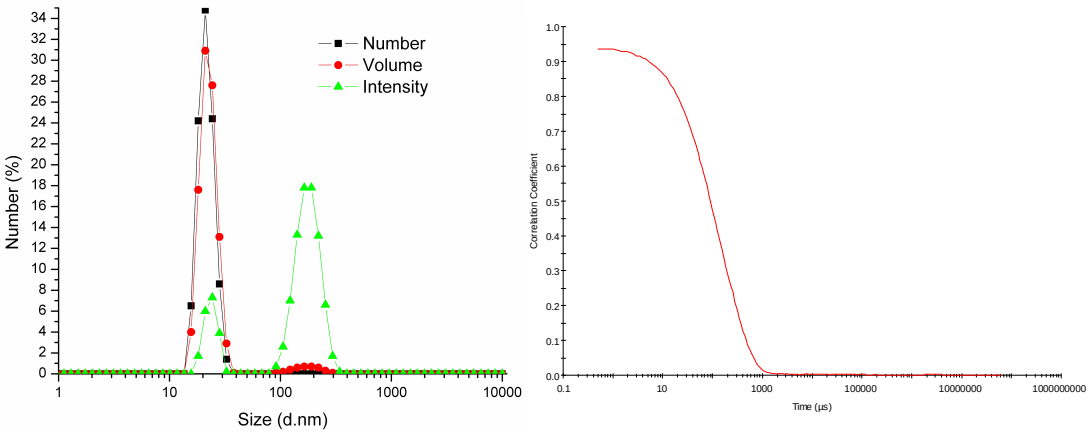

7.4 PEO_{2K}-b-P(L-BMA)$_5$ polymeric micelles

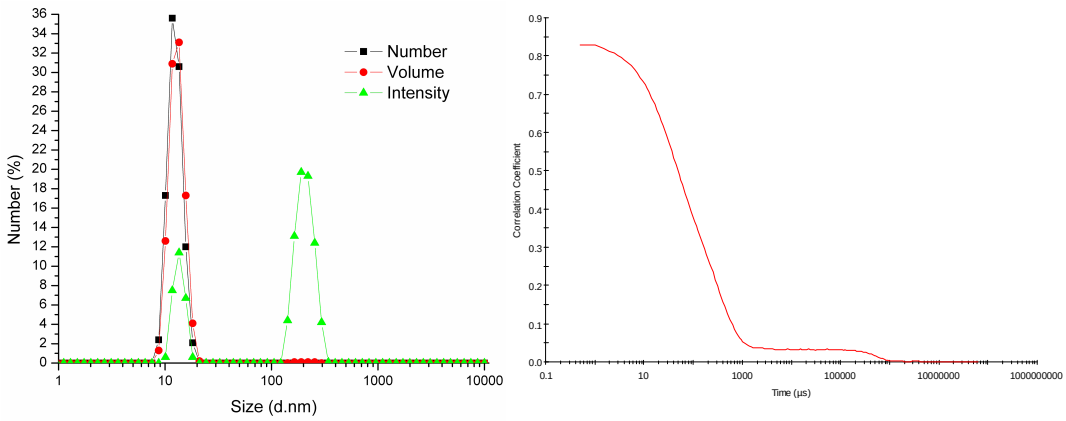

7.5 PEO_{10K}-b-P(L-BMA)$_{20}$ polymeric micelles

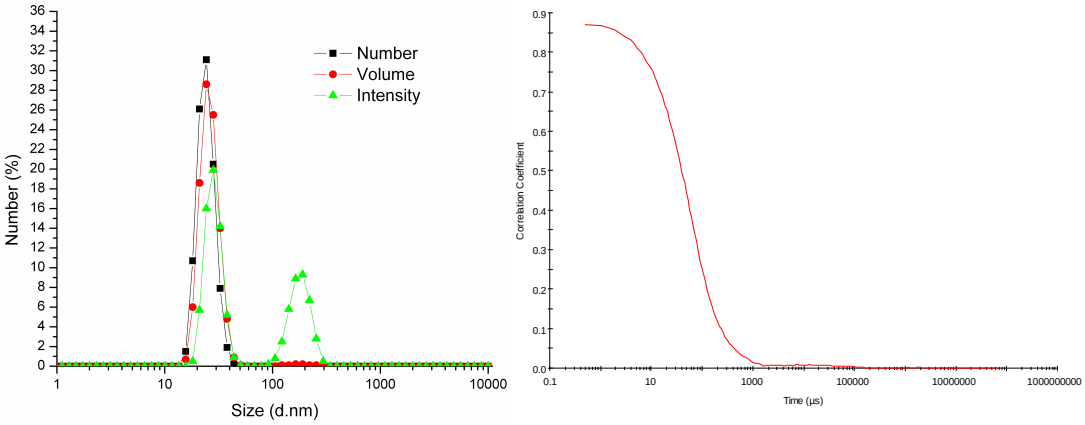

7.6 PEO_{5K}-b-P(L-BMA)$_{10}$ + PEO_{5K}-b-P(D-BMA)$_{10}$ stereocomplex polymeric micelles

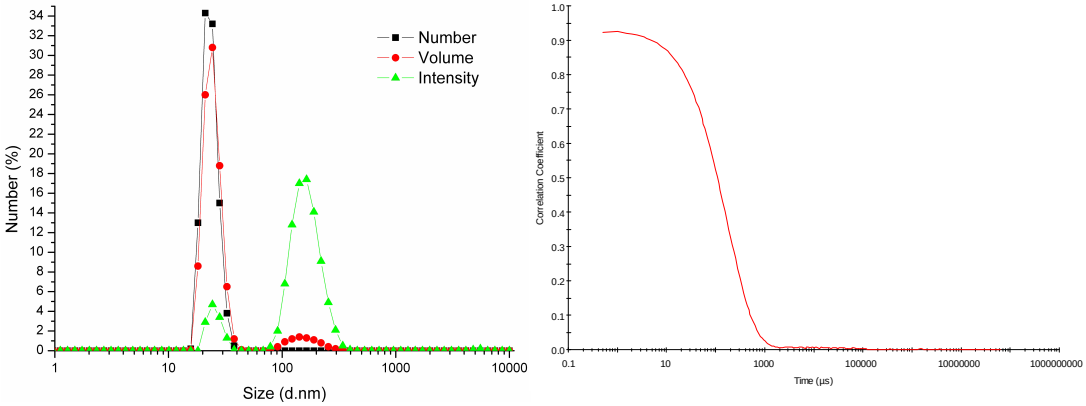

7.7 PEO_{5K}-b-P(L-BMA)$_{10}$ + PEO_{5K}-b-P(D-BMA)$_{10}$ stereocomplex polymeric micelles before redispersion

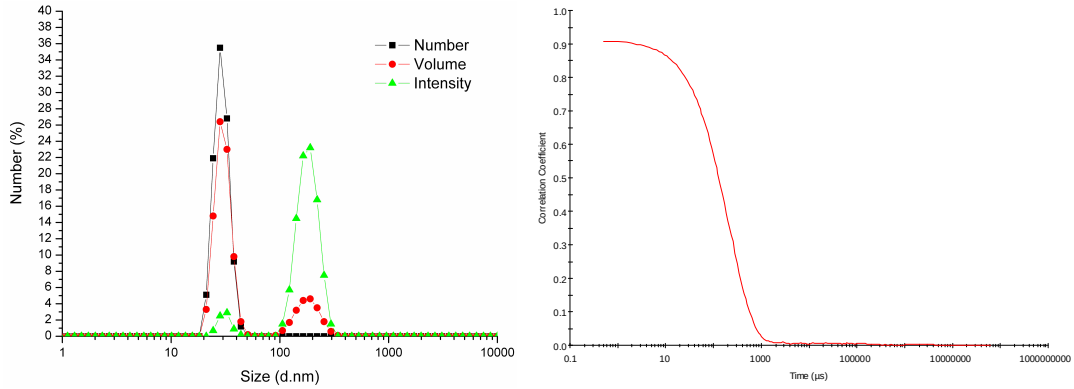

7.8 PEO_{5K}-b-P(L-BMA)$_{10}$ + PEO_{5K}-b-P(D-BMA)$_{10}$ stereocomplex polymeric micelles after redispersion

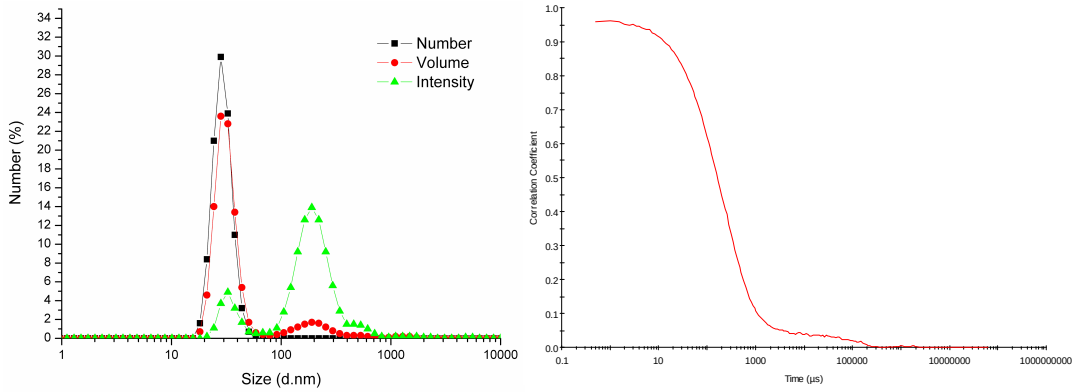

7.9 PEO_{5K}-b-P(L-BMA)$_{10}$ polymeric micelles before redispersion

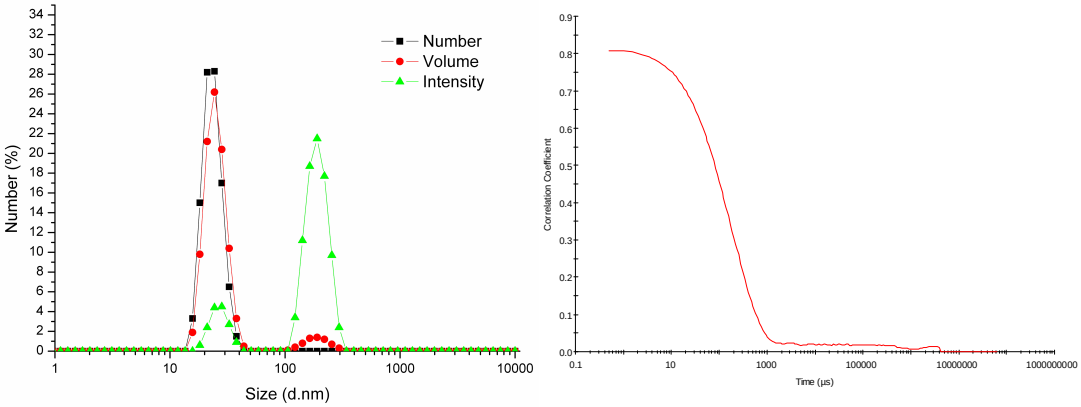

7.10 PEO_{5K}-b-P(L-BMA)$_{10}$ polymeric micelles after redispersion